Electrogenic Ion Transport in the Midgut of the Lepidopteran Larva, *Manduca sexta* (Tobacco Hornworm)

by

Jillian Mary Peacock B.Sc.

Department of Cell Biology, Faculty of Science

A thesis submitted to the University of Glasgow for the degree of Doctor of Philosophy

 May 1991

ProQuest LLC.
789 East Eisenhower Parkway
P.O. Box 1346
Ann Arbor, MI 48106 – 1346

ACKNOWLEDGEMENTS

First and foremost, I would like to thank my supervisor, Dr Julian Dow, for his support and encouragement during both the experimental work and the writing of my thesis, and also for being a continual source of ideas.

I am also grateful to Professor Adam Curtis for providing the facilities required to complete my work.

My thanks extend to all of the staff and students in the department of Cell Biology who made my time here most enjoyable with their friendship and advice. In particular Andrew Hart for his patience whilst teaching me photographic techniques, and both Susan Kitson and Scott Arkison for technical support.

I would also like my family to know that without their support and encouragement, this thesis may never have been written, at least with my sanity intact.

Finally, thanks to Jim who didn't want a mention.

TABLE OF CONTENTS

LIST OF FIGURES

ABBREVIATIONS

AC:	Alternating current
ADP:	Adenosine diphosphate
APTS:	Aminopropyl triethoxysilane
ATP:	Adenosine triphosphate
ATPase:	Adenosine triphosphatase
BCECF:	Bis-(carboxyethyl)-carboxyfluorscein
BSA:	Bovine serum albumin
Btk:	*Bacillus thuringiensis* δ- endotoxin var. *kurstaki*
cAMP:	Cyclic adenosine monophosphate
CCAM:	Columnar cell apical membrane
CCCP:	Carbonyl cyanide *m*-chlorophenylhydrazone
cDNA:	complementary DNA
CoA:	Coenzyme A
con A:	Concanavalin A
CoQ:	Coenzyme Q
CTP:	Cytosine triphosphate
Cyt a + a_3:	Cytochrome oxidase
Cyt. b:	Cytochrome b
Cyt. c:	Cytochrome c
Da:	Daltons
DC:	Direct current
DCCD:	N, N'- dicyclohexyl carbodiimide
DES:	Diethyl stilbestrol
DNA:	Deoxyribonucleic acid
DNP:	2,4-Dinitrophenol
EDTA:	Ethylenediamine tetraacetic acid
E.R.:	Endoplasmic reticulum
EtOH:	Ethanol
F:	Faraday's constant
FACS:	Fluorescence activated cell sorting
FCS:	Foetal Calf Serum
FDA:	Fluorescein diacetate
FITC:	Fluorescein isothiocyanate
FP:	Flavoprotein
GalNAc:	N-Acetyl galactosamine
GCAM:	Goblet cell apical membrane

GlcNAc:	N-Acetyl glucosamine
GTP:	Guanosine triphosphate
HS:	Horse Serum
kDa:	KiloDaltons
KSCN:	Potassium thiocyanate
mA:	Milliamps
ME	Microelectrode
MΩ:	Megaohms
M_r:	Molecular weight
mOsmol:	MilliOsmoles
mV:	Millivolts
NAD:	Nicotinamide adenine dinucleotide
NADH:	Nicotinamide adenine dinucleotide, reduced
NBDCl:	4-chloro-7-nitrobenzo-2-oxa-1,3-diazole
NEM:	N-ethyl maleimide
OCV:	Open circuit voltage
OSCP:	Oligomycin-sensitive connecting protein?
PBS:	Phosphate buffered saline
P.D.:	Potential difference
PHA:	Phaseolus Haemagglutinin
p.m.:	Plasma membrane
pmf, Δp:	Proton motive force
P:O:	Phosphate: Oxygen ratio
R:	Gas constant
RNA:	Ribonucleic acid
rpm:	Revolutions per minute
SBA:	Soybean agglutinin
SCC:	Short circuit current
SEM:	Scanning electron microscopy
S.R.:	Sarcoplasmic reticulum
T:	Temperature (in Kelvin)
TP:	Tip potential
TEM:	Transmission electron microscopy
TEP:	Transepithelial potential difference
TRIS:	Tris (hydroxymethyl) aminomethane
TRITC:	Tetramethylrhodamine isothiocyanate
UV:	Ultraviolet
v/v:	volume per volume

WGA:	Wheatgerm agglutinin
w/v:	weight per volume
$\Delta\psi$:	Membrane electrical potential
$\Delta\mu$:	Electrochemical equilibrium potential

SUMMARY

The midgut of *Manduca sexta* and other Lepidopteran larval types has a large electrical gradient approaching 150mV (lumen-side positive) or over 1mA cm^{-2} *in vivo.* This gradient is generated by electrogenic transport of K^+ from the blood to the midgut lumen *via* a unique K^+ ATPase located on the goblet cell apical membrane. Active transport of K^+ occurs in all three regions of the midgut, however morphological and functional differences result in generation of a high luminal pH of 11-12 only in the anterior and middle regions, with a return to dietary pH levels in the posterior region.

Microelectrode impalements of the goblet cell cavity and other midgut cellular compartments has shown that the electrical potential difference across the goblet cell apical membrane *in vivo* is 269mV which is sufficient to explain a pH of 11.6 in the cavity, using Nernstian dynamics. This evidence supports a primary role for the K^+ ATPase of providing the electrical gradient required for high pH generation. The advantages of having high luminal alkalinity for the insect larva are several; (1) Digestive hydrolysis may be accelerated resulting in faster growth and more efficient utilisation of dietary energy. (2) Limitation of gut living pathogenic microorganisms which normally prefer an acidic environment. (3) Protection from dietary tannins which bind to proteins at low pH and therefore reduce digestibility.

The presence of high $[K^+]$ in the diet led to the original theory that K^+ was actively excreted to prevent toxic accumulation in the haemolymph; however, now, there is evidence to suggest that excretion is not the primary role of the K^+ ATPase as; (1) Some phytophagous insect larvae do not possess goblet cells and therefore do not actively excrete K^+ via cavity-located ATPases, (2) The presence of a complex apical valve at the mouth of the cavity would restrict, rather than facilitate K^+ excretion, (3) The electrical gradient produced by active K^+ transport across goblet cells actually drives uptake of K^+ into the blood *via* an amino acid cotransport mechanism across columnar cell apical membranes, making a role in excretion seem irrational, (4) K^+ activity of the diet is not overly high, however Na^+ is low resulting in a larger than normal K: Na ratio.

The theories supporting active K^+ transport in Lepidopteran midgut have recently been challenged. Some workers believe the pump to be an

electrogenic H^+ ATPase which drives an electroneutral, or electroresponsive K^+ / H^+ exchange. This model explains the electrical potential difference and the transport of K^+ into the lumen, but it is difficult to reconcile with the high pH found in the midgut lumen, and the estimated pH of 11.6 thought to exist in the cavity following determination of the goblet cell apical membrane potential.

The work carried out during the course of this project attempted to resolve the discrepancies in models for active ion transport using electrophysiological, membrane biochemical and culture techniques. Microelectrode impalements of three midgut cellular compartments yielded the value of 269mV for the goblet cavity membrane mentioned above. In addition, these compartments were probed with a pH sensitive fluorescent dye, acridine orange, whilst monitoring transepithelial potential. When the pump was active (high TEP), no dye was found in the cavities, indicating alkalinity: However, when the pump was inactive (low TEP), for instance in the absence of K^+ from the bathing solution, cavity acidification occurred. Furthermore, permeabilization of isolated midgut, using steroid glycosides, abolished the TEP of isolated midgut. Subsequent addition of ATP induced a transient rise of TEP. These results support the hypothesis that an active K^+ ATPase located on the goblet cell apical membrane is responsible for generation of the high pH found in the midgut lumen of *Manduca sexta* larvae.

In addition, midgut cells, which were enzymically dissociated from the tissue, were shown to be maintained in culture for more than 2 weeks. This finding, together with the demonstrated lectin-specificity for columnar cells, could be applied in cell and membrane isolation procedures, which in turn would permit more precise biochemical and molecular biological determinations of enzyme characteristics.

For
Mum and Dad

Chapter 1

1. Chapter 1. INTRODUCTION

1.1. General Introduction to Insect Digestive System

Insects are the most numerous and diverse order of the animal kingdom having 1 million known species and probably 10-30 million uncharacterized species (Dow 1986). One reason for their success is their ability to adapt to their environment and exploit food sources unavailable to other members of the animal kingdom. In accordance with dietary preference, there are parallel changes in digestive system morphology and function, although external features, such as mouthparts, are equally important. For instance, phytophagous caterpillars which feed mainly on solid plant material possess a very different alimentary tract from mosquitos that feed on mammalian blood. The insect alimentary canal is a highly permeable organ responsible for functions such as osmoregulation, ion and water balance, and nutrient input and output. It can be divided into three regions; foregut, midgut and hindgut (Fig 1.1).

Figure 1.1 The alimentary canal of insect larvae

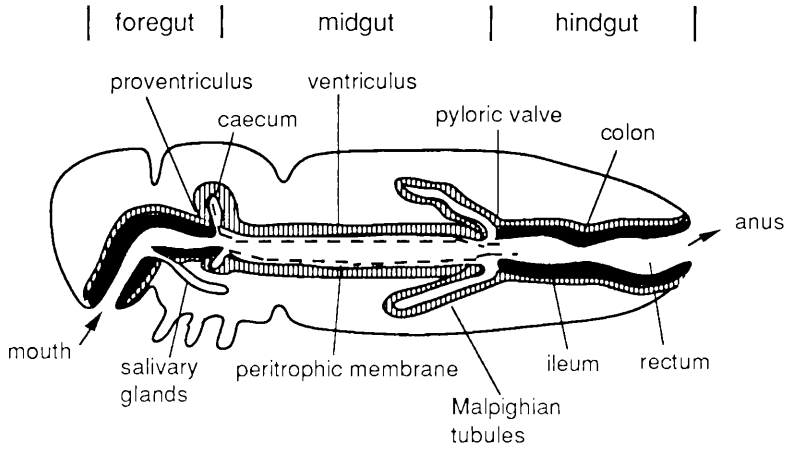

The alimentary canal is divided into 3 regions; foregut, midgut and hindgut, with access restricted by 4 sphincters; mouth, proventriculus, pyloric valve and anus. Cuticle lines the fore- and hindguts, as indicated by the heavy lines. The diagram also shows other organs such as salivary glands, caeca, Malpighian tubules, rectum and a chitinous peritrophic membrane delaminated from the midgut cells. (This figure was adapted from Dow 1986).

The foregut is lined with relatively impermeable cuticle and therefore does not play a significant role in absorption, being instead a major site of storage and digestion. The hindgut is also lined with cuticle, although it is more permeable than the foregut (Maddrell and Gardiner 1980). Its main function is to reclaim useful substances from food and urine before they are lost in the faeces. The midgut is the most permeable region of the alimentary canal and plays host to a variety of physiological processes encountered by the living insect. It is separated from the foregut and hindgut by valves at either end. The proventriculus is situated at the anterior entrance of the midgut and pyloric valve at the posterior exit. Other specializations that may occur in the alimentary canal include salivary glands which feed into the mouth to dilute ingested food and adjust the pH and ionic content, and Malpighian tubules which are blind sacs, located near the pyloric valve, involved in water and ion osmoregulation and urine production.

1.2. Morphological Characteristics of Insect Midgut

1.2.1. Basic Structure

The midgut is a simple epithelium, although there are present some endocrine cells, sparse innervation and an extensive tracheal supply, as well as underlying transverse and longitudinal muscles. As a simple epithelium, the midgut is ideal for physiological study and microscopy. Unlike neighbouring regions of the alimentary canal, midgut is endodermally derived and so does not secrete cuticle; instead it produces a peritrophic membrane which is a coarse meshwork of chitinous fibrils, coated with glycoprotein and full of pores ranging from 150-200nm depending on the species (Adang and Spence 1982; Baines 1978; Brandt et al. 1978; Skaer 1981). In Diptera, pore size of the peritrophic membrane has been estimated as low as 8nm (Terra 1983). In general, only very large molecules do not gain access to the epithelial layer through this membrane, thus providing protection against microorganisms and abrasion by food particles. In Lepidoptera, the peritrophic membrane is permeable to proteins of up to 10^5 Da (Wolfersberger et al. 1986), and may act as a barrier to certain enzymes (Santos et al. 1984).

1.2.2. Embryology

The development of the alimentary canal begins in the embryo when invaginations occur at the front and back of the insect, eventually forming the fore- and hind-gut. The midgut forms as an epithelial sac between the two invaginations which grow inwards eventually breaking through the sac and forming a continuous tube, which may explain why fore-and hind-gut are chitinous but midgut is not. Midgut is ancestrally derived from yolk cells, which are endodermal in origin; however, the midguts of higher order insects are derived from division of special anlagen cells which migrate from the tips of the ectodermal invaginations forming ribbons. This is known as bipolar formation (Anderson 1973; Kobayashi and Ando 1983; Miya 1976; Mori 1983; Suzuki and Ando 1981) and might result in structurally and/ or functionally distinct regions in the midgut, as suggested by Dow (1986). For example, the front two thirds of the midgut in *Manduca sexta* may be derived from anlagen cells from the stomodaeal invagination, whereas the morphologically and functionally different posterior third could be derived from migration of anlagen cells from the proctodaeal invagination (Dow 1986). The appearance of goblet cells in Lepidopteran midgut is a sign of epithelial maturity (Miya 1976). Displacement of the nucleus to a basal location is the first step in goblet cell formation in the embryo, followed closely by appearance of a microvillus-lined vacuole (Hakim et al. 1986; Miya 1976). Microvilli are later penetrated by mitochondria and the goblet cavity forms a connection valve with the midgut lumen. Septate junctions form as short, linear particles which join to form ribbons and eventually sinuous bands which are characteristic of septate junctions (Lane and Swales 1982). Nearly all insect epithelia display pleated septate junctions; however, smooth septate junctions have been reported in both midgut and Malpighian tubules (Flower and Filshie 1976; Lane and Skaer 1980). Gap junctions, responsible for cell:cell communication, coalesce at a similar time and are in place just before larval emergence (Lane and Swales 1982).

1.2.3. Developmental Changes in Growing Larvae

The surface area of midgut, and other epithelia, increases as the larva grows. In Malpighian tubules of Hemiptera, cell number remains constant but the area of the cells increases with larval growth (Maddrell 1985). It is unlikely that midgut epithelial surface area increases in this way as the

small size of cells in mature insects would imply an almost prokaryotic size on hatching. Lepidopteran larvae instead retain and add to their midgut cells (Turbeck 1974), whereas, other insect orders, such as Apterygota, turn over the whole epithelium at each moult (Humbert 1978). The presence of regenerative cells in Lepidopteran midgut suggest that a certain amount of turn-over is possible although this is limited to repair of sublethal damage occuring between moults (Spies and Spence 1985).

During metamorphosis from caterpillar to moth, the gut epithelium is completely transformed as the feeding habit changes from phytophagous plant eater to nectar drinker. The now almost redundant midgut shrinks to about a quarter of its larval size and the hindgut becomes seven times longer (Ryerse 1979). Prior to metamorphosis, various physiological as well as morphological changes take place. When the larvae stop feeding, electrogenic potassium ion transport across the gut ceases, goblet cell morphology alters, Malpighian tubule secretion is shut down and their lumens become occluded with concretion bodies, mitochondria retract from tubule microvilli, which then shrink (Cioffi 1984; Harvey et al. 1968; Ryerse 1978; Ryerse 1979). The changes observed in Malpighian tubules are hormonally regulated and can be mimicked *in vitro* by application of 20-hydroxyecdysterone. On the other hand, Juvenile hormone, topically applied, retards metamorphosis in the final instar and results in supernumerary larvae (Ryerse 1980).

1.2.4. Lepidopteran Midgut Cell Types

There are two main cell types in the caterpillar midgut, both with specializations for transport (Anderson and Harvey 1966). Columnar cells have long, even, type I microvilli which are coated with glycocalyx, and deep basal infoldings interspersed with mitochondria (Cioffi 1984) (Fig 1.2 a). Goblet cells are characterized by the presence of a 20μm diameter intracellular cavity, fringed with apical projections which have mitochondria inserted within them (Fig. 1.2 b and c): These are sometimes termed type II microvilli (Cioffi 1984). Insertion of mitochondria into microvilli is a feature characteristic of highly active transporting systems, as the distance between ATP source and destination is minimized (Bradley 1984). A complex interdigitating valve connects the cavity with the midgut lumen and allows restricted movement of certain components at specific times during the animal's life cycle (Fig 1.2 a)

Figure 1.2 Transmission electron micrographs of *Manduca sexta* midgut epithelium.

a. Transverse section through the epithelium showing both goblet and columnar cells. The goblet cell has been sectioned at an oblique angle through the top of the cavity and apical valve. Within the cavity cross sections of the apical projections can be seen as small circles. The apical valve is very complex consisting of many narrow channels which restricts movement of solutes. Columnar cells possess large centrally located nuclei (out of view) and apical microvilli that meet above the goblet cell apical valve. Their cytoplasm is filled with granules and vacuoles suggestive of protein packaging and degradation, reflecting their function as the nutrient absorbing cells of the midgut. 630x. scale bar = 50μm.

b. Transverse section through a goblet cavity from the middle region. The apical projections into the cavity possess inserted mitochondria indicating an energy-dependent role. The flocculent material in the lumen of the cavity is acid mucopolysaccharide matrix. 1700x. scale bar = 25μm.

c. Cross section through the goblet cavity apical projections showing inserted mitochondria. Those that do not display inserted mitochondria may have them further along the projection outwith this sectional plane. With the eye of a believer one may be able to see small regular electron-dense components on the cytoplasmic face of the plasma membrane.surrounding the mitochondria. These could be the 'portasomes' described by Harvey and Cioffi (1981) which are associated with active K^+ and H^+ transport. 5100x. scale bar = 8μm

d. Transverse section through the epithelium showing the junction between two columnar cells. Septate (invertebrate 'tight') junction is the dense band of very closely apposed membrane. Moving towards the basal side, possible gap junctions can be seen at intervals. 17000x. scale bar = 2.5μm

Figure 1.2 Transmission electron micrographs of *Manduca sexta* midgut epithelium.

a

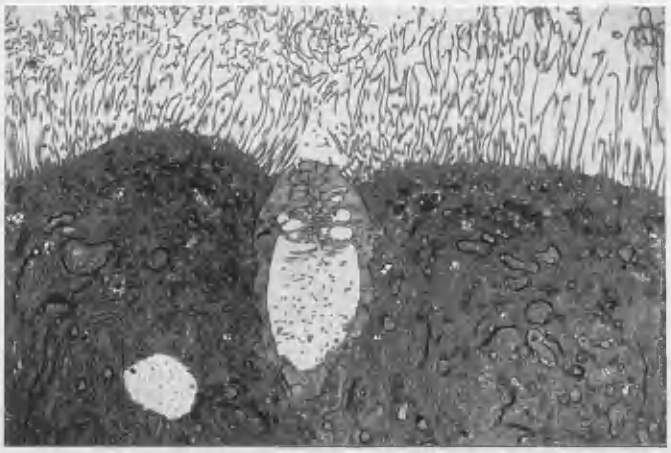

b

c

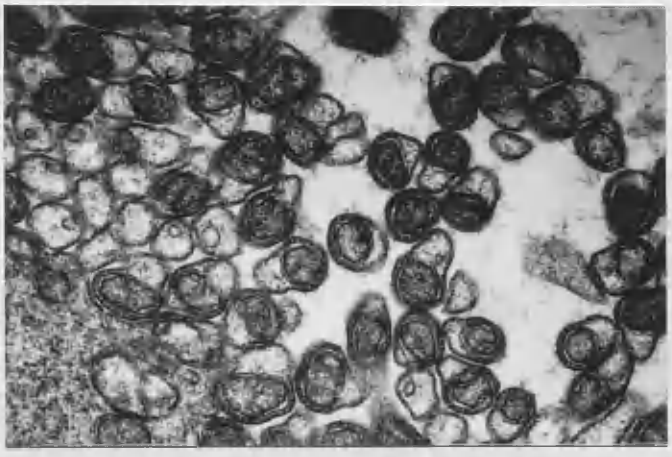

d

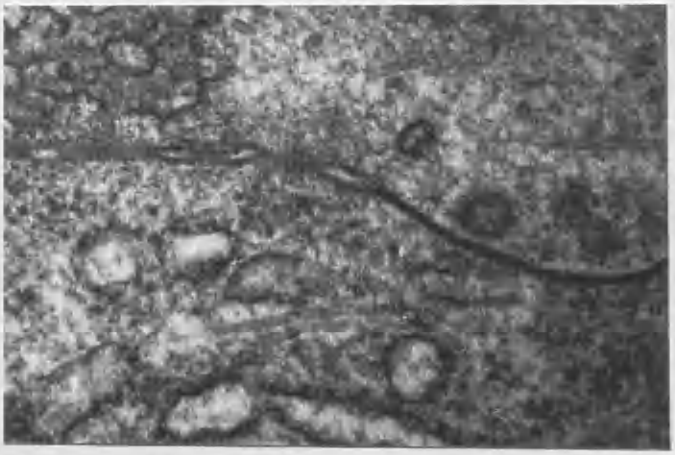

(Anderson and Harvey 1966; Cioffi 1984). The flocculent material contained within a cavity is rich in sulphur and is probably mucopolysaccharide in nature (Dow et al. 1984; Turbeck 1974).

Two other cell types can be found in the midgut, although they are rare. Regenerative cells are found clustered between epithelial cells on the basal membrane and can be distinguished from the other cell types by the absence of basal infoldings (Smith et al. 1969). They mostly remain inactive whilst the larvae are feeding, but begin to divide in the prepupae to form the pharate pupal epithelium (Waku and Sumimoto 1971). Some regenerative cells have been known to differentiate in larvae between the 4th and 5th instar moult suggesting some involvement in gut renewal (Turbeck 1974), and they also respond to injury (Spies and Spence 1985). Endocrine cells were discovered fairly recently (Endo and Nishiitsutsuji-Uwo 1981), and also have a basal location. They are filled with membrane-bound vesicles which react with antibodies to vertebrate hormones. However, evidence for their existence is such that they could easily be confused with regenerative cells.

1.3. Physiological Characteristics of Insect Midgut

1.3.1. Ions in the Midgut

Caterpillars are solid plant feeders and therefore have short broad guts with strong musculature. Their diet is abundant, but low in nutrients, and therefore is passed rapidly through the gut. Almost all Lepidopteran larvae are phytophagous and can grow three orders of magnitude within a few weeks, exemplifying the success of their feeding characteristics. The Na^+:K^+ ratio for plant material is low (195mM K^+ and 0.5mM Na^+.(Sutcliffe 1963)) and this is reflected in their blood ion composition which can consist of a Na^+:K^+ ratio of 1:3-5, unlike cockroaches which are not specialized plant feeders and have a ratio of 10:1 (Vitellaro-Zuccarello 1985). Analysis of body fluids has shown that a high level of potassium and magnesium is characteristic of Lepidopteran blood as well as a low level of sodium (Jungreis et al. 1973). This ratio is similar for midgut tissue and gut contents, as determined by flame photometry and electron probe X-ray microanalysis (Dow et al. 1984; Harvey et al. 1975). Ion concentrations can be measured quite easily using these techniques; however, it is the activities of the ions present that are important.

Monovalent ions within cells have an activity coefficient of 0.7, but divalent cations are usually bound to charged macromolecules (Dow 1986). In 1982, Moffett et al. measured intracellular potassium activities for *Manduca sexta* midgut epithelium using ion-selective microelectrodes, resulting in an activity coefficient for K^+ of about 0.8 (Moffett et al. 1982).

pH is very high in the alimentary canal, and especially in the midgut with measurements of over pH 12 on record, but it is nearly neutral in the blood (Dow 1984; Waterhouse 1949). High luminal pH corresponds with a tannin-rich diet and may serve as a protection against toxic tannin compounds that bind to proteins at low pH, thereby limiting digestive hydrolysis (Berenbaum 1980), although this controversial view has been challenged (Bernays 1981).

1.3.2. Midgut Toxins

Many toxins are inactivated by metabolism and high pH in Lepidopteran midgut (Ivie et al. 1983); however, one naturally occuring toxin, the δ-endotoxin of several *Bacillus thuringiensis* subspecies is effective. *Bt.* var *kurstaki (Btk)* is particularly effective for Lepidopteran larvae (Fast 1981).

Inert parasporal crystals from *Btk* are ingested by larvae and are then activated by the high pH and enzymes in the midgut lumen, yielding potent lytic proteins which proceed to destroy the cells of the midgut epithelium. The effect can be demonstrated *in vitro* as there is rapid loss of K^+ transport and K^+ content in the cavity within a matter of minutes (Gupta et al. 1985). The first morphological effects are; disruption of columnar cell microvilli followed by swelling of the goblet cavity (Endo and Nishiitsutsuji-Uwo 1980; Griego et al. 1980; Spies and Spence 1985). Eventually the whole epithelium is disrupted and blood and gut contents mix causing paralysis and death.

Btk causes a drop in short circuit current when it is applied *in vitro* (Harvey and Wolfersberger 1979). This is due to a back-flux of potassium rather than direct inhibition of active transport, as the toxin opens a K^+ conductance in columnar cell membranes. The mechanism of action is likely to be similar to K^+ ionophores, such as valinomycin, which produce their own ion-selective channels in membranes.

Using cultured cells it has been possible to show that the first step of insecticide action is a lectin-like binding to the cell surface, as the effects of *Btk* were reduced by preincubation with N Acetyl galactosamine (Knowles et al. 1984). Cell death by *Btk* seems to be ion-specific, requiring the presence of Na^+ or K^+ externally; however, these findings were obtained from the TN-368 cell line which is derived from ovary and not likely to be the site of action of the δ-endotoxin *in vivo* (Himeno et al. 1985).

1.3.3. Ion Transport in *Manduca sexta* Midgut

The midgut of *Manduca sexta* is by far the largest part of the alimentary canal in this species and can be divided into 3 regions based on appearance, ultrastructural morphology and function. The extent of folding of the epithelium is region-dependent, the least folded region being the middle of the midgut. Goblet cells from the posterior region have a reduced cavity, in which the apical projections no longer house mitochondria (Cioffi 1979) (Fig 1.3). The midgut possesses unique ion transporting capabilities, due to the presence of a highly active K^+ ATPase discovered in 1964 by Harvey and Nedergaard (Harvey and Nedergaard 1964), and defined since as a Keynes type V pump (Harvey et al. 1983a; Keynes 1969). Despite the differences in appearance and ultrastructural morphology, the rate of active K^+ transport remains the same in all three regions.

Ion transport in caterpillars has been extensively reviewed (Harvey 1980; Harvey et al. 1983a; Harvey et al. 1981; Harvey et al. 1983b; Wolfersberger et al. 1982; Zerahn 1977). The midgut is capable of generating a transepithelial potential difference of up to 150 mV at rest, and under short-circuit, a current of 0.5-1 mA cm^{-2} can be measured (Cioffi and Harvey 1981; Dow et al. 1984; Giordana and Sacchi 1977; Harvey and Nedergaard 1964; Moffett 1980; Wood and Moreton 1978). The short circuit current agrees very closely with net flux of radiolabelled potassium (Wood and Moreton 1978). Tissue resistance is typically 100 Ωcm^2.

The potassium pump has been proposed as being an alkali-metal ATPase which transports ions with the following order of efficacy; K = Rb > Na > Li > Cs (Harvey and Zehran 1972; Wolfersberger et al. 1982).

Figure 1.3 Midgut epithelial cell types display regional morphological differences

a. Anterior and Middle

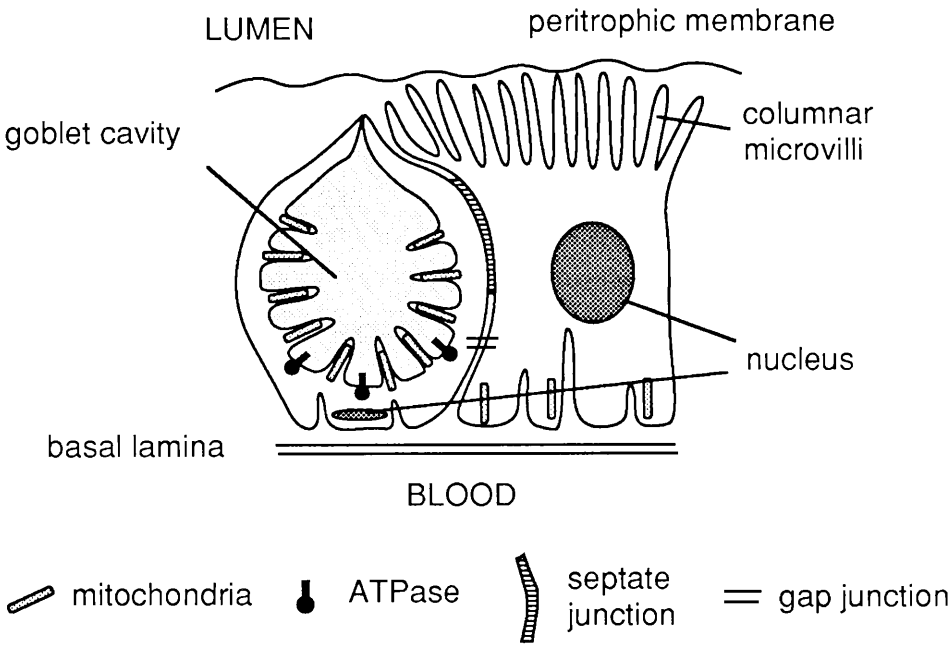

b. Posterior

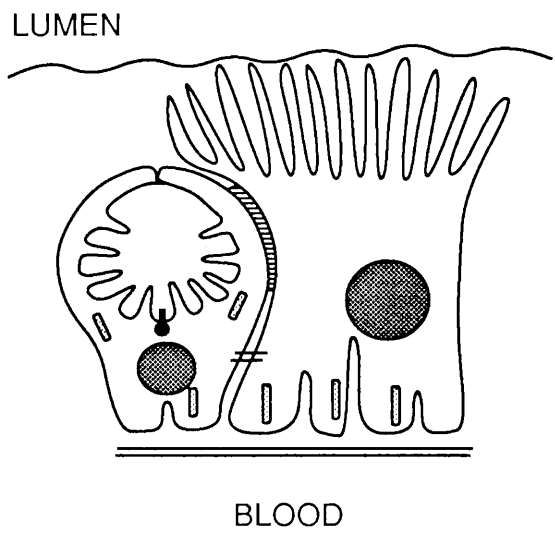

a. Anterior and Middle regions of *Manduca sexta* midgut possess goblet cells with large cavities and reduced cytoplasm. Apical projections into the cavity have mitochondria inserted. Columnar cell apical microvilli are relatively short but still overlap with the microvilli of an adjacent columnar cell (not shown) above the cavity apical valve.

b. The goblet cells in the posterior region have a reduced cavity with apical projections devoid of mitochondria. Columnar microvilli are elongated in this region and also overlap above the apical valve.

Active transport requires oxidative phosphorylation, as was shown by anoxia experiments, but conversely, changes in ion transport do not affect O_2 consumption (Harvey et al. 1967). This lack of respiratory control is thought to be because the free energy for ATP hydrolysis is low due to rapid use of ATP by K^+ -stimulated ATPases as it is formed (Mandel et al. 1980). The ATPase is capable of hydrolysing ATP even when their are no ions available for transport (Wieczorek et al. 1986).

Potassium is pumped across isolated midgut at a comparable rate to *in vivo* transport; however, there is an initial decline thought to be caused by adaptation to short-circuit conditions, followed by a slower exponential fall in K^+ transport (Cioffi 1980). This slow decline can be minimized by addition of various factors such as blood extracts and amino acids (Thomas and May 1984a). The short-circuit current can be reduced by general metabolic inhibitors such as 2,4-DNP (Haskell et al. 1965), cyanide (Mandel et al. 1980), azide (Dow et al. 1985) and tri-methyl tin (Thomas and May 1984a), but is only slightly affected by caffeine, calcium ionophores (Moffett et al. 1983; Wolfersberger and Giangiacomo 1983) and high external Ca^{2+} concentration (Wood and Harvey 1976), and slightly stimulated by cAMP. Transport is also inhibited by 25% CO_2 and carbonic anhydrase inhibitors. Ouabain does not inhibit ion transport indicating that the pump is not a Na^+ / K^+ ATPase (Harvey et al. 1981). If the pump is a K^+ ATPase, then it is unique to insect tissues.

10nm portasomes, which are an indication of active ion transport, have been seen on various insect membranes, such as those of the salivary glands, Malpighian tubules and epidermal sensilla (Harvey et al. 1983a; Harvey et al. 1981; Wieczorek and Gnatzy 1985).

The pump has been isolated, partially purified and characterized (Wieczorek et al. 1986). It is an Mg^{2+} and K^+ stimulated ATPase which can utilize ATP and GTP, but not CTP, ADP or AMP. The biochemical activity of the pump is not sensitive to ouabain, oligomycin, azide, vanadate or fluoride, but is sensitive to DCCD and nitrate (Wieczorek 1982). K^+: ATP stoichiometry is possibly 3 (Wieczorek 1982) and the pH optimum is around 8.

1.3.4. Location of the Potassium Pump

There is much evidence for the goblet cell apical membrane as the location of electrogenic K^+ transport, dating back to the discovery of portasomes studding the cavity membrane (Anderson and Harvey 1966). Early tracer flux studies with radioactive K^+, employed to investigate the transport 'pool', indicated that only one third of the tissue K^+ was involved in transport, which is similar to the proportion of goblet cells in the epithelium (Wood and Harvey 1976; Wood and Harvey 1979). Using microelectrodes, Woods discovered that, of the two potential steps measured when a microelectrode is advanced through a midgut epithelium, only the apical potential was affected by anoxia, suggesting that the apical membrane is the site of active transport (Wood et al. 1969). Moffett et al. in 1982 obtained similar electrical profiles using microelectrodes (Moffett et al. 1982). Electron probe X-ray microanalysis was employed by Dow et al. in 1984 to determine the ionic distribution across actively transporting tissue and non-transporting tissue under anoxia (Dow et al. 1984). They found that K^+ in goblet and columnar cytoplasm was unaffected by anoxia, whereas the level dropped considerably in the goblet cavity, showing that the cavity membrane was the site of active K^+ transport. Finally, biochemical evidence has been obtained which demonstrated the presence of K^+ ATPase activity which copurified with portasome studded membranes in a membrane fractionation study (Cioffi and Wolfersberger 1983; Wieczorek et al. 1986). These portasomes have been detected on goblet cell apical membranes.

1.3.5. Function of Goblet Cells.and Electrogenic Ion Transport

Goblet cells were traditionally believed to be specialized for K^+ excretion from the blood after feeding on high K^+ diet. However, as a primary function of goblet cells this role should be demoted for the following reasons; (1) The diet is not overly rich in K^+ at 150-200mM (Florkin and Jeuniaux 1974), and as Lepidopteran larvae have evolved a haemolymph in which potassium replaces the sodium found in more primitive insects, there seems little requirement for its active excretion. (2) Some phytophagous insects do not possess goblet cells, even though they have low blood Na^+ levels similar to those of Lepidoptera. (3) The uptake of K^+ into the blood is driven by an electrochemical gradient,

which has been estimated at -15kJ mol^{-1} (Giordana et al. 1982). This gradient is generated primarily by electrogenic K^+ transport, so why drive uptake of the ionic species that is to be excreted? Also, the activity gradient for potassium is much less than the concentration gradient, as K^+ activity in the lumen of *Manduca sexta* is only 70 mM (Dow 1986). High pH causes K^+ to bind to anionic sites of luminal proteins, thus lowering the activity coefficient. (4) Possibly the strongest argument against K^+ excretion as the primary role of K^+ transport is the evolution of the goblet cavity with its tight, complex apical valve, which would only reduce the efficiency with which the gut could excrete potassium.

The electrochemical gradient, once established across the midgut epithelium, can be used by the larva in several ways: It drives the uptake of amino acids and other nutrients across columnar cell apical membranes (Giordana et al. 1985; Giordana et al. 1982; Hanozet et al. 1989; Nedergaard 1977; Sacchi et al. 1984). Amino acid flux is inhibited by anoxia and DNP (Sacchi et al. 1981), and reduced by removing K^+ *in vitro*, suggesting a K^+: amino acid cotransport mechanism (Giordana et al. 1982). K^+ is driven passively from the lumen to the haemolymph by the K^+ pump-generated electrical PD. This pump-leak system accounts for much of the observed constancy of blood and midgut cellular K^+ concentrations; however, the Malpighian tubules and cryptonephridial system are also employed for regulation of K^+ levels in the blood and gut lumen, particularly when there are changes in dietary potassium load (Dow and Harvey 1988).

The existence of a constant high luminal pH also suggests tight regulation (Dow 1984; Dow and Harvey 1988). The electrochemical gradient could be used to drive this high pH (Dow 1984).

The presence of 17mM bicarbonate and 33mM carbonate in the midgut tissues of *Manduca sexta*, whereas there are only trace amounts in the blood, suggest active transport of these components (Turbeck and Foder 1970). Bicarbonate transport is also indicated by the presence of high levels of carbonic anhydrase in the tissues, particularly around the cavities in the front two thirds of the midgut, and associated with the columnar microvilli in the posterior third (Ridgway and Moffett 1986; Turbeck and Foder 1970). Transport of carbonate into the lumen is alone

enough to generate the high pH recorded in the lumen; however, there are no known carbonate ATPases to date. Dow (1984) suggested that the goblet cavity acts as an electrically isolated membrane which is charged to a very high potential by electrogenic K^+ transport. In his model, protons are stripped from bicarbonate in the cavity and are driven across the membrane into the cytoplasm, resulting in net secretion of potassium carbonate (Fig 1.4a). The driving force for passive proton flux is the electrogenic K^+ ATPase, so the equilibrium proton distribution is calculable from the Nernst equation together with estimates of the electron motive force for the K^+ ATPase. The estimates are in the range 140-220mV which would correspond to a pH gradient of 2-4 units and therefore a luminal pH of 9-11, which is closer to the measured pH than can be predicted from bicarbonate transport alone and also explains the presence of such a cavity. It seems likely, therefore, that the primary function of electrogenic K^+ transport is to establish and maintain the high midgut luminal pH.

The advantage to the insect of having such a high pH is not clear. High pH is known to prevent tannins binding to dietary proteins and digestive enzymes in the gut lumen; however, a pH of around 8 would be sufficient (Berenbaum 1980; Martin and Martin 1983). If however tannins are costly to overcome, which is doubted by some workers (Bernays 1981), then the enormous amount of energy expended may be necessary if the larvae is to feed almost continually. The metabolic cost of high pH may be compensated by other advantages, such as, acceleration of digestive hydrolysis enabling the larva to grow faster and reducing contamination by pathogenic microorganisms (Dow 1986).

1.3.6. Potassium or Proton ATPase?

The model described above and accredited to Dow (1984) is actually an expansion of the models previously proposed by several authors (Harvey and Nedergaard 1964; Haskell et al. 1965). Until recently it was generally accepted that the pump was a unique potassium translocating ATPase; however, an alternative model for the presence of the large potential difference across goblet cell apical membranes is that proposed by Wieczorek et al. (1989), who suggest that net K^+ transport from the blood to the lumen occurs by activation of a K^+/ H^+ electroneutral exchanger located on the goblet cell apical membrane (Fig 1.4b). The exchanger is

Figure 1.4 Models for active ion transport across Lepidopteran midgut

a. Electrogenic K^+ ATPase generating high luminal pH. (Dow 1984)

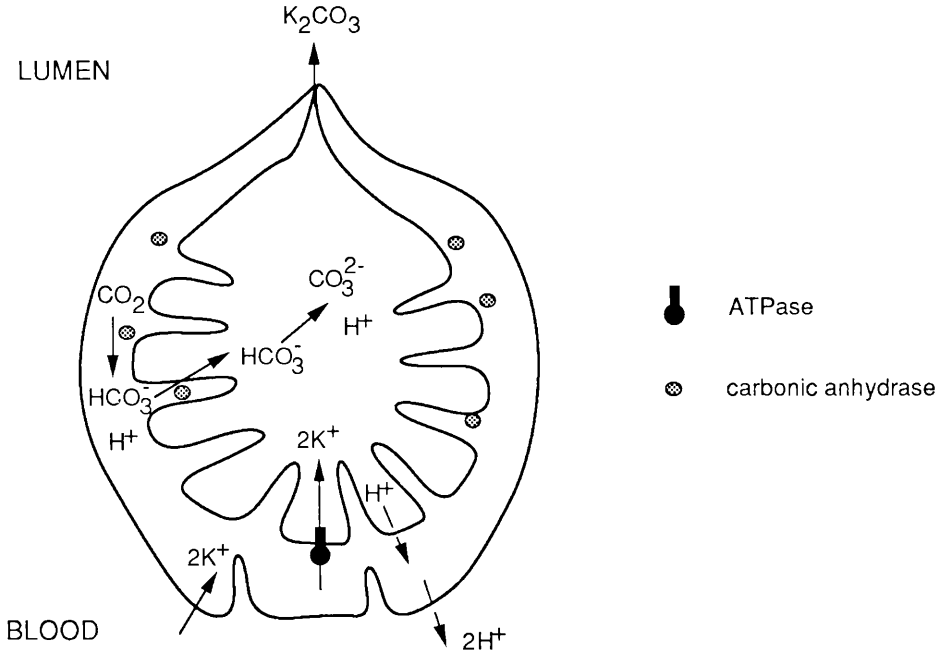

b. Electrogenic H^+ ATPase driving K^+/ H^+ electroneutral exchange. (Wieczorek et al 1989)

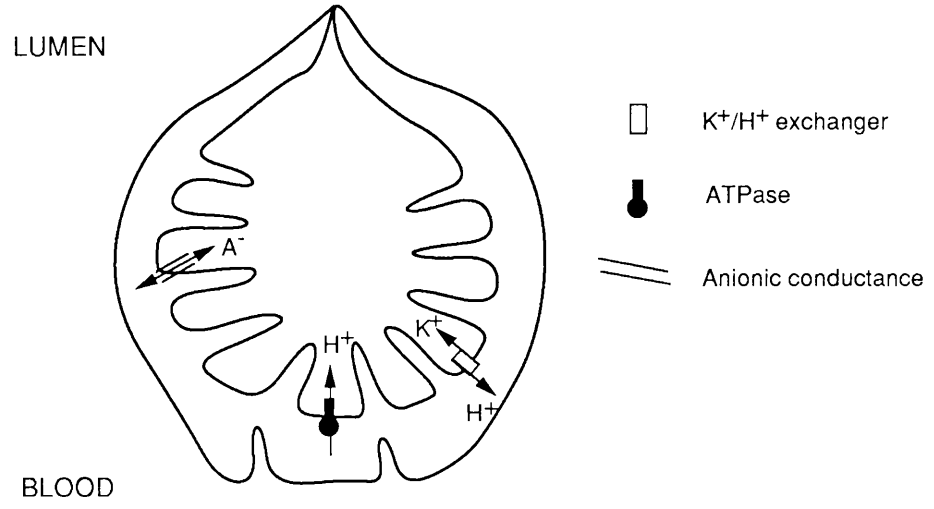

a. Electrogenic transport of K^+ polarizes the goblet cavity membrane (cavity side positive) which drives protons towards the cytoplasmic side in a Nernstian fashion. Carbonic anhydrase associated with the goblet cell apical membrane generates bicarbonate in the cavity which dissociates forming carbonate. K_2 CO_3 leaves the cavity via the apical valve resulting in high luminal pH.

b. K^+ stimulated electrogenic H^+ transport into the cavity energizes an electroneutral exchange of H^+ in the cavity for K^+ in the cytoplasm. This results in net K^+ movement from blood to lumen. The anion conductance enables mass potassium flux across the membrane which in turn determines the pH gradient.

driven by membrane potential generated from K^+-stimulated electrogenic H^+ transport through a V-type H^+ ATPase. The presence of an anionic conductance enables mass influx of K^+ which in turn causes mass efflux of H^+ thus determining the pH within the cavity. Their work was carried out on posterior midgut which is a region not thought to be involved in generation of the high luminal pH (Dow 1984), making it difficult to reconcile this model with high pH generation in anterior and middle midgut. Despite this discrepancy, the ion transport mechanism is believed to be similar in all 3 midgut regions, and evidence is emerging which indicates that the pump, whether a K^+ ATPase or an H^+ ATPase, is of the V-type and not closely homologous with F-type ATPases as was previously suggested (Harvey et al. 1983a)

1.4. Types of Ion Transport ATPase

In both prokaryotic and eukaryotic organisms, most ion-pumping ATPases that have been characterized fit into one of three structural types; P-type, V-type and F-type. Some examples of each class are given in Table 1.1 (Pedersen and Carafoli 1987a).

1.4.1. F-type ATPases

F-type ATPases (F_1F_0-ATPase) are the most complicated of the ion-motive ATPases. They consist of two moieties; F_1 is the water-soluble catalytic domain, i.e. the site of ATP synthesis/ hydrolysis. F_0 is the proton translocating domain (Pedersen and Carafoli 1987a). The main role of active ion transport by F-type ATPases is the transformation of free energy derived from the electron transport chain into the chemical form of ATP, some of which is supplied to ion-motive ATPases of the other classes (see Fig. 1.10) (Hofer 1981).

Mitochondria are the major sites of ATP production in a cell. It is here that the Tricarboxylic acid cycle (Krebs) provides the hydrogen atoms (or their equivalent in electrons) which are fed into the electron transport chain (Fig. 1.5) (Hall and Baker 1977).

Table 1.1. P-type, V-type and F-type ATPases.

The table shows the different structural types of ATPase, the ions transported and their membrane location. P-type ATPases transport a range of cations, however, V- and F-types so far have been found to transport only H^+.

ATPase	Ion	Source		Membrane
P-type:	H^+	Lower eukaryote (e.g. yeast)		plasma membrane
	H^+	Higher eukaryote	plant	p.m. *(Serrano 1984)*
		" "	animal	p.m. (bladder)
	K^+	*E. coli, S. faecalis*		Inner membrane *(Epstein 1985)*
	H^+/K^+	Higher eukaryote	animal	p.m. (gastric) *(Sachs et al. 1982)*
	Na^+/K^+	" "	"	p.m. *(Jorgensen 1982)*
	Ca^{2+}	" "	"	p.m.
	Ca^{2+}	" "	"	sarcoplasmic reticulum
	Ca^{2+}	" "	"	lysosomes, golgi
V-type:	H^+	Lower eukaryote		vacuoles
	H^+	Higher eukaryote	plant	tonoplasts *(Bowman and Bowman 1986)*
	H^+	" "	animal	lysosomes
	H^+	" "	"	endosomes
	H^+	" "	"	secretory granules
	H^+	" "	"	storage granules
	H^+	" "	"	Clathrin-coated vesicles *(Xie and Stone 1986)*
F-type:	H^+	Most bacteria		Inner *(Futai and Kanazawa 1983)*
	H^+	Eukaryotes	animal and plant	Mitochondrial inner *(Hatefi 1985)*
	H^+	"	plant	Chloroplast thylakoid

Figure 1.5. The electron transport chain.

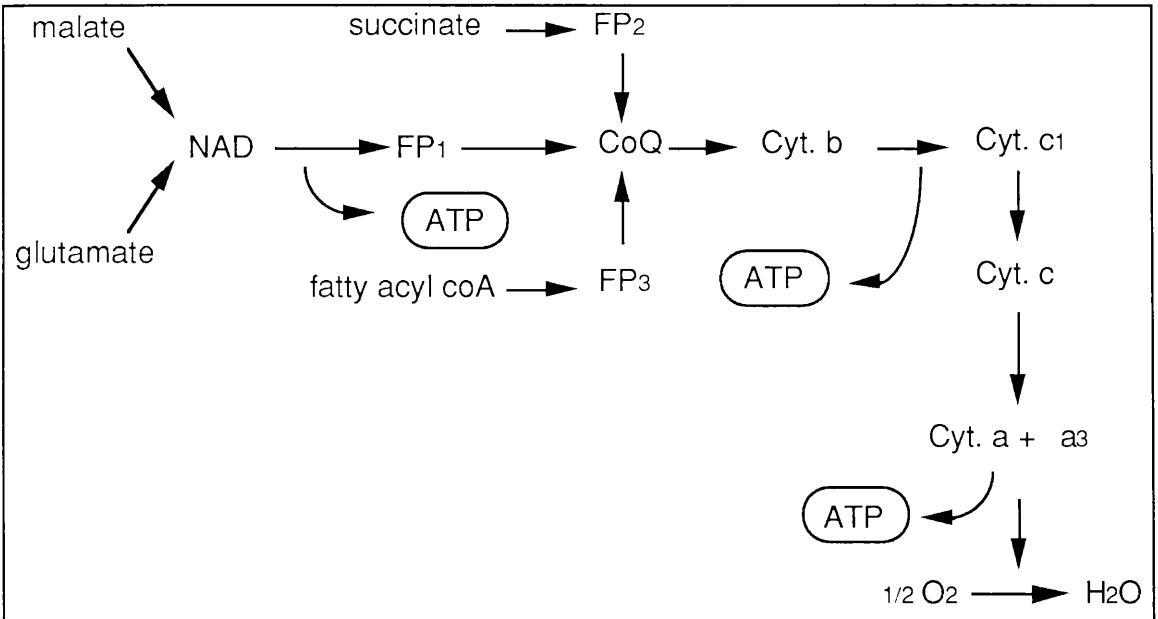

In the mitochondrial inner membrane electrons are transferred from the tricarboxylic acid cycle via cytochromes and other compounds to oxygen. Energy is produced at points along the chain in the form of ATP. NAD, nicotinamide adenine dinucleotide, FP, Flavoprotein, Co A, coenzyme A, CoQ, coenzyme Q, Cyt., cytochrome, Cyt a + a3, cytochrome oxidase.

Free energy is conserved at three sites along the chain by converting ADP to ATP by the process of oxidative phosphorylation (Hall and Baker 1977). The free energy of oxidation is stored in the form of an electrochemical gradient of protons across the membrane, which attracts protons back across into the mitochondria (Al-Awqati 1986). The Proton Motive Force (pmf) can be used directly for ATP synthesis. This is the basis for Mitchell's Chemiosmotic hypothesis summarized in figure 1.6 (Mitchell 1966).

If the pmf decreases, for example by lack of substrate for oxidative phosphorylation, then the pump will operate in reverse; protons will move out of the mitochondria and ATP will be hydrolysed. Most ion motive ATPases operate in this direction, although the F_1F_0-ATPases of mitochondria, bacteria and chloroplasts all tend to synthesize ATP (Al-Awqati 1986).

Figure 1.6. The Chemiosmotic Hypothesis.

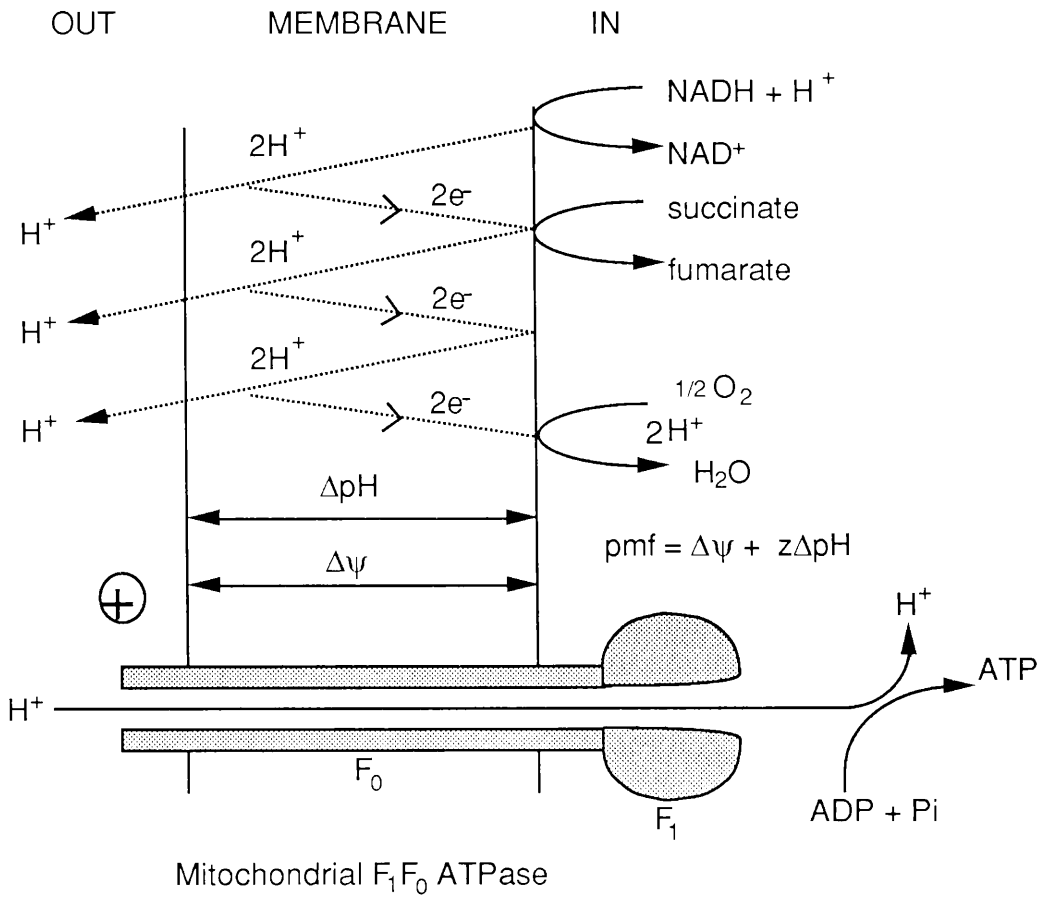

Cytochrome oxidase pumps protons across the mitochondrial inner membrane and ATP synthesis is driven by re-entry of protons through the ATP synthesizing protein complex (F_1F_0 ATPase). NAD nicotinamide adenine dinucleotide, NADH reduced form of NAD, ΔpH pH gradient across the membrane, $\Delta\psi$ membrane potential difference, pmf proton motive force.

The F_1F_0-ATPase can have between 8 and 13 different polypeptide chains, hence a molecular weight of around 450 kDa. F_1 always has five subunits with stoichiometry ($\alpha 3\ \beta 3\ \gamma\ \delta\ \varepsilon$). It has three $\alpha\beta$ pairs, one which is tagged by the three smaller subunits γ, δ and ε. A possible function of the δ and ε subunits is binding of F_1 to F_0 (Fig. 1.7).

F_0 has three different peptides; $\alpha\ \beta\ \gamma_{10}$. '$\gamma$' is the DCCD-binding protein and it may form the channel for proton translocation. In some F-type ATPases, such as bovine heart H^+ ATPase, F_0 has up to eight subunits, one of which may be the key protein in energy coupling in this ATPase (Pedersen and Carafoli 1987b).

Figure 1.7. Structure of an F-type ATPase.

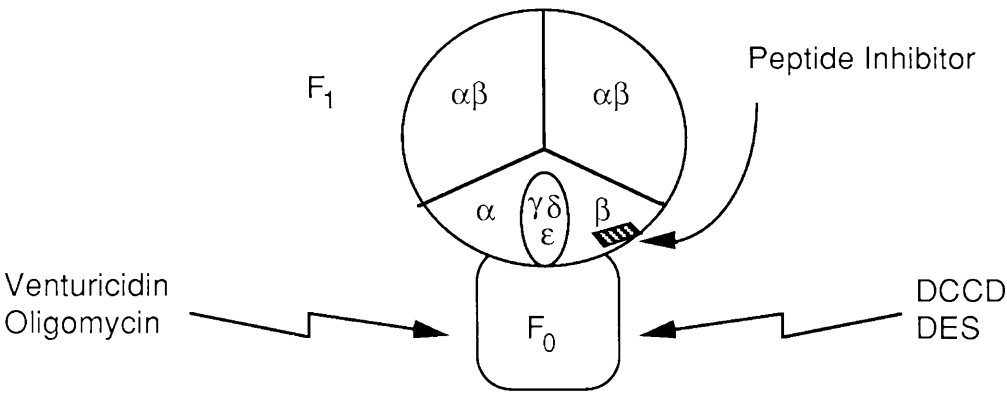

F-type ATPases are multisubunit (α,β,γ,δ,ε). The F_1 subunits constitute the catalytic portion which is responsible for providing the energy for ion transport through the translocating F_0 subunit. Peptides have been identified and characterized, and inhibitors specific to these F-type ATPases are known. DCCD dicyclohexyl carbodiimide, DES diethyl stilbestrol.

It is still not clear whether coupling between ion translocation and ATP synthesis/ hydrolysis is direct or indirect (Pedersen and Carafoli 1987b). Evidence for both P- and F-type ATPases suggests that it is an indirect coupling involving conformational changes in the enzyme. Energy coupling and transduction in F-type ATPases may be mediated by proteins, such as OSCP (Oligomycin-sensitive connecting peptide), which is a peptide connecting F_0 to F_1. Here the electrochemical proton gradient may induce conformational alterations in OSCP which are transmitted to F_1 effecting release of ATP tightly bound at αβ interfaces, which, prior to this change, is optimised by the hydrophobic nature of the catalytic site.

1.4.2. P-type ATPases

P-type ATPases are characterized by the formation of a covalent phosphorylated intermediate during the reaction cycle. They were originally termed the E_1-E_2-ATPases after the two conformational states of the enzyme during ion-translocation, however, other enzymes undergo this change without the involvement of a phosphorylated intermediate. The γ phosphate of ATP reacts with a single aspartic acid residue, which is absolutely conserved, in the α chain of the P-type ATPase. They are often distinguished from other ion-motive ATPases by their sensitivity to vanadate, which is a transition state analogue of phosphate (Pedersen and Carafoli 1987a).

Structurally, they consist of an α peptide which is about 100kDa and contains both the phosphorylation and the ATP binding sites. The Na^+/ K^+ ATPase, which is the most extensively studied P-type ATPase, also has a β peptide of about 40-60 kDa, its function unknown. It is however heavily glycosylated suggesting a role in specificity (fig. 1.8) (Rossier et al. 1987).

Figure 1.8. The Na^+/ K^+ ATPase, a P-type enzyme.

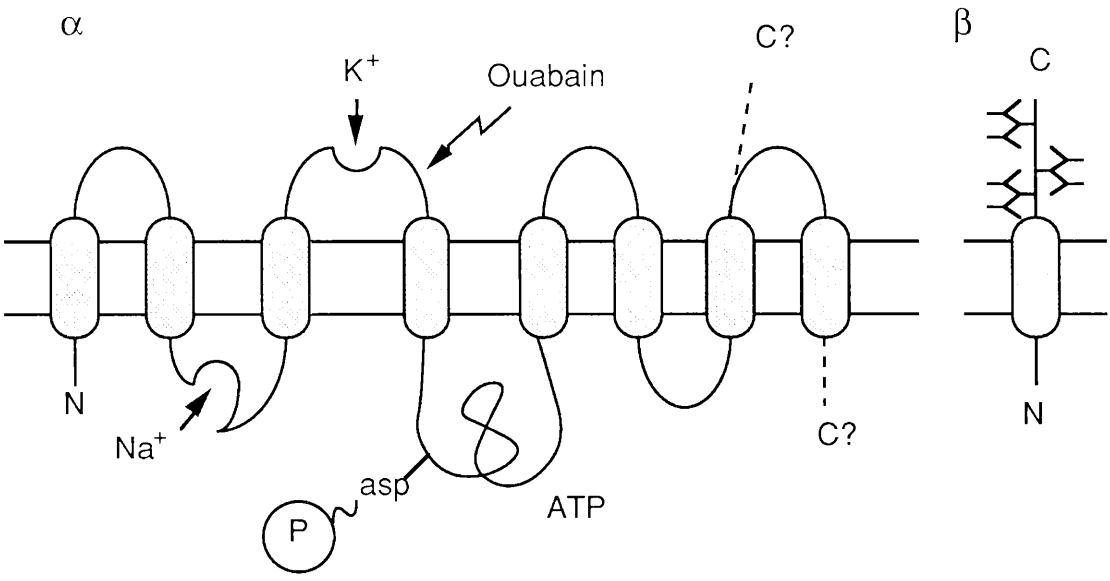

Diagrammatic representation of the structure of the Na^+ K^+ ATPase displaying membrane spanning segments and binding sites for Na^+, K^+, ouabain and ATP. Both α and β subunits are shown. The location of the C terminal of the α subunit is still unknown. Also shown is the aspartyl residue which becomes phosphorylated during the enzymic cycle.

There is a high degree of homology among the P-type ATPases; however, there must be subtle differences in amino acid sequence in order to specifically transport one type of ion. This is shown also in the different inhibitor specificity, such as ouabain for the Na^+/ K^+ ATPase (Jorgensen 1982) and DCCD (dicyclohexyl carbodiimide) and DES (diethyl stilbestrol) for the plasma membrane H^+ ATPase (Pedersen and Carafoli 1987a). In the P-type ATPase, binding of a phosphate exposes an ion binding domain and/ or pathway through the membrane. Energy coupling and transduction are transmitted through the stalk resulting in translocation of ions from a high to low affinity binding domain. Movement

of helixes in the stalk region may lower affinity for the ion which moves across to the luminal surface.

P-type ATPases have two highly conserved transmembrane segments, H-3 and H-4, which lie between the covalent phosphorylation site and the ion binding domains and may be involved in mediating ion transport. A hydrophobic microenvironment at the catalytic site optimises formation of aspartyl phosphate in P-type ATPases, in a similar manner to tight binding of ATP in F-type ATPases.

1.4.3. V-type ATPases

V-type ATPases are probably the largest class of ion-motive ATPases, but the least is known about them (Pedersen and Carafoli 1987a). They are associated with membrane-bound organelles and those described so far all translocate protons without a phosphorylated intermediate. Sites for ATP hydrolysis and proton translocation may reside on different polypeptides of this multisubunit enzyme. The subunits vary in size and number but an average M_r for a V-type ATPase is greater than 400 kDa (fig. 1.9).

Figure 1.9. Structure of a V-type ATPase.

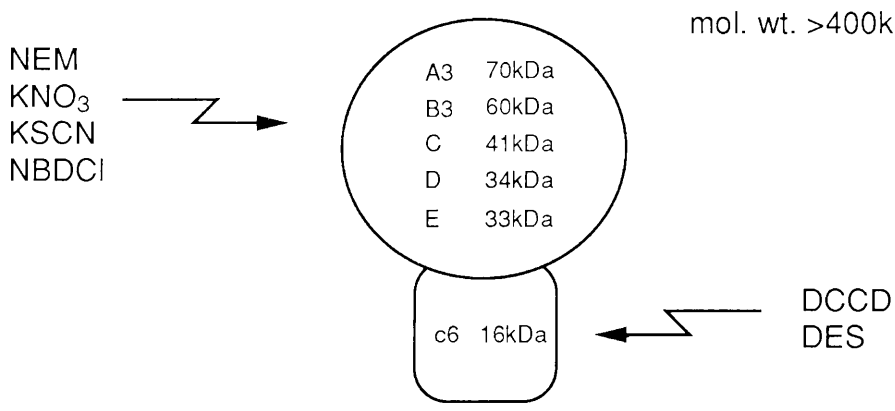

V-type ATPases are multisubunit membrane proteins which have their catalytic site on the cytoplasmic domain. Catalytic subunits are inhibited by N ethyl maleimide (NEM), nitrate (KNO_3), thiocyanate (KSCN) or chloronitrobenzooxadiazole (NBDCl). The transmembrane ionic pore is directly affected by DCCD (Dicyclohexyl carbodiimide) and DES (Diethylstilbestrol). Subunit Mr and stoichiometries are shown.

This group of ATPases is distinguished from the other two by its inhibitor specificity; DCCD, DES, NBDCl (Nitrobenzodiazole chloride), NEM,

KNO_3, KSCN, and more recently bafilomycin A_1 (Bowman et al. 1988), are inhibitors of vacuolar ATPases. They are insensitive to other ATPase inhibitors, vanadate, ouabain (P-type), azide and oligomycin (F-type) (Pedersen and Carafoli 1987a). V-type ATPases are involved in uptake of amino acids and amines into granules, e.g. catecholamine uptake associated with H^+ ATPase in chromaffin granules. They are also critical for receptor recycling as they lower the pH in endocytic vesicles which promotes ligand-receptor dissociation.

The ATP synthesized by F_1F_0 ATPases is hydrolysed by the both P- and V- type ATPases during ion translocation (Fig. 1.10).

Figure 1.10. Interaction between P-, V- and F-ATPases.

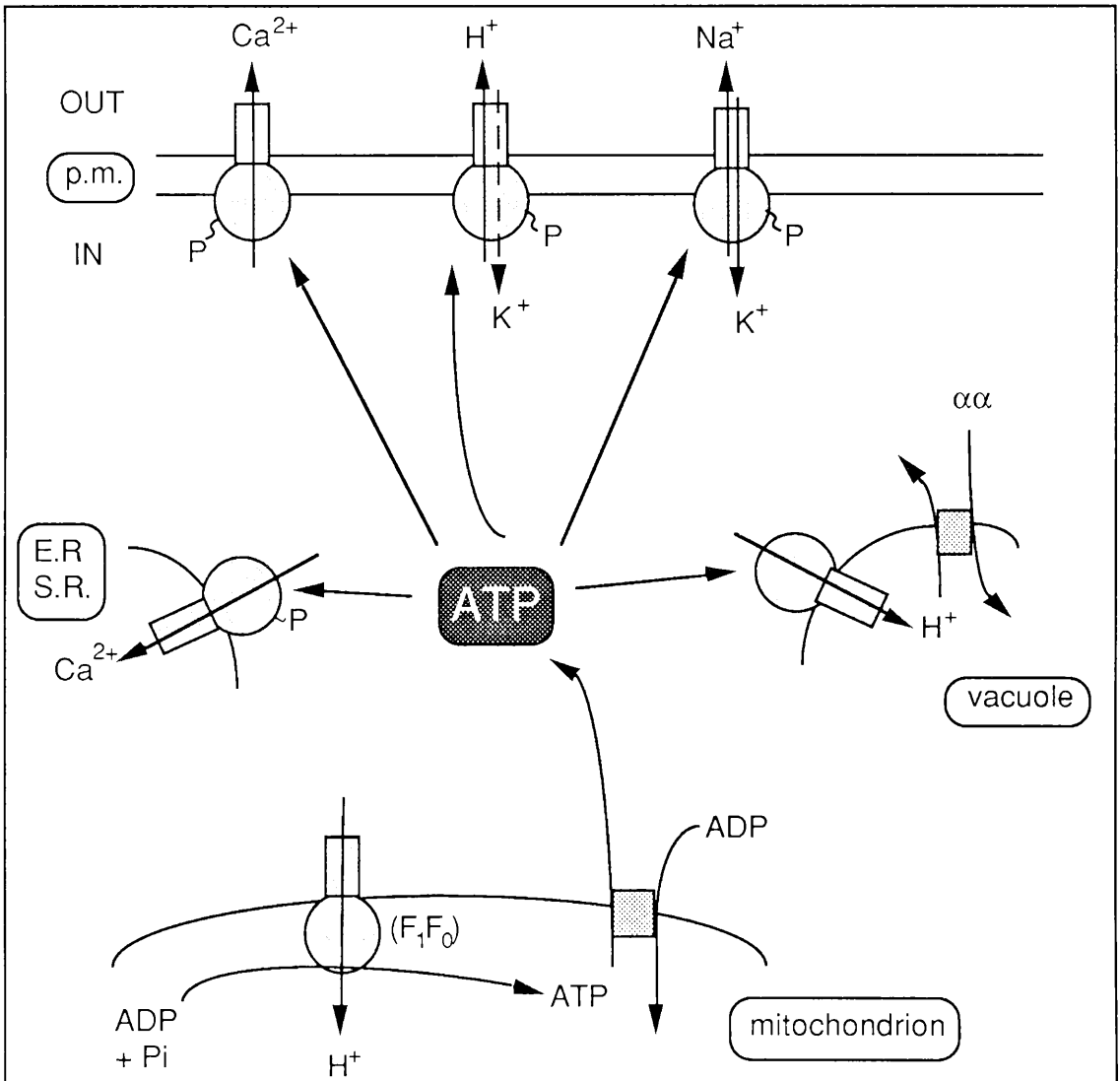

F- type ATPases work in a cell mainly to produce ATP which can then be used by ATPases of the other 2 classes as illustrated in this hypothetical model.

1.4.4. Sequence Homology between ATPase Types

Although sequence homology is negligible between F and P-type ATPases, there is a short sequence which contains the phosphorylation region in P-type ATPase that is also found in F-type (Fig. 1.11) (Pedersen and Carafoli 1987b).

Figure 1.11. Amino acid sequence homology of P- and F-type ATPases.

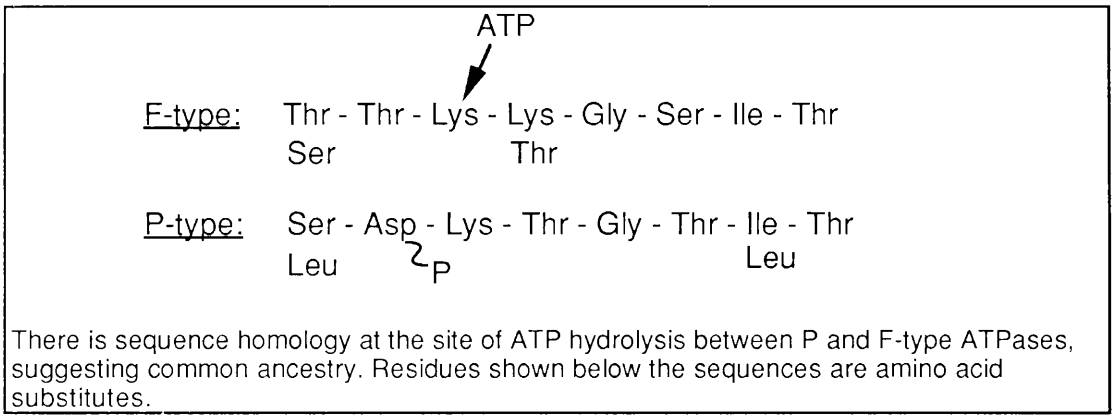

There is sequence homology at the site of ATP hydrolysis between P and F-type ATPases, suggesting common ancestry. Residues shown below the sequences are amino acid substitutes.

If the threonine which replaces the aspartic acid in F-type sequence could be mutated to an aspartic acid, then it would be interesting to see if the F-type now had a phosphoenzyme intermediate. The implication being that perhaps common regions in the different classes of ATPase are involved in energy coupling, maybe even evolution from a common gene.

Some workers (Mandel et al. 1988) have isolated and cloned the gene coding for the DCCD-binding protein from the vacuolar H^+ ATPase. They found amino acid sequence homology with vacuolar proteolipid and with the proteolipid of F_1F_0 (eubacterial-type) H^+ ATPase, as well as plant and yeast F-ATPases. This suggests that the proteolipids of the vacuolar H^+ ATPases were evolved in parallel with the eubacterial proteolipid from a common ancestral gene that underwent gene duplication (Fig. 1.12).

Figure 1.12. Evolution of proteolipids of eubacterial and vacuolar ATPases.

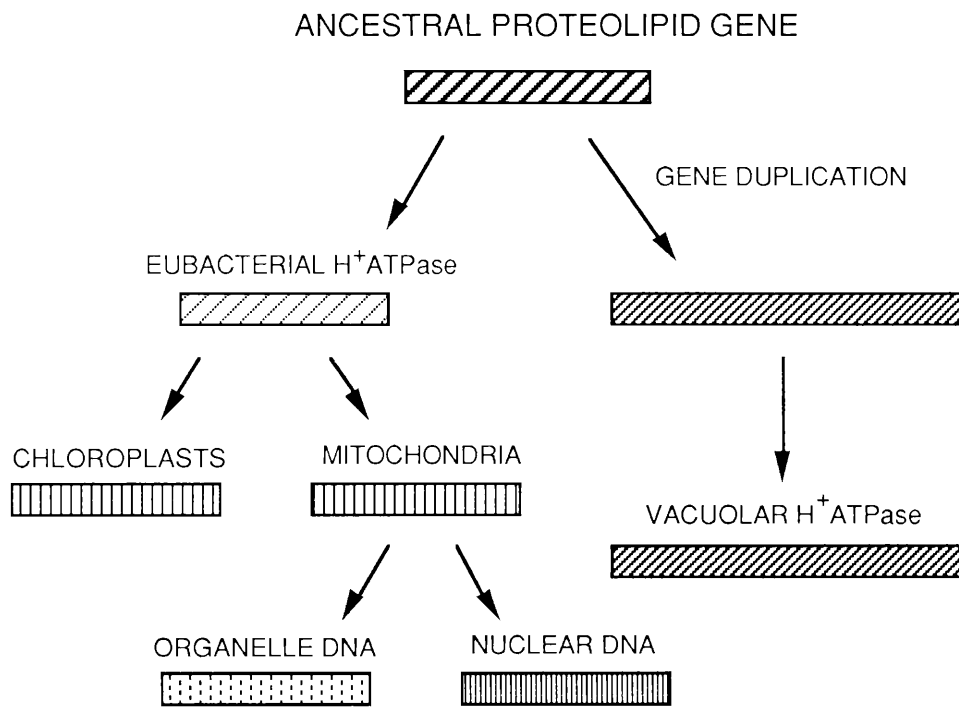

Possible ancestry of vacuolar and F-type ATPases showing an early split in the coding genes. The split between P-, F- and V-type ATPases may have occured even earlier.

The split between the F- and V-type ATPases is an ancient event, preceding the appearance of eukaryotes (Nelson and Taiz 1989). The split between P-, F- and V-type ATPase (assuming they had a common precursor) occurred even earlier.

1.4.5. The Midgut K^+ Pump is a V-type ATPase

The electrogenic K^+ ATPase of insect epithelia has been compared to the F_1F_0 ATPase of mitochondria, working in reverse as an ATPase, as it has similar structure, thermodynamics and stoichiometry, with two K^+ translocated for every one Mg ATP^{2-} (Harvey et al. 1983a; Harvey et al. 1983b). Figure 1.13 shows this chemiosmotic model, although it has now been superseded and should therefore be regarded as historical interest only.

The pump is not an H^+/ K^+ antiport ATPase of the type found in gastric mucosa (Rabon et al. 1983), as this would have the wrong sidedness, pumping K^+ into the blood and H^+ out. It has also been described as a type 5 pump by Keynes (Keynes 1969). There is now evidence that it could be a V-type ATPase (Schweikl et al. 1989). If so, it would be the first discovered that transported an ion other than H^+, although protons have been suggested as the ion of active transport (Klein et al. 1988; Wieczorek, et al. 1989). One of the subunits has been identified as having a mass of 69kDa, similar in size to one of the catalytic subunits of characterised V-type ATPases, and is probably also a catalytic subunit (Schweikl et al. 1989).

As the pump is located on the goblet cavity membrane, then the origin of the cavity itself could indicate the class to which this ATPase belongs. For instance, it has been described as an invagination of the goblet cell apical membrane (Cioffi 1979), which would indicate the pump is a P-type ATPase. Alternatively, the cavity could have evolved from fusion of an intracellular vesicle with the apical membrane (Hakim et al. 1986), which is the generally accepted model, suggesting a V-type ATPase. All V-type ATPases so far described translocate protons and a model for proton transport across the cavity membrane has been proposed which fits this requirement (Fig 1.4b) (Wieczorek et al. 1989). (For details see section 1.3.6)

In order to categorize the midgut and other ion transport ATPases, a more detailed understanding of the mechanisms of energy coupling is required, although this has been reviewed with respect to insect epithelial K^+ pumps (Harvey et al. 1983a). Further amino acid sequencing of the protein subunits would reveal the evolutionary origin of these ion-motive ATPases, which in turn may provide the solution to the K^+ / H^+ controversy.

Figure 1.13. Chemiosmotic K^+ pump of insect ion transporting membranes.

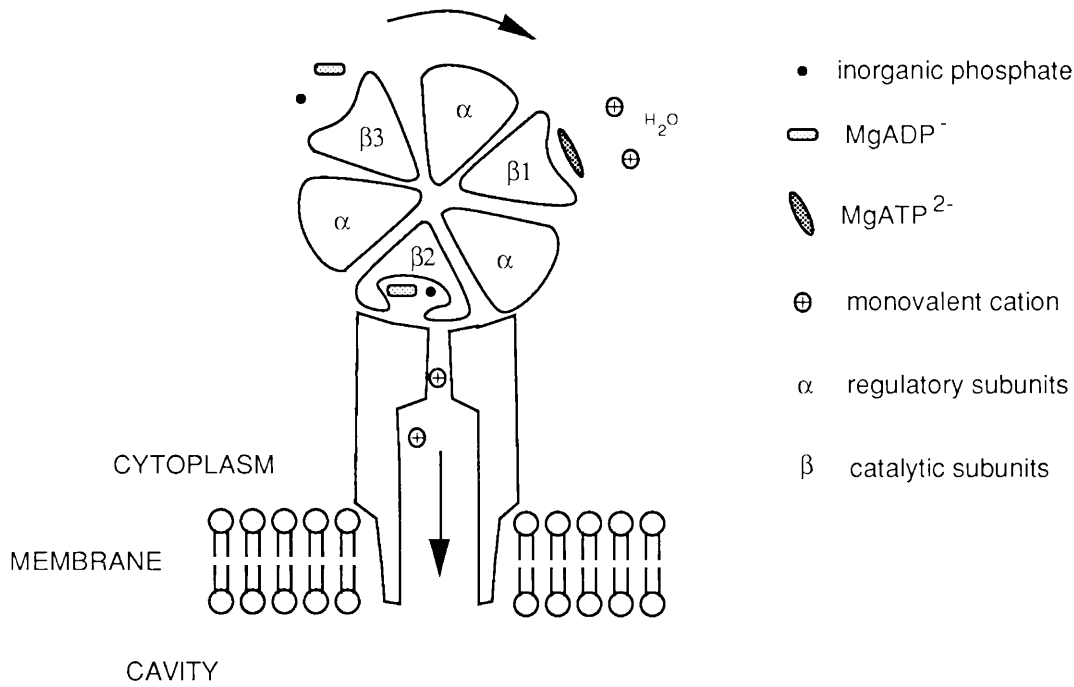

This historical model taken from Harvey et al. (1983), shows the possible mechanism by which monovalent cations (K^+) are translocated across the midgut goblet cell apical membrane and into the cavity following ATP hydrolysis. Within the catalytic domain are regulatory and catalytic subunits which regulate ion transport; $2K^+$ cross the membrane for every 1 ATP molecule that is hydrolysed.

1.5. Aims

The main aims of this study, combining the techniques of electrophysiology, transport physiology, membrane biochemistry and cell biology, were;

1. To identify the alkali-pumping site in *Manduca sexta* larvae.
2. To understand the function of the insect goblet cell.
3. To elucidate the mechanisms of K^+ and other ion transport across *Manduca sexta* midgut.
4. To isolate, separate and culture the cell types from the midgut.
5. To obtain a physiologically relevant *in vitro* assay system for the potential application of screening insecticides and other pharmacologically active agents.

Chapter 2

2. Chapter 2 MATERIALS AND METHODS

2.1. Obtaining and Rearing Larvae

3rd instar *Manduca sexta* larvae were obtained from the Department of Zoology at the University of Cambridge. They were reared on an artificial diet based on that of Yamamoto 1969 (Yamamoto 1969) (Table 2.1). Eggs of *Manduca sexta* were kindly donated by Dr. Stuart Reynolds at Bath University. They were hatched in a chamber containing artificial diet and a climbing frame which allowed new 1st instar larvae to avoid drowning during non-feeding periods. All larvae were maintained in a Scotlab-VSL incubator at 25°C, ambient humidity and with a 16h:8h light dark photoperiod. Except where otherwise stated, feeding 5th instar larvae weighing 4-6g were used in all experiments.

Table 2.1. Composition of artificial diet for *Manduca sexta* larvae.

Ingredients	
Wheatgerm	150g
Casein (BDH)	70g
Sucrose	60g
Dried baker's yeast	30g
Wesson's salt mix (ICN)	20g
Cholesterol (SIGMA)	4g
Sorbic acid (SIGMA)	3g
Choline chloride (SIGMA)	2g
Methyl hydroxybenzoate (SIGMA)	2g
Boiling distilled H_2O	700ml
Agar (DIFCO)	40g
Distilled H_2O	1000ml
Linseed oil	4ml
Corn oil	4ml
10% formaldehyde	8ml
Ascorbic acid (SIGMA)	8g
Vanderzant vitamin mixture (ICN)	0.2g
Chlortetracycline (SIGMA)	0.2g

2.2. Physiological Salines

Physiological saline used in many experiments, was modified from that used by Cioffi and Harvey (1981) which was based on the ionic composition of *Manduca sexta* larval haemolymph (Cioffi and Harvey 1981; Florkin and Jeuniaux 1974). Certain metabolic substrates were added after stimulatory properties had been reported (Chamberlin 1989; Dow and O'Donnell 1990). For convenience it was termed *Manduca* saline. The constituents of this saline were further modified to suit experimental conditions, as seen in table 2.2.

Table 2.2 *Manduca* saline composition and modifications

(values given in mM except where otherwise stated. mOsmol l^{-1} is the calculated osmolality)

Constituents	Standard	Divalent-free	K-free	TRIS-free
Sucrose	200	200	200	200
Glucose	5	5	5	5
Succinic acid	5	5	5	5
Caproic acid	5	5	5	5
KCl	22	22	-	22
Choline Chloride	-	-	22	-
$CaCl_2$	1	-	1	1
$MgCl_2$	1	-	1	1
TRIS	5	5	to pH 6.7	-
$NaHCO_3$	-	-	-	10
EDTA	-	5	-	-
KOH/HCl	to pH 6.7	to pH 6.7	-	to pH 6.7
mOsmol l^{-1}	290	290	275	290

2.3. Culture Media

Two types of media were used, Grace's insect tissue culture medium and TC100 medium (GIBCO). These were also based on haemolymph composition but contained components necessary for longer term maintenance of insect cells and tissues (Grace 1962). Media composition is detailed in table 2.3. In addition to the listed components, both types of media were supplemented with 10% heat-inactivated foetal calf serum (FCS) (GIBCO), 50µg ml^{-1} gentamicin (Sigma), 2.15µg ml^{-1} amphotericin

Table 2.3. Composition of Insect Tissue Culture Media

	GRACE'S		TC100	
	mg ml^{-1}	mM	mg ml^{-1}	mM
Ions:				
$CaCl_2$	750	6.8	-	-
$CaCl_2.H_2O$	-	-	1320	8.9
KCl	4100	55	2870	36
$MgCl_2.6H_2O$	2280	11.2	-	-
$MgCl_2$	-	-	2280	11.2
$MgSO_4.7H_2O$	2780	11.3	-	-
$MgSO_4$	-	-	2780	11.3
$NaHCO_3$	350	4.2	350	4.2
$NaH_2PO_4.H_2O$	1013	10.9	1140	12.4
Other:				
α-ketoglutaric acid	370	2.8	-	-
Fructose	400	2.2	-	-
Fumaric acid	55	0.5	-	-
Glucose	700	3.9	1000	5.6
Malic acid	670	5	-	-
Succinic acid	60	0.5	-	-
Sucrose	26680	77.9	-	-
Bactotryptose Broth	-	-	2600	?
Amino acids:				
β-alanine	200	2.3	-	-
L-alanine	225	2.5	225	2.5
L-arginine HCl	700	3.3	-	-
L-arginine	-	-	550	3.2
L-asparigine	350	2.7	350	2.7
L-aspartic acid	350	2.6	350	2.6
L-cysteine	22	0.1	22	0.1
L-glutamic acid	600	4.1	600	4.1
L-glutamine	600	4.1	600	4.1
Glycine	650	8.7	650	8.7
L-histidine	2500	16.1	-	-
L-histidine mono HCl	-	-	3380	17.7
L-isoleucine	50	0.4	50	0.4
L-lysine HCl	625	3.4	625	3.4
L-methionine	50	0.4	50	0.4
L-phenylalanine	150	0.9	150	0.9
L-proline	350	3	350	3
DL-serine	1100	10.5	-	-
L-serine	-	-	550	5.2
L-threonine	175	1.5	175	1.5
L-leucine	75	0.6	75	0.6
L-tryptophan	100	0.5	100	0.5
L-tyrosine	50	0.3	50	0.3
L-valine	100	0.9	100	0.9
Vitamins:				
Biotin	0.01		0.01	
D-Ca pantothenate	0.02		0.11	
Choline chloride	0.2		-	
Cyanocobalamin	-		0.01	
Folic acid	0.02		0.02	
i-inositol	0.02		0.02	
Niacin	0.02		0.02	
Para-amino benzoic acid	0.02		0.02	
Pyroxidine HCl	0.02		0.02	
Riboflavin	0.02		0.02	
Thiamine HCl	0.02		0.02	

B (Sigma), 0.35 μg ml^{-1} sodium bicarbonate (BDH) and 5 drops of phenyl red indicator (Sigma). Bactotryptose broth, which is included in the TC100 composition, contains; 0.5mg ml^{-1} thiamine HCl, 2g ml^{-1} bacto-tryptose, 500mg ml^{-1} NaCl and 100mg ml^{-1} bacto-dextrose.

The calculated osmolalities for these media are; 378 mOsmol l^{-1} for Grace's medium and 270 mOsmol l^{-1} for TC100 medium. Osmolality was also measured directly using a Wescor 5500 vapour pressure osmometer. Grace's medium was found to be 386mOsmol l^{-1} and TC100 was 250mOsmol l^{-1}, which was consistent with the calculated values. Some of the macromolecules present in bactotryptose broth may have been removed during filter sterilization which could explain the lower measured osmolality for TC100.

2.4. Dissection

Larvae were cold anaesthetized in crushed ice for 30 min before dissection. This numbs the animal and prevents contraction of the muscles underlying the midgut once isolated. For experiments requiring sterility, the larvae were surface sterilized with 70% ethanol before dissection. Cross-sectional cuts were made between segments 2 and 3 and between segments 8 and 9 of the larva, which is equivalent to approximately 1 cm from the head and tail respectively, in a 5g 5th instar. A blunt ended probe was inserted longitudinally through the centre of the midgut lumen. The body wall was carefully dissected away leaving the midgut intact around the probe. Sometimes this midgut tube was used without further dissection, for instance in the enzyme dissociation assay, but if a flat sheet or a specific region were required, the midgut was simply cut to suit. The dissection was similar to that described by Cioffi and Harvey (Cioffi and Harvey 1981).

2.5. Construction of Sylgard Chambers

Sylgard 184 silicon elastomer was obtained from Dow Corning. This syrup-like compound sets as a clear rubber when mixed 9 + 1 with 184 curing agent and cured overnight at 60°C. By building walls of Silicon rubber (RS components) around the perimeter of a glass slide, the

elastomer can be poured in before curing, giving a flat clear surface for pinning out sections of gut. Chambers of this type were used in a number of experiments, ranging from cell isolation to visually guided microelectrode impalement of specific cellular compartments. For the latter, some modifications were made to the design of the chamber to allow perfusion of the midgut and measurement of transepithelial potential, (see section 2.7.5).

2.6. Ussing-type Chamber set-up

For measurement of short circuit current (SCC) and open circuit voltage (which is equivalent to transepithelial potential, TEP), a chamber designed by, and described in, Dow et al. 1985 was used (Figure 2.1) (Dow et al. 1985). It was essentially a modification of the chamber designed by Ussing and Zerahn for measurement of ion transport in frog skin (Ussing and Zerahn 1951). A flat piece of midgut epithelium was secured to an aperture which exposed 0.5 cm^2 of the tissue. This was inserted into the chamber using a "lollipop" -like holder. The set-up allowed separate and continual perfusion of basal and apical sides of the midgut with oxygenated saline, whilst current and voltage electrodes, wired to a home-made voltage clamp unit, measured short-circuit current and transepithelial potential, respectively. Short circuit is similar in principle to voltage clamping. The short circuited tissue is supplied, from a high gain differential amplifier, with sufficient current to maintain the transepithelial potential at 0mV. The magnitude of the current required can be recorded and except for brief capacitative transients, all current is ionic, therefore only actively transported ions moving across the tissue will be detected. The net flux of these charged species can be measured precisely by the short-circuit current. Because of the low resistivity of the tissue (100 Ωcm^2 (Wood and Moreton 1978)), three voltage electrodes were arranged to compensate for the resistivity of the saline during short-circuit. Each chamber half had a volume of 3ml, and along with rapid gas lift circulation, this allowed any additions to mix quickly and uniformly with the bathing solution. SCC and TEP were recorded on a Goertz Servoscribe chart recorder.

Figure 2.1 Short circuit chamber for midgut tissue.

Front-view, plan, end view and perspective sketch. The 'lollipop' has an aperture over which a section of midgut can be mounted. The voltage sensing electrodes (A,B,C), current electrodes (D,E) and gas inlet pipes (F,G) are labelled. This chamber can also measure open circuit voltage across a midgut (transepithelial potential). Figure taken from Dow et al. (1985.)

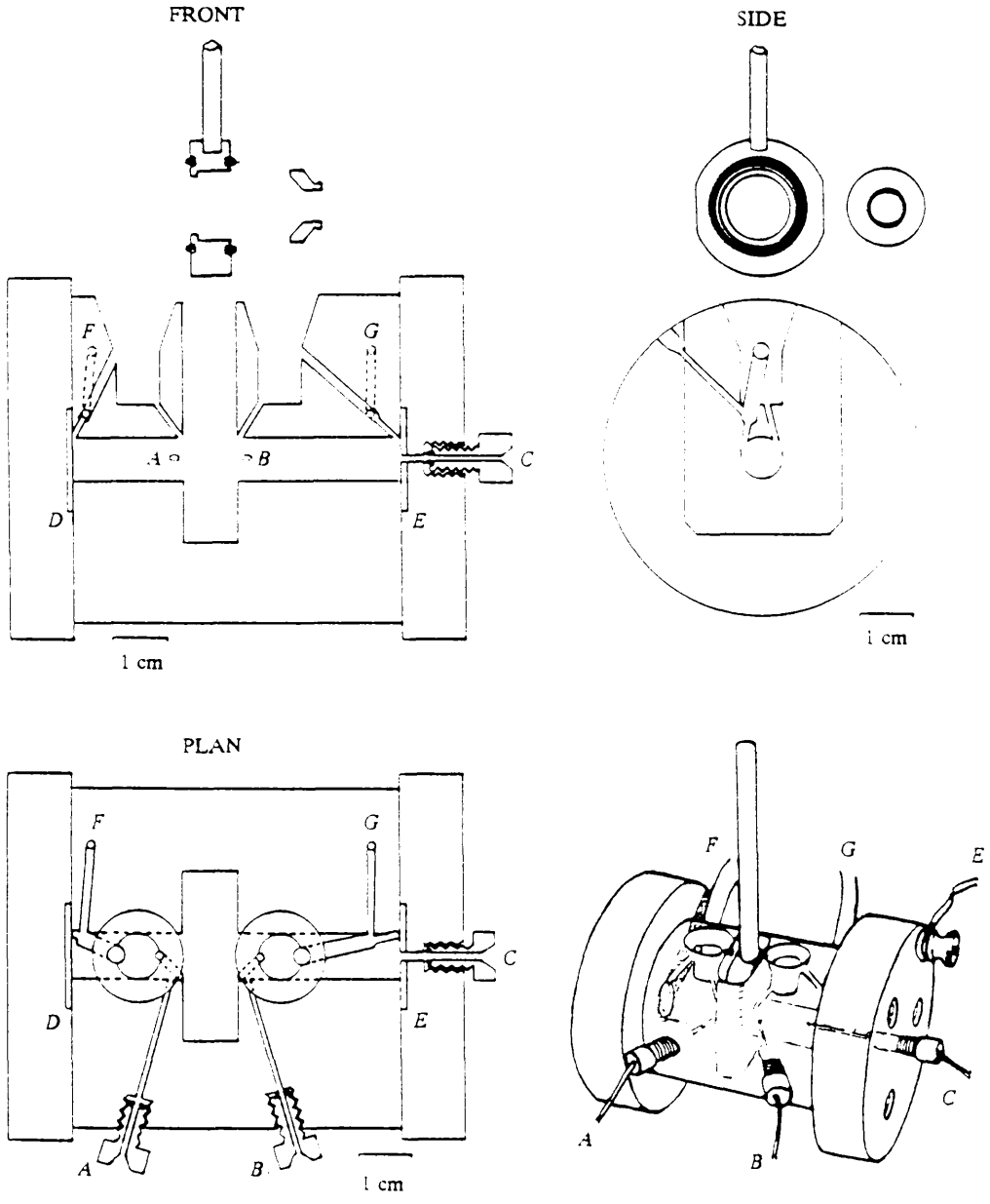

2.7. Microelectrode Methods

2.7.1. Microelectrodes

Microelectrodes were pulled from borosilicate glass (Clark GC100TF-10) using a Campden Instruments microelectrode puller. Electrodes were back-filled with Lucifer Yellow CH (5 mg ml^{-1} in 1% LiCl) to yield final resistances of approximately 100 MΩ. Microelectrodes were inserted into holders containing Ag/ AgCl half-cells, and fitted to an electronic Leitz micromanipulator.

2.7.2. Electrical Equipment for Microelectrode Recording.

The amplifier system was made in the Zoology Department at Cambridge, with facilities for bridge balancing, current injection and resistance measurement (Figure 2.2). It was connected to a Gould 20 MHz digital storage oscilloscope (OS 1420) which displayed the resting potentials of impalement sites. All potentials were measured relative to the apical side *via* an earthed Ag/AgCl wire immersed in the bathing solution. The electrode resistance was electrically nulled before an impalement by manipulating the stimulus balance while passing depolarizing and hyperpolarizing currents alternately, until there was no trace deflection when a current was passed. This meant that when current was injected into a cell, any deflection of the scope trace reflected a change in the cell membrane potential only.

2.7.3. Chloridizing Silver Wires

To measure voltages across membranes in solution, a piece of metal (or conductive material) must be on either side. Bare metal does not give stable recordings. By electrolytically depositing a film of grey AgCl onto a bright silver electrode an extremely good reference electrode was obtained. This was done by immersing silver wires, cleared of grease using acetone, in a 0.1M HCl solution, then repeatedly passing current first one way and then the other (figure 2.3).

2.7.4. Transepithelial Recording of Potential Difference

Midgut transepithelial electrical potential differences (TEPs) were measured with a pair of Ag/ AgCl wires on either side of the epithelium,

Figure 2.2 Electrical equipment required for microelectrode recording

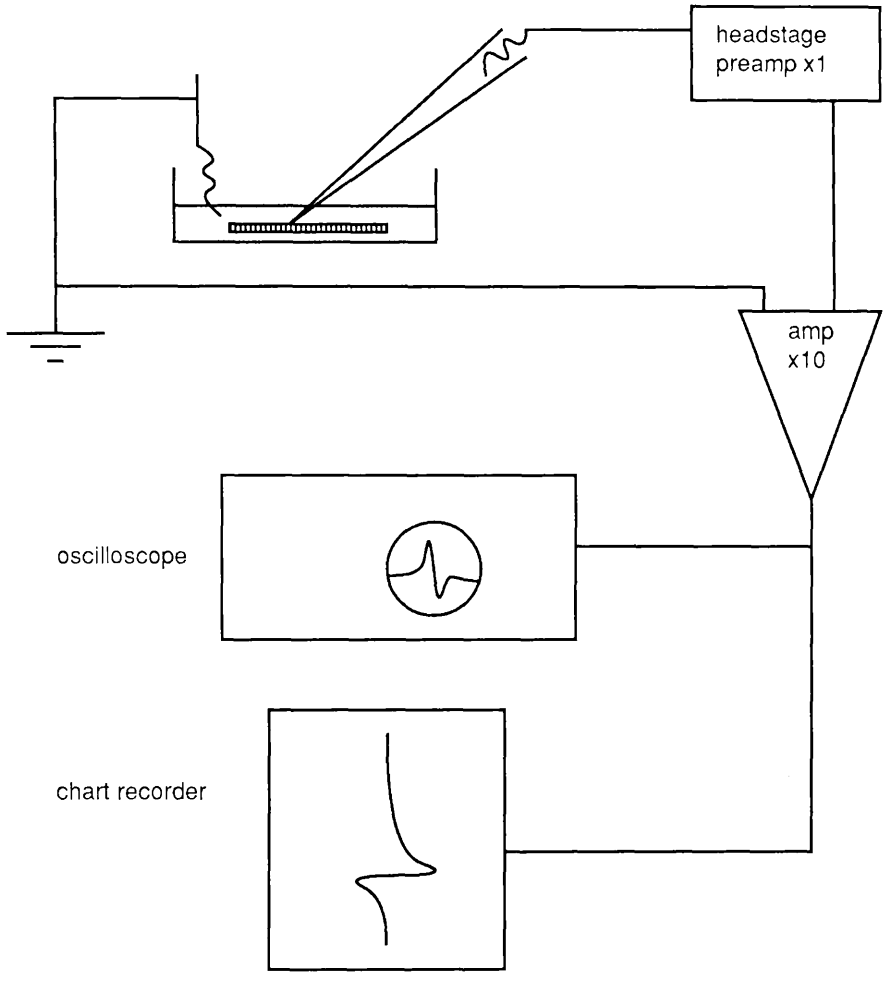

A glass microelectrode is used to make impalements in an earthed chamber. The earth wire also acts as an apical reference for recordings. The electrode has a conductive Ag/AgCl pellet and this is connected to an amplifier via a preamplifier which filters out noise. The amplifier, which has a 10x gain, carries the signal from the impalement to both an oscilloscope and a chart recorder, where voltage deflections can be stored and measured.

Figure 2.3 Chloridizing silver wires

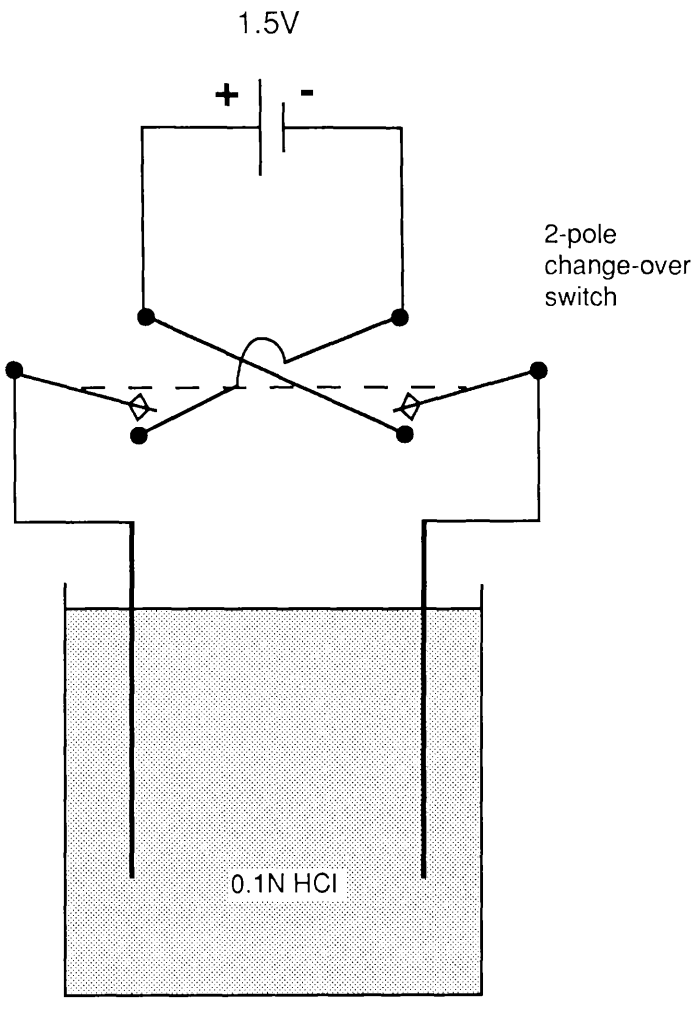

Anode reaction: $H^+_{(aq)} + e^- \rightarrow \frac{1}{2} H_{2\,(g)}$

Cathode reaction: $Ag_{(s)} + Cl^-_{(aq)} \rightarrow AgCl_{(s)} + e^-$

Silver wires immersed in 0.1 N HCl are connected to a 1.5V battery source via a 2-pole change-over switch. The switch allows current to pass alternately in both directions. AgCl is deposited on the cathode whilst hydrogen gas is produced at the anode.

connected to a Beckman 3050 voltmeter and/ or a chart recorder. Potentials typically varied between 120 and 20mV during an experiment.

2.7.5. Perfusion

A perfusion system was designed to provide isolated stretched midguts with oxygenated saline, and allow simultaneous measurement of transepithelial potential and membrane potential difference (Figures 2.4 and 2.5). The flat midgut sheet was mounted, haemolymph-side down, on the perfusion chamber which was made from Sylgard 184 elastomer (Dow Corning), as described in section 2.5. Polythene tubing was cast into the chamber and connected to gravity sources of oxygenated *Manduca* saline (standard, Table 2.2), which independently perfused the basal and apical sides of the tissue. Perfusate was removed with a vacuum line.

2.7.6. Tissue

The tissue was viewed under bright field or epifluorescence optics on a Leitz Ortholux microscope, through a 25x water immersion objective; the barrel of which was lacquer coated to prevent earth loops. This configuration allowed the live epithelium to be viewed in considerable detail and the electrode to be advanced into identified, preselected sites.

The middle midgut was used in all experiments because (i) although it has not been as thoroughly studied as the posterior midgut, it is believed to be involved in generating the high pH found in the alimentary canal (Dow 1984); and (ii) it is the least folded region of the midgut (Cioffi 1979) and therefore the most transparent for microscopy, especially the area directly above the longitudinal muscles.

2.7.7. Iontophoresis

Iontophoresis was used to eject charged fluorescent molecules from the pipette by applying positive or negative going current, depending on the charge polarity of the molecule. Blockage of the pipette tip can and did occur, but was temporarily relieved by reversing the polarity of the current for a short time. The capacity compensation control on the amplifier allowed brief over compensation which effectively sent the system into

Figure 2.4 System for perfusion of midgut with oxygenated saline

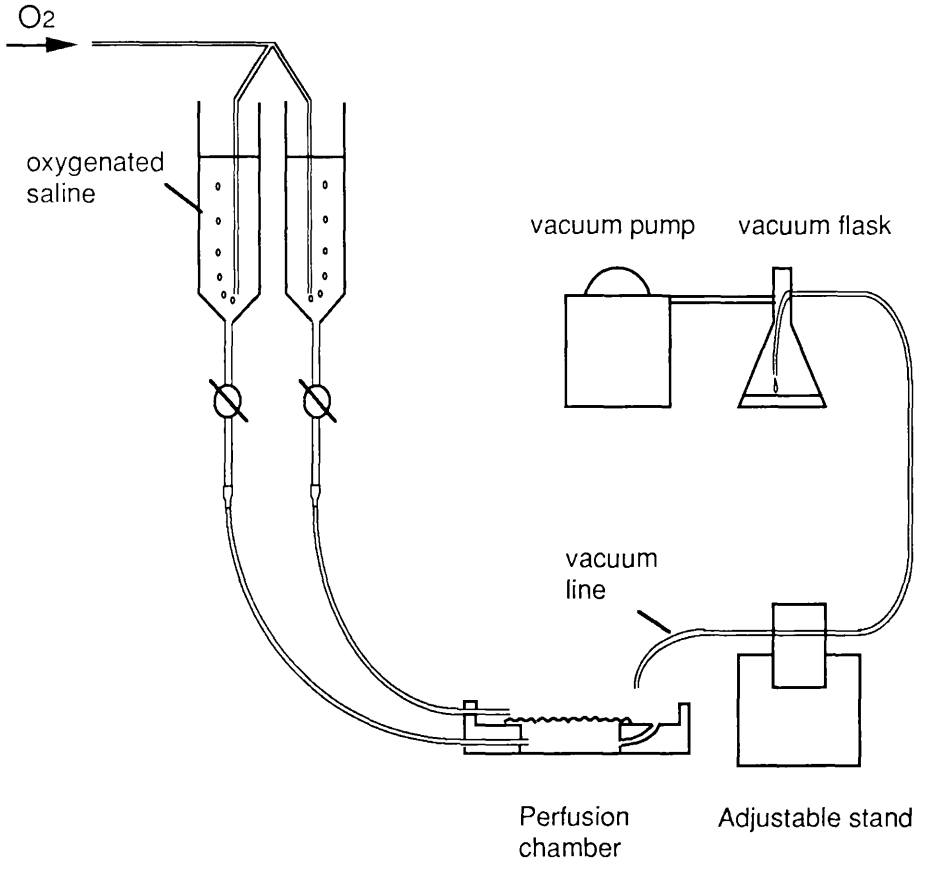

Manduca saline was oxygenated in burettes before allowing controlled gravity perfusion of the isolated midgut via polythene tubing. The tubing was cast into the chamber so that basal and apical sides of the tissue could be simultaneously perfused. Waste perfusate was removed via a vacuum line.

Figure 2.5 Perfusion chamber for microelectrode impalements

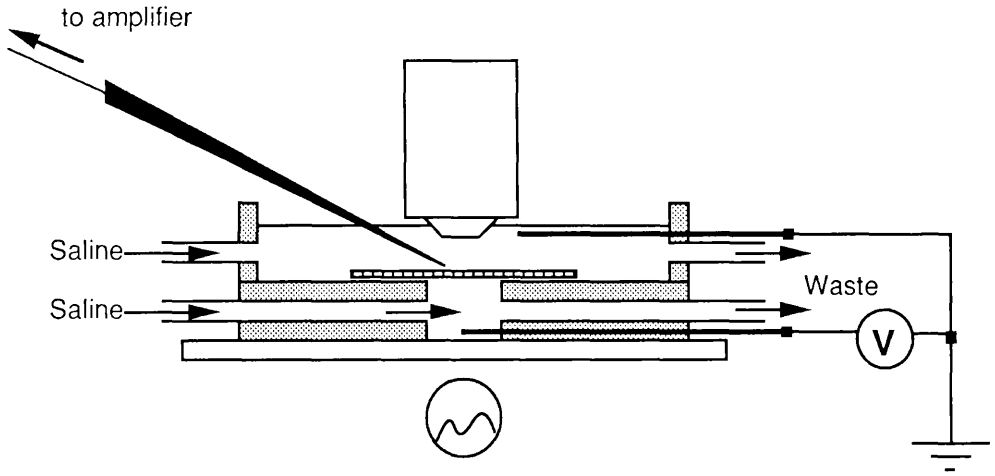

The chamber, made from sylgard elastomer, allows a midgut to be pinned out as a flat sheet over a gap through which oxygenated saline is passed. Under perfusion of both the basal and apical sides of the epithelium, the microelectrode is visually guided into a compartment. The tissue is illuminated from below. The transepithelial potential is measured simultaneously with membrane potential, using Ag/AgCl electrodes, which are placed on either side of the midgut and are connected to a voltmeter. The apical Ag/AgCl electrode is earthed to provide an apical reference for intracellular recordings.

oscillation. This physically vibrates the tip clearing away any air bubbles or debris.

Hyperpolarizing current injection was carried out after intracellular recording had been made so avoiding the effects of iontophoresis on membrane potential. Lucifer Yellow CH (M_r 457) was used most frequently for marking impalement sites (Warner and Bate 1987). It diffused rapidly between cells via gap junctions, although it can form an insoluble precipitate with potassium and had to be dissolved in 1% LiCl. 6 carboxy fluorescein (Mr 332) was also used for injection as it had the advantage that it was not precipitated by high potassium levels (Warner and Bate 1987).

The injection site could readily be identified by its morphology without fixation or other intervention, allowing recordings to be made from many sites in a single preparation. To determine whether the observed slow loss of fluorescence from a goblet cavity was due to a gradual photobleaching of Lucifer Yellow within an intact cell, or whether the impalement site was 'leaky', allowing dye to escape, a short experiment was conducted wherein a time course of bleaching of fluorescence was estimated. Continuous bleaching was compared with bleaching at intervals, to see whether loss of colour was due to length of exposure to U.V., or to time in the cavity.

2.8. Culture Methods

2.8.1. Enzymes.

Standard *Manduca* saline (Table 2.2) or serum-free media were used to dissolve the following proteolytic enzymes at 1 or 2 mg ml^{-1} for dissociation of midgut tissue; Collagenase/ dispase (Boeringer Mannheim), Collagenase (type IV), Elastase (type IV), Pronase E (type XXV), Hyaluronidase and Trypsin (all SIGMA). Bicarbonate-containing solutions were gassed with 5%CO_2/ 95% O_2 mixture.

2.8.2. Enzymic Dissociation of Midgut Epithelial Cells.

The midgut was dissected out from a surface sterilized larva, as described above, then two different methods were used for dissociation,

both of which provided selective access of proteolytic enzymes to the apical surface of the midgut. This effectively removed the possibly of contamination of epithelial cultures with muscle or Malpighian tubule cells, both of which lie below the basal lamina.

Inverted sac method: The midgut tube was flushed through with serum-free medium containing 5x the normal concentration of antibiotics (5x A) and inverted to expose the epithelial cells. It was left non-inverted when attempting to isolate muscle cells. The tube was then inflated with 5xA serum-free medium and tied at both ends to form a 'sac' which opened up the folds of the midgut allowing easier access by the rinsing solution and the proteolytic enzyme. The sac was rinsed several times in 5xA medium to achieve sterility. Inverted, inflated and rinsed sacs were incubated in 1ml of an enzyme solution at 37°C, or at room temperature, for 30 min, with occasional agitation. Enzyme action was stopped by dilution with 10ml serum-containing medium and the remaining midgut tube discarded. The resulting cell suspension was agitated, filtered through 100µm Nitex mesh to remove cell clumps, centrifuged at 1500 rpm for 5 min and resuspended in medium. Cells which were isolated for culture were given additional washes in 5xA medium. A slower centrifugation step of 500 rpm aided the removal of less dense microorganisms and damaged cells. The cells were finally resuspended in 1xA medium for culturing.

Flat sheet method: The isolated midgut tube was opened up as a flat sheet and stretched over pins placed strategically on a Sylgard-coated slide, lumen side up. This method also allowed access of high antibiotic rinsing solutions and enzymes, however flushing of the cells during incubation was improved, producing a higher cell yield. The extent of stretching of the tissue was made reproducible using this method. The flat epithelial sheet was incubated at 30°C for 40 min in 1 mg ml^{-1} collagenase/ dispase dissolved in serum-free medium. At 30 min the enzyme solution was flushed gently with a stream of medium from a pasteur pipette over the luminal surface to dislodge the epithelial cells from the basal lamina and the tissue replaced in the incubator for a further 10 min. Flushing with serum-containing medium was continued until a turbid single cell suspension was collected.

2.8.3. Cell Viability Assessment.

Cell suspensions were incubated with a 1:500 dilution of 1% fluorescein diacetate (FDA) for 15-30 min in the dark before washing and resuspending in medium for counting. Using a haemocytometer and epifluorescence optics, the percentage of viable (fluorescent) cells was obtained. For cell cultures, FDA was added to the dish in a 1:500 dilution and after incubation the supernatant containing unattached cells was removed and the cells centrifuged and resuspended for counting. Cells which had adhered to the surface of the dish were assessed by counting the percentage of fluorescent cells in 10 fields and an average for the whole dish was estimated. Cells were viewed using 20x or 32x phase contrast and epifluorescence optics on a Leitz Ortholux fluorescence microscope.

2.8.4. Cell Culture

Small tissue culture plastic dishes were mainly used for maintaining midgut cells *in vitro*. However, some other surfaces were tested for their ability to support growth and viability of primary insect culture, including; 25cm^2 tissue culture plastic flasks and 3.5cm^2 dishes (FALCON) coated with a 2% (w/v) gelatin / 10µg ml^{-1} poly-l-lysine mixture by incubating for 1h at 37°C. The coated surface was rinsed thoroughly with Hepes saline before plating. Once plated, cells were kept in a humidified, gassed and sealed container to prevent evaporation of media, and incubated at 15-25°C with a 16h:8h light:dark photoperiod.

2.9. Electron Microscopy Methods

2.9.1. Transmission Electron Microscopy

2.9.1.1. Solutions

Fixation Buffer: 2.5% glutaraldehyde, 0.1M Phosphate Buffered Saline (PBS), 0.18mM $CaCl_2$, 270 mOsM.

Rinsing Buffer: 2% sucrose, 0.1M PBS, 0.18mM $CaCl_2$.

2.9.1.2. Preparation of Tissue for Fixation

2.5% glutaraldehyde solution was applied to the midgut tissue as soon as it was exposed during the dissection. The middle region was cut into small ($1mm^3$) pieces and stored in 2.5% glutaraldehyde solution.

2.9.1.3. Fixation and Post-fixation

Pieces of tissue were selected and fixed in 2.5% glutaraldehyde solution for 1 h at room temperature. They were then rinsed three times for 5 min in 0.1M PBS rinsing buffer, leaving a small amount of buffer at the bottom of the phial after the last rinse.

2.9.1.4. Staining

An equivalent volume of 2% osmium tetroxide (OsO_4) was added to the tissue pieces in buffer and incubated for 1 h. The phial was topped up with distilled water for 5 min before three 10 min rinses in distilled water. After rinsing, the distilled water was drained down and the phial filled up with uranyl acetate solution. The tissue pieces were allowed to incubate in this solution in the dark for 1 h. Two rinses in distilled water readied the samples for dehydration.

2.9.1.5. Dehydration

After draining down the distilled water in the phial, the tissue pieces were dehydrated through a graded series of alcohols, as follows (15 min in each); 30%, 50%, 70%, 70%, 90%, 100%, 100%, 100% (dry). There was an additional step between 70% ethanols which was 1 h in p-phenyl amine diamine/ 70% ethanol with rotation. This enhances the OsO_4 effect.

2.9.1.6. Embedding

Most of the alcohol was removed and the phial filled with epoxy 1, 3-propylene oxide for 5 min. this was drained off and epoxypropylene oxide was added for 5 min. This too was drained off and a 1:1 mixture of epoxypropylene and araldite, prewarmed in the oven before shaking together, was added and left overnight on a rotator which allowed evaporation. The epoxy resin mixture was warmed in the oven at 62°C,

then pipetted into the wells of a setting plate. The samples were implanted into the unset resin as close to one end as possible, to avoid over-sectioning later. The plates were placed in the oven for two days.

2.9.1.7. Sectioning

The embedded samples were trimmed into a pyramid shape with razor blades, and the whole block mounted on an LKB microtome. A blunt glass knife was chosen to remove the initial Araldite. A sharp knife was used once the sample started to appear in the thick sections. Only sections with a gold or silver appearance were collected on a copper mesh grid.

2.9.1.8. Staining Sections

Grids containing samples were placed in 2% methanolic uranyl acetate solution for 5 min in the dark. They were rinsed using 2 droplets of distilled H_2O, followed by repeated submergence (20x) in consecutive phials of distilled H_2O. The grids were put into a droplet of 0.02N NaOH. After draining off the the excess NaOH, the grids were dipped into a drop of lead citrate solution in a CO_2 free environment, i.e. NaOH pellets around, for 5 min. They were then rinsed in 2 droplets of 0.02N NaOH, followed by a droplet of distilled water and then dipped 20 times in consecutive phials of distilled H_2O. Excess water was drained and the grids allowed to dry under a glass petri dish lid. They were then ready for viewing in the transmission electron microscope.

2.9.2. Scanning Electron Microscopy

2.9.2.1. Fixation and Post-fixation

Pieces of midgut tissue, (and whole 1st day 1st instar larvae), were immersed in 2.5% glutaraldehyde solution for 1 h. Glutaraldehyde was removed and the samples rinsed three times with buffer for 5 min leaving a small amount of buffer to cover the samples. An equal volume of 2% osmium tetroxide was added and the mixture incubated for 1 h. The phial was topped up with distilled H_2O for 5 min, before three 10 min washes in distilled water.

2.9.2.2. Staining

The distilled water was drained down and the phial filled with uranyl acetate solution. Samples were incubated in this solution for 1 h in the dark. After incubation, the samples were rinsed twice in distilled H_2O.

2.9.2.3. Dehydration

Dehydration of the samples was carried out using a graded series of acetones, made by equilibriating neat acetone with different volumes of H_2O, as follows; 30%, 50%, 70%, 90%, 100%, 100%, 100% dry acetone. Samples were then critical point dried.

2.9.2.4. Sputter Coating

Fixed and dehydrated samples were mounted on stubs using either silver paint or double sided tape, depending on the size of the sample. The stubs were mounted in a sputter coater which coated the samples with gold. The samples were transferred directly to a scanning electron microscope for viewing.

2.10. Acridine Orange Methods

2.10.1. Staining of Isolated Midgut Cells

Test solutions dissolved in *Manduca* saline included; 10, 50, 100 and 200 mM NaCl or NH_4Cl, 10 and 20 mM $NaHCO_3$ (BDH) , or K^+-free saline for a set period of time. Depending upon experimental requirements, cell-solution mixtures were bubbled with O_2, CO_2 or nothing. All cell suspensions were incubated for 5 min with 80μM acridine orange diluted in saline from a 0.25% stock (Sigma). Acridine orange (3,6-bis (Dimethylamino) acridine) had an excitation wavelength of 480 nm, and an emission wavelength of 530 nm. Cells were centrifuged and then resuspended in 1ml medium for counting. Occasionally samples were removed from the original cell suspension and incubated with fluorescein diacetate (FDA) for 30 min in order to determine viability.

2.10.2. Staining of the Intact Epithelium: TEP

5th instar middle midguts were isolated as flat sheets and mounted in an open circuit chamber (Dow et al. 1985). Both apical and basal sides of the epithelium were bathed in saline gassed with either O_2 or CO_2 depending on the experimental requirements. (Saline recipes are given in table 2.2). TEP was monitored throughout the experiment using a voltmeter (homemade Voltage Clamp) and plotted using a Goertz Servoscribe 1s chart recorder. Stock solutions of NH_4Cl, $NaHCO_3$, NaCl, KCl, ATP, azide, acridine orange and quinacrine (Sigma) were dissolved in saline and used to make additions to either or both sides of the epithelium. Equivalent volumes of saline were used for control additions. At the end of the recording, acridine orange or occasionally quinacrine was added for 5 min before the gut was removed, rinsed with saline and viewed under U.V. epifluorescence using a Leitz Ortholux microscope, for determination of dye accumulation.

2.11. Lectin Methods

2.11.1. Fluorescent Lectin Binding.

2.11.1.1. Lectins

Lectins were stored in 100µl aliquots at a concentration of 1mg ml^{-1} in saline containing 1% BSA to aid freezing. In initial experiments, one 100µl aliquot of WGA-TRITC was added to a 5ml cell suspension, and one 100µl aliquot of SBA-FITC was added to the other. The mixtures were allowed to incubate at room temperature for 30 min in the dark to avoid photobleaching of the fluorescent molecule. Kidney bean lectin (PHA) binding was also investigated following a similar protocol, and WGA-FITC was used in the later region-specific experiments.

2.11.1.2. Cell Isolation

Cells were isolated using collagenase/ dispase enzymic dissociation, either of an inverted sac or a flat sheet. Initially, cell suspensions were rinsed several times with saline and eventually resuspended in 5 ml saline aliquots. After incubating with lectin, cells were centrifuged and resuspended in saline before viewing under the ortholux fluorescence microscope. The flat sheet method, employed later, enabled cells to be

collected from the three morphologically distinct regions of the midgut. 100µl of lectin was incubated with the cells during isolation to prolong the exposure time (45 min at 30°C), and background fluorescence was removed by rinsing the cells in medium. Cells were resuspended finally in 1 ml medium in order to concentrate them for counting on a haemocytometer.

2.11.2. Cell Adhesion to Glass-Coupled Lectin.

2.11.2.1. Preparing the coverslips

Ten 25mm^2 glass coverslips were immersed in 20% H_2SO_4 for 1 h. Then they were individually immersed in 0.1 M NH_4OH (1:100 dilution of a 35% solution (10 M)) and dried on a paper towel. Dry coverslips were transferred to petri dishes where 1% APTS (aminopropyl triethoxysilane) was pipetted on until a meniscus was formed. This was left for 4 min, then the petri dishes filled with distilled water and the coverslips washed several times. 1% (v/v) glutaraldehyde in PBS was added to the dishes and left for more than 1 h at room temperature. It was rinsed off 3 times with PBS. 100 µg ml^{-1} of the lectin in PBS was added to the coverslips and the dishes covered and left for 1 h at room temperature. Coverslips were washed 3 times with PBS in which they were also stored. 1% APTS was dissolved in acetone, 1% glutaraldehyde in PBS. This method is outlined in a diagram (Figure 2.6).

PBS (10x stock): 1.37M NaCl, 0.027M KCl, 0.1M Na_2HPO_4, 0.015M KH_2PO_4, pH 7.2.

2.11.2.2. Differential adhesion assay

Cells isolated from the midgut were rinsed before finally resuspending in medium. 1ml aliquots of cell suspension containing 0.15-0.6 x 10^6 cells were plated onto coverslips coated with either WGA, SBA or PBS (control). They were allowed to settle and attach to the substrata for 2 hs. Unattached cells were removed with the supernatant and replaced with 1ml of a 4% (v/v with a 0.25% (w/v) stock) acridine orange solution to stain attached cells. The supernatant was centrifuged and the pellet of unattached cells resuspended in a 4% acridine orange solution. Incubation in acridine orange was 15 min at room temperature.

Figure 2.6 Covalent coupling of protein (or lectin) to glass

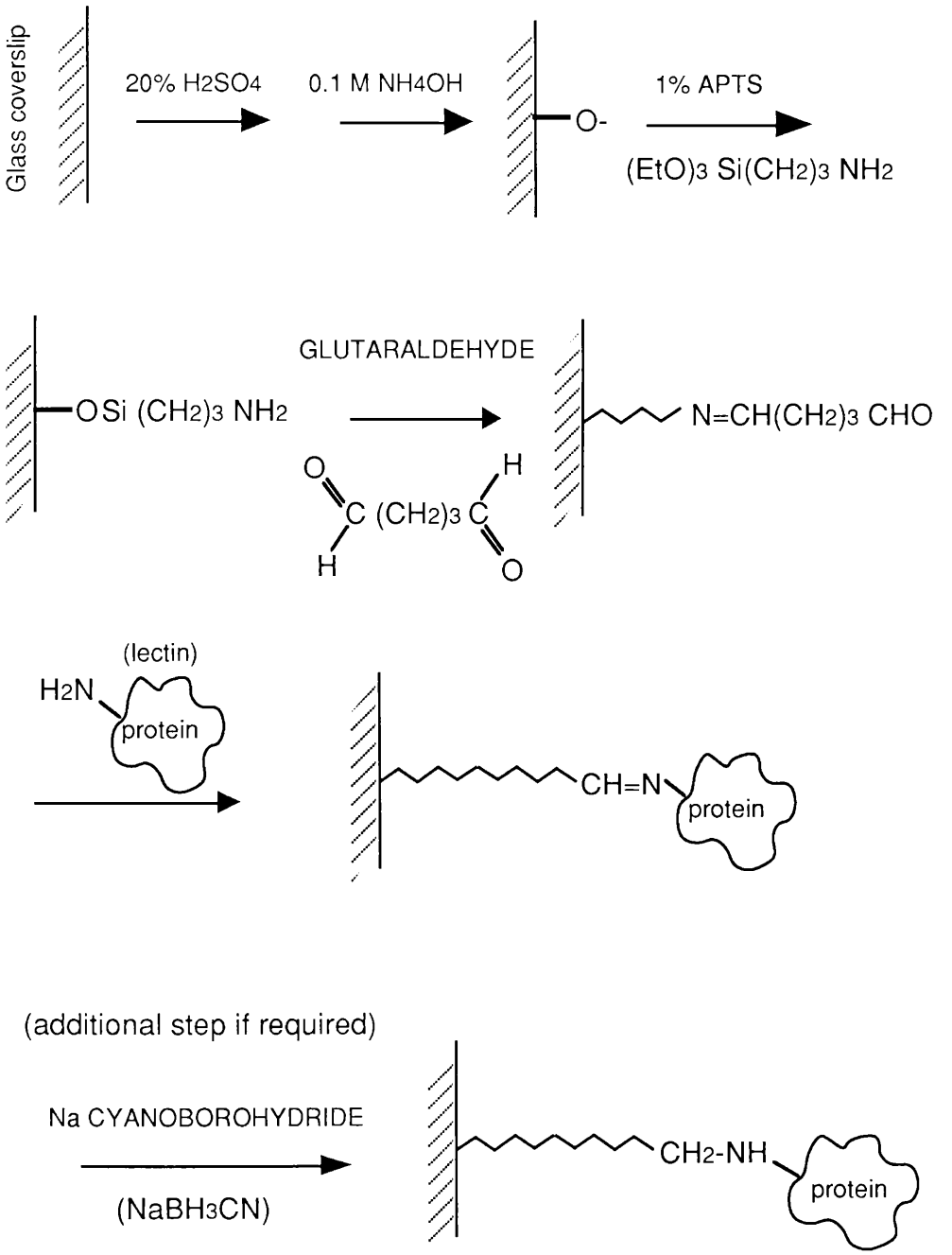

Method of J. D. Aplin (1981) for covalently coupling proteins or peptides to glass. The chemical structures of the compounds used for each step are given. APTS is aminopropyltriethoxysilane. The desired lectin (or protein) is incubated with the glass coverslips after treatment and therefore becomes covalently bound.

Coverslips were rinsed with medium and then inverted in clearmount onto a glass slide. Attached cells were quantified by counting fields of known area. Cell suspensions were centrifuged and the pellets resuspended in 1 ml of medium for counting of unattached cells on a haemocytometer.

2.11.3. Lectin Affinity Chromatography

2.11.3.1. Buffers

Column buffer: 20mM KH_2PO_4, 150mM KCl, 0.1% BSA, 0.02% azide, pH7.3

Elution buffer: 20mM KH_2PO_4, 150mM KCl, 0.1% BSA, 0.02% azide, 0.1M (25mg ml^{-1}) GlcNAc, pH7.3

Regeneration buffer: (a) 100mM TRIS-HCl, 500mM KCl, pH 8.5
(b) 100mM Na Acetate, 500mM KCl, pH 4.5

Storage buffer: 20mM KH_2PO_4, 150mM KCl, 0.1% BSA, 0.5% azide, pH7.3

2.11.3.2. Preparing the Column

A 1ml syringe was plugged with glass wool (or 80μm Nitex) and the column sterilized with 70% ethylene oxide. It was filled with 1ml WGA-sepharose 6MB beads (Pharmacia) (5mg ml^{-1}) then the column was connected to a peristaltic pump with polythene tubing. The column was equilibriated with 10-20 column volumes of column buffer at room temperature.

2.11.3.3. Cell Separation Protocol

A cell suspension containing 10^6-10^8 cells was prepared in 300μl of column buffer (i.e. 30% of the column volume). The column was allowed to run until the buffer level reached the level of the adsorbant. The cell suspension was added and the sample allowed to run onto the column bed. The buffer flow was stopped and the whole column incubated at room temperature for 10-15 min. The non-bound cells were eluted off by extensive washing with column buffer (20 column volumes) at a rate of 4-5 ml min^{-1} using gravity or 1ml min^{-1} using a peristaltic pump. The bound cells were eluted off by incubating the column with buffer containing 25mg ml^{-1} GlcNAc at room temperature for 20 min. Occasionally a

second bound fraction was obtained by agitating the column with a pipette. Cells were collected by washing through the column with elution buffer at a similar flow rate to the above. Cells were spun down and resuspended in 1ml medium. To regenerate the column, 10ml of regeneration buffer (a) was run through the column, followed by 10 ml regeneration buffer (b). The column was stored in column buffer plus 0.5% azide at 4°C.

2.11.3.4. Quantification.

Cells collected in 5 ml medium were stained with acridine orange (400µl of stock 0.25% acridine orange solution). They were incubated for 5-10 min and then spun out before resuspending the cell pellet in 1ml saline. Differential staining was assessed by eye using an epifluorescence microscope and a haemocytometer. In some experiments cell type was assessed by morphology and stained for viability using FDA.

2.12. Permeabilization Methods

2.12.1. Isolated Cells

Midgut cells were dissociated from the tissue using collagenase dispase and were resuspended in divalent-free *Manduca* saline to promote the permeabilizing effects of some agents. Aliquots of cells were resuspended after centrifugation in 2ml of saline containing the permeabilizing agent which could be 1mM ATP, 50 or 100 µg ml^{-1} Saponin and 50 or 100 µg ml^{-1} Digitonin (all Sigma). Control suspensions contained saline or saline with 5% ethanol as this was used initially to dissolve the detergents. The cell suspensions were incubated for either 15 min or 2 min in ATP solutions, or 2.5 min in detergent solutions.

2.12.2. Ethidium Bromide Fluorescence Assay For Cell Permeability

Following permeabilization, cells were exposed for 30 sec to 50µM ethidium bromide in divalent-free *Manduca* saline. Divalent-free saline was used to maintain the conditions under which permeabilization occurs as, in some cases, addition of the divalent cations, Mg^{2+} and Ca^{2+}, results in reversal of permeabilization (Gomperts and Fernandez 1985). The cells were washed and resuspended in saline before a sample was

removed to a haemocytometer for visual assessment of fluorescence uptake under epifluorescence optics. Cells were scored either bright, medium or faintly fluorescent.

2.12.3. Whole Tissue

The middle region of an isolated midgut was mounted in an Ussing-type chamber which could measure either short circuit current (SCC) or open circuit voltage (TEP) across the epithelium. Additions of the permeabilizing agents, ATP^{4-}, digitonin and saponin were made to either side of the epithelium and the results recorded on a chart recorder. The concentrations added are specified in the text.

2.13. Statistics

Statistical tests used include;
Microelectrode scattergrams: Spearman's correlation
Enzyme dissociation assays: Wilcoxon's sum of ranks and Yate's χ^2
Acridine orange differential staining of isolated cells: χ^2 and Yate's χ^2
Lectin differential affinity: χ^2 and Yate's χ^2
Differential cell permeabilization: χ^2 and Yate's χ^2
Significance levels were set at 5% throughout, to give the best compromise between type I and II errors.

Chapter 3

3. Chapter 3 Microelectrodes

3.1. Introduction

3.1.1. Model for Active Potassium Transport in Manduca Midgut

A model has been proposed suggesting that the main function of active K^+ transport across the midgut of Lepidopteran larvae (from blood to lumen) is to generate and maintain the high pH of 12 characteristic of caterpillar midgut contents (Dow 1984). K^+ ATPases present on goblet cell apical membranes pump K^+ from the goblet cytoplasm into the goblet cavity. The cavity membrane becomes polarised (apical side positive) which according to this model causes protons to distribute passively away from the cavity interior in accordance with the Nernst equation. This renders the goblet cavity extremely alkaline. The predictions of the model are that the goblet cavity membrane is not at the same resting potential as the midgut lumen, and that it is therefore more highly polarised than could be estimated from measurements of transepithelial potential differences (150mV) and intracellular resting potentials (-70mV). The maximum pH attainable in the midgut lumen should also be proportional to the extent of polarisation of the goblet cavity apical membrane.

Moffett and Koch recently measured cavity potentials in the posterior region of *Manduca sexta* midgut, and found that they were indeed not isopotential with the midgut lumen, however the posterior region is not thought to play a direct role in high pH generation (Dow 1984; Moffett and Koch 1988a). A technique was developed which, for the first time, allowed microelectrodes to be guided by eye to specific sites, such as goblet cavities, in the middle midgut, which is believed to be involved in the alkalinization of the gut lumen (Dow 1984). Site of impalement was confirmed by iontophoresis of the dyes Lucifer Yellow and 6-carboxyfluorescein whose diffusion was restricted by the apical valve. The electrical measurements obtained supported the predictions of the model, and it was shown that the cavity was an extremely high resistance compartment. Estimates were made for the likely extent of polarisation of the goblet cavity apical membrane *in situ*. These estimates agreed closely with the transmembrane Nernst potential calculated for protons.

3.1.2. History of Microelectrodes.

Ling and Gerard were amongst the first to pioneer the use of microelectrodes as a physiological tool. They developed the first glass micropipette which could be filled with an electrolyte solution and thus act as a conductor of electricity (Ling and Gerard 1949). Since then microelectrodes have been used not only in studies of the membrane properties of cells, but also for measuring intracellular free ion concentrations, injecting markers for determining cell: cell connections and cell structure, and, using patch clamp, for examining membrane activity at the level of the single ion channel.

Microelectrodes can be used for potential recording and current injection, the basic procedures required for conventional voltage- and patch-clamping; and also, using ion-selective resins, the free concentration of cytoplasmic constituents can be determined (Halliwell and Whitaker 1987).

3.1.3. Microelectrode Characteristics

When microelectrodes are made they generally have tip dimensions of the order of 1μm. This is achieved usually by heating glass capillaries until molten and then drawing apart to the extent where the tip breaks. It is possible to do this by hand but most people use microelectrode pullers, the best of which can produce tips so fine that the resistance across them is up to 300-500 MΩ, which is much higher than would be usable in most systems, 50-100MΩ is more reasonable (Halliwell and Whitaker 1987).

The conductor is often a salt solution which can be introduced by capillary action along channels which form either side of a fibre fused into the lumen of the micropipette. Small tipped pipettes draw up about 100μl by this action. Connections between recording subject and the electrical circuitry are made *via* non-polarizable reversible electrodes. Ag/AgCl pellets are usually employed to make the connection as they have the advantage of large current carrying capacity. Also the Ag/AgCl reference electrode is reversible and of constant potential because AgCl is slightly soluble and the solution therefore always saturated.

3.1.4. Electrical Equipment for Microelectrode Recording

Amplifiers used for microelectrode recording usually have an input resistance at least 100-1000 times the microelectrode resistance in order to measure the full signal at the microelectrode tip and draw negligible current from the signal source. A low leakage current (i.e. less than that which causes a 1mV drop across the microelectrode) and an adequate response time will overcome low pass filtering properties of a voltage recording set-up.

Bridge balance circuits are required when testing passive membrane properties, such as input resistance, by passing current into the cell. This can be done by having two microelectrodes in the same cell, one for recording voltage, the other for current injection, or with a single electrode; however, the potential difference between the microelectrode barrel and the tip resulting from the voltage drop caused by current flowing through the microelectrode resistance (R_{ME}), must be eliminated. This can be very large, for instance, 1nA through a 50 MΩ electrode will produce a 50 mV voltage drop. Using bridge balance circuits, a scaled proportion of the input signal driving the current injection can be subtracted electronically from the voltage output. The amplifier gains can be scaled so that the microelectrode resistance can be read off a dial in MΩ.

3.1.5. Iontophoresis

The best pipettes for intracellular injection have; (a) relatively short shanks, (b) relatively large tip diameters, as small diameters have high electrical resistance which can hinder movement of the dye, and (c) thin walled glass for obtaining lower resistance. However, normal microelectrodes can be used if the substance is easily injected (Warner and Bate 1987).

Iontophoresis ejects the substance from the pipette by the application of positive or negative going current, depending on the polarity of the overall charge of the substance (negative going pulses to inject negatively charged molecules). The magnitude of the current should be kept to a minimum in order to avoid blocking the electrode and damaging the cell. Blockage can be temporarily relieved by reversing the polarity of

the current for a short time. Bulk flow out of the tip can be achieved by high frequency electronic oscillation. The capacity compensation control on the amplifier allows for brief over compensation which effectively sends the system into oscillation. Current injection is carried out after intracellular recording has been made to avoid inducing an electrical imbalance across the membrane and measuring an artificially altered membrane potential.

6 carboxy fluorescein (low M_r ~332) as a substance for injection has the advantage that it does not bind to cellular components It may however, cross cell surface membranes (Warner and Bate 1987). Lucifer Yellow (M_r 457) can be CH or VS form, although most workers use the CH form. It diffuses through the cell rapidly, but forms an insoluble precipitate at high levels (>200mM) of potassium and has to be dissolved in LiCl (Warner and Bate 1987). LY-filled electrodes can block during iontophoresis as Lucifer Yellow becomes precipitated with K^+ in the cytoplasm. This block can be relieved by passing depolarizing pulses.

Several molecules are available which can act as fluorescent indicators of cellular ionic concentrations. Most have been developed to measure free calcium levels, such as aequorin, Quin-2, Fura-2 (Blinks et al. 1982), however, others are becoming available, for instance BCECF (2',7'-bis-(carboxyethyl)-5(6')-carboxyfluorescein) for measuring hydrogen activity (Rink et al. 1982). The AM form of the dye (BCECF-AM) acts as an ester which readily crosses the plasma membrane. Inside the cell BCECF-AM is hydrolysed by cellular esterases and becomes membrane impermeable and is therefore trapped. Hydrolysis releases hydrogen ions and therefore this method of introducing the substance into the interior of the cell results in a small drop in pH, so for accuracy of measurement of H^+ concentration it is perhaps best to micro-inject the membrane impermeable form (BCECF).

Before impaling a cell the electrode resistance must be checked. 1% LiCl is a poor conductor and so resistances of 30-100MΩ are normal. Electrodes are often quite unstable and drift markedly, usually because the tip is blocked. An extremely noisy or drifting trace can sometimes be corrected by pressing the capacitance compensation for a few seconds. This physically vibrates the tip clearing away any air bubbles or debris.

The resistance can be cancelled out by manipulating the stimulus balance while passing depolarizing and hyperpolarizing currents alternately, until there is no trace deflection when a current is passed. This means that when current is injected into a cell, any deflection of the scope trace reflects a change in the cell membrane potential only. After an impalement has been made and a stable resting potential recorded, the hyperpolarizing current can be applied and increased until the scope trace is deflected by about 50mV for 1-2 min, periodically adjusting the current. This injects the dye into the cell or compartment which can then be viewed using epifluorescence optics.

Glass capillary microelectrodes filled with Lucifer Yellow dissolved in 1% LiCl, and with resistances of 30-100MΩ, were used for all midgut cell impalements.

3.2. Results

3.2.1. Experimental Procedure

Using visual guidance, it proved very easy to obtain good impalements of goblet and columnar cells, and reasonably easy to impale goblet cavities. The site of impalement was verified readily after Lucifer Yellow filling, by comparing phase and epifluorescence views of the impalement site (Figure 3.1). It was noted that dye injected into either goblet or columnar cell cytoplasm spread rapidly to neighbouring cells, confirming that middle midgut cells are normally linked by gap junctions under open circuit conditions (Figure 3.1d) (Moffett et al. 1982; Thomas and May 1984b). However, impalements giving potentials and resistances consistent with basal extracellular space (Moffett et al. 1982) showed no accumulation of dye, even when viewed during iontophoresis.

In contrast, dye leakage was not observed from any of the goblet cavities (figure 3.1b). No loss of fluorescence, other than that due to photobleaching, was detected up to 30 min after making fills. This result confirmed resistance measurements relative to the apical side of the epithelium, in which cavity resistance was found to be very high (34 ± 8 MΩ, n = 11). In contrast, the resistances of the cytoplasm of goblet cells (6 ± 2 MΩ, n = 10) and columnar cells (4 ± 1 MΩ, n = 18) were low, which is

Figure 3.1 Microelectrode impalement sites in *Manduca sexta* midgut marked by iontophoresis of lucifer yellow.

a. Light micrograph of stretched middle midgut showing donought-shaped goblet cells interspersed with granular columnar cells. Underlying longitudinal and transverse muscle layers can be made out just below the plane of focus.

b. Epifluorescence micrograph of (a) showing a goblet cavity filled with lucifer yellow by iontophoresis after a successful impalement. The jagged effect is caused by apical projections into the cavity. The apical valve is tight to outward movement of lucifer yellow from the cavity.

c. Mixed light and epifluorescence micrograph of stretched middle midgut showing a lucifer yellow-filled microelectrode approaching from the left and penetrating a goblet cell.

d. Epifluorescence micrograph of (c) showing that the impalement was made in the goblet cell cytoplasm as there is rapid spread of lucifer yellow via gap junctions to the neighbouring cells.

Scale bars = 50μm

Figure 3.1 Microelectrode impalement sites in *Manduca sexta* midgut marked by iontophoresis of lucifer yellow.

a

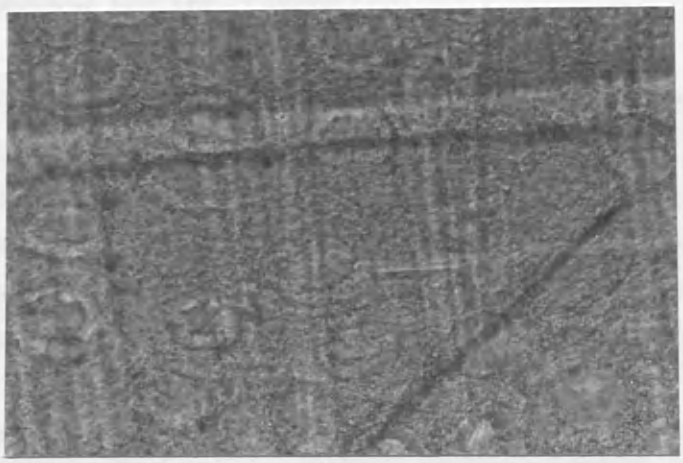

b

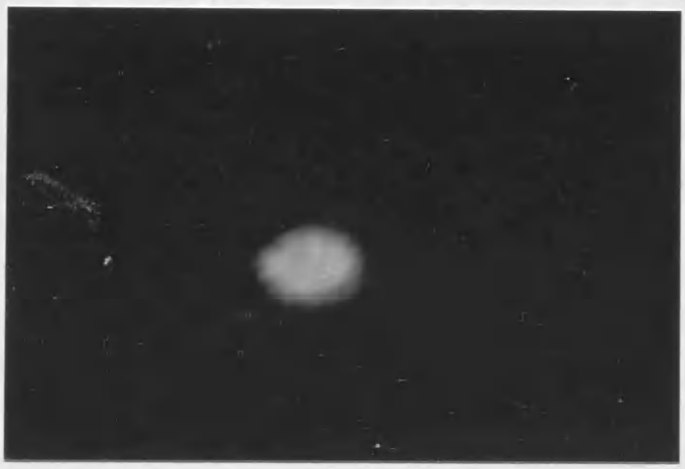

c

d

close to the average resistance measurement in *Spodoptera* midgut of 6.2 MΩ (Thomas and May 1984b).

As Lucifer Yellow can be precipitated by high potassium levels (Warner and Bate 1987), it is possible that the lack of dispersion of Lucifer Yellow could arise from immobilisation, rather than restriction by the tight apical valve. This is unlikely, as the potassium activity of goblet cavities (90mM) is no higher than that of the cytoplasm (Moffett and Koch 1988a), a level which should not precipitate Lucifer Yellow (Warner and Bate 1987). The possibility was tested by filling impalement sites with 6-carboxyfluorescein, which has a lower relative molecular mass than Lucifer Yellow, but does not suffer from the problem of precipitation (Warner and Bate 1987). It was found that the same pattern of dye accumulation was obtained as for Lucifer Yellow. The dye filled all three compartments successfully, but photobleached much more rapidly than Lucifer Yellow. It diffused from goblet or columnar cytoplasm within 1 min, but did not diffuse out of goblet cavities in 20 min.

3.2.2. Microelectrode Impalement Potentials

As the transepithelial potential across an isolated midgut was oxygen-dependent, microelectrode impalements were made following perfusion with oxygenated saline, the effect of which is illustrated in figure 3.2. Fig. 3.3 shows the potentials of each compartment impaled, relative to the apical side of the tissue. As the TEP measured varied widely among guts, and among impalements, the potentials are presented as functions of TEP. It can be seen that, for all three sites, the measured potentials correlate significantly, and approximately linearly, with gross TEP.

The TEP across midgut *in vivo* is generally agreed to be approximately 150 mV (Dow 1986; Harvey et al. 1986). As there was a clear relationship between polarization of the three impalement sites and TEP, it was possible to estimate *in vivo* values of membrane potential by extrapolation to 150mV TEP. These are presented in Table 3.1, and are expressed relative to the apical side, as measured, and relative to the basal side, in order to compare them with previously published results (Blankmeyer and Harvey 1978; Moffett, Hudson et al. 1982; Moffett and Koch 1988a; Moffett and Koch 1988b; Thomas and May 1984b)

Fig. 3.2 Effect of perfusion with oxygenated saline on midgut TEP

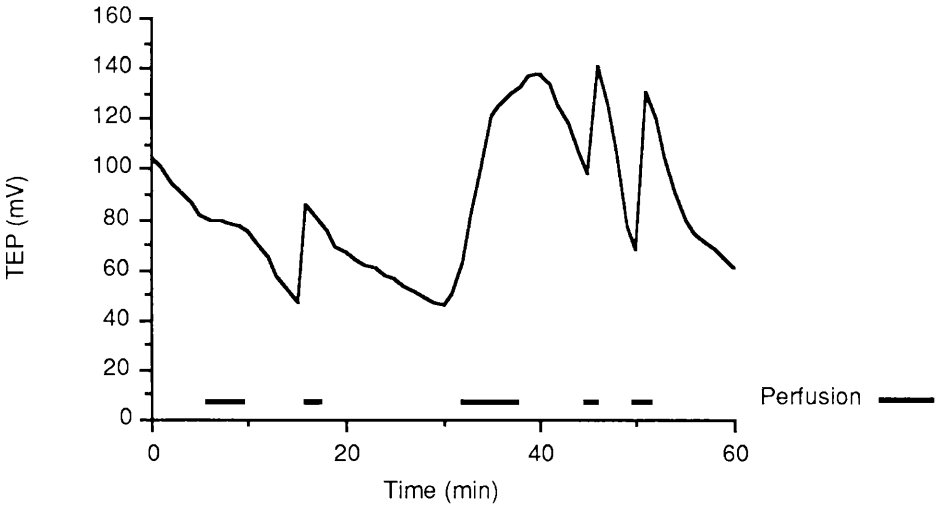

Transepithelial potential was measured with a voltmeter across an isolated midgut during microelectrode impalements. Prior to an impalement being made, the tissue was perfused on both basal and apical sides with oxygenated saline, resulting in a dramatic rise in TEP. Interval and duration of perfusions are indicated by solid lines below the recorded trace.

Figure 3.3 Microelectrode impalements of three midgut compartments

Scattergrams of membrane potential differences recorded in three sites of *Manduca sexta* middle midgut, relative to the apical lumen, as a function of gross transepithelial potential difference (TEP). Lines were fitted by eye. All impalements were confirmed by dye fills. Spearman *r* values are shown. All correlations were significant.

a. Goblet cell cytoplasm (n= 135 impalements)

b. Columnar cell cytoplasm (n= 106)

c. Goblet cell cavities (n= 53).

Figure 3.3 Microelectrode impalements of three midgut compartments

a. Goblet cell impalemnts

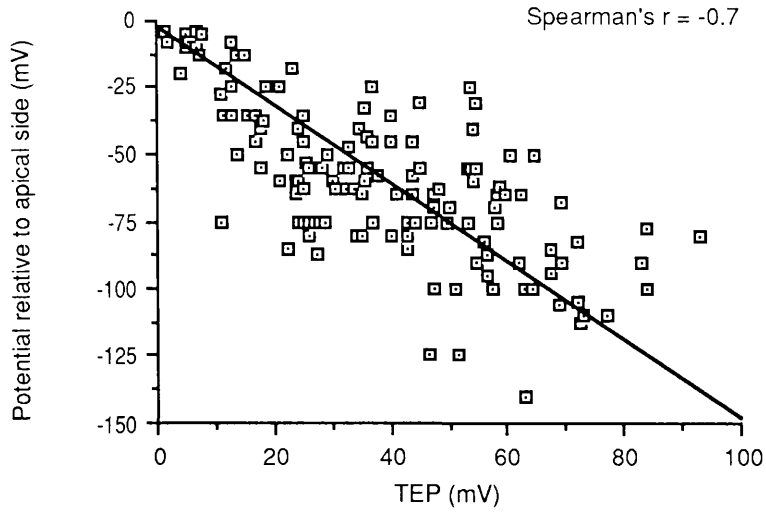

b. Columnar cell impalemnts

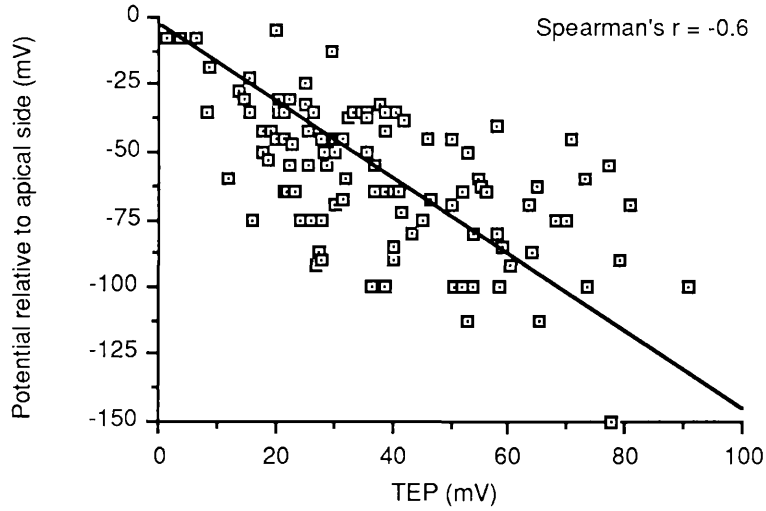

c. Goblet cavity impalements

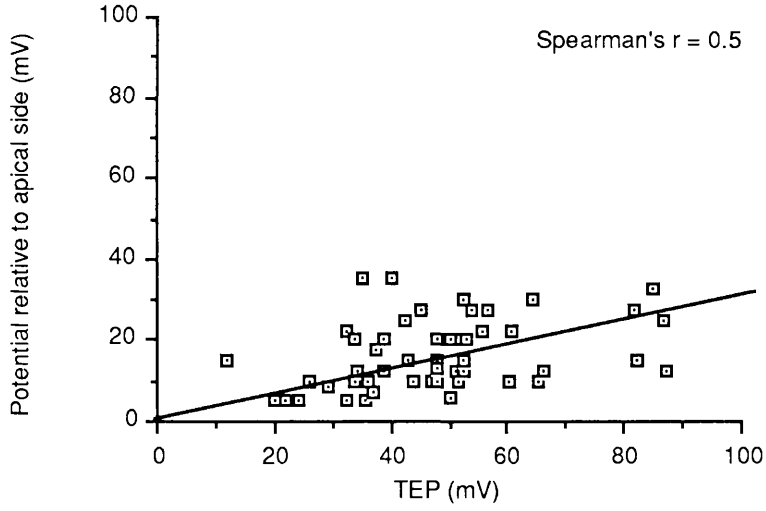

Table 3.1. Estimated electrical potentials of *Manduca* middle midgut compartments relative to basal and apical sides *in vivo*

Compartment	Estimated PD (mV) Relative to basal side	Relative to apical side
Goblet cytoplasm	-72	-222
Columnar cytoplasm	-80	-230
Goblet cavity	+197	+47

3.2.3. Calculation of Electrochemical Gradients

Electrochemical gradients for potassium between various midgut compartments were calculated using: electrical potentials (shown in Table 3.1); potassium activities in blood (25 mmol l^{-1}) and middle midgut contents (65 mmol l^{-1}) (from Dow and Harvey 1988); and potassium activities of goblet and columnar cells (95 mmol l^{-1}) and goblet cavities (94 mmol l^{-1}) of posterior midgut (from Moffett and Koch 1988a). The resulting values are presented in Table 3.2, with chemical and electrical components of the electrochemical gradient shown separately.

Table 3.2. Estimated electrochemical potentials for potassium movements between *Manduca* middle midgut compartments *in vivo*

Compartments	Estimated electrochemical PD for potassium (kJ mol^{-1}) Component Chemical	Electrical	Total Electrochemical
Transport pathway *via* goblet cells			
Goblet cytoplasm relative to blood	+4.3	-6.9	-2.7
Goblet cavity relative to cytoplasm	-0.03	+26.0	+25.9
Apical lumen relative to goblet cavity	-0.3	-4.5	-4.8
Absorptive pathway *via* columnar cells			
Columnar cytoplasm relative to apical lumen	+0.3	-22.2	-21.9
Blood relative to columnar cytoplasm	-4.3	+7.7	+3.5
Recycling pathway from columnar to goblet cells			
Goblet cytoplasm relative to columnar cytoplasm	0	+0.7	+0.7

All the values used in the calculation, except intracellular and cavity potassium activities, relate to middle midgut. However, the use of posterior midgut data in the calculation is justified as: (i) the ionic environment bathing both blood and luminal sides of both middle and posterior midguts is similar (Dow and Harvey 1988), (ii) potassium transport in the three midgut regions is similar in terms of open-circuit voltage, short-circuit current and flux ratios (Cioffi and Harvey 1981), (iii) the potentials recorded in goblet cavities of middle midgut (this study) are similar to those published for posterior midgut by Moffett and Koch (1988) and (iv) most significantly, the calculations shown in Table 3.2 are insensitive to variations in potassium activity values, as the electrical term dominates the electrochemical PD in all cases where significant electrochemical PDs were obtained. However, these assumptions should be considered when interpreting the calculations.

3.2.4. Energetics of Transport

The electrochemical PD for potassium across the pump site (the goblet cavity membrane) represents the minimum work required for transport, given 100% efficiency in the pump. This allows certain estimates of pump energetics to be made (Harvey et al. 1981; Harvey and Zehran 1972). Data obtained from these impalements, and from those of Moffett and Koch (1988), allow these estimates to be made with greater precision.

The stoichiometry of the pump can be estimated by comparing the electrochemical PD for potassium (26 kJ mol^{-1}) with generally accepted values for the free energy of ATP hydrolysis (50-55 kJ mol^{-1}), yielding a K^+: ATP ratio of 2: 1.

The minimum energy expended on the pump by a 5g larva can be calculated by multiplying the electrochemical PD (26 kJ mol^{-1}) by the estimated transport rate across the entire midgut (150 µmol h^{-1}: based on Cioffi and Harvey (1981), which yields an expenditure of 3.9 J h^{-1}, or around 3.9/ 52000 = 75 µmol ATP h^{-1}. By comparing this with the larva's gross metabolic product, calculated from the oxygen consumption of a 5g larva at 25°C (2.85 ml h^{-1}: Reynolds et al. 1985), and a P: O ratio of 3: 1 (Mandel et al. 1980), a total ATP production rate of 832 µmol ATP $larva^{-1}$ h^{-1} is estimated. The minimum fraction of the larva's total ATP budget utilised by the K^+ pump would then be 9%.

In saline containing 32 mmol l^{-1} K^+, which resembles haemolymph, the K^+: O ratio measured by Harvey and Zerahn (1972) in isolated *Cecropia* midgut was 1.23: 1. Assuming a P: O ratio of 3: 1, and that pump stoichiometry is 2: 1, then the K^+ pump uses 1.23 X 100 / (2 X 3) = 21% of the total ATP production in the midgut.

3.3. Discussion

3.3.1. Experimental Procedure

Use of the microscope configuration described allowed easy impalement and verification of three midgut recording sites. The observation that the polarisation of all three compartments correlated with TEP validates the scatterplot approach used in Fig. 3.3 for open circuit measurements. These values for potentials in midgut compartments were made more meaningful by standardizing to *in vivo* conditions.

3.3.2. Testing the Model

The model for generation of high pH (Dow 1984; Dow et al. 1984) predicts that the PD across the apical membrane of the goblet cavity determines the distribution of protons between the goblet cavity lumen and the goblet cytoplasm according to the Nernst distribution. It also predicts that the function of the complex apical valve of the cavity is to electrically isolate the apical membrane, so that it is not isopotential with the apical lumen, and that it is the potential across the goblet cavity membrane, rather than the gross TEP, which determines the maximum pH that can be generated by the midgut.

Evidence to support these predictions was obtained by comparing microelectrode impalements in three compartments; goblet cell cytoplasm, columnar cell cytoplasm and the goblet cavity. The goblet cavity was found to be electrically isolated from the apical lumen, as measured by; (i) its consistently positive potential relative to the apical side; (ii) its uniformly high resistance; and (iii) its tightness to Lucifer Yellow and 6-carboxyfluorescein.

3.3.3. The Nernst Potential Difference for Protons

The Nernst PD for protons across the goblet cavity was calculated from the maximum pH observed in midgut contents in *Manduca* (11.3 in middle midgut: Dow 1984), and an estimate of pH 7 for cytoplasmic pH. This value is justified by the finding that intracellular pH is regulated close to pH 7 in all animal cells measured to date (Roos and Boron 1981). In fact a cytoplasmic pH of 7 was subsequently measured in *Manduca* midgut cells by Dow and O'Donnell (1990). It was therefore possible to compare the polarisation of the goblet cavity apical membrane with the calculated Nernst PD for protons across the membrane, by extrapolation to *in vivo* conditions. The expected polarization of the goblet cavity apical membrane *in vivo* would be +269 mV. As the maximum pH measured in *Manduca sexta* midgut is 11.3 in the middle midgut (Dow 1984), the Nernst potential for protons across the goblet cavity apical membrane would then be 254mV, calculated using the following derivation of the Nernst equation;

$$\Delta\psi = \frac{-RT}{zF} \ln (C_{in}/C_{out}) \qquad \textit{Equation 3.1}$$

where $\Delta\psi$ is the membrane electrical potential, R is the gas constant, T is temperature in K, z is the charge of the ion, F is the Faraday constant and C is the concentration of the ion inside and outside respectively.

254mV is in excellent agreement with the calculated electrical PD for this membrane. Alternatively, the PD estimated across the goblet cell membrane would account for a luminal pH of up to 7 + 269/ 58 = 11.6.

The microelectrode technique for estimation of goblet cavity polarisation must underestimate the true values, as potentials recorded on impalement of high-resistance compartments, such as the goblet cavity, will be reduced by damage artefacts and the sealing of highly structured membranes around the electrode is probably poor. It might therefore be more appropriate to consider only the steepest slope through the points obtained in the goblet cavity impalements of Fig. 3.3. This would increase further the measured polarization of the cavity membrane.

3.3.4. Potassium Activity Gradients *in vivo*

There are believed to be two main pathways for potassium movement across the midgut (Dow 1986). In the pump pathway, potassium enters from the basal surface of the goblet (and perhaps columnar) cells, and is pumped out through the apical goblet cavity. In the leak, or absorptive, pathway potassium enters the apical side of the columnar cells *via* cotransport with nutrients, and leaves at the basal surface, returning to the blood. Additionally, there is thought to be recruitment of columnar cell K^+ into the pump pathway *via* gap junctional communication between cells. The data from Table 3.2 is presented in diagrammatic form in Fig. 3.4, which shows the directions of hypothesized potassium fluxes across the midgut, together with the associated energy steps, in three pathways.

These data suggest that, in the middle midgut of the living insect, basal potassium entry is energetically favourable, and so there is no need for transbasal active transport (although this may occur in posterior midgut: Moffett and Koch 1988b). The major energy step is across the goblet cell apical membrane, where the K^+ -ATPase is located. Exit of K^+ from the goblet cavity is favoured by a small electrochemical gradient into the midgut lumen: this can be considered as the energy 'overhead' imposed on the potassium pump by the presence of the apical valve.

Potassium entry across the columnar cell apical microvilli in the absorptive pathway is strongly favoured, although the electrical gradient is far larger than the chemical gradient. These data are particularly relevant to studies of amino acid uptake, which is believed to be mediated by the electrochemical PD for K^+ across the columnar cell brush border *via* a cotransport mechanism. The estimate for this PD (-22 kJ mol^{-1}) is somewhat larger than that of -15 kJ mol^{-1} in *Bombyx mori* made by Giordana et al. (1982). Here, a lower chemical component is made negligible by a larger electrical component. However, the two estimates are broadly compatible.

It has often been suggested that the K^+ transport pool for the goblet cell ATPase is drawn from both goblet and columnar cells (Dow 1986). Microelectrode data obtained in this study and elsewhere (Dow and Peacock 1989; Moffett et al. 1982) implies communication between the cell types and therefore supports this view. Figure 3.4 reveals that the

Figure 3.4 Electrochemical gradients for potassium across midgut cell membranes

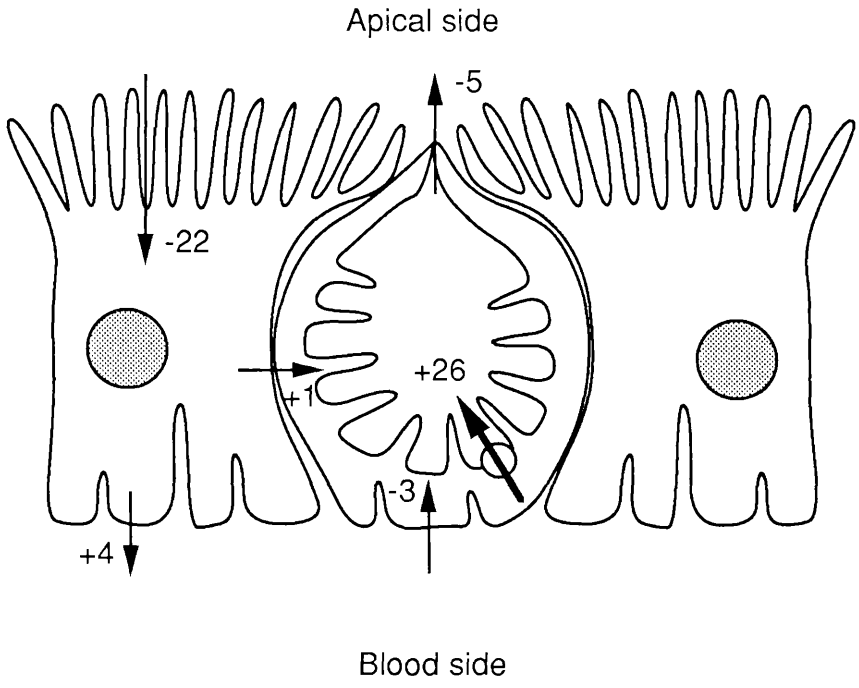

Schematic representation of the midgut cell types showing the major routes for K^+ movements between compartments in the pump, absorptive and shunt pathways. The values given are estimates for the electrochemical potential difference for K^+ ions (in kJ mol^{-1}) moving in the directions indicated (arrows) *in vivo*. The heavy arrow and circle indicates the K^+ATPase.

electrochemical PD between goblet and columnar cytoplasm is almost zero. Also, the energetic gradient favouring K^+ entry from the apical side (-22 kJ mol^{-1}) greatly exceeds the gradient favouring K^+ entry from the basal side (4 kJ mol^{-1}). Rather than recruitment of blood-side potassium to the goblet cell *via* the columnar cell basal membrane, as was argued by the K^+ excretory hypothesis (Harvey et al. 1983a), the dominant K^+ movement through the columnar cells may be a recycling of K^+ to the goblet cells *via* the columnar apical membrane. This idea is consistent with flux data obtained from Bt-intoxicated midgut tissue (Harvey and Wolfersberger 1979).

3.3.5. Energetics of Transport

It is significant that the estimate for the work needed to pump potassium across the goblet cavity membrane (26 kJ mol^{-1}) is approximately half that of the generally accepted value for the free energy of ATP hydrolysis in cells (50-55 kJ mol^{-1}). This suggests a stoichiometry of $2K^+$: 1ATP for the pump, which has long been favoured (Harvey et al. 1981). However, in the middle midgut, mitochondria actually insert into the goblet cavity projections (Cioffi 1979), shortening the diffusion path for ATP and metabolites, and so the free energy of ATP hydrolysis may be somewhat higher than normal. This could have the effect of shifting the stoichiometry towards an alternative value of 3: 1.

This pump uses a large fraction of the larva's gross metabolic product. The total ATP production rate calculated does not account for 'housekeeping' metabolism, so the fraction of the larva's disposable metabolic income which is expended on the midgut K^+ ATPase may be considerably higher than that calculated. This calculation, though preliminary, supports the suggestion (Dow 1986) that midgut K^+ transport is an expensive process, and must produce tangible benefits. Such benefits might include not only the regulation of blood potassium levels (Harvey et al. 1983a), and the absorption of nutrients (Giordana et al. 1982), but also the alkalinization of the midgut lumen which in itself has several advantages for the insect (Dow 1984; Dow et al. 1984).

3.3.6. Comparing Middle and Posterior Midgut

With microelectrode impalement data now available for both posterior midgut (Moffett and Koch 1988a; Moffett and Koch 1988b), which is not thought to alkalinize the midgut lumen, and for middle midgut (Dow and Peacock 1989), which is thought to do so, it is instructive to compare them. The potentials recorded for the goblet cavity relative to the apical lumen are comparable with those obtained by Moffett and Koch (1988) in short-circuited posterior midgut. This similarity implies that the ability of the potassium pump to polarize the goblet cavity apical membrane is not the only prerequisite for generation of an alkaline fluid. If the potassium-transporting activities are similar in middle and posterior midgut (Cioffi and Harvey 1981), then where might the necessary differences lie? The goblet cells in the two regions differ morphologically (Cioffi 1979); the goblet cells in the anterior and middle regions have a vastly reduced cytoplasm, and their microvilli all contain mitochondria, in contrast with the goblet cells of the posterior midgut. Similarly, carbonic anhydrase, an enzyme associated with acid-base regulation in many tissues, is associated with the goblet cell apical membranes only in the anterior and middle midgut regions; in the posterior midgut, it associates with the columnar cell apical membrane (Ridgway and Moffett 1986). Another possibility is that the H^+ permeability of the goblet cell apical membrane in the posterior midgut may be lower than that in the middle and anterior midgut; in that case, although an electrical gradient for H^+ equilibriation may exist, the ability to produce alkalinity may be reduced.

Whatever the details of the mechanism for generation of high pH that may emerge, certain points arise from these data: the electrical isolation of the midgut cavities precludes their role primarily as K^+ excretory cells; and the electrical, rather than the chemical, work performed by the goblet cell K^+ pump dominates its impact on midgut nutrient absorption and high pH generation models. Further work is required to explain the roles of midgut potassium pumping, an extraordinarily energy-intensive process, in ionic homoeostasis, nutrient absorption and midgut alkalinization.

Chapter 4

4. Chapter 4 Midgut Cell Culture

4.1. Introduction

4.1.1. History of Insect Cell Culture

The first recorded attempt at maintaining insect tissue *in vitro* was by Goldschmidt early this century using explants from testes of diapausing Cecropia silkmoth, *Hyalophora cecropia* (Goldschmidt 1915). He observed spermatocytes in a hanging drop of pupal haemolymph. However, due to a lack of adequate medium to promote cell growth and maintenance, his success was limited. Interestingly, he was working at the time in a laboratory in New Haven, where, in 1907, R. Harrison set up the first ever vertebrate tissue culture (Harrison 1907). This was a piece of explanted nerve tube from frog embryos in a hanging drop culture, also developed by Harrison, from which he observed axonal outgrowth. Several years later, Trager (Trager 1935) was first to systematically develop medium based on the physico-chemical properties of haemolymph. The cells survived and remained physiologically active outside the organism, but they could not be maintained for more than a few days. Later, Wyatt (Wyatt 1956) grew cells from ovarian tissue of the silkworm, *Bombyx mori*, again using medium based on insect haemolymph and it promoted *in vitro* cell growth and survival for up to three weeks.

T.D.C. Grace (Grace 1958) advanced insect cell culture using the Australian emperor gum moth, *Antheraea eucalypti*, by becoming the first person to set up a continuous insect cell line. Initially he used Wyatt's medium, in which cells divided for 3-4 weeks before ceasing growth, although remaining viable for several additional weeks. In other words, the cells had become quiescent. Grace then modified Wyatt's medium, by addition of a group of B vitamins, to more closely mimic the haemolymph of *Antheraea* (Grace 1962). This was an improvement, however, after 2 months he found that cell growth and migration had decreased to very low levels, even though the cells were still healthy. The cultures were maintained at this level for more than 1 year when 4 of the cultures showed a rapid increase in cell number and division rate. These were the first established insect cell lines.

Since then improvements have been made in media formulation. Investigators such as Mitsuhashi, Maramorosch, Kitihari and McIntosh have developed media based on vertebrate media formulations, for example, foetal bovine serum was shown to be an efficient replacement for insect haemolymph (Mitsuhashi 1982), although there is always a residual requirement for molecular components from insect blood. Lactalbumin hydrosylate, tryptose broth and yeast extract have often been included in insect media to improve the nutritive properties of the medium, although these have often been at concentrations which could not be tolerated by many vertebrate cells.

In general, insect media differs from vertebrate media in three major respects, based on the following *in vivo* characteristics:

1. The pH of insect body fluids is more acidic, ranging from 6.3 to 6.9 pH units, however it has been suggested that insect tissues tolerate wide pH variations (Jones 1962).

2. Often the osmotic pressure of insect fluids is more than twice that of vertebrates, due to high concentrations of amino acids which contribute to the buffering capacity of insect blood. However, caterpillar haemolymph has a lower osmotic pressure (320 mOsM) than vertebrate blood.

3. The ionic ratios of insect blood differ from vertebrate blood. Frequently the Na^+/ K^+ ratio is low as is the Ca^{2+}/ K^+ ratio. Insect blood also has a higher phosphate concentration in the form of organic phosphates (Paul 1975).

4.1.2. Recent Advances in Insect Cell Culture

Both primary and established cell culture have been widely documented for both vertebrate and many invertebrate cells of varying types (Freshney 1986; Paul 1975), there being currently in excess of 200 invertebrate cell lines representing more than 75 species from 8 orders of arthropods on record (Hink and Hall 1989). The majority of these cell lines are derived from the insect orders, Lepidoptera and Diptera, the rationale being that the former are agricultural pests and the latter

includes *Drosophila*, which are used widely in molecular genetics (Sang 1981).

Most of the cultured cell lines that are available remain unidentified as they were mainly derived from ovaries or whole minced larvae; however, there has been some success with primary embryonic cell culture of nerve, blood, larval and adult, muscle and fat, and imaginal disc (Currie et al. 1988; Grace 1962; Harvey and Sohi 1985; Kurtti 1976; Marks 1976; McIntosh 1976; Mitsuhashi 1976; Sohi 1980) and also with short term organ culture (Fistrom et al. 1973; Milner and Muir 1987).

Satmary and Bradley (1984) achieved enzymic isolation and viable maintenance of Malpighian tubule cells in culture. These highly differentiated cell types tend not to multiply *in vitro* as they would first have to de-differentiate into a mitotic cell type before beginning replication. It would therefore seem advantageous to maintain cells such as these in primary culture complete with their original functions for reasonably extended periods of time.

This is true also for the larval midgut cells of *Manduca sexta.* Two main cell types exist which have defined morphologies (see Fig. 1.3 in Introduction); Goblet cells are characterized by the presence of a relatively large cavity which is isolated from the midgut lumen by a complex apical valve (Cioffi 1979). Columnar cells are more regular in shape, appearing polygonal in section and have an apical brush border of microvilli (Hanozet et al. 1989). In accordance with their morphology, the midgut cells have specific functions (Harvey et al. 1983a). Columnar cells are the nutrient absorbing cells of the gut (Giordana et al. 1985; Giordana et al. 1982; Nedergaard 1977) and are therefore the site of potassium and amino acid coupled uptake from the gut lumen. The function of the goblet cavity is still under debate. There is evidence to indicate that the goblet cell apical membrane is the site of electrogenic K^+ transport from the blood to the lumen (Blankmeyer and Harvey 1978; Dow et al. 1984; Dow and Peacock 1989; Harvey et al. 1981; Moffett et al. 1982; Wieczorek et al. 1986). It is probably also involved in generation of the extremely high pH of 12 found in the midgut contents (Dow 1984; Dow and O'Donnell 1990).

Most investigations of the osmoregulatory system have been made on whole isolated midgut, but there is still some doubt as to whether the unique K^+ ATPase resides on the goblet cell apical membrane and even whether it exists at all, as a recently proposed model suggests a primary electrogenic proton pump driving a K^+: H^+ electroneutral exchanger (Klein et al. 1988; Schweikl et al. 1989; Wieczorek et al. 1989). By isolating and separating the two individual cell types much of the present controversy could be clarified, for example, by enabling cellular manipulations to be carried out, as well as reducing membrane contamination during biochemical analyses.

The Lepidopteran larvae under investigation in this study are agricultural pests of tobacco crops, thus their feeding behaviour and physiology are also of interest. By setting up a cell culture system, in particular of the midgut cells, one has many avenues to explore, for instance the molecular biology of the tissue incorporating a baculovirus expression system could be exploited, as well as the hormonal control of cellular development *in vitro*, both of potential use in pest control (Haider and Ellar 1987; Hammock et al. 1990; Riddiford 1976; Ryerse 1980). Cells in isolation could also facilitate access to the plasma membrane required for patch-clamp studies.

This chapter describes a simple method for isolation and maintenance of a heterogeneous primary culture of cells from the midgut epithelium of *Manduca sexta* and discusses possible applications of insect cell culture.

4.2. Results

4.2.1. Enzyme Dissociation Assay

It was necessary to establish the optimum conditions for isolating single cells from the midgut epithelium. This was done by exposing inverted midgut sacs to various enzyme treatments comparing enzyme type, concentration and temperature of incubation. As the insects were reared at around 25°C, dissociation at room temperature was employed to optimise viability and cell stability *in vitro*. However, the enzymes used were often derived from bacteria which grow at 37°C, so in order to test the ability of these enzymes to cleave proteins at their optimum temperature, dissociation at 37°C was also carried out.

Viability of the isolated cells was monitored to ensure that enzyme action did not damage cells irreparably by degrading essential membrane proteins as well as disrupting cell-cell and cell-matrix adhesion. It was assessed using fluorescein diacetate (FDA) which is an ester that readily crosses cell membranes. Once inside an intact and viable cell, cellular esterases cleave the molecule thus trapping fluorescein which has a fluorescence emission at 510nm (Guilbault and Kramer 1964) (Figure 4.1.). It proved straightforward to distinguish two subclasses of goblet and columnar cells: those which stained brightly and were deemed viable, and those which stained weakly or not at all, and were deemed non-viable.

Yields and viabilities of isolated cells were determined following each enzyme treatment and are presented in Table 4.1. The highest yields were obtained when midgut sacs were incubated at 37°C. After subtraction of the appropriate controls, the greatest enrichment was found during treatments with collagenase or collagenase mixtures, especially when dissolved in serum-free medium, regardless of temperature of incubation. Comparing the results for collagenase treatments with those from other enzymes, which were not statistically significant from the controls, indicated that collagen was probably a major constituent of the extracellular matrix of this epithelium. For clarity these results were presented graphically in figure 4.2.

The results for enzymes of 2 mg ml^{-1} concentration were also tested, and are presented in table 4.2. Yields were only slightly higher in some cases than for 1 mg ml^{-1} although not statistically so, and there was no significant difference between viabilities, in fact quite often cells were less viable, probably due to the degradative properties of the enzymes involved. For comparison these results were also presented graphically (Figure 4.3.)

Columnar cell viability was highest when trypsin/ versene was used at either temperature. For goblet cells, however, viability appeared to be independent of the enzyme type involved. In general, these cells were more robust than columnar cells which had delicate microvilli that could be sheared off easily during isolation. This might actually be

Figure 4.1 Fluorescein diacetate (FDA) staining of viable midgut cells isolated by enzymic dissociation.

a. Light micrograph of an isolated goblet cell displaying irregular shaped cavity and stalk-like apical valve region.

b. Epifluorescence micrograph of (a) showing FDA uptake by the goblet cell. The brightness of staining in the cytoplasm indicates viability. The impression of faint staining in the cavity is probably a reflection of the surrounding cytoplasm.

c. Light micrograph of an isolated columnar cell characterized by granular cytoplasm and apical microvilli. The large central nucleus can also be made out.

d. Epifluorescence micrograph of (c) showing FDA uptake by the columnar cell. The brightness of staining indicates high viability. Note that the brush border stains only at the base and not at the tips of the microvilli.

Scale bars = 50μm

Figure 4.1 Fluorescein diacetate (FDA) staining of viable midgut cells isolated by enzymic dissociation.

a

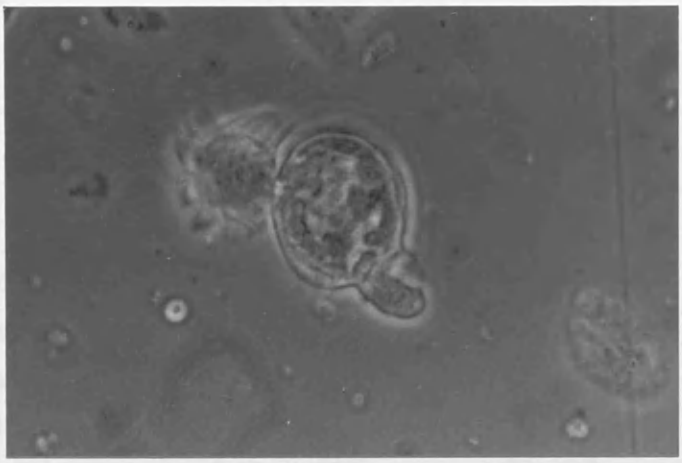

b

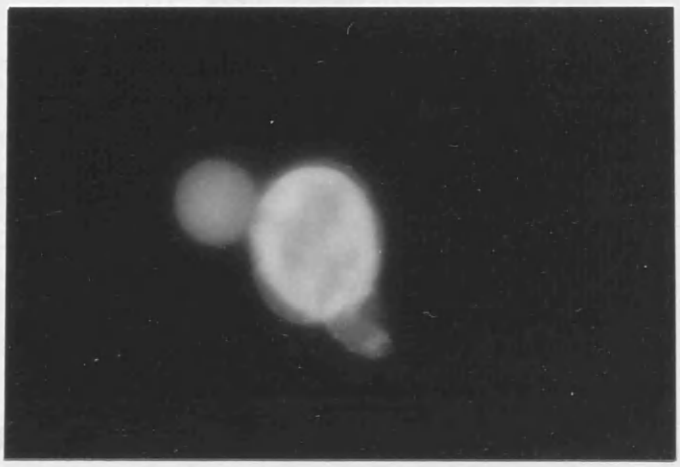

c

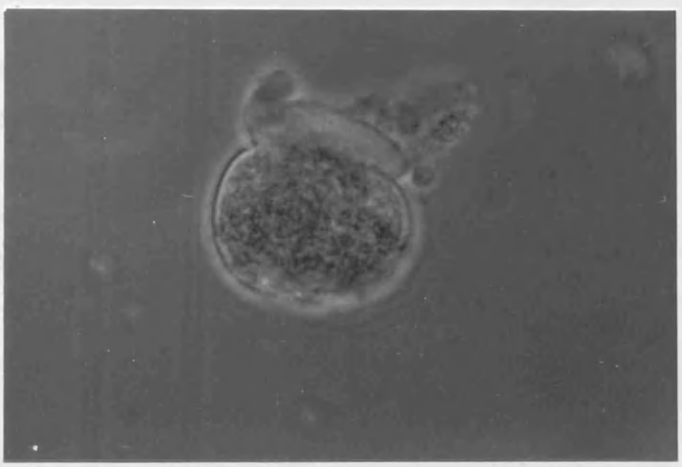

d

Table 4.1. Enzyme Dissociation Assay.(1mg ml^{-1})

Cells were isolated from inverted midgut 'sacs' under the conditions shown. Enzymes dissolved in media are shown in brackets. Results are given as total number of cells in suspension per g of original tissue ± SEM. Viable cells were fluorescent after exposure to FDA. (n=4)

ENZYME (1mg ml^{-1})	TOTAL YIELD $x10^6 g^{-1}$ tissue	Goblet viability (%)	Columnar viability (%)
30 min at 37°C:			
Collagenase	**0.56** ± 0.13	44 ± 9.2	29 ± 5.9
Collagenase (TC100)	**0.79** ± 0.1	68 ± 8	52 ± 13.2
Collagenase/ dispase	**0.44** ± 0.06	74 ± 5.6	52 ± 7.7
Collagenase/ dispase (TC100)	**0.74** ± 0.11	83 ± 5.1	44 ± 6.7
Collagenase/ Elastase	**0.52** ± 0.09	63 ± 5.1	40 ± 8.4
Elastase	**0.43** ± 0.06	74 ± 5.6	49 ± 13.4
Trypsin	**0.43** ± 0.1	58 ± 6.3	45 ± 12.1
Trypsin/ Versene	**0.29** ± 0.08	80 ± 11.5	72 ± 10.2
Pronase E	**0.46** ± 0.04	53 ± 8.5	57 ± 9.2
Hyaluronidase	**0.32** ± 0.02	67 ± 10.1	42 ± 8.8
CONTROLS			
Manduca Saline	**0.32** ± 0.02	81 ± 9.7	61 ± 19.2
TC100 medium	**0.55** ± 0.14	91 ± 3.5	75 ± 10
Graces medium	**0.4** ± 0.11	77 ± 4.4	48 ± 8.3
30 min at room temp:			
Collagenase	**0.34** ± 0.09	69 ± 7.8	56 ± 6.4
Collagenase (TC100)	**0.41** ± 0.13	86 ± 3.1	54 ± 15.6
Collagenase/ dispase	**0.39** ± 0.09	76 ± 4.7	62 ± 6.7
Collagenase/ dispase (TC100)	**0.5** ± 0.26	72 ± 9.4	54 ± 5.9
Collagenase/ dispase (Graces)	**0.5** ± 0.11	65 ± 7.2	39 ± 2.9
Collagenase/ Elastase	**0.37** ± 0.08	78 ± 9.6	42 ± 6.9
Elastase	**0.3** ± 0.05	72 ± 11.5	57 ± 9.6
Trypsin	**0.34** ± 0.07	72 ± 7.5	46 ± 9.9
Trypsin/ Versene	**0.29** ± 0.07	67 ± 10.3	81 ± 8.9
Pronase E	**0.3** ± 0.06	64 ± 2.7	49 ± 10.4
Hyaluronidase	**0.22** ± 0.04	57 ± 5.4	45 ± 12.3
CONTROLS			
Manduca saline	**0.25** ± 0.06	61 ± 10.1	63 ± 8.7
TC100 medum	**0.22** ± 0.07	74 ± 5	72 ± 10.5
Graces medium	**0.11** ± 0.01	84 ± 5.6	47 ± 13.6

Figure 4.2 Enzyme Dissociation Assay (1mg ml^{-1})

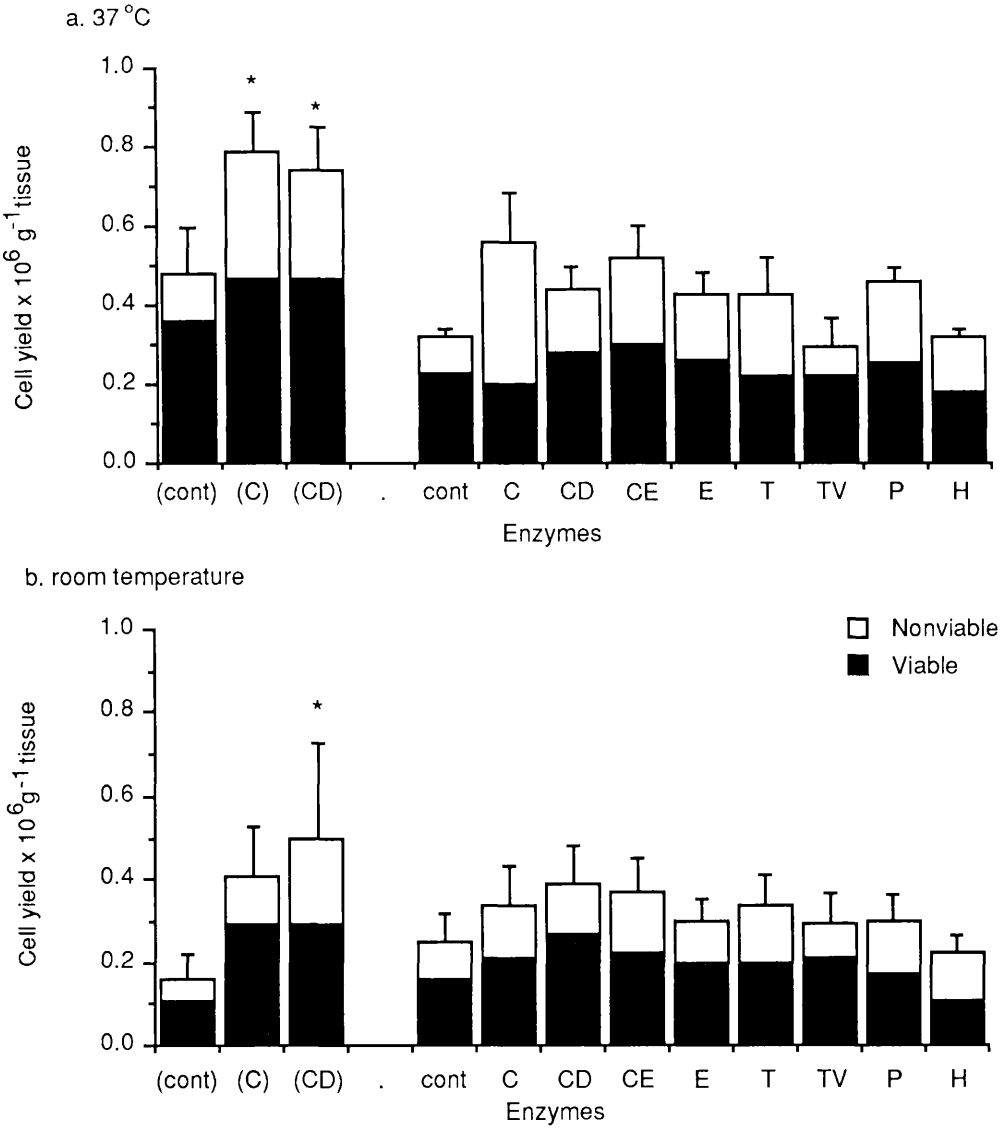

Graphical presentation of Table 4.1. The bars represent the total number of cells isolated per g of midgut tissue, under the conditions shown. The shaded areas are the total number of viable cells present in the cell suspension as determined by FDA uptake. For separate goblet and columnar cell viabilities see table 1. cont, is control isolation in medium (brackets) or saline; C is collagenase; CD is collagenase dispase; CE is collagenase / elastase; E is elastase; T is trypsin; TV is trypsin versene; P is pronase E and H is hyaluronidase. All enzymes were dissolved at a concentration of 1 mg ml^{-1} in saline or medium (in brackets). a. Isolation was carried out at 37°C for 30 min. b. Isolation was carried out at room temperature for 30 min. ± S.E.M. (n=4)

Statistics: Yields which are statistically significant from the controls are indicated by an asterisk. For all enzymes tested there was no significant difference between yields at room temp. and 37°C, although there was a significant difference between medium controls.

Table 4.2. Enzyme Dissociation Assay.(2mg ml^{-1})

Cells were isolated from inverted midgut 'sacs' under the conditions shown. Enzymes dissolved in media are given in brackets. Results are given as total number of cells in suspension per g of original tissue ± SEM. Viable cells were fluorescent after exposure to FDA. For controls see table 4.1. (n=4)

ENZYME (2mg ml^{-1})	TOTAL YIELD $x10^6 g^{-1}$ tissue	Goblet viability (%)	Columnar viability (%)
30 min at 37°C:			
Collagenase	**0.55** ± 0.18	57 ± 13.3	31 ± 9
Collagenase (TC100)	**0.7** ± 0.1	67 ± 5.1	38 ± 9.9
Collagenase/ dispase	**0.44** ± 0.08	56 ± 8.3	46 ± 9
Collagenase/ dispase (TC100)	**0.82** ± 0.12	73 ± 6.5	60 ± 8
Collagenase/ Elastase	**0.58** ± 0.08	76 ± 7.4	56 ± 10.4
Elastase	**0.35** ± 0.05	75 ± 4.7	67 ± 4.1
Trypsin	**0.3** ± 0.04	55 ± 11.3	34 ± 10.7
Pronase E	**0.49** ± 0.13	67 ± 10.7	61 ± 12.7
Hyaluronidase	**0.36** ± 0.07	67 ± 4.8	51 ± 16.6
30 min at room temp:			
Collagenase	**0.46** ± 0.16	62 ± 7.4	44 ± 5.7
Collagenase (TC100)	**0.27** ± 0.09	86 ± 6.4	54 ± 10
Collagenase/ dispase	**0.31** ± 0.08	61 ± 5.1	46 ± 8.4
Collagenase/ dispase (TC100)	**0.6** ± 0.18	76 ± 4.3	49 ± 11.6
Collagenase/ dispase (Graces)	**0.58** ± 0.13	69 ± 10.8	35 ± 7.4
Collagenase/ Elastase	**0.42** ± 0.11	61 ± 11.3	33 ± 13.1
Elastase	**0.4** ± 0.08	78 ± 4.4	42 ± 8.6
Trypsin	**0.29** ± 0.08	72 ± 10.2	48 ± 8.6
Pronase E	**0.39** ± 0.09	71 ± 6.5	55 ± 11.5
Hyaluronidase	**0.35** ± 0.11	59 ± 13.4	46 ± 18.1

Figure 4.3 Enzyme Dissociation Assay (2mg ml^{-1})

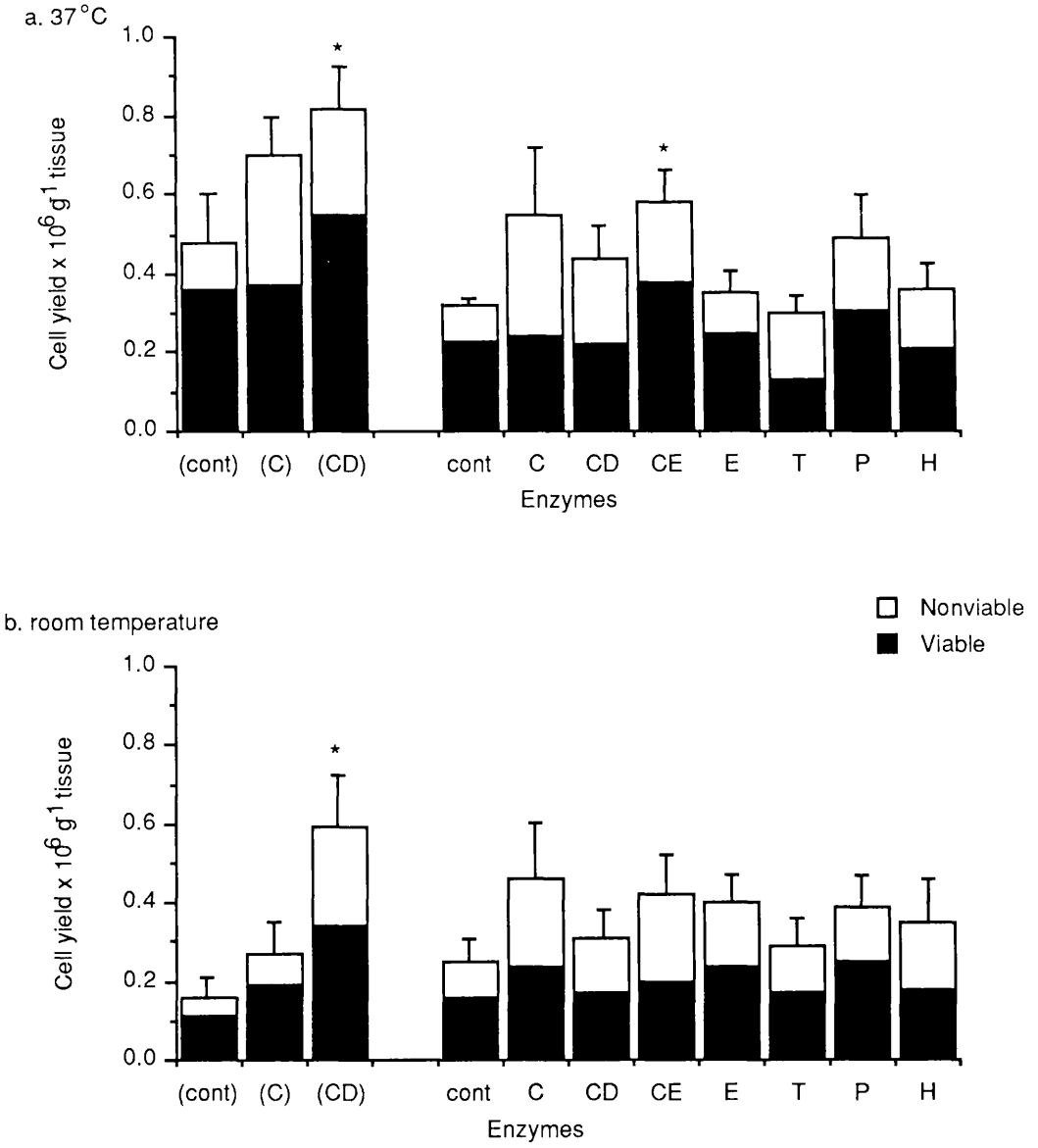

Graphical presentation of Table 4.2. The bars represent the total number of cells isolated per g of midgut tissue, under the conditions shown. The shaded areas are the total number of viable cells present in the cell suspension as determined by FDA uptake. For separate goblet and columnar cell viabilities see table 4.2. cont, is control isolation in medium (brackets) or saline; C is collagenase; CD is collagenase dispase; CE is collagenase / elastase; E is elastase; T is trypsin; TV is trypsin versene; P is pronase E and H is hyaluronidase. All enzymes were dissolved at a concentration of 2 mg ml^{-1} in saline or medium (in brackets). a. Isolation was carried out at 37°C for 30 min. b. Isolation was carried out at room temperature for 30 min. ± S.E.M. (n=4)

Statistics: Yields which are statistically significant from the controls are indicated by an asterisk. Yields using 2mg ml^{-1} enzyme were not statistically significant from 1mg ml^{-1} enzyme.

advantageous as goblet cells could be selectively enriched merely by reasonably vigorous agitation of the cell suspension.

Taking both viability and yield into consideration, the optimum conditions for isolating goblet and columnar cells with high viability were; 2 mg ml^{-1} collagenase dispase dissolved in TC100 medium at 37°C for 30 mins. This concentration of enzyme also gave the best results at room temperature. These conditions were applied later in a technique which improved on the existing cell isolation method, namely the flat sheet isolation.

4.2.2. Flat Sheet Dissociation.

From the results of the enzyme dissociation assay, a method was designed which greatly enhanced the yield of cells isolated from the anterior and middle midgut regions, whilst maintaining a high viability. This flat sheet dissociation method also minimised contamination by muscle cells and Malpighian tubule cells and allowed the isolation to be carried out at an intermediate temperature of 30°C.

The epithelium was stretched out as a flat sheet onto a Sylgard coated slide allowing the enzyme better access to the highly folded epithelium compared with the midgut 'sac' which often failed to inflate. This set up also allowed gentle flushing to be carried out during the incubation, a procedure which dislodged the upper layer of the epithelium. After 30-40 min of incubation, flushing with the enzyme solution caused the cells to detach in sheets which then dissociated easily during pipetting of the cell suspension. A comparison of yields and viabilities of cells isolated using both methods is presented in figure 4.4. There was a significantly higher yield obtained using the flat sheet method compared with the sac method of enzymic isolation, although both produced similar cell viability.

The flat sheet method was beneficial for isolating cells for cell culture as the tissue could be flushed with medium containing a high concentration of antibiotic, whereas only limited rinsing was possible with the previous sac dissociation technique. Epithelial cells were removed cleanly from the basal lamina, which could also lead to the possibility of using the basal lamina to grow these or other cells *in vitro*.

Fig 4.4 Flat Sheet vs Sac Dissociation

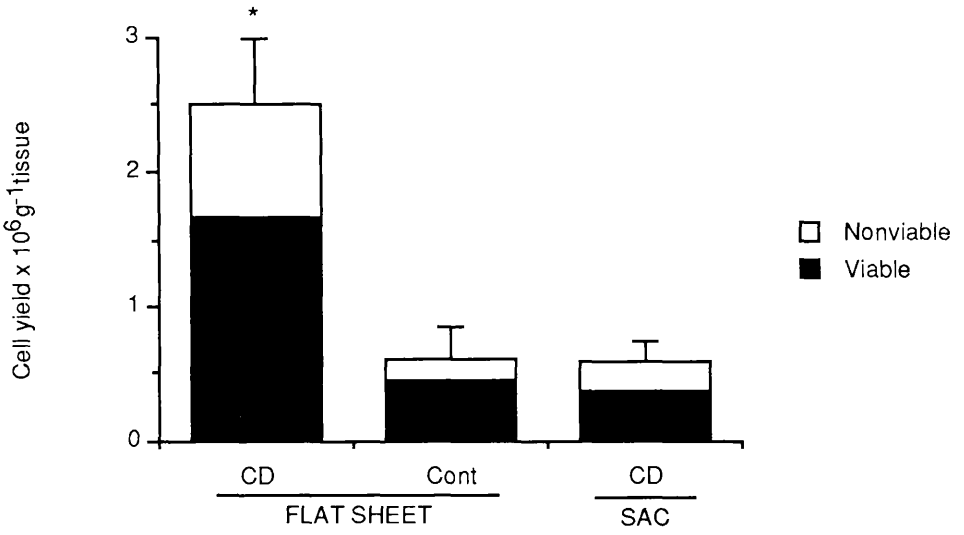

Cells were dissociated from the midgut using either the flat sheet dissociation method or the 'sac' dissociation method. The bars represent the total number of cells isolated per g of midgut tissue ±S.E.M. The shaded areas are the number of viable cells in the population. CD is 1 mg ml^{-1} collagenase dispase in serum-free medium; Cont is serum-free medium. Incubations lasted 40 min at 30 ^{o}C. (n=4)

Statistics: Yields which were statistically significant are indicated by an asterisk. A chi-squared value of 2.3 indicated that there was no significant difference between cell viabilities for all three conditions.

4.2.3. Maintenance of Midgut Cells in Culture

4.2.3.1. Gelatin/ poly-l-lysine-coated Flasks:

In initial culture attempts, cells were isolated from inverted midguts using collagenase and plated onto gelatin/ polylysine-coated culture flasks. Viability of the isolated cells was high at approximately 85% as determined by FDA staining.

The 0.5ml cell suspension was swirled and the flask inverted for 1 h at 37°C before adding 2ml of medium and upturning the flask. The initial swirling allowed any serum factors in the medium to adsorb onto the substratum, providing an adhesive surface for the cells after the flask was inverted. Cells were incubated at 25°C for 2 days without disturbance. This method was supplied by Barbara Knowles at Cambridge (pers. comm.).

After 2 days the cells were floating or very loosely adherent to the gelatin/ polylysine surface, however, they were healthy with very little contamination. In order to keep contamination to a minimum, the original cell culture was removed and rinsed once in 5xA medium. The cells were resuspended in 1xA medium and then half of the cells were aliquoted into the original flask and the other half into a fresh gelatin/ polylysine-coated flask. Most cells at this stage were viable, however, goblet cells showed the brightest FDA fluorescence.

Midgut cells still retained their differentiated morphology 6 days after dissociation from the tissue. Goblet cells had stalks and cavities and a robust phase bright appearance. Columnar cells could be seen with defined microvilli (Fig 4.5). The advantages of using flasks for culture were; (a) they could be inverted to allow adsorption of proteins from the medium to the culture plastic surface, and (b) sterility of the cultures could be more successfully maintained. However, one disadvantage was that a large number of cells were required to fill the flask and this limited the number of cultures that could be set up and later assessed. So, a similar experiment was carried out on smaller petri dishes.

Figure 4.5 Maintenance of midgut cells in culture on gelatin / poly-l-lysine-coated flasks.

a

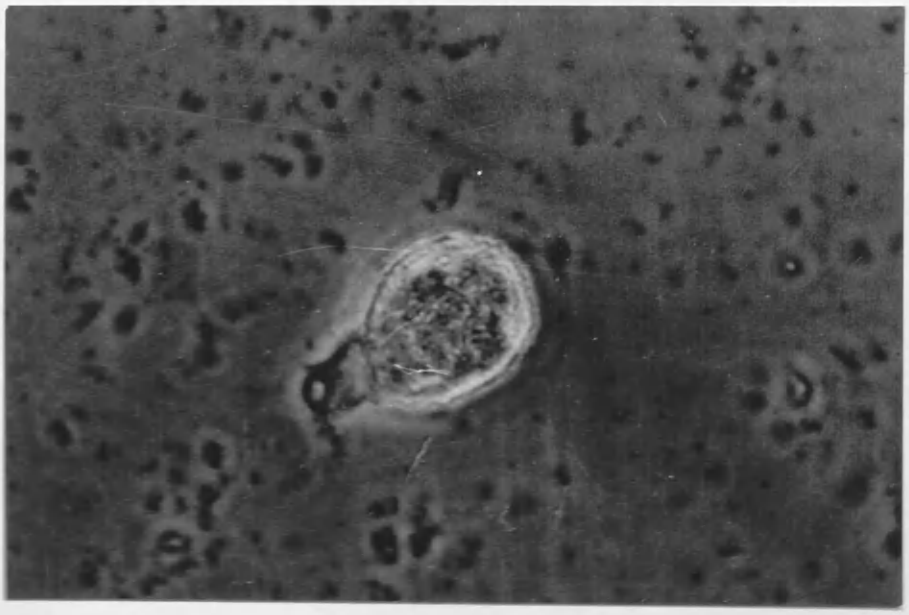

b

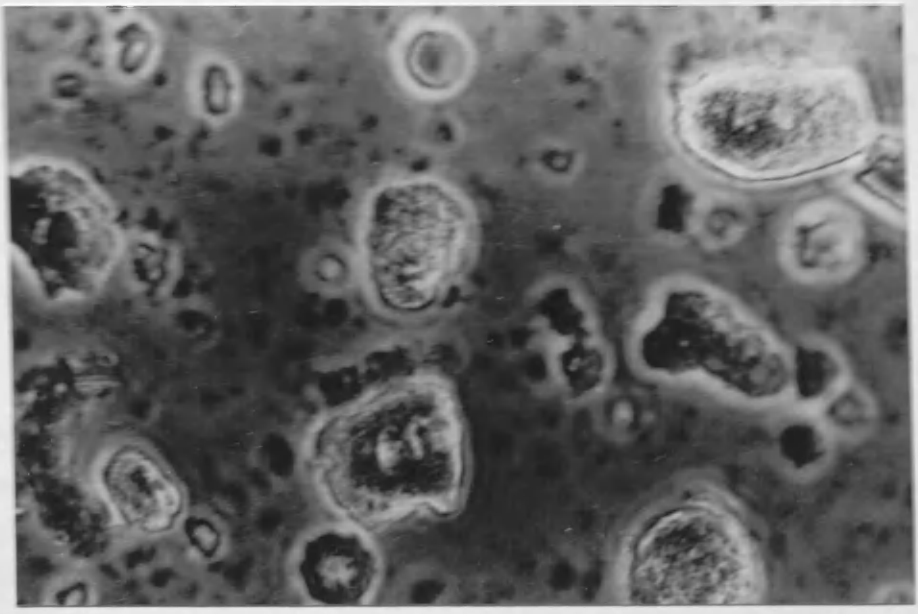

a. Light micrograph of a goblet cell in culture for 6 days. The cell still retains its original isolated morphology with irregular shaped cavity and apical valve (stalk-like structure) well defined.

b. Light micrograph of columnar (and other) cells in culture for 6 days. The columnar cell at the centre of the picture still retains its characteristic morphology with centrally located nucleus and apical brush border evident. Cell fragments and gut particles are also present.

Scale bar = 50μm

4.2.3.2. Gelatin/ poly-l-lysine-coated Dishes:

Gelatin/ poly-l-lysine-coated dishes were used to maintain and assess *Manduca sexta* midgut cell survival in culture. Cells were isolated by the sac dissociation method and rinsed thoroughly with 5xA Graces medium. Approximately 5 x 10^6 cells were aliquoted in 0.5ml volumes onto 10 dishes and incubated at room temperature in the dark with fresh medium added every 2-3 days. At intervals, viability was assessed using FDA. The supernatant containing cells which had not adhered to the substratum was removed and the cells were spun down, resuspended in medium and counted on a haemocytometer. Cells remaining on the dish were assayed by counting fields and determining the total number of cells attaching. The results are presented in Figure 4.6.

The total number of cells remained relatively stable throughout the experiment, the only deviation from this being the counts taken on day 14 which was possibly the result of adding more cells initially. The number of cells remaining on the dish after gentle rinsing increased slightly after 1 week in culture but then decreased towards the end of the total culture period. This coincided with an increase in contamination by yeast and bacteria that could not be constrained by the antibiotics present in the medium. The results showed, however, that midgut cells could be maintained for more than 2 weeks in culture with a high viability for both types of cell. Cell types became difficult to distinguish from each after this time.

Viability of the cells in suspension remained high throughout the experiment, rarely falling below 80%, however, the viability of cells on the substratum was low in comparison. Other putative adhesive substrates, including collagen, concanavalin A, fibronectin and laminin, had been tested in preliminary experiments and they too failed to stimulate midgut cell adhesion (J.Peacock Honours project) It may be that a prerequisite for adhesion of midgut cells is cell death.

Figure 4.6 Midgut cell culture on gelatin polylysine coated dishes.

a. Cells attached to the substrata

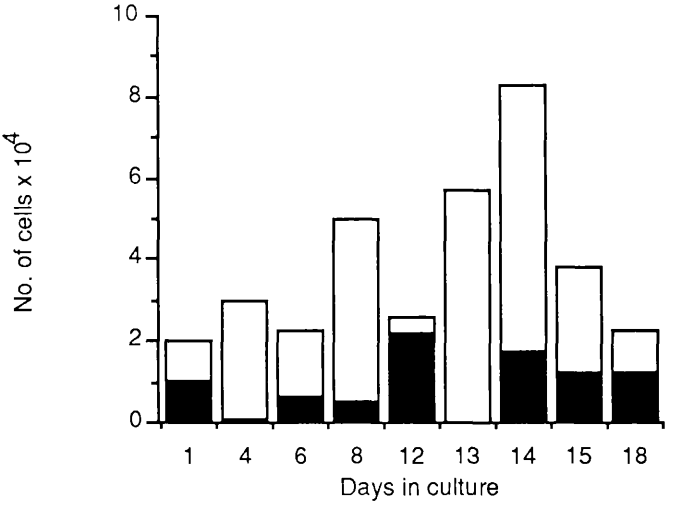

b. Cells unattached to the substrata

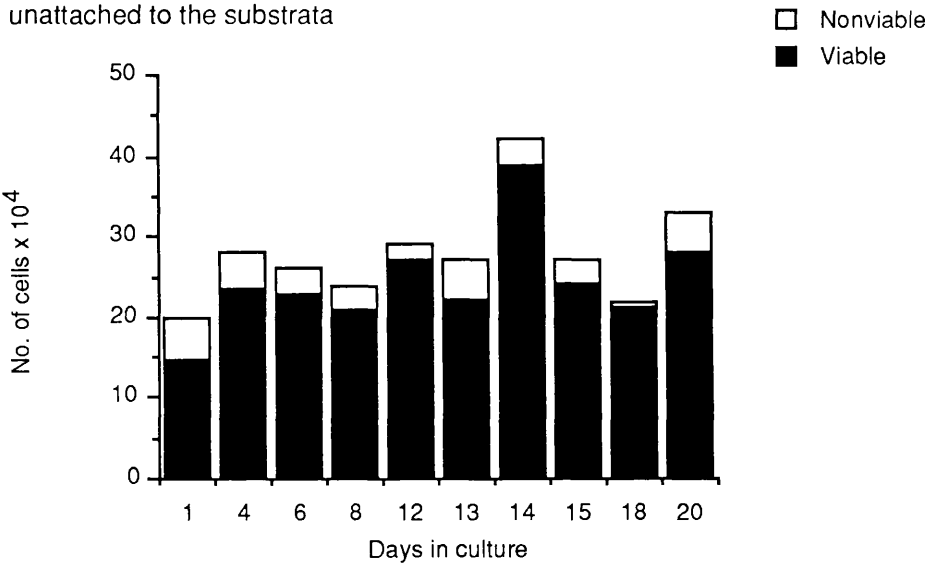

Midguts cells were plated at a concentration of 0.5 x 10^6 cells per dish onto gelatin poly-l-lysine coated dishes and were maintained in Graces medium for a period of 20 days. Cells were assayed at intervals for adhesion to the substrate and viability with FDA. a. Number and viability of cells which remained attached to the substrata after removal of the supernatant. b. Number and viability of cells which were found in the supernatant and had not therefore attached to the gelatin polylysine coated surface.

4.2.3.3. Cell Culture on Tissue Culture Plastic

Cells isolated from the midgut using the flat sheet dissociation method were plated onto tissue culture plastic dishes and incubated at 15-20°C. This temperature maintained the cells in a healthy condition whilst impeding microbial contamination.

Although there may have been some loose attachment, most of the epithelial cells remained floating in the culture medium, as with the gelatin polylysine coated dishes. In order to assess viability of cells in culture, the supernatant was removed from the dish after FDA incubation. Cells were spun down and then resuspended in 1ml of medium before counting with a haemocytometer. Cells remaining on the dish were assessed by counting the total number of cells in 10 fields, thus determining the total number of cells on the dish. The results are presented as a histogram in figure 4.7.

Viability for cells in the supernatant increased after isolation on day 0, then remained high for the duration of the culture experiment. This may have been due to non-viable isolated cells disintegrating, thus the relative viability was higher. Cells remaining on the dish, however, displayed poor viability.

The results from culture on both tissue culture plastic and gelatin/ polylysine dishes again suggest that cells which adhere to these substrata must be dead or dying in order to do so. The problem of adhesion could be partly due to the derivation of the adhesive molecules. Many are derived from mammalian and other vertebrate sources, so it is not surprising that these insect cells appear not to have receptors for them. One answer to the problem may be the basal lamina that remains after a flat sheet isolation. This could potentially be used as an adhesive surface for these epithelial cells.

The results of this culture attempt showed, however, that highly differentiated insect epithelial cells could be maintained in primary culture for at least 2 weeks without losing their morphological characteristics (Figure 4.8). Whether or not they retained their functional differences could easily be investigated, for instance using pH or voltage

Figure 4.7 Midgut cell culture on tissue culture plastic

a. Cells attached to the substrata

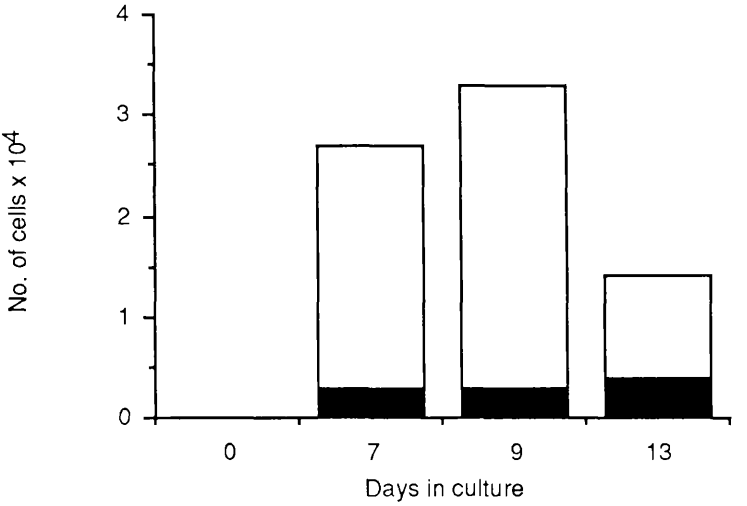

b. Cells unattached to the substrata

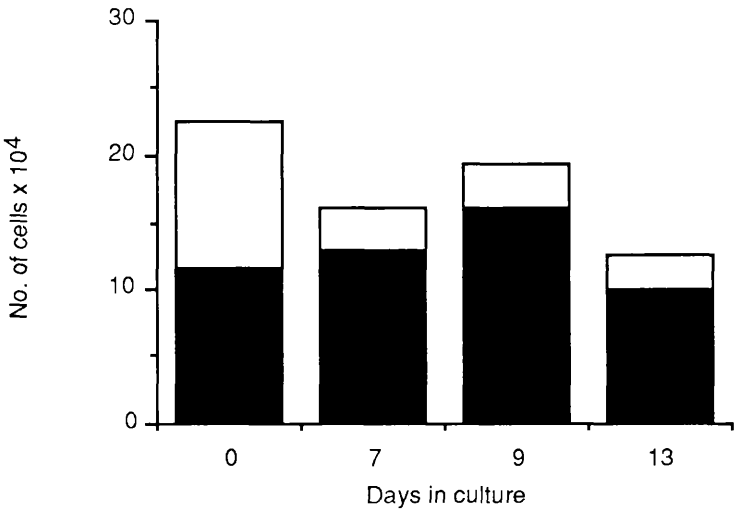

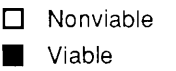

Midgut cells were plated onto tissue culture plastic at a concentration of 0.3 x 10^6 cells per dish and maintained in insect media for a period of 13 days. At intervals, cell adherence to the substrate and viability were assessed. a. Cells which attached to the substrata after removal of the supernatant. b. Cells which did not attach to the tissue culture plastic surface but remained in the supernatant.

Figure 4.8 Midgut cells maintained on tissue culture plastic for 13 days.

a. Light micrograph showing a goblet cell which has retained its characteristic morphology after 13 days in culture. The cavity and apical valve region (stalk-like structure) can be easily defined.

b Epifluorescence micrograph of (a) showing faint staining with the viability indicator fluorescein diacetate (FDA).

c. Light micrograph showing a columnar cell which has retained its characteristic morphology after 13 days in culture. The apical microvilli are still intact and the centrally located nucleus is definable.

d. Epifluorescence micrograph of (c) showing faint staining with the viability indicator fluorescein diacetate (FDA).

Scale bar = 50μm

Figure 4.8 Midgut cells maintained on tissue culture plastic for 13 days

a

b

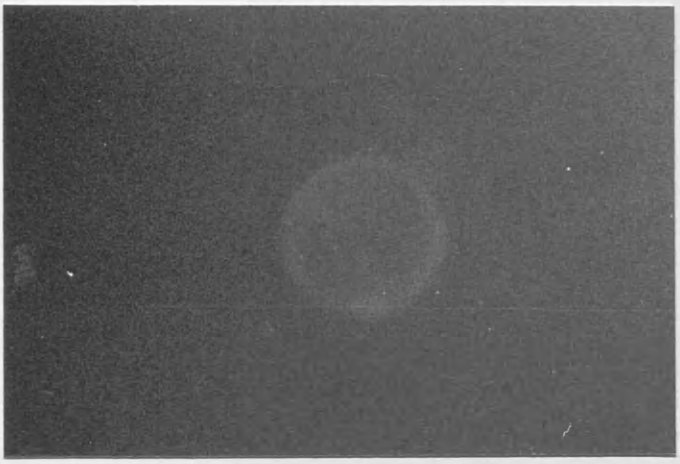

c

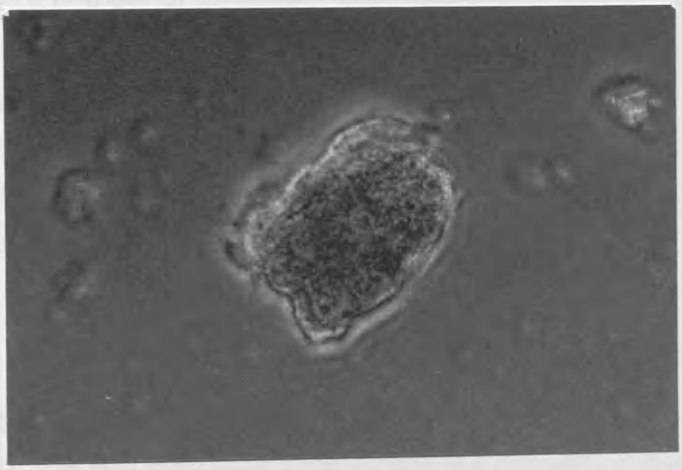

d

sensitive dyes to probe goblet cavity function. Acridine orange was used on these cells in this capacity (see chapter 5)

4.3. Discussion

Successful insect tissue culture is becoming increasingly important in a number of fields including biochemistry, endocrinology, molecular biology, physiology and virology. Cultured insect cell lines can support growth and replication of arthropod-borne parasites and viruses, making them an essential tool in the study of such pathogens. For instance, they could be used to produce virulent insect viruses and recombinant proteins using insect virus expression vectors (Fraser 1989; Hammock et al. 1990).

Of particular commercial significance is the use of an insect culture system to produce and assay for viral, and other pesticides. Many successful insecticides act primarily in the digestive tract of the insect larva, for example *Bacillus thuringiensis* δ–endotoxin runs down the electrochemical gradient in the midgut of Lepidopteran larvae and disrupts the ultrastructure of Malpighian tubule cells (Crawford and Harvey 1988; Knowles et al. 1986; Maddrell et al. 1989; Sacchi et al. 1986; Spies and Spence 1985; Wolfersberger et al. 1985). Even the viruses currently being used in insect cell culture are normally activated by gut pH and proteases (Vaughn et al. 1989). The gut is necessarily a route for all systemic insecticides and so the ability to culture cells from the insect alimentary canal would provide a useful assay system for insecticides and viruses that specifically affect these cells.

4.3.1. Enzyme Dissociation Assay

The results of the enzyme dissociation assay showed that it was possible to selectively dissociate epithelial cells from a midgut 'sac' using enzymes, with limited contamination by other cell types such as muscle, tracheal or Malpighian tubule cells. The basal lamina which separates luminally situated goblet and columnar cells from basally located muscle cells, was impervious to enzymatic degradation under the conditions employed. Some effort has been made previously to remove the basal lamina from insect epithelia by both mechanical (Koefoed 1985) and

enzymic means (Levinson and Bradley 1984). In the latter, elastase was most successful, however the incubation required was at least 1h and as the enzyme dissociation incubation required here was just 30 min, elastase treatment did not penetrate the basal lamina so there was no serious contamination problem.

Vertebrate epithelial cells have also been isolated enzymically (Kimmich 1970; Metz et al. 1977; Romrell et al. 1975). Amsterdam and Jamieson (1972) used hyaluronidase, chymotrypsin and collagenase to remove connective tissue and basal laminae from pancreatic acinar cells. Insect epithelial cells are joined by septate junctions which differ from those in other epithelia in that they can occupy approximately the apical two-thirds of the intercellular space (Bradley 1983; Lane and Skaer 1980). From these results this implies that either insect midgut septate junctional proteins have a collagen-like structure or cleavage site, or that cell:cell adhesion was broken mechanically during trituration and was therefore an indirect effect of enzyme action. Collagenase is relatively specific for digestion of the triple-helical native collagen fibres found in connective tissue and is best used for dissociation of tissues in conjunction with other proteases, such as less specific dispase. The presence of dispase did enhance cell yield but not significantly, therefore, it seems likely that mechanical disruption was partly responsible for cell isolation as all enzymes, and even the controls, yielded some single cells.

Insect basal lamina is a complex containing collagen, laminin, elastic fibres, acid and neutral mucopolysaccharides and numerous other unidentified fibrous components (Ashhurst 1968), hence the inability of 1 or 2 enzymes alone to break through in 30 min. The results with collagenase suggest that collagen is a major constituent of the basal lamina underlying *Manduca sexta* midgut epithelium and that the enzyme probably serves to release cells more effectively from this basal lamina, especially when used in combination with other less specific degradative enzymes such as dispase. Collagenase treatment has also been successful in dissociation of imaginal disc cells (Fausto-Sterling 1983; Fehon 1983) suggesting that collagen is abundant in connective tissue of various insect species (Ashhurst and Bailey 1980; Harper et al. 1967).

4.3.2. Flat Sheet Dissociation

The flat sheet dissociation method was superior to the previous 'sac' dissociation method in terms of yield. There are several possible reasons for this;

(1) The extent of inflation of a midgut sac varies depending on the integrity of the midgut tube. Fluid can also escape from the site of injection as the gut swells and forces it back out. With the flat sheet method the midgut can be stretched lumen-side upwards over a fixed area, thus the extent of stretch is reasonably constant throughout the experiment and also from one experiment to the next. This means that enzyme solutions have similar access to their site of action.

(2) As the gut is inflated with saline for the 'sac' method, any leakage during incubation would dilute the enzyme outside the sac, rendering it less effective for dissociation. There is no extra saline present in the flat sheet method meaning that enzyme concentration remains constant throughout the experiment.

(3) An added advantage for the flat sheet method is that the tissue is fixed down and so a stream of medium can be flushed over to aid release of cells from the basal lamina, whereas a 'sac' is floating and would move away from any attempt at flushing.

4.3.3. Culture

There was no apparent advantage to culturing cells on typically adhesive substrates such as collagen-, laminin-, gelatin/ polylysine- or fibronectin-coated plastic, therefore these molecules may not be sufficiently homologous to the insect molecules to provide good substrates for adhesion of insect cells (J. Peacock Honours project 1987).

Growing cells in tissue culture dishes as opposed to flasks was favourable as fewer cells were required per dish allowing more dishes to be set up per midgut for later assessment of viability and attachment. In all experiments very few cells attached to the substrate regardless of whether or not it was coated. Most cells came off when the culture medium was removed with a pipette and were therefore assayed in

suspension. The apparent lack of cell adhesion may have been due to adhesion molecules becoming enzymically or mechanically cleaved during cell isolation. Cells do not divide during the length of time in culture, as determined by a lack of increase in cell number from that initially plated, suggesting that the cells were probably terminally differentiated. However, viability of cells in the supernatant remained relatively high for periods exceeding 2 weeks. This is encouraging as it allows for manipulations to be carried out in culture where viability is of importance, such as hormonal regulation of cellular differentiation from regenerative cells and influence of various factors on cellular physiology and metabolism *in vitro*, including cell-specific effects in a heterogeneous population.

Establishment of a midgut cell line might be possible if the cells divided in culture, that is, if regenerative cells were manipulated with insect hormones. With a primary culture such as that described, many other assays are possible. Pesticides could be tested for their ability to disrupt one cell type over the other, using FDA as an indicator of viability which in turn would allow quantification of results in a spectrofluorimeter. If a cell-specific inhibitor was found it could then be applied to whole midgut mounted in an short circuit chamber to investigate electrical effects of that agonist and correlate them with the cell type affected. This would produce further information about the ion transport processes in caterpillar midgut, in particular the role played by each cell type.

Other advantages of separating isolated cells in culture include biochemical analysis of membrane constituents of one cell type. Cioffi and Wolfersberger (Cioffi and Wolfersberger 1983) attempted to isolated pure membrane fractions from the midgut epithelium using ultrasonication of epithelial pieces; however, it is likely that contamination by membranes other than those of interest would occur. Having a pure population of goblet or columnar cells would eliminate this problem and one could then search biochemically for the K^+ ATPase on both cell types. Once located it could be manipulated, for instance introducing stimulatory agents like ATP and the effects monitored using voltage-, ion- or pH-sensitive techniques such as microelectrodes or fluorescent dyes. Some preliminary experiments carried out using acridine orange staining showed that when the cells were dissociated, the cavity became acidic,

indicating that, if the model for pH generation is reliable, the K+ATPase had been switched off (Dow 1984)

On a molecular biology aspect, cDNA libraries could be set up for cells from different midgut regions to try to establish embryonic origin and presence of active ATPase. This in turn could allow a probe to be used to screen for vacuolar ATPases in order to clarify recent controversy (Dow 1984; Wieczorek et al. 1989) and ultimately to unveil mechanisms of action and control at the molecular level.

It is feasible that methods developed from insect cell culture could be applied to other invertebrate and even vertebrate tissues. These techniques would be of particular use with a heterogeneous population of cells where previous separation methods have proved unsuccessful. The ability to quickly set up and maintain a simple primary insect culture of identified origin would be invaluable for investigation into modes of action of pesticides and other agents in a cell specific manner, without the need to establish cell lines from highly differentiated tissue. This is an attractive system to use for research in this area, especially in a commercial environment such as the insecticide industry.

Chapter 5

5. Chapter 5 Acridine Orange

5.1. Introduction

Three characteristics of the midgut of *Manduca sexta* are generally accepted, regardless of whether the K^+ ATPase theory (Dow 1984) or the H^+ ATPase theory (Wieczorek et al. 1989) is applied, and these are; (1) There is a large electrical potential difference across the goblet cell apical membrane (Dow and Peacock 1989; Moffett and Koch 1988a), (2) Potassium is transported from basal to apical side of the midgut (Dow et al. 1984; Dow and Harvey 1988; Harvey et al. 1983a; Moffett et al. 1982; Moffett and Koch 1988a; Moffett and Koch 1988b) and (3) pH in the midgut lumen is very alkaline (Berenbaum 1980; Chamberlin 1990; Dow 1984).

According to the model of Dow (1984) and the estimations from microelectrode measurements of cavity membrane potential (see Chapter 3), the predicted pH within the cavity is approximately 11.6, i.e. alkaline (Dow and Peacock 1989). However, when considering the model of Wieczorek et. al. (1989) in which protons are pumped into the cavity energizing a proton/ K^+ electroneutral exchange, the expected pH in the cavity would not be alkaline, but slightly acidic. It has in fact recently been reported that the measured pH in the cavity in the posterior region is 7.2 (Moffett et al. unpublished). This region however, is not thought to be involved in luminal alkalinization and measurements of pH in the anterior and middle regions may prove to be higher (Dow 1984).

The work presented in this chapter was carried out to investigate the pH characteristics of the midgut tissue in general, and goblet cavities in particular, especially in the middle region, under control conditions and conditions in which the pH was manipulated. The properties of a fluorescent weak base, acridine orange, were exploited as a possible probe of pH in the goblet cavity.

5.1.1. General Properties of Weak Bases

Weak bases, such as neutral red and acridine orange, accumulate in acidic compartments and also cause formation in the cytoplasm of large

vacuoles (Figure 5.1). de Duve et al. (1974) proposed a theory to account for this accumulation in lysosomes (de Duve et al. 1974).

Three assumptions were made:
(1) Plasma and lysosomal membranes are highly permeable to the neutral forms of weak bases.
(2) These membranes are mostly impermeable to the protonated forms of the weak bases.
(3) The pH inside the lysosomes is lower than it is outside.

The consequences are:
(1) Neutral weak bases, which diffuse freely across the lysosomal membrane, are trapped by protonation and so accumulate in the lumen of the lysosomes.
(2) When concentration of the base inside the lysosomes approaches isotonicity, water enters osmotically and the lysosomes swell to form large vacuoles.
Thus the pH within the lysosome rises in the presence of weak bases.

Fig 5.1 Model of lysosomal pH maintenance and uptake of weak bases

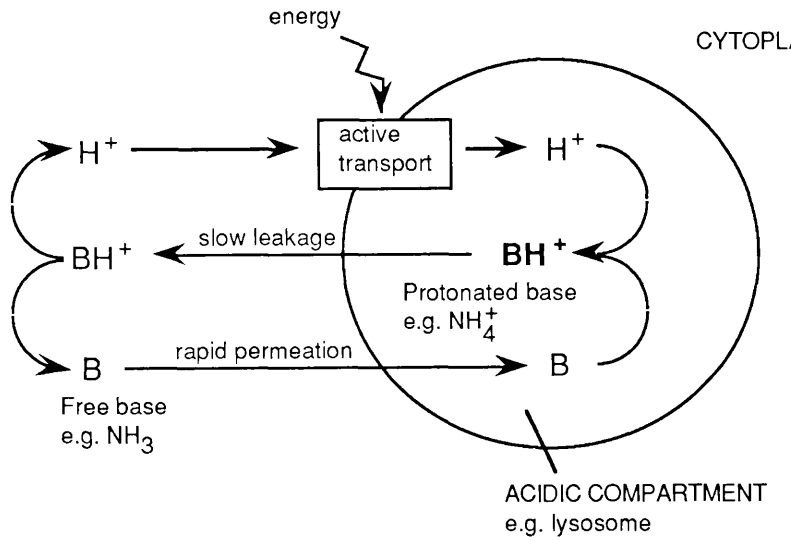

An acidic compartment is maintained at low pH by active transport of protons into the lumen of the vesicle. This requires energy often in the form of ATP which fuels a proton ATPase. Weak bases in the free form (B) rapidly permeate the vesicle membrane and once inside become protonated (BH^+). The protonated form of the weak base does not readily cross the membrane and so there is net accumulation of the base within the acidic compartment, causing osmotic influx of water. Protons consumed by the weak base during this cycle result in raised pH within the vesicle.

The vacuoles that form after exposure, correspond to an increased uptake of weak base. The increase in lysosomal volume is the consequence of osmotic uptake of water, but, by increasing the osmotic potential of the medium the size of the vacuoles in treated cells should decrease (Ohkuma and Poole 1981).

Another weak base which accumulates in acidic compartments is ammonium. It is the concentration of the free base form (NH_3) in medium that determines uptake and vacuolation. The protonated base (NH_4^+) has no effect on intralysosomal pH, nor does the pH of the medium. With a concentration of 10 mM NH_4Cl, lysosomal pH can be raised from 4.6 to 6.3 and sustained until it is removed from the medium by rinsing (Poole and Ohkuma 1981).

The effective concentration range of NH_4Cl is 10^{-5} M - 10^{-4} M. The cytoplasmic pH is relatively unaffected by the pH of the medium, meaning that the relative concentration of free and protonated base in medium can be controlled by changing medium pH, without affecting intralysosomal pH.

In the absence of base, some energy dependent mechanism (an ATPase) transports H^+ into lysosomes producing a proton concentration gradient. In the presence of weak base, the free base form diffuses rapidly across the plasma and lysosomal membranes. Due to acidity inside lysosomes, the base is trapped there by protonation and the concentration builds up.

Osmotic influx of water causes the lysosomes to swell. However, the finite diffusion rates of the protonated base out of the lysosome and down the very large concentration gradient that is formed, limit the process and increase the intralysosomal pH by transporting H^+ out, thereby partially short-circuiting the "proton pump". Differences in back diffusion rates of different bases explain the different response of pH change, vacuolation and base uptake.

There are two phases for uptake of weak bases into lysosomes:

(1) A steady state is rapidly attained when protonated base leakage balances H^+ pumping with the pH inside the lysosomes at a steady, elevated value.

(2) Accumulation of the base continues and the lysosomal compartment swells progressively to provide room for more base.

If leakage rate of H^+ out is low, pH within vacuoles could be maintained using little energy. In the presence of weak bases, however, energy is required to replace the H^+ that are consumed in the protonation of the incoming free base.

With 10mM NH_4Cl the pH difference is ~ 1.5, therefore the difference between chemical potentials of H^+ inside and outside the lysosomes (ignoring membrane potential effects) is;

$$\Delta\mu = RT \ln (H_i / H_o) = 2(310) \ln 32 = 9 \times 10^3 \text{ J mol}^{-1}$$

Work performed is;

$$5 \times 10^{-8} (9 \times 10^3) = 4.48 \times 10^{-4} \text{ J min}^{-1} \text{ mg protein}^{-1}$$

Heat production in mouse macrophages has been measured at 4.18 mJ min^{-1} mg $protein^{-1}$, thus even under stress of 10 mM NH_4Cl, the additional work of pumping H^+ into lysosomes is within the capacity of the cells (Ohkuma and Poole 1981).

5.1.2. Properties of Acridine Orange

Acridine orange similarly accumulates within acidic compartments and has been used widely as a tool for studying the acidification mechanism of organelles such as lysosomes and liposomes containing reconstituted membrane proteins, the vacuolar H^+ ATPases in particular (Decker et al. 1985; Harikumar and Reeves 1986; Moriyama et al. 1982; Pope and Leigh 1988; Rabon et al. 1983). It is also used by histologists and biochemists as it differentially stains DNA green and RNA red.

As with other weak bases, acridine orange crosses membranes in the free form and accumulates due to protonation. The advantage of using

this, as opposed to other weak bases, as a visual (fluorescent) pH probe is that acridine orange undergoes a metachromic shift to red fluorescence emission when concentrated within a compartment. For this reason it was chosen as the probe for investigating pH changes in goblet cavities under various conditions.

5.1.3. Acridine Orange as a pH probe in the Midgut

Preliminary experiments showed that when cells were dissociated from the ion transporting epithelium, goblet cell cavities, which are the site of active transport, appeared to stain red indicating acidity in this compartment, whereas columnar cells, the nutrient absorbing cells of the gut, stained green. This was probably due to acridine orange binding to DNA in organelles, such as mitochondria, which are dispersed throughout the cytoplasm.

In a healthy intact midgut displaying a high transepithelial potential (TEP), it was found that both cell types displayed green cytoplasm, but goblet cavities remained unstained and appeared black under U.V. epifluorescence. If the gut was not actively transporting ions, then the cavities stained red as with the cavities of isolated goblet cell (Figure 5.2). This lends support to the theory that active transport is closely linked with generation of high pH in the gut lumen and possibly in the cavities (Dow 1984; Dow and Peacock 1989).

The conditions for accumulation of acridine orange within the cavity were investigated in both isolated cells and intact epithelia. Various manipulations were carried including attempts to artificially raise or lower the pH of the cavity and also to inhibit or enhance transepithelial potential, following which acridine orange staining patterns were observed.

5.2. Results

5.2.1. Isolated Cell Studies

An average of 0.9×10^6 cells g^{-1} of midgut tissue were isolated from the midgut epithelium following enzymic dissociation. The isolated cells were

Figure 5.2 Effect of Ion Transport Competence on Acridine Orange Accumulation

a. Actively transporting epithelium

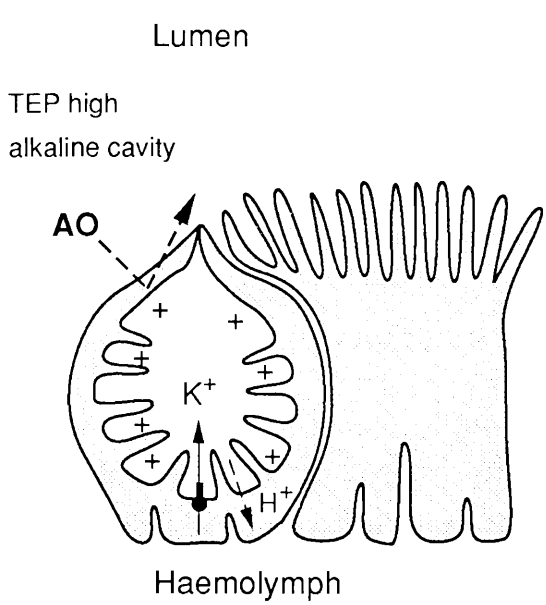

Acridine orange staining pattern.

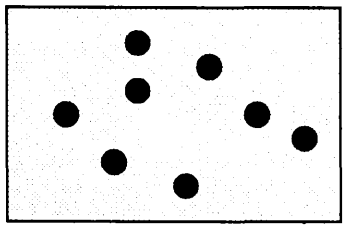

Goblet cavities appear as black holes on a green fluorescence background.

Electrogenic transport of potassium ions into the cavity electrically polarises the membrane (inside positive) which in turn drives protons out, rendering the cavity alkaline. Acridine orange (AO) does not accumulate, as it is not rendered membrane impermeable by protonation.

b. Non-transporting epithelium

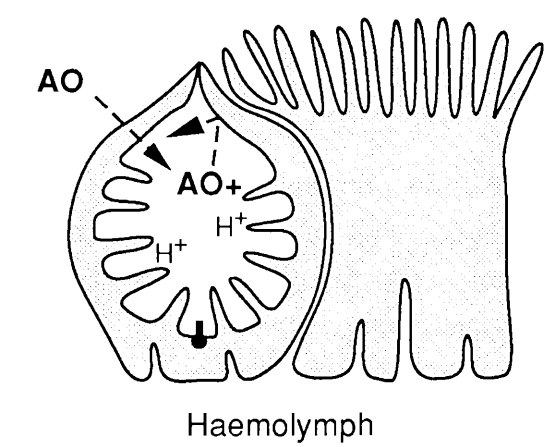

Acridine orange staining pattern.

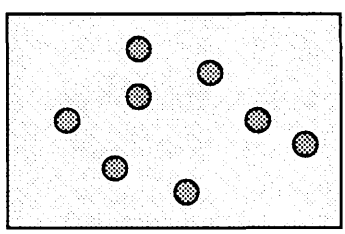

Goblet cavities appear as red circles on a green fluorescence background.

When there is no electrogenic ion transport, protons remain in the cavity rendering it acidic. Acridine orange passively enters the cavity in the membrane permeable form (AO), but becomes protonated and therefore membrane impermeable (AO+). The accumulation of AO+ induces a hyperchromic shift to red fluorescence emission.

subjected to various experimental conditions and the resulting acridine orange staining patterns observed and quantified.

5.2.1.1. Control Staining.

Figure 5.3a is a histogram showing the staining patterns of cells isolated under "normal" conditions. Photomicrographs of control isolated cells are shown in Figure 5.3b and c. The effect of enzymic dissociation using the flat sheet method was compared with the sac isolation method. Collagenase dispase was used as this was found to be the most effective enzyme for dissociation of viable midgut cells (see Chapter 4).

There were proportionally fewer goblet cells staining red with acridine orange when the sac method was applied, suggesting that goblet cavities were more acidic when isolated from a flat sheet. This could have been caused by over-exposure of cells to the enzyme, or some other experimental parameter, during flat sheet isolation, as the epithelium was stretched in such a way that there was greater access to the folds of the tissue. This extent of stretching, and access by the enzyme, was not achieved during sac dissociation.

The inclusion of exogenous ATP during sac dissociation, in an attempt to enhance pump activity and render cavities alkaline, had no effect on reducing red fluorescence in the sample, probably because ATP would not readily cross the cell membrane in this form and therefore did not gain access to the catalytic site of the pump.

The results of a control isolation replacing the enzyme with serum-free Graces medium, which repeatedly yielded cells of high viability despite low cell numbers (Chapter 4), are also presented. The number of cells obtained was only 0.07×10^6, however, there was a significant reduction in the percentage of goblet cells accumulating acridine orange, indicating that in the absence of enzyme less cavity acidification occured. Collagenase dispase may have had a detrimental effect on the isolated cells which resulted in more goblet cavities becoming acidic.

The effect of omitting O_2 gassing of the dissociation chamber did not significantly enhance red fluorescence emission as might be expected, suggesting that oxygenation, to this extent, did not help to maintain

Figure 5.3 Acridine orange staining: Flat sheet vs Sac dissociation

a. Acridine orange differential staining of midgut cells isolated using either the flat sheet dissociation method (bars on the left of the histogram) or the sac dissociation method (bars on the right). Cd is collagenase dispase, Graces is Graces medium used as a control for enzymic dissociation, O_2 is oxygenated conditions, non O_2 is non-oxygenated conditions, 60' and 30' is the length of time of incubation in minutes. Percentage acumulation of acridine orange in goblet cell cavities (top histogram) is compared with accumulation in columnar cells (lower histogram) ± S.E.M. (n=4).
Statistics: The asterisks denote significant differences in goblet red staining between CD flat sheet dissociations and the Graces contols. These values were also significantly different from those obtained during sac dissociation.

b. Light micrograph of an isolated columnar cell (left) and goblet cell (right).

c. Epifluorescence micrograph of (b) showing acridine orange differential staining of the 2 midgut cell types. The columnar cell emits green fluorescence whereas the goblet cell emits red fluorescence due accumulation of acridine orange in the cavity. Goblet cytoplasm, although sparse, can be seen to emit some green fluorescence, as can the flattened nucleus near the base of the cell.

Scale bar = 50μm

Figure 5.3 Acridine Orange staining: Flat Sheet vs Sac Dissociation

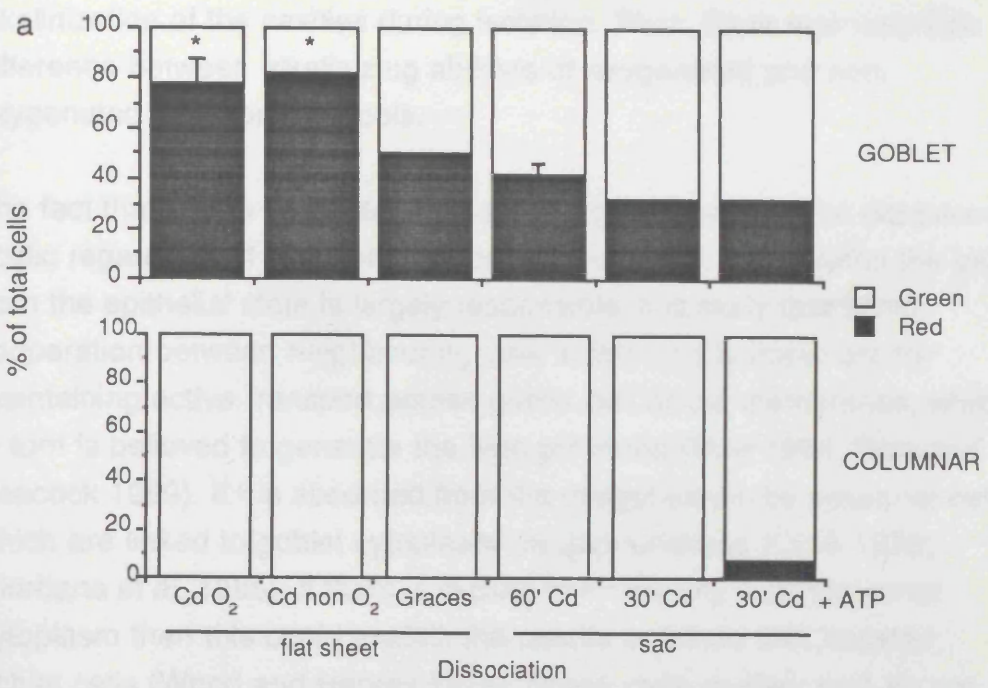

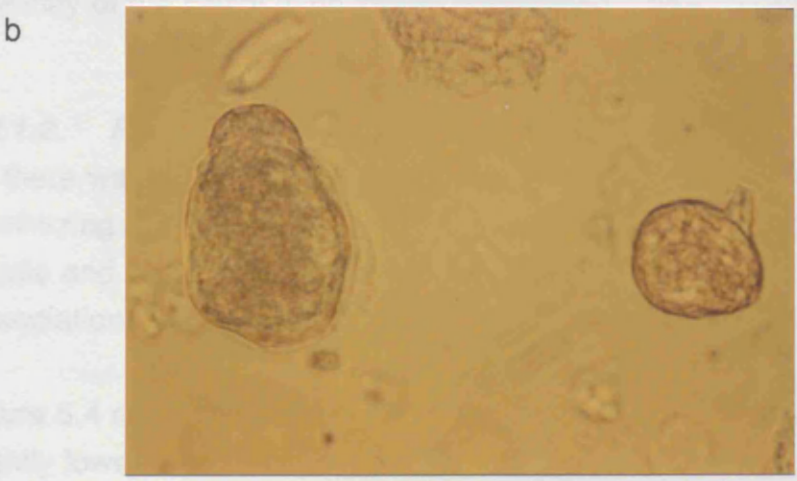

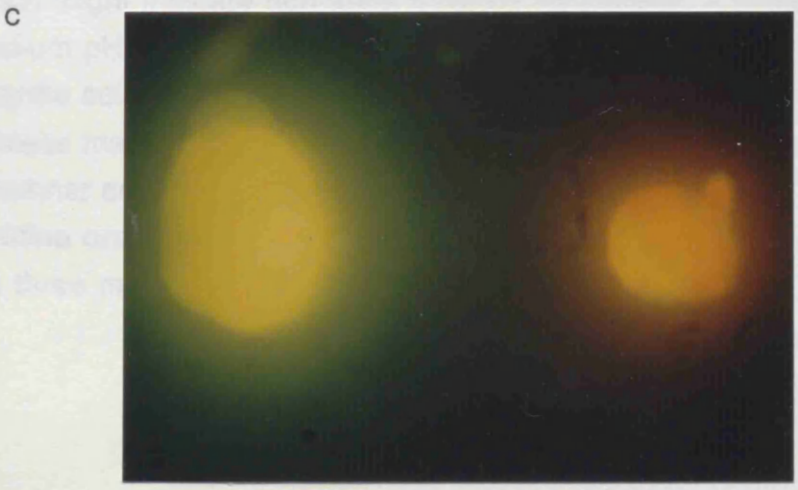

alkalinization of the cavities during isolation. Thus, there was very little difference between alkalinizing abilities of oxygenated and non-oxygenated isolation protocols.

The fact that a high percentage of isolated goblet cell cavities did become acidic regardless of isolation protocol suggests that dissociating the cells from the epithelial state is largely responsible. It is likely that some cooperation between neighbouring cells exists and is important for maintaining active transport across goblet cell apical membranes, which in turn is believed to generate the high pH found (Dow 1984; Dow and Peacock 1989). K^+ is absorbed from the midgut lumen by columnar cells which are linked to goblet cytoplasm via gap junctions (Cioffi 1979; Giordana et al. 1985). If there is cycling of K^+ directly from columnar cytoplasm then this could explain the results obtained with isolated goblet cells (Wood and Harvey 1979). These cells on their own do not have a large enough K^+ ion pool, so transport rapidly stops and the alkalinity of the cavity is no longer maintained.

5.2.1.2. Regional Differences

As there was thought to be differences in the ion transporting and alkalinizing abilities of the three midgut regions (Dow 1984), anterior, middle and posterior regions were separated before flat sheet dissociation and the resulting cells stained with acridine orange.

Figure 5.4 reveals that the ratio of red goblet cells: green goblet cells was slightly lower in cells from the middle region although not significantly so. An unusual finding was that ~25% of the columnar cells also stained red, which might indicate non-ideal isolation conditions. A change in the medium pH could have affected columnar cytoplasmic pH, or if the enzyme solution used had a lower activity than usual, then the flushing process may have been rather vigorous causing damage to sensitive columnar cells. In general though, there is no significant difference in acridine orange accumulation within cavities of goblet cells isolated from the three midgut regions.

Figure 5.4 Acridine Orange: Regional staining of the midgut

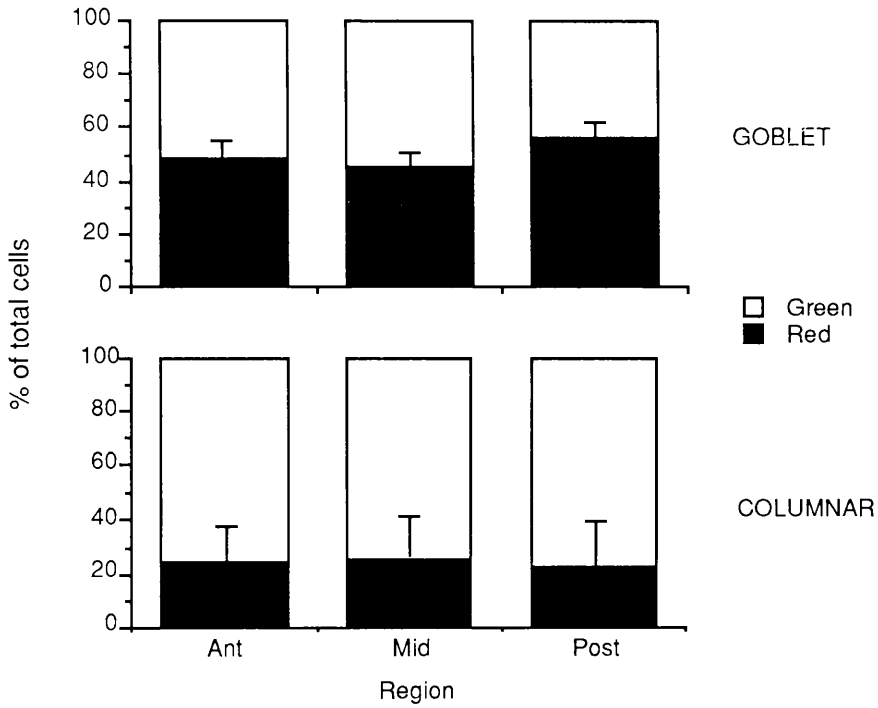

Acridine orange differential staining of midgut cells isolated from three separate regions of the midgut, using collagenase dispase under oxygenated conditions. Ant = anterior midgut, Mid = middle midgut and Post = posterior midgut. The histogram bars display the ratio of green to red staining for each cell type ±S.E.M. (n=2)

Statistics: There was no significant diference in % red staining of goblet cells between the 3 midgut regions.

5.2.1.3. Manipulating the pH within the Cavity

In order to confirm that the red staining seen within isolated goblet cell cavities was due to accumulation of acridine orange as the cavities were rendered acidic, the pH was raised using a lysosomotropic agent, NH_4Cl (Makarow and Nevalainen 1987; Ohkuma and Poole 1981; Poole and Ohkuma 1981; Rothman et al. 1989). This, like acridine orange, is a weak base which crosses membranes of acidic vesicles in the form of NH_3 and then becomes protonated producing NH_4^+. The protonated form is membrane impermeable and does not readily leave the vesicle, so as protons are consumed, the vesicle pH is raised (Poole and Ohkuma 1981). Indeed, NH_4Cl reduced acridine orange accumulation in cavities in a dose-dependent manner (figure 5.5). 100-200mM NH_4Cl was optimal for inhibiting that accumulation.

There are two possible explanations, both of which result in the same basic conclusion that the red cavities of isolated goblet cells were acidic. (1) NH_4Cl raised the pH within the cavity and acridine orange molecules were no longer trapped by protonation, as there would be a lack of protons in the alkalinized cavity. (2) There could have been competition for the protons in the acidic cavity and NH_3 had a higher affinity for them than unprotonated acridine orange. This second point was highlighted by the finding that pre-stained red cavities were rendered unstained upon administration of NH_4Cl (fig 5.5b and c).

At present it is not known to what extent pH was raised by NH_4^+, however it requires only 10 mM NH_4Cl to raise the pH of yeast vacuoles by 2 units (Poole and Ohkuma 1981). NaCl was used as a control in these experiments to ensure that the observed effect was not due to increasing the Cl^- concentration or the osmotic pressure. For all concentrations of NaCl, ranging from 10-200 mM, the percentage of goblet cells staining red was 60-70%, a value comparable with control levels. The small reduction in red staining compared with controls could have been due to an effect on Cl^- conductance, but as some swelling of the goblet cavities was observed, it is probable that the increase in volume of the compartment led to a reduction in acridine orange concentration without a direct pH affect. Alternatively, as some swelling was seen, perhaps percentage red staining was slightly reduced by lysis of the cavities. This could also be partly responsible for the reduction of red staining in NH_4Cl

Figure 5.5 Acridine orange staining: Effects of Ammonium chloride

a. Ammonium chloride affects the ratio of acridine orange differential staining of isolated midgut cells in a dose-dependent manner. Increasing mM concentrations of NH_4Cl in standard *Manduca* saline were tested and compared to increasing concentrations of NaCl in standard *Manduca* saline (control). Histogram bars display the ratio of red to green staining for both cell populations ± S.E.M. (n=2).
Statistics: All NH_4Cl treatments were significantly different from equivalent concentrations of NaCl with respect to red: green staining of goblet cells,as indicated on the graph by the asterisks. There was also significantly less red staining in 100 and 200mM NH_4Cl compared with 50 (and 10) mM.

b. The epifluorescence micrograph shows no acridine orange red staining in the cell suspension after exposing cells to 200mM NH_4Cl. Goblet cavities were therefore rendered non-acidic upon treatment and did not accumulate acridine orange.

c. In the control, cells were exposed to 200mM NaCl. The micrograph shows a large proportion of the goblet cells in the sample staining red after accumulation of acridine orange in the acidic cavities.

Scale bar = 100μm

Figure 5.5 Acridine Orange staining: Effects of Ammonium Chloride

a

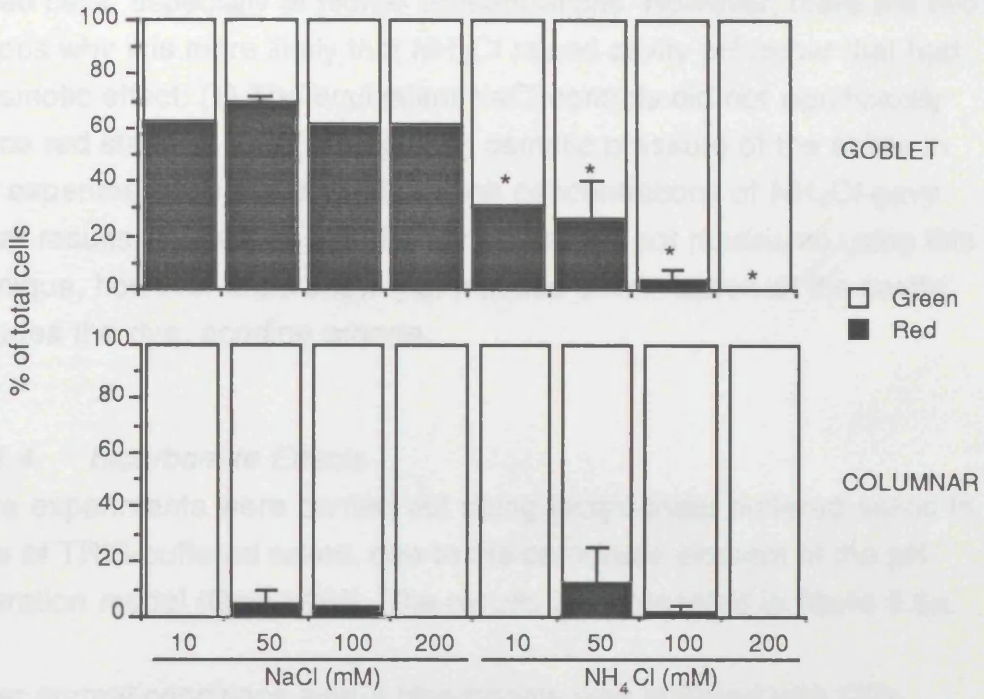

b

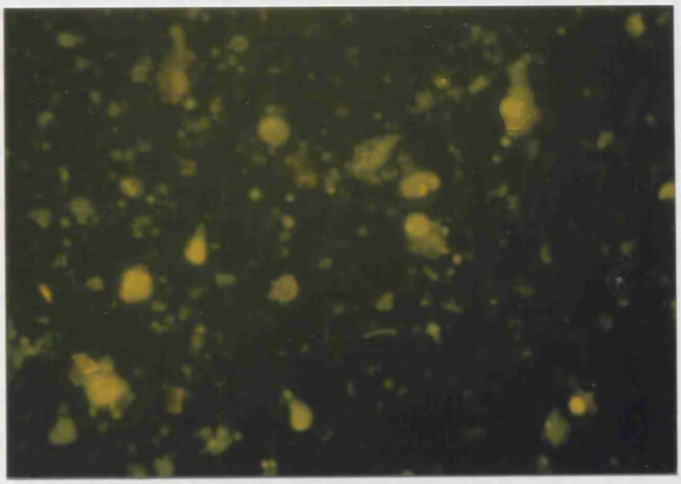

c

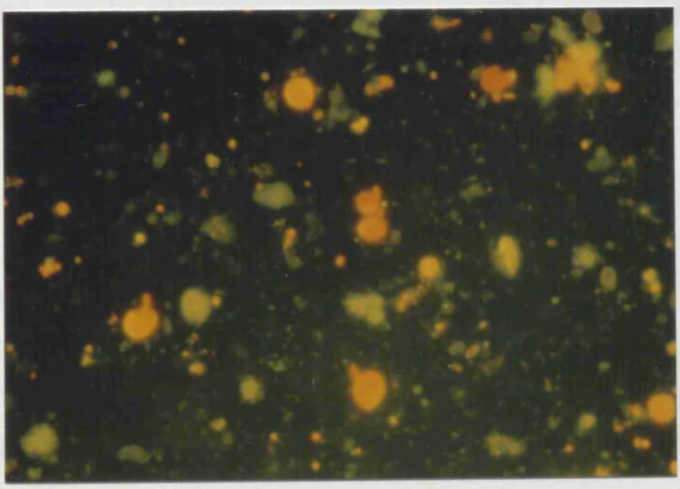

treated cells, especially at higher concentrations. However, there are two reasons why it is more likely that NH_4Cl raised cavity pH rather that had an osmotic effect; (1) The equivalent NaCl controls did not significantly reduce red staining, and (2) Adjusting osmotic pressure of the saline in later experiments to accommodate high concentrations of NH_4Cl gave similar results. The actual pH of the cavities was not measured using this technique, however it did show that induced alkalinization of the cavity excludes the dye, acridine orange.

5.2.1.4. Bicarbonate Effects

Some experiments were carried out using bicarbonate buffered saline in place of TRIS buffered saline, due to the carbonate element of the pH generation model (Dow 1984). The results are presented in figure 5.6a.

Under normal conditions where bicarbonate was buffered with CO_2, approximately 50% of goblet cells stained red (Fig 5.6b), which was lower than the value obtained when oxygenated TRIS saline was used (Figure 5.3). Addition of azide should deplete the energy source for active transport (ATP); however, it did not result in significantly increased goblet cavity acidification. The pump itself is not sensitive to azide (Schweikl et al. 1989; Schweikl et al. 1987; Wieczorek et al. 1986), but the mitochondria supplying ATP for the pump would be inhibited. As the concentration of $NaHCO_3$ was increased from 10 to 20 mM, there was an insignificant reduction in the ratio of red goblet cells, however columnar cells also accumulated the dye with 60% staining red. The presence of external bicarbonate in this sample may have buffered the columnar cytoplasm, or the vesicles within, to an acidic pH. However, the 20mM solution was not gassed with CO_2 or O_2, and may therefore have been slightly alkaline due to equilibration with O_2 in the atmosphere. The resulting pH gradient across the columnar cell membranes may have caused the effects seen.

Gassing with oxygen in the presence of bicarbonate serves to alkalinize the saline as CO_2 is driven out (Burton 1975). The pH gradient between external medium and internal compartments would then be steeper than before and may therefore explain the enhanced accumulation of acridine orange within the cavities of cells subjected to these conditions. Columnar red staining was also slightly higher. More care should

Figure 5.6 Acridine orange staining: Effects of Bicarbonate buffering

a. Bicarbonate buffering affects the ratio of acridine orange differential staining of isolated midgut cells. [10] and [20] = concentration (in mM) of sodium bicarbonate in in *Manduca* saline. O_2 = oxygenation, CO_2 = gassing with carbon dioxide. Wher no gas is specified, the cell isolation chamber was not gassed. NaCl is a control for addition of Na azide, both of which were present at a concentration of 10mM. Histogram bars display the ratio of red to green staining for both cell populations (n=1).
Statistics: Only oxygenation of bicarbonate saline significantly increased the % red staining of goblet cells. Both oxygenation and azide enhanced red staining of columnar cells compared with their respective controls. 20mM bicarbonate (not gassed) also enhaced red columar cell staining even compared with oxygenation of 10mM bicarbonate. Significant differences are indicated on the graph by asterisks.

b. The epifluorescence micrograph shows a goblet cell which has accumulated acridine orange in the cavity and in particular around the apical valve region. Some goblet cavities appear unstained possibly due to continuing active transport, after cell isolation, which maintains non-acidic cavities. A columnar cell is also shown emitting green fluorescence.

Scale bar = 50μm

Figure 5.6 Acridine Orange staining: Effects of Bicarbonate Buffering

a

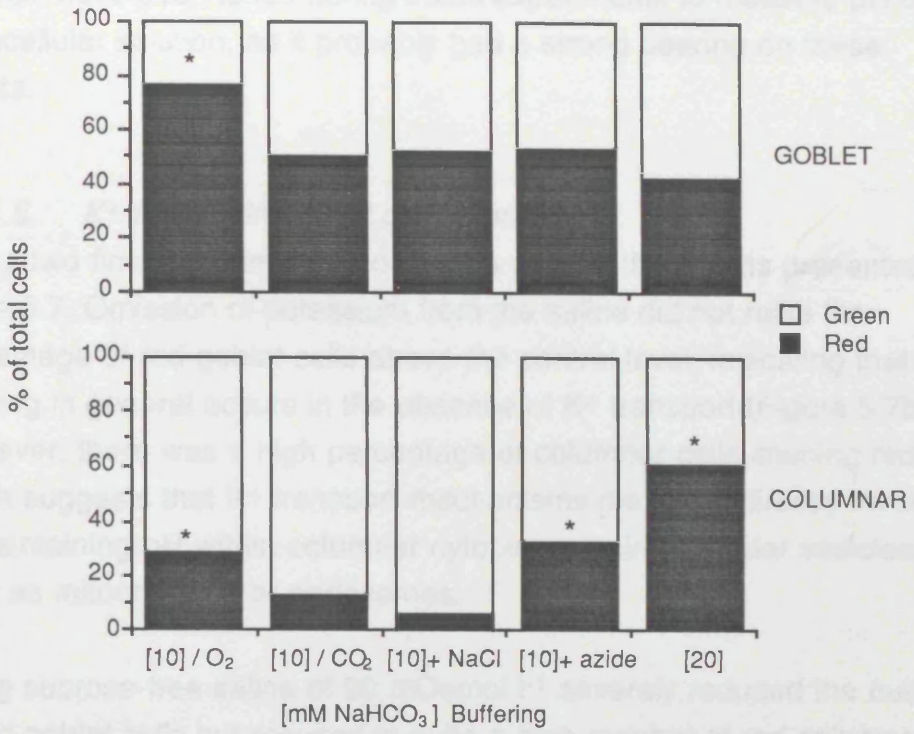

b

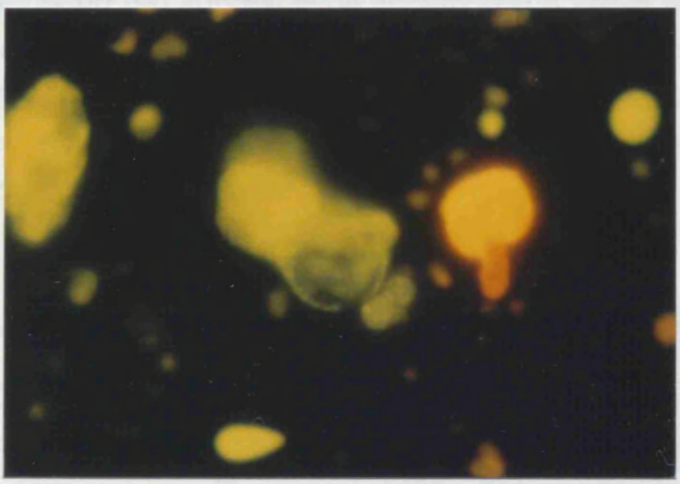

perhaps have been taken during these experiments to measure pH of the extracellular solution, as it probably had a strong bearing on these results.

5.2.1.5. K^+-free Saline and Low Osmolality

These two final experimental conditions yielded the results presented in figure 5.7. Omission of potassium from the saline did not raise the percentage of red goblet cells above the control level, indicating that red staining in general occurs in the absence of K^+ transport (Figure 5.7b). However, there was a high percentage of columnar cells staining red, which suggests that K^+ transport mechanisms may be indirectly involved in maintaining pH within columnar cytoplasm or intracellular vesicles, such as mitochondria or endosomes.

Using sucrose-free saline of 90 mOsmol l^{-1} severely reduced the number of red goblet cells but resulted in quite a high number of red columnar cells. Intracellular compartments swell under these conditions as the cavity did, thus the volume to be occupied by acridine orange was greater and would require a higher degree of dye protonation to fill it. Hence the reduced red fluorescence accumulation within the cavity. Many cavities probably swelled and burst and this may be the real reason for the low percentage of red staining. The enhanced red fluorescence seen in columnar cells was probably an effect of the osmotic imbalance.

5.2.2. Intact Epithelium Studies: Transepithelial Potential (TEP)

5.2.2.1. Control Conditions

The middle midgut region was mounted in an Ussing-type chamber adapted for midgut tissue (Dow et al. 1985). This enabled transepithelial potential to be monitored under various experimental conditions. Acridine orange staining following TEP measurement, gave an indication of the pH status of the epithelium, in particular of the goblet cavities in the intact tissue.

Figure 5.8a shows TEP traces recorded from midguts under control conditions, i.e. normal oxygenated saline. Transport-competence was

Figure 5.7 Effect of no K^+ and low osmotic pressure on acridine orange staining

a. The effects of potassium-free saline and sucrose-free saline on acridine orange differential staining of isolated midgut cells. K^+-free saline was made by substituting 22mM KCl for 22mM choline chloride in standard *Manduca* saline. 90mOsmol l^{-1} saline is the calculated osmolality of sucrose-free saline. Histogram bars display the ratio of red to green staining for each cell type (n=1).
Statistics: Asterisks indicate a significant difference in % red staining compared with control conditions.

b. The epifluorescence micrograph shows a goblet cell in K^+ free conditions with a bright red cavity indicating strong accumulation of acridine orange into an acidic compartment. A columnar cell is also pictured displaying the green fluorescence emission characteristic of control cell staining.

Scale bar = 50μm

Figure 5.7 Effect of no K^+ and low osmotic pressure on acridine orange staining

a

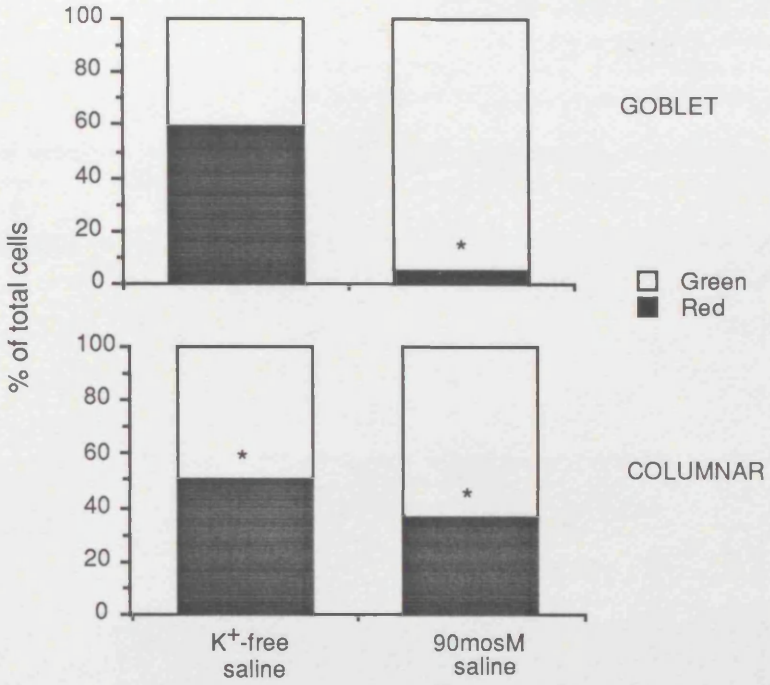

b

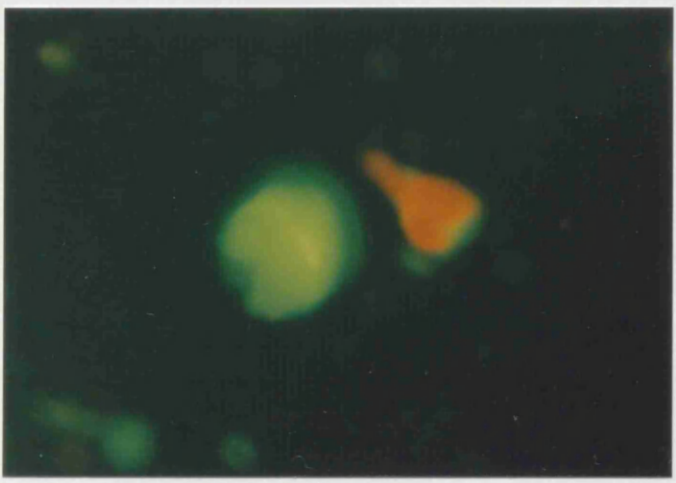

Fig 5.8 TEP of middle midgut; Standard saline.buffered with 100% O_2

a. Transepithelial potential difference (TEP) of isolated middle midgut bathed in normal oxygenated saline. Acridine orange was added to each side of the epithelium 5 min before termination of the experiment. Original chart recordings were converted into the graph shown. Traces from 2 separate experiments are shown.

b. Light micrograph of the middle midgut mounted on an open circuit chamber for monitoring TEP.

c. Epifluorescence micrograph of (b) showing little or no accumulation of acridine orange within cavities, which coincides with electrogenic ion transport (high TEP).

Scale bar = 50μm

Figure 5.8. TEP of middle midgut: Standard saline buffered with 100% O_2

a

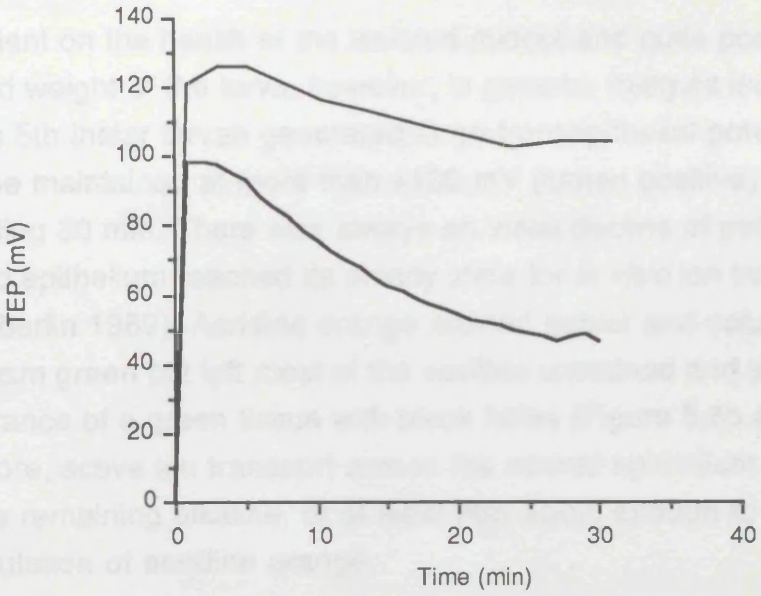

b

c

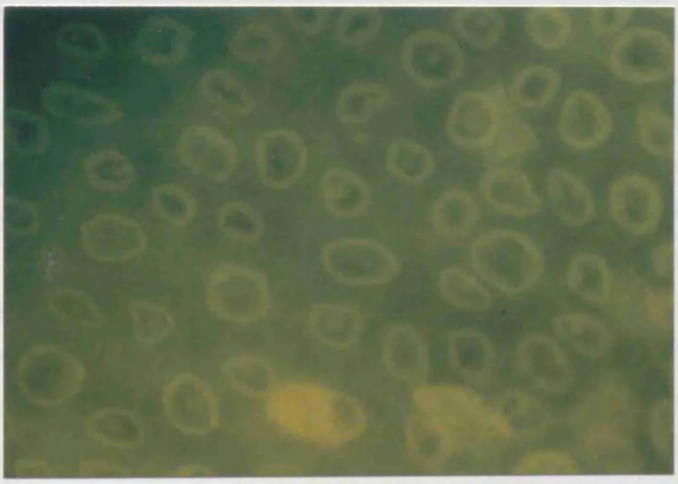

dependent on the health of the isolated midgut and quite possibly the age and weight of the larva, however, in general, midguts isolated from feeding 5th instar larvae generated large transepithelial potentials which could be maintained at more than +100 mV (lumen positive) for periods exceeding 30 min. There was always an initial decline of potential as the isolated epithelium reached its steady state for *in vitro* ion transport (Chamberlin 1989). Acridine orange stained goblet and columnar cell cytoplasm green but left most of the cavities unstained and so gave the appearance of a green tissue with black holes (Figure 5.8b and c). Therefore, active ion transport across the normal epithelium resulted in cavities remaining alkaline, or at least non-acidic enough to prevent accumulation of acridine orange.

Occasionally some cavities were seen to be filled with a pale green fluorescence which may indicate a certain amount of protonation of acridine orange. Also there appeared to be patches of differential staining suggesting possible localized active transport (Cioffi and Harvey 1981).

5.2.2.2. K^+-free Conditions

From the model for active K^+ transport, the electrogenic step is the pumping of K^+ ions across the goblet cavity membrane, which drives H^+ from the cavity resulting in alkalinization (Dow 1984). If this is so, then omitting K^+ from the saline bathing the gut should result in loss of transepithelial potential, as there is no electrogenically transportable ion present. H^+ would no longer be driven back across the membrane and acidification should occur.

Figure 5.9a shows the effects on TEP of omitting K^+. TEP began reasonably high at around 60-80 mV but quickly declined towards zero as the residual K^+ within the tissue was utilised. Often the membrane potential was reversed producing negative values, possibly reflecting other transport processes that become evident following elimination of electrogenic K^+ transport. Under these conditions, acridine orange readily accumulated within cavities and underwent a hyperchromic shift to red fluorescence emission (Figure 5.9b). Addition of 22mM KCl to both sides of the epithelium reversed the decline of TEP, which then fell at a slower rate, comparable to the decline rate in control tissues.

Figure 5.9. TEP of middle midgut: K^+ -free saline

a

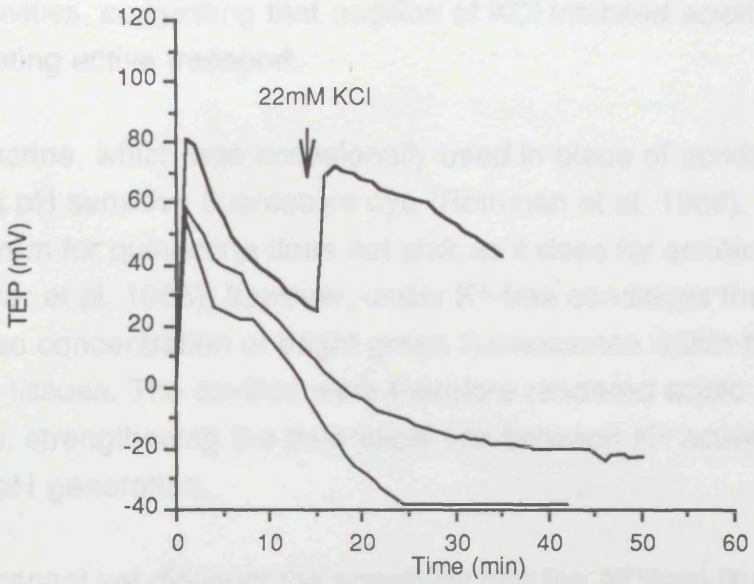

b

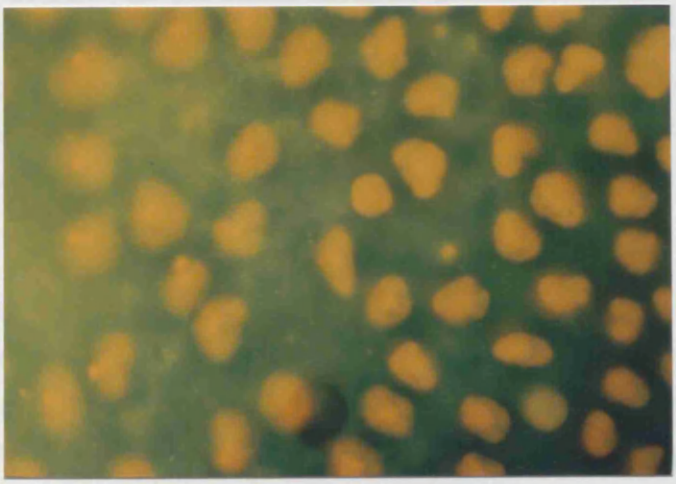

a. Transepithelial potential difference (TEP) of isolated middle midgut bathed in potassium-free saline. The arrow indicates addition of 22mM KCl to the bathing solution (upper trace only). Acridine orange was added to each side of the epithelium 5 min before the end of recording. Traces from 3 separate experiments are presented.

b. Epifluorescence micrograph showing accumulation of acridine orange within cavities, coincident with low TEP caused by omitting K^+ from the bathing solution.

Scale bar = 50μm

This maintenance of TEP was accompanied by a lack of red staining in the cavities, suggesting that addition of KCl inhibited acidification by facilitating active transport.

Quinacrine, which was occasionally used in place of acridine orange, is also a pH sensitive fluorescent dye (Rothman et al. 1989). The emission spectrum for quinacrine does not shift as it does for acridine orange (Decker et al. 1985); however, under K^+-free conditions there was a marked concentration of bright green fluorescence within the cavities of these tissues. The cavities were therefore rendered acidic in K^+ free saline, strengthening the theoretical link between K^+ active transport and high pH generation.

One cannot yet discount the possibility that the ATPase is a K^+-stimulated H^+ ATPase as has been recently suggested (Wieczorek et al 1989). However, if this were the case, then one would expect omission of K^+ to result in loss of TEP, as the pump is no longer stimulated by K^+, but one would not expect acidification of the cavity, as no protons will be pumped into the cavity and none will be exchanged for potassium. The observations presented here, on the other hand, suggest an inverse correlation between electrogenic K^+ transport and acidification.

5.2.2.3. Buffering Effects

Normal *Manduca* saline contained TRIS as a buffer, however with bicarbonate reputedly playing an important role in this osmoregulatory system, saline containing 10 mM bicarbonate and buffered with 5% CO_2 was used as the bathing solution (Dow 1984).

High TEPs of around 90 mV were maintained in this saline (Figure 5.10a). As a result, there was little or no accumulation of acridine orange within goblet cavities (Figure 5.10b). Addition of 3 mM azide caused the TEP to fall, although only to 65mV. The cavities in this midgut appeared mainly black, with a few green ones evident. In the trace where TEP did fall to 0mV, 15 mM azide had to be administered, and there was no significant increase in red cavities. Some green and red cavities could be seen, especially around the areas of the folds, but most remained black. The initial presence of bicarbonate may have had an effect on maintaining alkalinity in these midguts.

Figure 5.10. TEP of middle midgut: Bicarbonate buffered with 5% CO_2

a

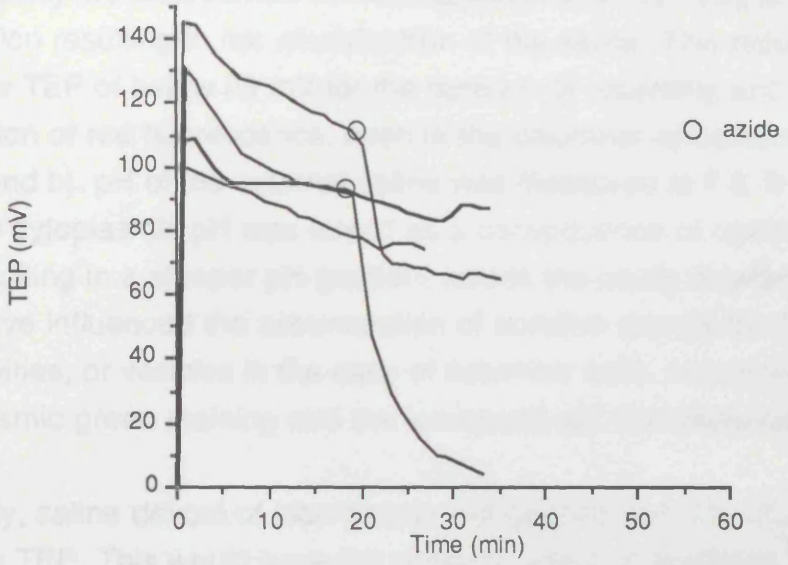

b

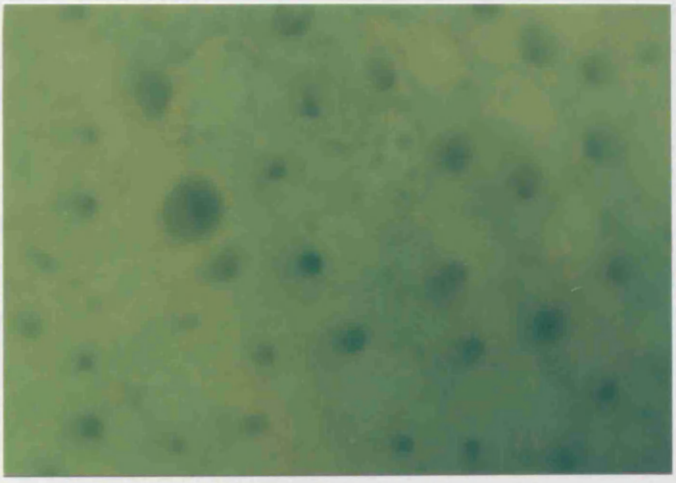

a. Transepithelial potential difference (TEP) of isolated middle midgut bathed in saline containing 10mM sodium bicarbonate and buffered with 5% CO_2 / 95% O_2. Azide was added during 2 experiments as indicated by the open circles. This caused a sharp fall in TEP. Acridine orange was added to each side of the epithelium 5 min before the end of recording. Traces from 4 separate experiments are presented.

b. Epifluorescence micrograph showing little or no accumulation of acridine orange within goblet cavities of the midgut, as with standard oxygenated saline. This coincides with a high measured TEP.

Scale bar = 50μm

By bubbling the bicarbonate-containing saline with O_2, CO_2 is driven out of solution resulting in net alkalinization of the saline. This resulted in a very low TEP of below 20 mV for the duration of recording and a high proportion of red fluorescence, even in the columnar cytoplasm (Figure 5.11a and b). pH of the external saline was measured at 7.6. It is likely that the cytoplasmic pH was raised as a consequence of raised external pH, resulting in a steeper pH gradient across the cavity membrane. This may have influenced the accumulation of acridine orange by driving it into cavities, or vesicles in the case of columnar cells, hence the lack of cytoplasmic green staining and the increased red fluorescence seen.

Similarly, saline devoid of bicarbonate but gassed with 5% CO_2, resulted in a low TEP. This would have the opposite effect of acidifying the saline as CO_2 solubilizes and forms H_2CO_3 (H^+ and HCO_3^-). pH was measured at 5.6. There were no black cavities but there were surprisingly few red ones. Again it may have been the gradient which due to acidification of the cytoplasm was shallower across the cavity membrane and therefore acridine orange may have been partially protonated in the saline before it could cross any cellular membranes.

5.2.2.4. Effect of NH_4Cl

As NH_4Cl increased the pH in cavities of isolated cells, its effect on the intact tissue was investigated. TEP was used as an indicator of ion transport competence in order to relate this to acridine orange staining ability.

A preliminary experiment involved adding NH_4Cl sequentially to alternating sides of the epithelium. The results indicated that apical additions caused a rapid drop of TEP, and basal additions caused temporary increases in the potential (Figure 5.12a). The size of the effect was proportional to the concentration of NH_4Cl administered. 10mM induced a rise of 2-4 mV and a fall of 6-10 mV, and 150 mM caused a 20-30 mV decrease on the apical side and a 10-15 mV transient increase when added to the basal side. Despite the final TEP reading of less than 20 mV, there was no red accumulation of acridine orange (Figure 5.12 d). The pH had therefore been raised by addition of the weak base which consumed H^+ in the cavity. This effect has been seen in lysosomes and the result was that the H^+ ATPase increased pumping to make up for the

Figure 5.11. TEP of middle midgut: Effects of incorrect buffering

a

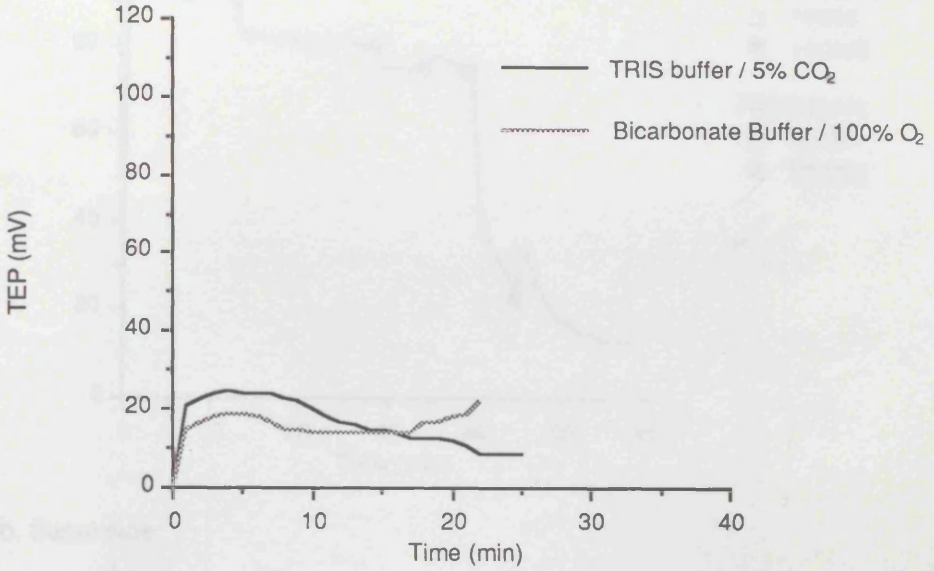

b

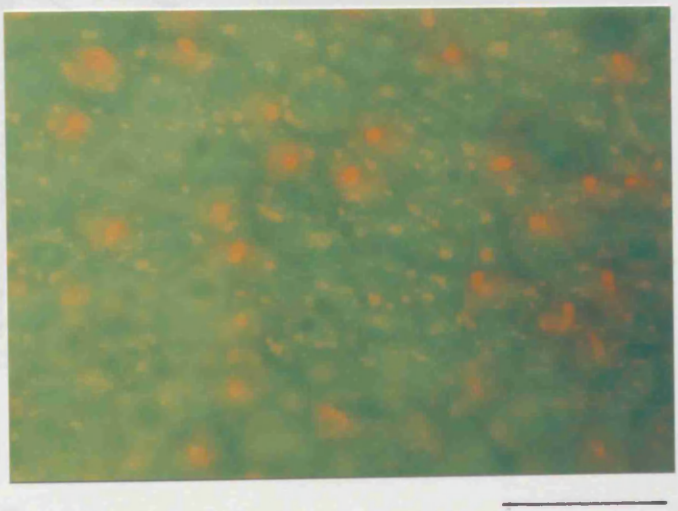

a. Transepithelial potential difference (TEP) of isolated middle midgut bathed in saline containing either TRIS buffer or sodium bicarbonate. TRIS salin was gassed with 5% CO_2 / 95% O_2 (solid line), and bicarbonate saline was gassed with 100% O_2 (dashed line). Acridine orange was added to each side of the epithelium 5 min before the end of recording. Traces from 2 separate experiments are shown.

b. Epifluorescence micrograph showing accumulation of acridine orange within goblet cavities of the midgut. This suggests acidity which was caused by the buffering imbalance of gassing bicarbonate saline with 100% O_2 .This staining pattern coincides with low measured TEP.

Scale bar = 50μm

Figure 5.12 TEP of middle midgut: Ammonium chloride additions

a. Alternating sides

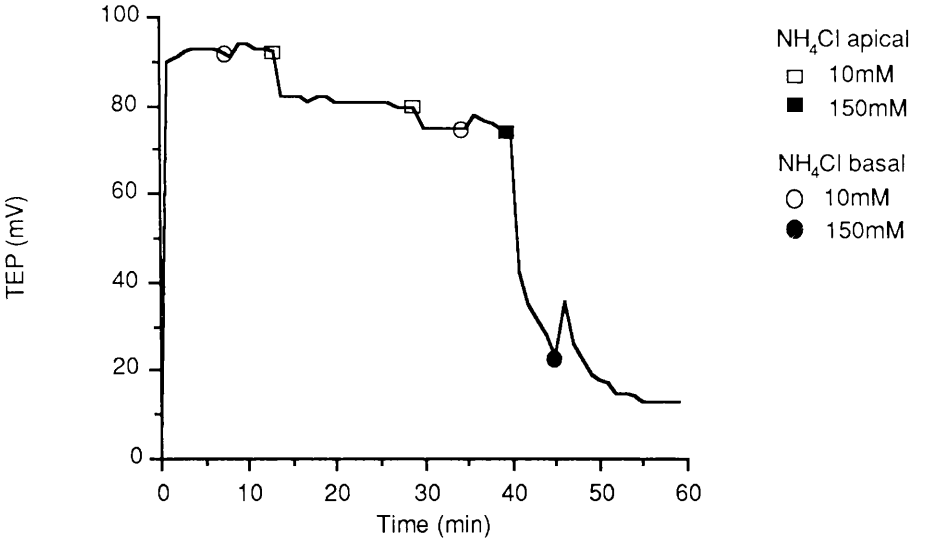

b. Basal side

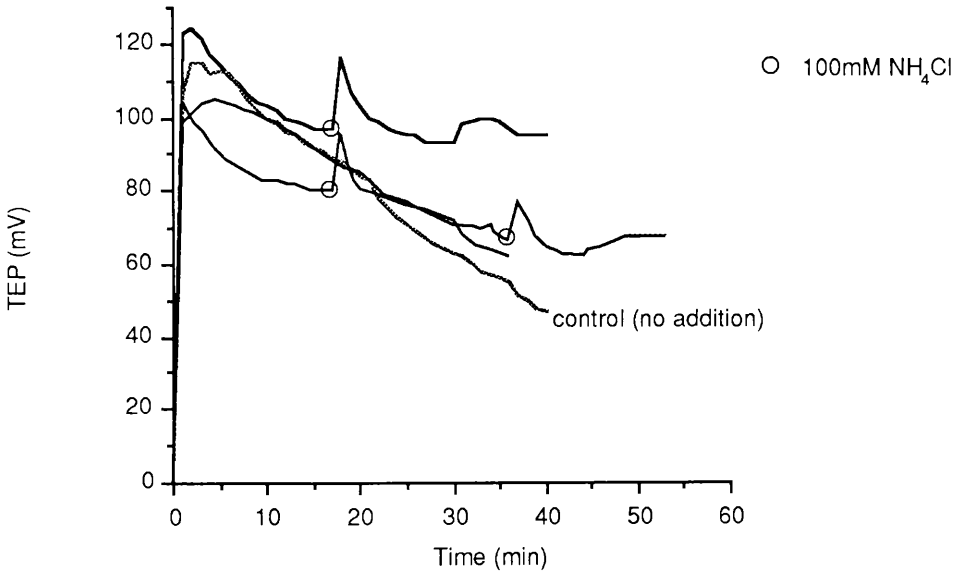

c. Apical side

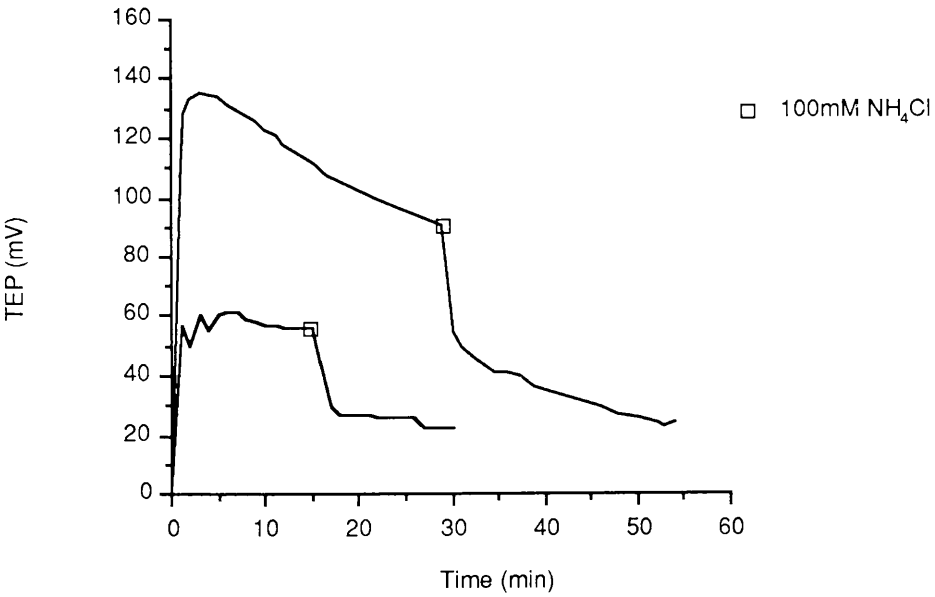

contd.

Figure 5.12 (contd)TEP of middle midgut: Ammonium chloride additions

d

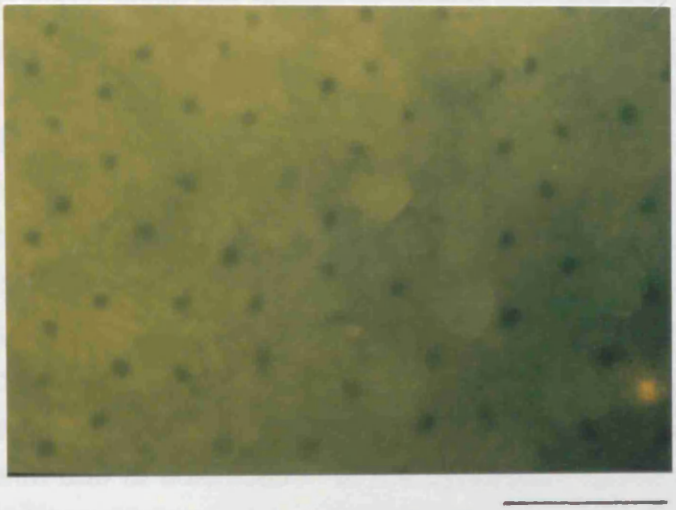

a. The effects on TEP of sequentially adding 10mM (open symbols) and 150mM NH_4Cl (closed symbols) to the basal (circles) and apical (squares) sides are shown.

b. The effects on TEP of basal additions of 100mM NH_4Cl are shown for 3 midguts (open circles). A control trace, where no addition was made, is given for reference. Basal additions caused a transient rise in TEP.

c. The effects on TEP of apical additions of 100mM NH_4Cl are shown for 2 midguts (open squares). Apical additions caused a sustained drop of TEP.

Acridine orange was added 5 min before termination for all traces.

d. Epifluorescence micrograph showing acridine orange staining pattern after addition of 150mM NH_4Cl to each side of an isolated middle midgut. This coincided with a TEP of near 0mV, but no accumualtion of acridine orange in goblet cavities, which suggests that the cavities were not acidic.

Scale bar = 50μm

loss in protons (Poole and Ohkuma 1981). There was also an effect of short-circuiting the pump. These explanations could apply to the TEP results shown here, particularly if the pump was an H^+ ATPase and not a K^+ ATPase.

Figure 5.12 b and c show the results of adding 100 mM NH_4Cl to the basal and apical sides, respectively. Addition to the basal side boosted the TEP by about 20 mV but this was followed by a decline back to the original level. Addition to the apical side caused a fall in TEP of between 30 and 60 mV loosely depending on the initial TEP. The effect on membrane potential was more sensitive when NH_4Cl was added to the apical side. Some red fluorescence was seen around the edges of midguts with apically applied NH_4Cl, but most goblet cells had black or pale green cavities. Similar staining was seen in basally applied midguts. Columnar cells in some of the preparations looked slightly orange, this may have been due to acidification of the cytoplasm caused by raising the pH of the intracellular vesicles.

One explanation for the differential effects of NH_4Cl on TEP, depending on application site, could be access. The basal membrane is less sensitive to many agents such as *Btk (Bacillus thuringiensis* var. *kurstaki endotoxin)* (Crawford and Harvey 1988; Harvey and Wolfersberger 1979; Knowles et al. 1986; Knowles et al. 1984; Wolfersberger et al. 1985), and permeabilizing agents (see chapter 6), partly due to the underlying muscle cell layer and connective tissue. The only barrier on the apical side is the peritrophic membrane which was removed before mounting the midgut on the chamber. The TEP was more sensitive to NH_4Cl addition on the apical side, which would be expected; however, why the electrical element of the TEP was altered is a mystery. An explanation could be that the pump is sensitive to pH in the cavity and a sudden increase in pH inhibited pump activity. NH_4Cl probably affected organelles other that the cavity, such as the mitochondria. The ATP synthase present on mitochondrial inner membranes could have been affected resulting in a block of ATP production and subsequent inhibition of the cavity membrane ATPase.

5.2.2.5. ATP Permeabilization

ATP in the free base form of ATP^{4-}, acts as a membrane permeabilizing agent in some systems (Findlay 1988; Gomperts and Fernandez 1985; Gordon 1986). As the pump is an ATPase, administering ATP to the catalytic site may stimulate ion transport in a non-transporting epithelium.

Figure 5.13a shows the effects of adding ATP to the basal side of a midgut mounted on an Ussing-type chamber in divalent-free conditions. Under these conditions ATP should be present in the free base form. This concentration (20mM) induced a decline of TEP when added to the basal side. TEP was allowed to continue its decline until it reached a new steady state, at which point a further addition of ATP was made. This caused a very small rise of about 2 mV, possibly as a result of fuelling the ATPase. Only black cavities were seen after staining with acridine orange, despite the final low values of TEP that normally result in red cavities (Figure 5.13d).

In divalent-containing saline (Figure 5.13b), ATP basally applied had a similar if not stronger effect of reducing TEP to zero mV. In only one of these samples did a second addition of ATP induce a small rise of TEP, however all cavities remained black after acridine orange staining. Addition of ATP to the apical side in divalent-containing conditions also caused a rapid decline to near zero mV (Figure 5.13c). However, a further addition instead of stimulating TEP actually induced a further decline. As a consequence of this, many cavities displayed red or green fluorescence indicating acidity.

The ATP stock was made up in divalent-free saline, which may explain why permeabilization still occurred in divalent-containing bathing solution. The rate of decline appeared to influence the ability of the second ATP addition to stimulate TEP. The slower rates of decline seen in figure 5.13a for basal addition in divalent-free conditions, resulted in stimulation by ATP, however, the faster rates seen in figures 5.13 b and c did not. The decline rates themselves may have been a compromise between the immediate loss of the electrochemical gradients following ATP permeabilization, and stimulation of the ATPase activity.

Figure 5.13 TEP of middle midgut: ATP additions

a. Basal side, divalent-free conditions

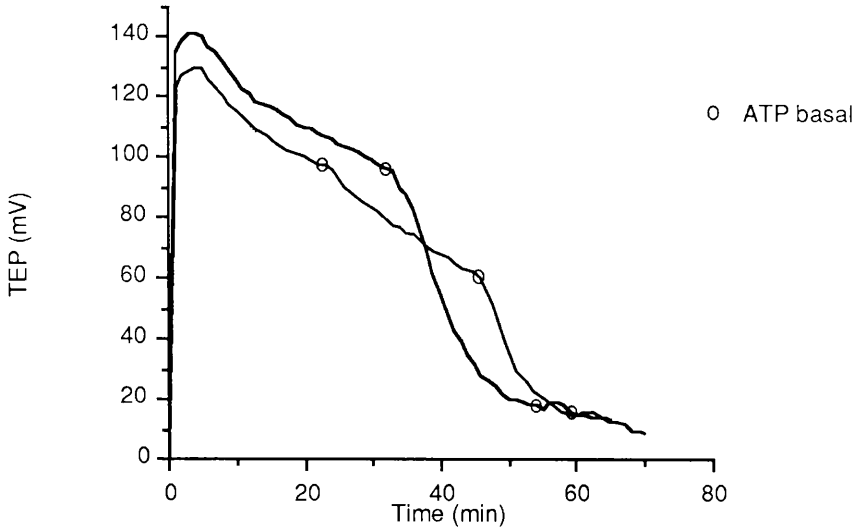

b. Basal side, divalent-containing conditions

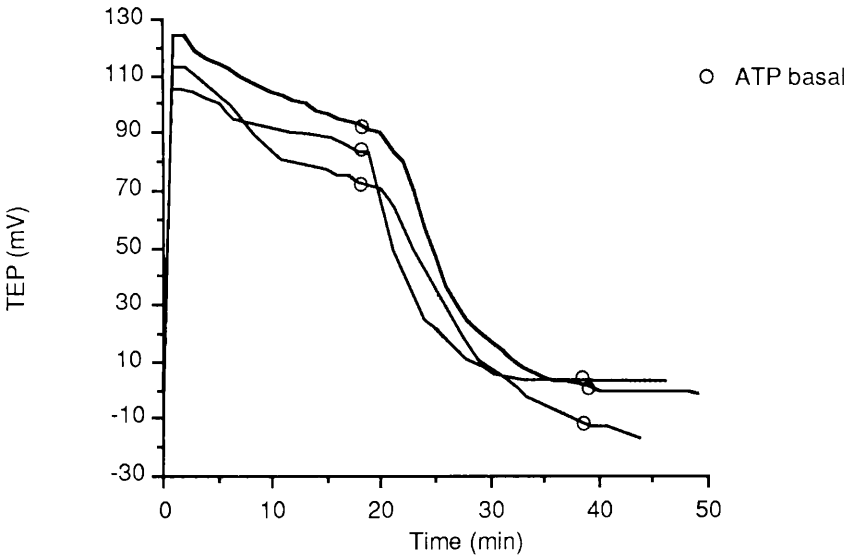

c. Apical side, divalent-containing conditions

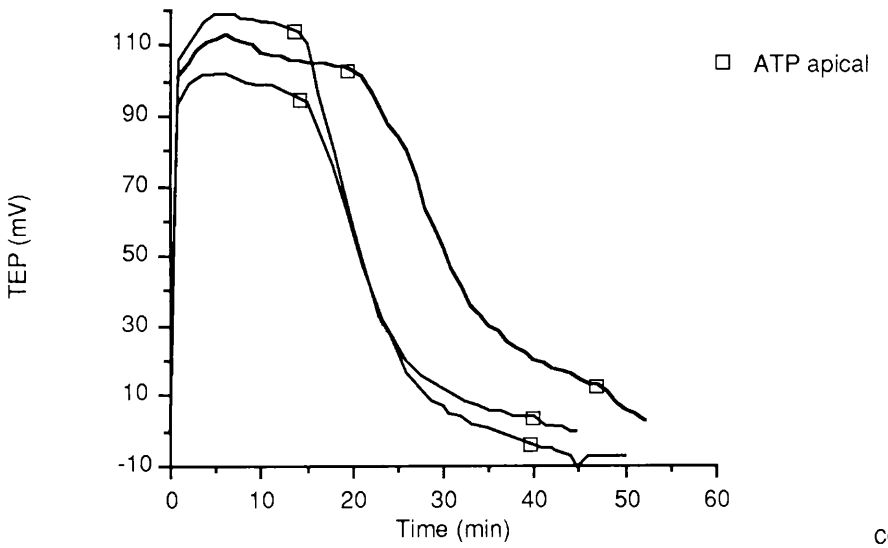

contd.

Figure 5.13 (contd) TEP of middle midgut: ATP additions

d

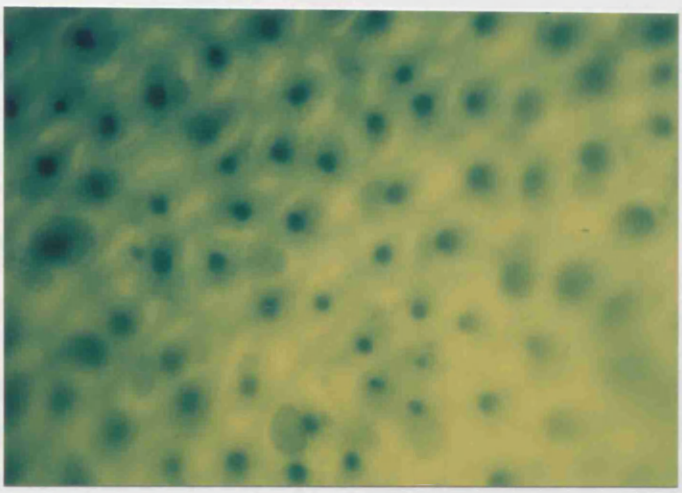

a. The effects on TEP of basal additions of 20mM ATP (open circles) in divalent-free saline are shown for 2 midguts. Additions were made before and after the resulting fall in TEP.

b. The effects on TEP of basal additions of 20mM ATP (open circles) in divalent-containing saline are shown for 3 midguts. Circles indictate time of additions for each trace which were made before and after the resulting fall in TEP.

c. The effects on TEP of apical additions of 20mM ATP (open squares) in divalent-containing saline are shown for 3 midguts. Squares indictate time of additions for each trace which were made before and after the resulting fall in TEP.

Acridine orange was added 5 min before termination for each trace.

d Epifluorescence micrograph showing the acridine orange staining pattern of middle midgut after a 2nd addition of 20mM ATP to the basal side in divalent-free conditions. This addition caused a transient rise in TEP and resulted in little or no accumulation of acridine orange in goblet cavities, despite the relatively low TEP value.

Scale bar = 50μm

As apical addition drove TEP to zero and yielded red and green filled cavities, it can be concluded that the ATPase was not stimulated either at the end of decline or during the descent. Permeabilization thus probably took place across the apical valve area allowing ATP access to the cavity but not to the cytoplasm where the catalytic sites of the enzyme are situated. However the appearance of all black cavities in the basally administered midguts, despite near zero TEPs, imply that ATP may have reached the ATPase catalytic site after permeabilization from the basal side.

5.3. Discussion

Acridine orange is a weak base which crosses membranes surrounding acidic compartments in the free base form. Once inside the compartment the dye is protonated and thus cannot readily cross the membrane which results in accumulation of the dye within the acidic compartment (Poole and Ohkuma 1981). In *Manduca sexta* midgut, acridine orange accumulates within cavities of isolated cells, suggesting acidity. It is possible that upon isolation, the pumping mechanism which renders the midgut lumen alkaline, shuts down, perhaps due to loss of cell:cell contact with columnar cells that may be housing the transporting ion pool.

From the results presented, it still remains unclear as to which of the current models is more viable. Is it K^+ transport facilitating H^+ export from the cavity, or is it electrogenic H^+ transport into the cavity energising an electroneutral or electroresponsive exchange of K^+ for H^+ in the cavity? The second model is maturing into the more favourable of the two for a number of reasons. Recently, Moffett measured the pH within the posterior midgut cavity using pH sensitive microelectrodes, the value being 7.2 (Moffett, unpublished observations). The prediction from the K^+ transport model of Dow and Peacock, was a cavity pH of 11.6 in the middle region. Until the middle region cavity pH is measured neither model can be discounted.

The presence of an anion conductance is an integral part of the proton pump model. In other H^+ transporting systems, presence of a Cl^- conductance as well as a K^+ pathway, results in acidification, however in goblet cavities the electroneutral exchanger moves H^+ to the cytoplasm

and K^+ to the cavity lumen. This would result in near neutral pH within the cavity. If export of H^+ from the cavity is blocked, a Cl^- conductance would facilitate acidification. HCO_3^- is another contender for an anionic conductance. This could bring about alkalinization perhaps by exchanging with Cl^- in the apical valve region with its array of tubular channels, thus alkalinization would occur but may not be detected in the cavity, only in the midgut lumen. The main function of the cavity may therefore be to house the matrix of mucopolysaccharides which being negatively charged could influence ion transport, particularly of anions, into and out of the cavity.

The experiments performed here were designed to test the validity of the proton pump model. If the electrogenic step is the pumping of protons into the cavity, then omitting K^+ from the bathing saline should have no effect on TEP, as transport of this ion is electroneutral. However TEP could not be maintained under these conditions and plummeted to 0 mV and even reversed to lumen negative values in some cases. But even this result cannot dismiss the new theory as Wieczorek claims that the pump is K^+ stimulated (Wieczorek et al. 1989; Wieczorek et al. 1986). This would explain why there is a drop in TEP in the absence of K^+, but not why acidification occurs. There are still a few problems with this model, however it does have in its favour the fact that from an evolutionary viewpoint, most similar transport systems are energized by a H^+ ATPase and an electroneutral exchange (Al-Awqati 1986; Nelson and Taiz 1989). In these other systems however the result is net acidification, which suggests that if H^+ pumping is the primary transport process, then there are some complicated secondary transport mechanisms occuring to cause the extreme alkalinization found in the anterior and middle midgut lumen.

Chapter 6

6. Chapter 6. Other Results

There were several additional experiments carried out during the course of this study which although related to the project, could not be categorized with ease. This chapter aims to present the results from these experiments, and discuss their importance to the overall study.

6.1. Lectins

6.1.1. Introduction

All eukaryotic cells have carbohydrate on their surface bound covalently to membrane proteins or lipids (Alberts et al. 1989). This can be demonstrated by administering carbohydrate binding proteins, or lectins, to the cell surface. Lectins are proteins with binding sites that recognize a specific sequence of sugar residues, for example, Soybean lectin recognizes α–galactose and N-acetyl-D-galactosamine residues, Wheat germ lectin recognises N-acetylglucosamine, and Concanavalin A recognizes -D-glucose and α-D-mannose residues. They originated from plants where they were found in abundance in the seeds, however, lectins have been discovered in other organisms, including mammals in which they are thought to be involved in cell: cell recognition.

As lectins bind to specific cell surface carbohydrates, they have often been used as a tool for isolating and localizing membrane proteins as well as fragments of membrane and even whole cells (Lis and Sharon 1986). Often clustering or patching of the membrane receptors occurs as lectins are polyvalent. This property can be exploited, for instance using lectins to agglutinate cells expressing the same glycoproteins.

The properties of lectins were exploited in an attempt to selectively isolate two populations of *Manduca sexta* midgut cells; namely the goblet and columnar cells. Three different techniques were applied:

(1). Fluorescence-labelled lectins were allowed to bind with a heterogeneous midgut cell suspension in order to determine whether there was any specificity for a certain cell type.

(2). Lectins conjugated with sepharose beads were used on cell affinity chromatography column in an attempt to retain one cell type only on the column.

(3). Lectins were covalently bound to glass coverslips and differential cell adhesion assays were carried out.

6.1.2. Fluorescent Lectins

In a personal communication, J.B. Harrison (Cambridge) reported some success in labelling *Manduca sexta* midgut cell apical membranes with peroxidase conjugated Wheat Germ Agglutinin (WGA) and Soy Bean Agglutinin (SBA), and also with Fluorescein isothiocyanate (FITC) labelled Phaseolus Haemagglutinin (PHA or kidney bean lectin). On this basis, FITC and TRITC (Tetramethylrhodamine isothiocyanate) conjugated WGA and SBA were used as probes for their specific carbohydrates (N-Acetyl Glucosamine and N-Acetyl Galactosamine respectively) on isolated midgut cells. The objective was to see if there was a lectin which would bind specifically to one cell type.

6.1.2.1. Results of WGA-FITC Labelling

Initial observations indicated that WGA bound strongly to columnar cell microvilli, but very little staining was observed on the goblet cell surface (Figure 6.1). SBA did not appear to label either cell type. Some faint staining was seen over both cell types but was accredited to either non-specific adsorption, or the presence of very few receptors. One experiment was carried out using Kidney bean lectin-FITC. Again some dull uniform staining was seen on more than 70% of both cell types, however goblet cells appeared to be slightly brighter. This was not pursued.

These observations were later supported by quantifying the number of each cell type displaying fluorescence. The results of three experiments with WGA-FITC are presented in Figure 6.2. There was selective binding of WGA to columnar cells and in particular to the apical microvilli. This occurred only in the anterior and middle regions, with almost no binding observed in posterior midgut cells.

Figure 6.1 Wheat-germ agglutinin-FITC labelling of midgut cells isolated from 3 regions.

a. Anterior midgut. Light micrograph showing a columnar cell and a goblet cell still associated with each other after isolation.

b. Epifluorescence micrograph of (a) showing WGA-FITC affinity for columnar cell microvilli. No goblet cells had bound WGA-FITC.

c. Middle midgut. Light micrograph showing a columnar cell (or possibly 2) still associated with a goblet cell (nearer the top of the picture) after isolation.

d. Epifluorescence micrograph of (c) showing WGA-FITC affinity for columnar cell microvilli but none bound to goblet cell membranes, as with anterior midgut cells in (b).

e. Posterior midgut. Light micrograph showing a columnar cell and 2 goblet cells after isolation. Note the longer length of the microvilli on the posterior region columnar cells compared with the anterior and middle region, and also the different shape of the goblet cells(a and c).

f. Epifluorescence micrograph of (e) showing no affinity of WGA-FITC for columnar microvilli. Goblet cells in this region also do not bind the lectin.

Scale bars = 50μm

Figure 6.1 Wheat-germ agglutinin-FITC labelling of midgut cells isolated from 3 regions.

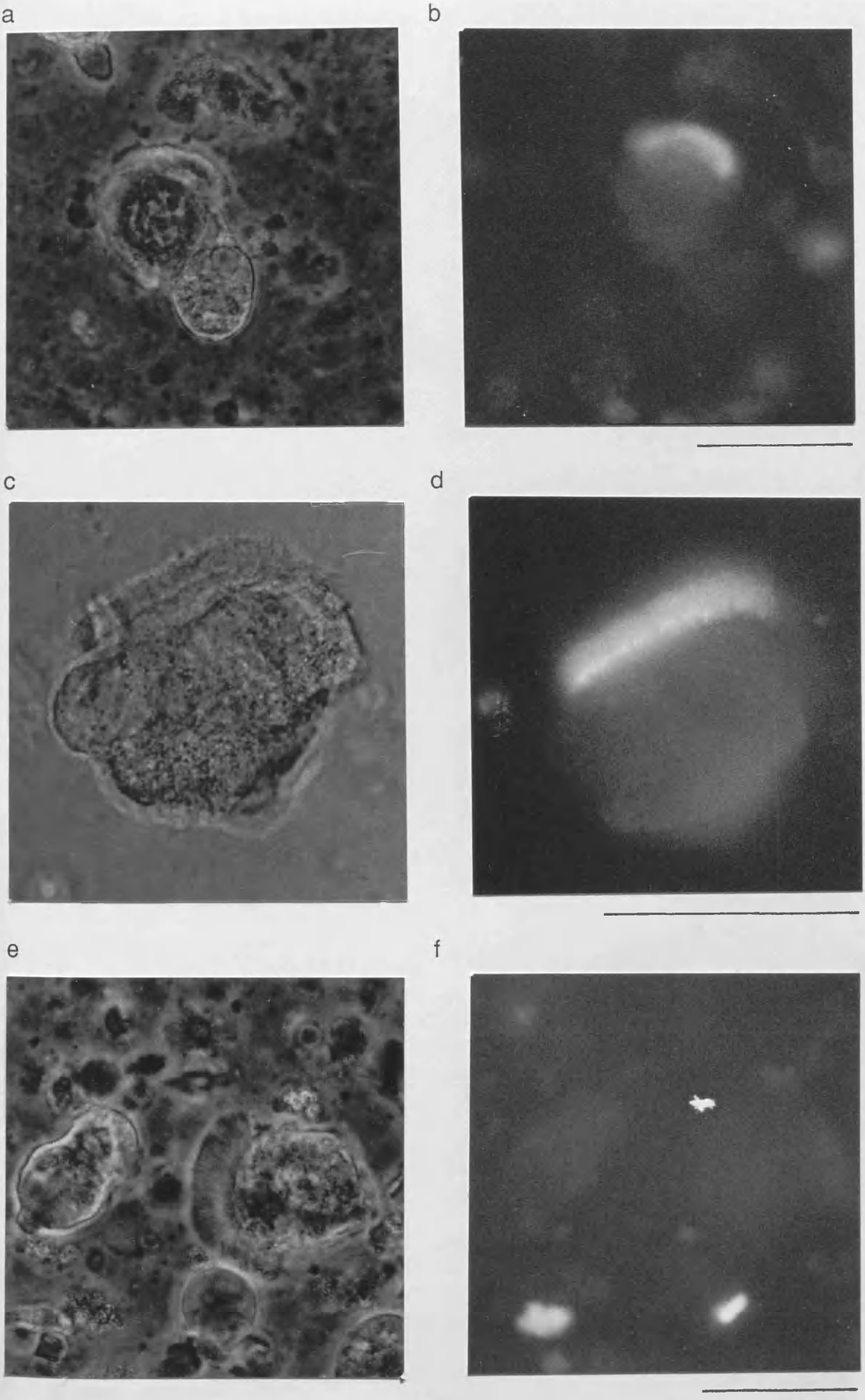

Figure 6.2 WGA-FITC staining of midgut cells

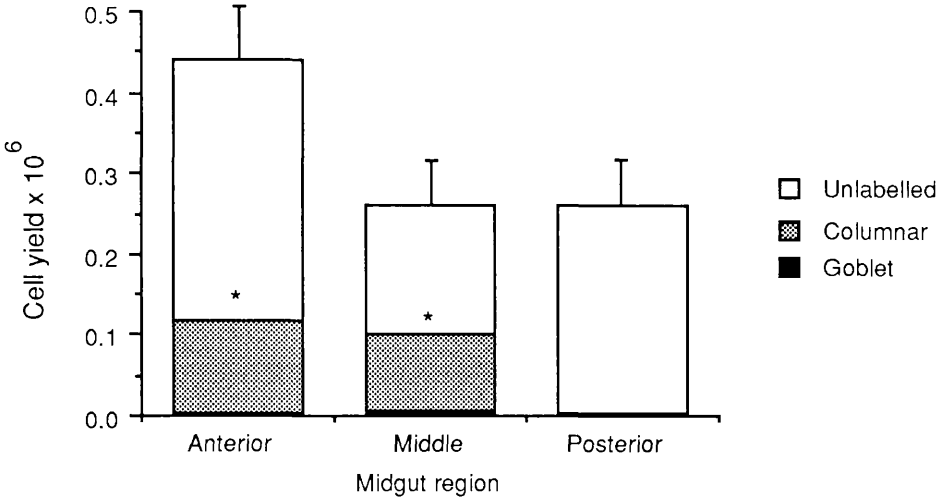

Midgut regions were incubated with FITC-labelled Wheat Germ Agglutinin during flat sheet dissociation of the cells. The number of goblet and columnar cells, in each region, which displayed affinity for WGA is indicated by the shaded portions of the stacked histogram. The combined height of the bars represents the total number of cells isolated ±S.E.M. (n=3)

Statistics: Asterisks indicate significant WGA-FITC labelling of columnar cells in anterior and middle regions compared with the posterior region. There was no significant difference in labelling of goblet cells in all three regions.

Whilst quantifying the binding, it was noted that columnar cells which possessed long microvilli did not take up the lectin, whereas short microvilli bound it very strongly. In the anterior and middle regions, columnar cells with both types of microvilli were seen, which may explain why approximately 50% of the columnar cells in these regions did not display staining. Another explanation may be that the delicate brush borders were often cleaved off during isolation and the resulting columnar cells would still be scored, but as non-fluorescent. Posterior region columnar cells all had long microvilli none of which were seen to bind WGA-FITC. The reason for having microvilli of different lengths may be related to the extent of folding. Short microvilli may be adequate for the tops of the folds, but longer ones may be required within a fold.

Middle midgut is the least folded region and displayed the highest percentage of WGA binding, whereas the highly folded posterior region bound no WGA. It is possible that the carbohydrates present on the short microvillate columnar cell surface, which may be exposed to the midgut lumen at the tops of the folds, have a role in absorption of certain proteins. The carbohydrates labelled by WGA lectin were NAcGlc meaning that certain proteins might be selected according to their ability to bind to this sugar residue. There are probably a range of carbohydrates present alongside NAcGlc for selection of other nutrients by these columnar cells, however the lectins tested so far have failed to detect them.

6.1.3. Lectin Coupling to Glass

Armed with the knowledge that WGA bound specifically to columnar cell microvilli, an attempt was made to separate the two midgut cell types based on their adhesive properties. In general, these cells do not adhere well to most putative 'adhesive' surfaces, such as collagen, fibronectin, con A, gelatine polylysine or laminin (J.M. Peacock, Honours project 1987), but this could be due to the use of unsuitable homologues of the protein in adhesion experiments. Many adhesive proteins are derived from mammalian and other non-insect sources. On finding that WGA did bind specifically to columnar cell membranes, it was used in a differential adhesion assay.

In order to ensure that lectin was present on glass coverslips, a method devised by J. D. Aplin, which allowed proteins (or peptides) to be covalently coupled to glass surfaces, was employed (see Figure 2.6 in Chapter 2) (Aplin 1981). The differential adhesion of isolated midgut cells to the covalently bound WGA substrate was assessed.

6.1.3.1. Results of Differential Adhesion to Lectins

The results of midgut cell adhesion to surfaces coated with lectins are presented as histograms in Figure 6.3. The number of cells attaching to any of the surfaces was very low compared with those that remained in the supernatant (Fig 6.3a), although there did appear to be a slight enhancement of cell attachment when lectin was bound to glass. Figure 6.3 b and c show acridine orange differential staining of both attached cells on substrata and unattached cells in suspension. Green fluorescence normally associated with columnar cell staining predominated in most assessments and was usually 70-80% of all stained cells. It does not follow that 70-80% of cells present were columnar cells, as it was shown that in a healthy cell isolation as much as 50% of goblet cells can be stained green due to the non-acidic nature of the cavity during active ion transport (see Chapter 5). Although WGA caused attachment of proportionally more cells than other surfaces, it was relatively non-specific, there being as many red stained cells present as in the controls (Fig 6.3b). On the other hand, SBA displayed a certain amount of selectivity for red cells, suggesting that the goblet cell surface expressed NAcGal. Due to the very low numbers of cells adhering, and lack of significant selectivity, this method of separating the two midgut cell types was far from ideal.

6.1.4. Cell Affinity Chromatography

Affinity chromatography exploits the properties of biospecific interactions. It is commonly used to adsorb specific proteins or other macromolecules from a heterogeneous population, for instance fibronectin from serum. By selecting the appropriate materials, whole cells can be separated into sub-populations based on their surface properties, using this technique. The affinity adsorbant material is packed in a column through which the substance to be separated is passed. Components with a high affinity for the chosen adsorbant will be retained in the column whilst incompatible moieties pass on and can be collected or discarded, as required. Binding

Figure 6.3. Adhesion of midgut cells to lectin-coated glass

(a) Histogram showing number of cells attaching to prepared surfaces compared with number remaining in the supernatant. Few cells attached to the any of the surfaces (black area). Far more remained in the supernatant above the slide (white area). # , is the total no. of cells originally added to each slide. WGA, Wheat Germ Agglutinin; SBA, Soy Bean Agglutinin; Control, processed glass. Values are the total no. of cells ± S.E.M. (n=3)

(b) Acridine orange differential staining of cells which had attached.as indicated in (a) Red staining indicates mainly goblet cells, green staining, mainly columnar cells.

(c) Acridine orange differential staining of cells which remained in the supernatant, i.e unattached to the substrata.

Statistics: The asterisk indicates a significant difference in the ratio of red: green acridine orange staining for cells attached to SBA compared with WGA and control substrates. All other comparisons were not significantly different.

Figure 6.3 Adhesion of midgut cells to lectin-coated glass

(a) Cell yields comparing attached and unattached to the substratum

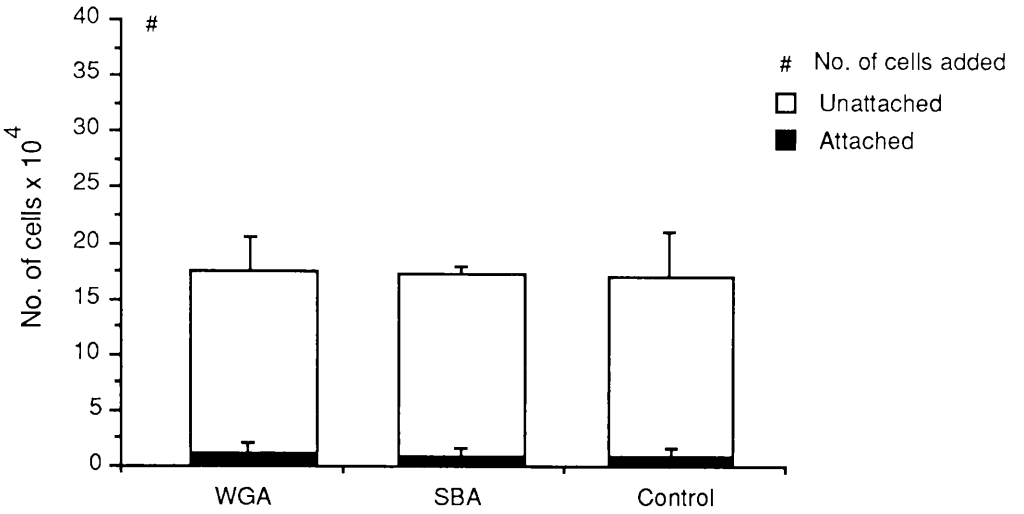

(b) Acridine orange staining of cells attached to lectin-coated slides

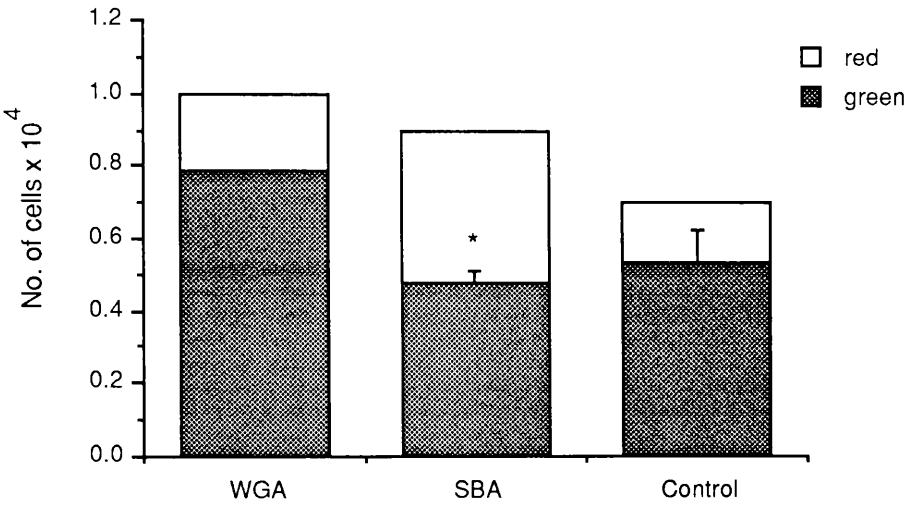

(c) Acridine orange staining of cells unattached to lectin-coated glass

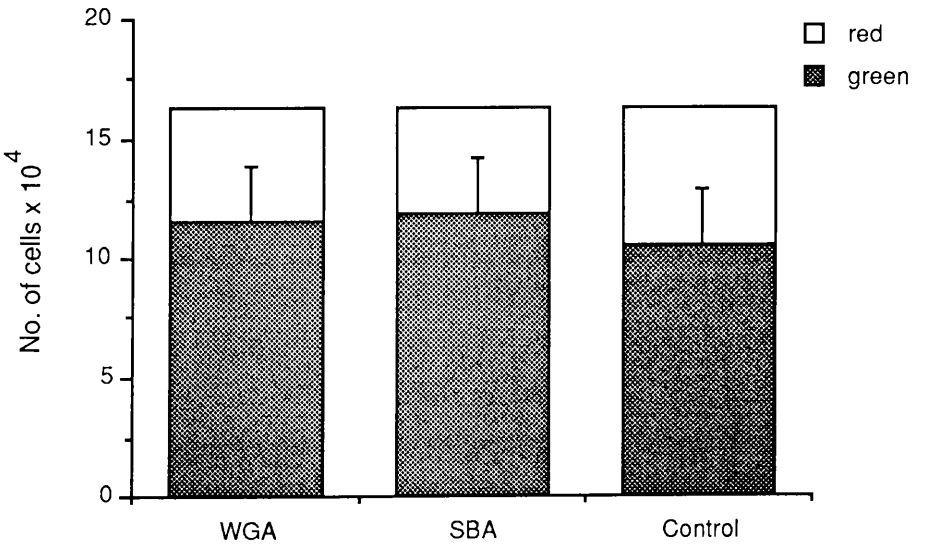

has to be reversible so that the adsorbed material can be eluted if needed.

For cell affinity chromatography, the affinity adsorbant is normally coupled to sepharose beads so that the column can be packed with sufficient space to allow free travel of cell suspension without physical trapping which could lead to retention of unwanted cell types. The adsorbant itself has to be specific for the components of the surface of the desired cell type, and is usually chosen on the bases of (a) selectivity and (b) strength of binding.

The advantages of using affinity chromatography over other cell purification methods are that it is rapid and produces good yields of cells with retention of cell viability. The column and adsorbant can also be used repeatedly giving economical and reproducible separations. Most of the early work with cell affinity chromatography used antibody-antigen interactions to separate specific blood cell types (Chess et al. 1974; Manderino et al. 1978). However, immobilized lectins have also proved valuable for fractionation of cell sub-populations (Hellstrom et al. 1976; Nicola et al. 1978).

Following the results with fluorescent lectins, where there appeared to be quite high specificity of WGA for columnar cell apical membranes, a WGA sepharose affinity column was used in an attempt to purify columnar cells from midgut cell suspensions.

6.1.4.1. Results of Lectin Affinity Chromatography

Figure 6.4a shows the cell yields for each elution from a WGA sepharose affinity column. *Non-bound* was the first elution where after incubation of the cell suspension on the column, cells which did not bind to WGA were washed through with normal column buffer and collected. *Bound1* was the first elution after incubating the column with NAcGlc which competes for the binding sites (i.e. the lectins) on the adsorption bed. This elution was obtained by simply running the elution buffer through the column. The second bound elution *(Bound2)* was the fraction collected after the column was agitated with a pipette to aid dislodgement of cells bound to WGA. Approximately half of the cells collected came off in the first elution and were therefore not bound to the column. This fraction contained

Figure 6.4 Midgut cell separation on a WGA affinity column

(a) Cell yields in each fraction

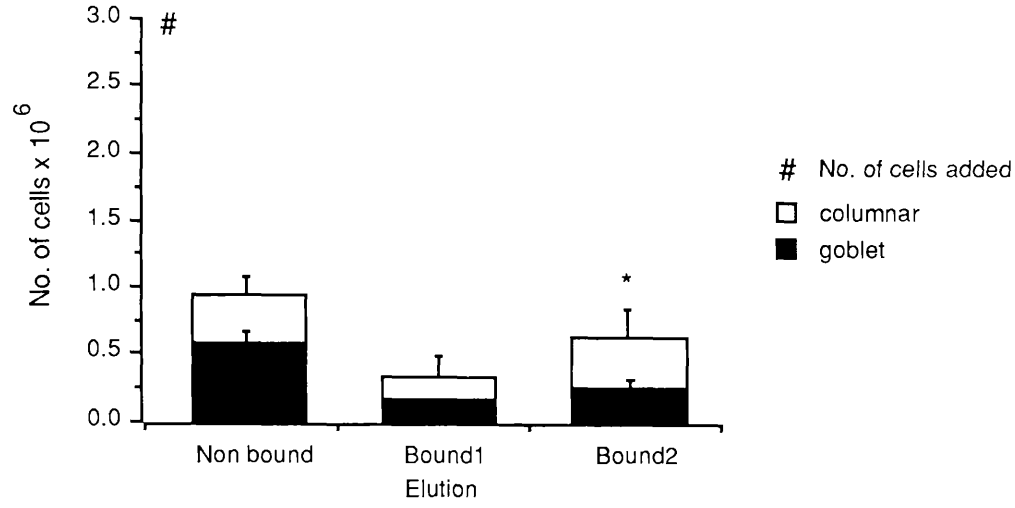

(b) Viability of midgut cells after elution from a WGA affinity column

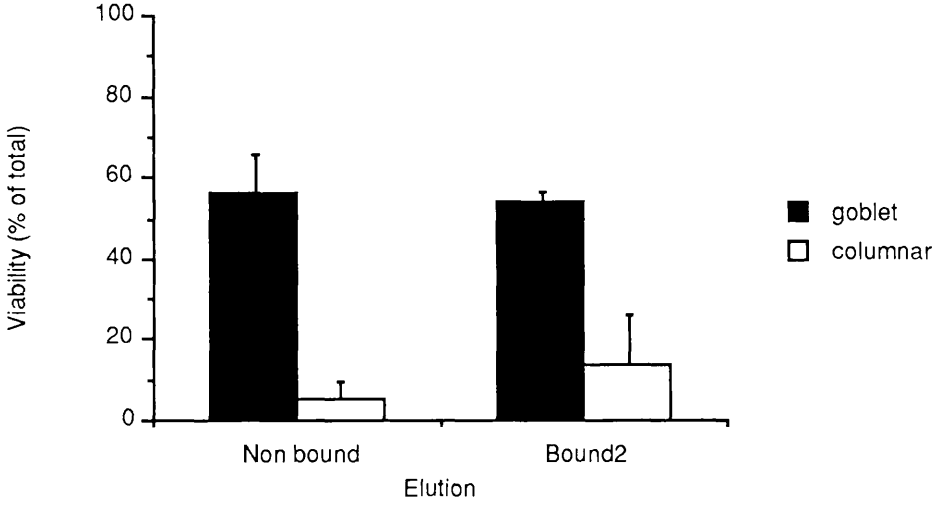

Isolated midgut cells were incubated on a Wheat Germ Agglutinin-sepharose column for 25 min before elution and collection of the fractions indicated. *Non bound* was the fraction containing cells which did not remain on the column bed after rinsing with normal column buffer, *Bound1* was the fraction containing cells which were eluted from the column bed after incubation in buffer containing N-acetyl glucosamine, *Bound2* was the fraction containing cells which were eluted only after additional agitation of the column. (a) The total no. of each cell type in the 3 elutions. (b) Viability of the cells collected from *Non bound* and *Bound2* elutions. ±S.E.M. (n=5)

Statistics: The asterisk indicates a significant difference in the goblet: columnar cell ratio in the *Bound2* elution compared with the *Non bound* elution. All other comparisons were not significant.

almost 40% columnar cells, which may have been the group with cleaved microvilli, or those from the posterior region which displayed no affinity for WGA-FITC. There is a steady increase in the proportion of columnar cells after elution with the dissociating buffer (elution buffer).

These results, taken from 5 experiments, suggest that there was a degree of selectivity for columnar cells, however as can be seen in figure 6.4b, viability was very low. As columnar microvilli were the site of specific interaction, these delicate cell processes could have become damaged by binding of the cell to the beads. It is possible that the strength of binding was sufficiently high for the cells to detach from their brush borders during elution. This need not be a major problem, as goblet cells could be selected and obtained as a pure fraction in the non-bound cell elution. These more robust cells seemed able to withstand the trauma of cell affinity chromatography, and with some refinements could prove to be a useful cell separation tool for *Manduca* midgut and other heterogeneous cell populations.

6.1.5. Discussion

Of the lectins tested for their ability to bind to specific cells in a midgut cell suspension, only WGA showed any significant selectivity. FITC-labelled WGA, which recognises NAcGlc, displayed strong affinity for columnar cell microvilli. The length of the microvilli seemed to be a factor in determining this binding, as only short brush borders were stained with fluorescence. Posterior columnar cells mainly possessed long microvilli, perhaps related to the role of this midgut region in osmoregulation of acid/ base equivalents, and as a result, no labelling of these membranes was found. In contrast, approximately 50% of columnar cells isolated from anterior and middle regions were labelled with WGA-FITC. It was thought that this finding could be exploited by using WGA to separate columnar cells from a heterogeneous midgut cell population. At least in the front two-thirds of the midgut.

Cells can be separated, in theory, by presenting a mixed cell suspension to selective adhesion factors. As there are no such factors specific for Lepidopteran midgut cell types, an attempt was made to use WGA to adsorb columnar cells from the cell suspension. The two methods used, adhesion to glass and affinity chromatography, proved unsuccessful,

there being no significant enrichment of either cell type. The reason for the discrepancy in success between WGA-FITC labelling and cell attachment to WGA could be that WGA-FITC molecules are quite small and can bind non-disruptively to delicate microvilli, whereas the other methods rely on the whole cell adhering to a relatively large WGA-coated surface. In the epithelium, columnar cells adhere to basement membrane and other epithelial cells, only by their basal and lateral membranes, never by their apical membranes. There was no evidence for lectin binding to these membranes and so it is probably futile to attempt cell separations based on this mechanism. However, specific labelling of columnar apical membranes by WGA-FITC could be still be used to produce homologous cell populations by using the FACS technique (Fluorescence-Activated Cell Sorting), whereby fluorescently labelled columnar cells would be separated from non fluorescent goblet cells in the front two-thirds of the midgut.

Further screening of lectins in midgut cell suspensions may yield more cell specific affinity, perhaps for goblet cell membranes or for other membranes on columnar cells. If a lectin specific for regenerative cell membranes was found, this could lead to establishing cell lines or at least midgut cultures which underwent cell division. Lectins shown to be specific could be used for administering toxins and other pharmacologically active agents to predetermined targets and observed effects could be interpreted at the molecular level, aiding our understanding of the mode of action of such agents. Lectins have a potentially important role to play as a tool for such studies.

6.2. Permeabilization

6.2.1. Introduction

6.2.1.1. Isolated Cells

The ability to permeabilize cell membranes allows direct control of cytoplasmic composition and introduction of pharmacologically active agents to the cytosolic face of cellular membranes. Permeabilization can be permanent or prolonged, by the use of high voltage discharge, enveloped viruses or detergents, or it can be reversible, for instance using exogenous ATP^{4-} (Gomperts and Fernandez 1985). Some of these

methods have been documented effective only on certain cell types, such as mast cells, whereas others can be used on a wide range of cells, although vertebrate cells have been the subject of most permeabilization experiments to date (Gordon 1986; Howell et al. 1987).

For this reason, both reversible and irreversible permeabilization techniques were used to isolated midgut cells from *Manduca sexta* larvae. The objective was to introduce agents across the membrane to the cytoplasm of the goblet cells in particular, and observe any effect on ion transport, using probes such as acridine orange or electrical measurement.

The reversible technique selected was exogenously applied tetrabasic ATP^{4-}. In the absence of divalent cations, the free acid form of ATP creates small lesions in the cell membrane which allow the passage of molecules less than 5000 M_r (Whetton et al. 1988). When ATP^{4-} is converted to its Mg^{2+} salt, the lesions close and anything which entered the cell is then trapped (Gomperts and Fernandez 1985). This also suggests that as ATP^{4-} enters the cytoplasm it will be converted to Mg_2.ATP by the endogenous divalent cations present and could then be hydrolysed by ATPase enzymes such as the catalytic site of the K^+ ion pump on the goblet cell apical membrane.

The alternative technique employed because of the reported specificity of ATP^{4-}, was irreversible detergent permeabilization using saponin and digitonin. Saponin is a cholesterol-complexing agent and forms lesions in cell membranes containing cholesterol. This has the advantage that it will not affect intracellular membranes such as those of the nucleus, mitochondria and granular vesicles, as these membranes do not contain cholesterol. The pores formed are large enough to allow proteins of 200kDa to pass through (Smolen and Stoehr 1985). Washing saponin away does not affect permeabilization but prolonged exposure may result in cell lysis. An optimum time course for exposure was therefore approximately 2.5-3 min (Brooks and Treml 1983). Digitonin is a similar steroid glycoside which also interacts with 3β -hydroxysterols (cholesterol) to produce pores large enough to introduce 134kDa proteins to the cell interior (Dunn and Holz 1983). It also requires over 2

min to be effective at the concentration range 50-100μg ml^{-1} (Wilson and Kirshner 1983).

Ethidium bromide uptake is often used as an indicator for determining effective permeabilization (Gomperts and Fernandez 1985). Ethidium bromide intercalates with double stranded DNA or RNA, but does not readily cross living cell membranes (De Jong et al. 1986; Garcia et al. 1988). Fluorescence can be quantified using spectrofluorimetry, however the presence of bright as opposed to weak fluorescence was an adequate indicator of permeabilization for these experiments.

6.2.1.2. Whole Tissue Permeabilization

In order to monitor the effects of introducing potential ion pump stimulatory agents to the cytoplasm of permeabilized cells, techniques of electrical measurement can be used. For instance, microelectrodes could be inserted into the goblet cavities; however, this procedure requires delicate micromanipulation, especially in isolated cells. Alternatively, the whole epithelial potential difference could be monitored, under short- or open-circuit conditions. The latter method was chosen as it allowed repeatable manipulation of the tissue as various agents were screened; (a) for their ability to permeabilize the tissue membranes, and (b) for their ability to fuel or switch on the ATPase after permeabilization. Using an Ussing-type chamber, short circuit current (SCC) and transepithelial potential (TEP) were monitored and the effect of permeabilization observed as a fall in current or voltage as the electrochemical gradient across the transporting membrane diminished.

6.2.2. Results

6.2.2.1. Isolated Cell Permeabilization

Figure 6.5a shows the results of incubating isolated cells with 1mM ATP in divalent free conditions for 15 min. Most of the cells displayed faint fluorescence although, compared to the controls (fig. 6.5b), there was a significantly higher proportion of cells fluorescing brightly, indicating that ATP^{4-} had some effect on cell membranes which enabled ethidium bromide uptake. Columnar cells in particular appeared to be more susceptible to this permeabilizing agent, although not significantly This

Figure 6.5 Ethidium bromide fluorescence after long exposure to ATP

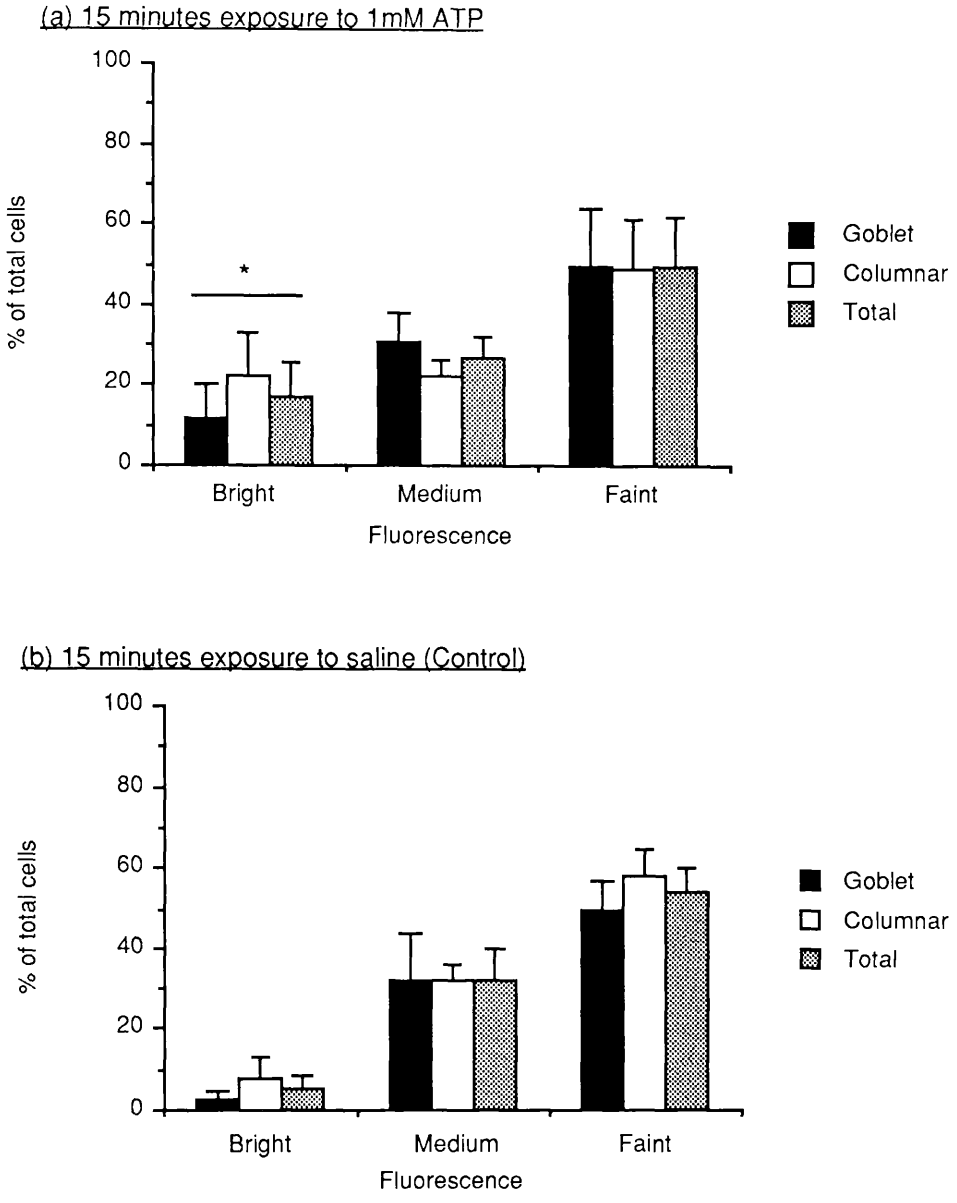

Ethidium Bromide uptake into isolated midgut cells. (a) Cells exposed to 1mM ATP in divalent-free saline for 15 min. (b) Cells exposed to divalent-free saline for 15 min as a parallel control for ATP permeabilization. Ability to permeate goblet cell membranes was compared with ability to permeate columnar cell membranes. Bright fluorescence indicates the percentage of cells in the sample which were permeabilized to the extent of permitting a high degree of dye uptake. Medium fluorescence represents cells which took up the dye but were not fully permeabilized, and faint fluorescence is baseline or control permeation. ±S.E.M. (n=4)

Statistics: The asterisk indicates significantly more bright fluorescence in ATP treated cells of both types compared with the control. Extent of medium and faint fluorescence was similar for both treatments. There was no significant difference between goblet and columnar cells.

effect may have been due to the delicate constitution of these cells after isolation, as microvilli become cleaved. This in turn would increase passive uptake of the probe by the cell. In contrast, a short exposure of 2 min was insufficient to yield many brightly fluorescing cells, although there were fewer cells with background (faint) fluorescence uptake compared to the control (Figure 6.6a, b). A longer incubation in ATP was required for any real permeabilizing effects to occur suggesting that midgut cell membranes may not be ideal substrates for ATP^{4-} action.

The results with detergents were more promising. Both saponin and digitonin significantly enhanced the ratio of bright fluorescence in the cell samples compared to the controls (compare Figures 6.7, 6.8 and 6.9). The presence of 5% ethanol in the saline did not have any apparent effect on ethidium bromide uptake and therefore did not contribute directly to the effects seen with the detergents (Figure 6.9b), other than perhaps enhancing their solubility. Increasing the concentration of detergent had little effect on permeabilization ability suggesting that 50μg ml^{-1} was probably a saturated concentration (Figure 6.7).However, fewer goblet cells stained faintly with 100μg ml^{-1} than with 50μg ml^{-1} digitonin (Figure 6.8a). Both detergents caused a significantly lower ratio of faint staining in goblet cells compared with columnar cells, perhaps reflecting differences in membrane composition of the two cell types. There was little difference between the two detergent types; however, at 50μg ml^{-1}, saponin did have a greater permeabilizing effect on the whole cell population (Figures 6.7b and 6.8b). Figure 6.10 shows epifluorescence micrographs of isolated midgut cells after uptake of ethidium bromide. Permeabilized cells (Fig. 6.10b and c) displayed brighter staining than the control (Fig. 6.10a), although due to compensation by the photographic apparatus it may not appear so.

6.2.2.2. Whole Tissue Permeabilization; Short Circuit Conditions

From the results with isolated cells, it seemed that there could uses for the permeabilizing ability of these agents. One application was the potential switching on or fuelling of the ATPase ion pump on the goblet cell apical membrane. Short circuit current measurement was used initially to monitor the electrogenic condition of the epithelium as varying concentrations of detergent were added to the membrane. Figure 6.11 shows that 100μg ml^{-1} digitonin (a concentration which permeabilizes

Figure 6.6 Ethidium bromide fluorescence after short exposure to ATP

(a) 2 minutes exposure to 1mM ATP

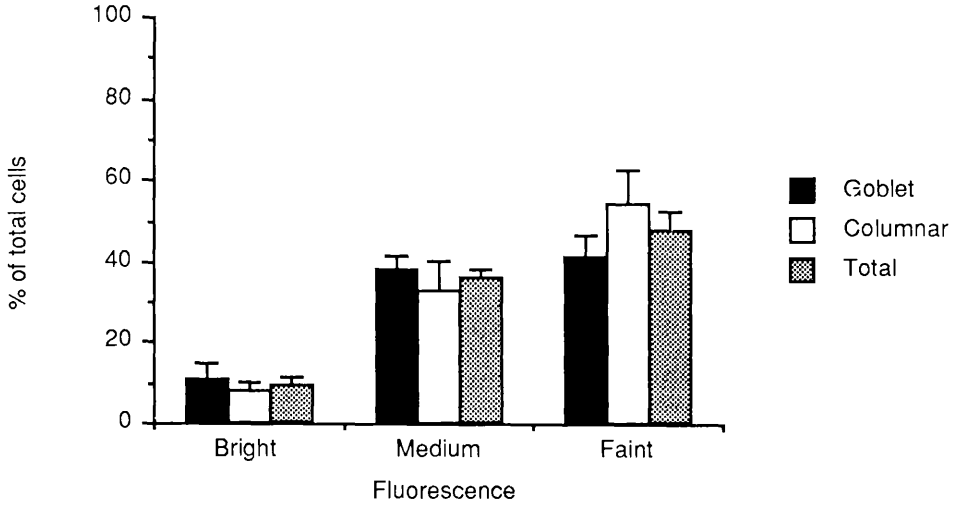

(b) 2 minutes exposure to saline (Control)

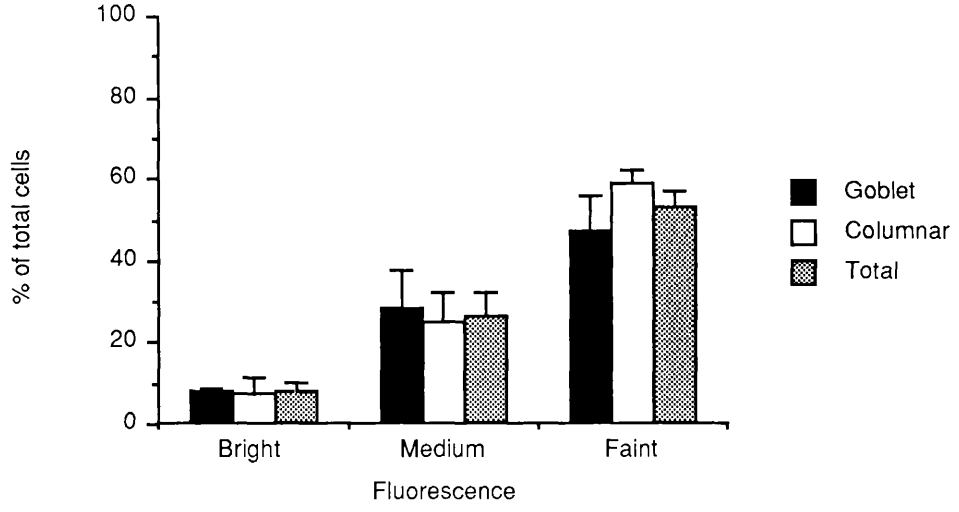

Ethidium Bromide uptake into isolated midgut cells. (a) Cells exposed to 1mM ATP in divalent-free saline for 2 min. (b) Cells exposed to divalent-free saline for 2 min as a parallel control for ATP permeabilization. Ability to permeate goblet cell membranes was compared with ability to permeate columnar cell membranes. Bright fluorescence indicates the percentage of cells in the sample which were permeabilized to the extent of permitting a high degree of dye uptake. Medium fluorescence are cells which took up the dye but were not fully permeabilized, and faint fluorescence indicates baseline or control permeation. ±S.E.M. (n=4)

Statistics: There was no significant difference in extent of fluorescence uptake between short ATP treatment and the control. Nor between goblet and columnar cells.

Figure 6.7 Ethidium bromide fluorescence after exposure to detergents

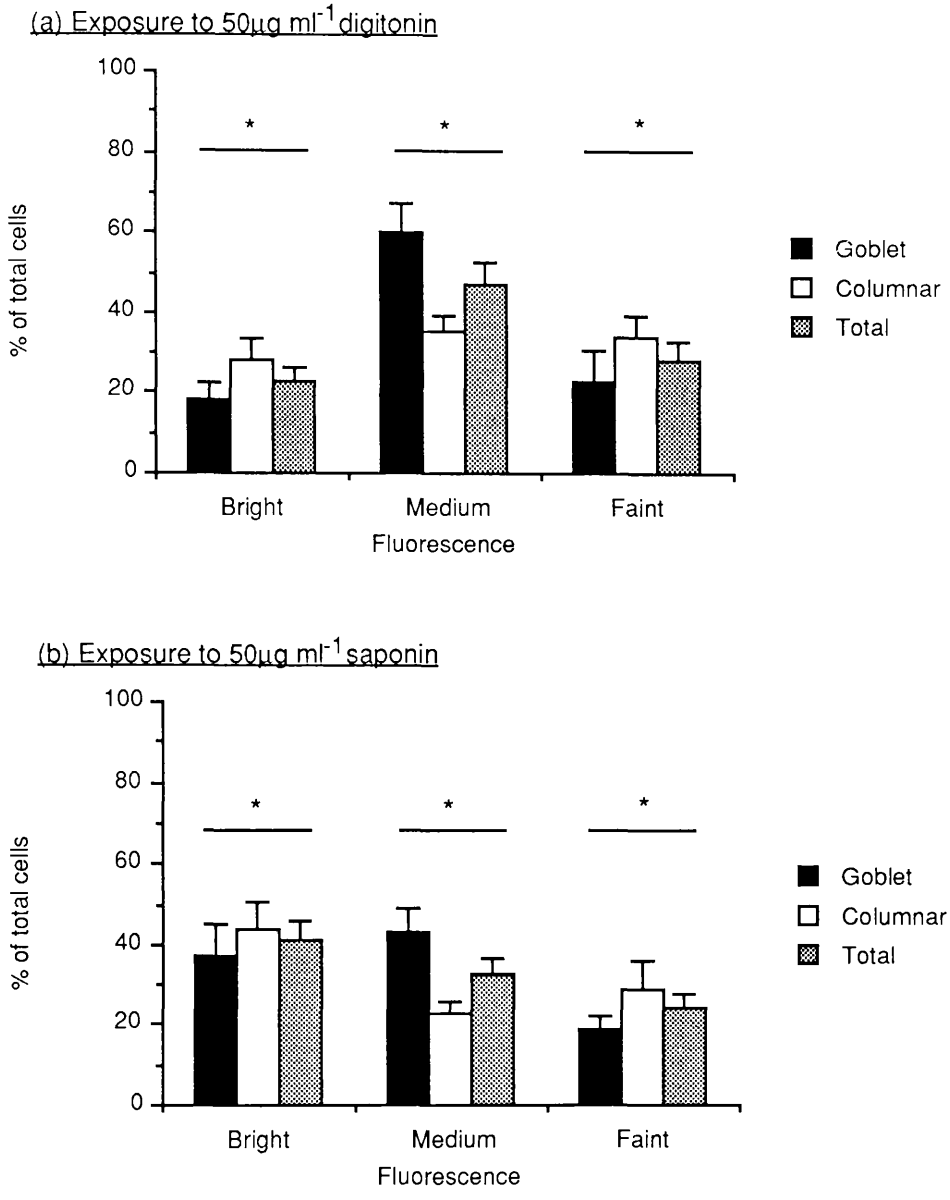

Ethidium Bromide uptake into isolated midgut cells. (a) Cells exposed to 50µg ml^{-1} digitonin in divalent-free saline (n=8). (b) Cells exposed to 50µg ml^{-1} saponin in divalent-free saline (n=6). ±S.E.M. Ability to permeate goblet cell membranes was compared with ability to permeate columnar cell membranes. Bright fluorescence indicates the percentage of cells in the sample which were permeabilized to the extent of permitting a high degree of dye uptake. Medium fluorescence represents cells which took up the dye but were not fully permeabilized, and faint fluorescence is baseline or control permeation.

Statistics: Asterisks indicate significant difference in fluorescence uptake for both saponin and digitonin treatments compared with controls (fig. 6.9). Saponin treatment yields significantly more bright fluorescnce and less medium fluorescence than digitonin. Both detergents significantly increased medium fluorescence and decreased faint fluorescence in goblet cells compared with columnar cells.

Figure 6.8 Ethidium bromide fluorescence after exposure to detergents

(a) Exposure to 100µg ml^{-1} digitonin

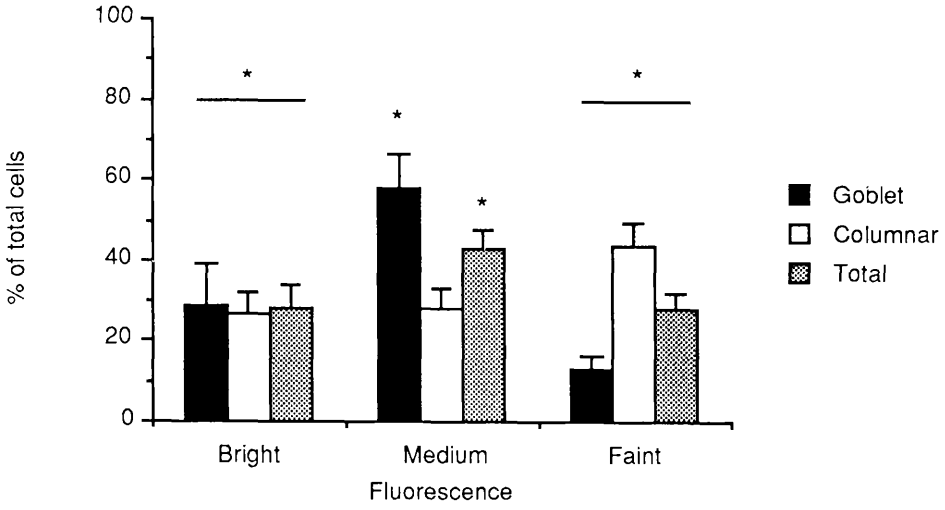

(b) Exposure to 100µg ml^{-1} saponin

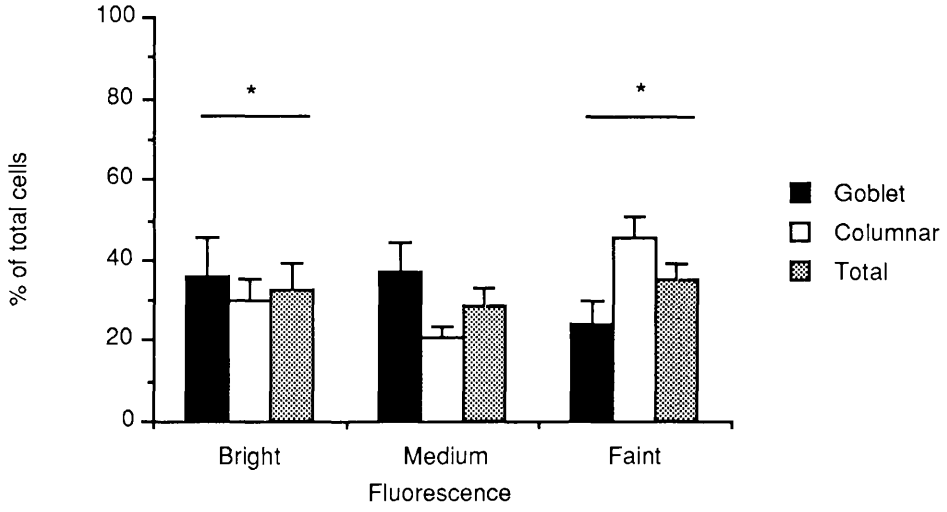

Ethidium Bromide uptake into isolated midgut cells. (a) Cells exposed to 100µg ml^{-1} digitonin in divalent-free saline (n=7). (b) Cells exposed to 100µg ml^{-1} saponin in divalent-free saline (n=9). ±S.E.M. Ability to permeate goblet cell membranes was compared with ability to permeate columnar cell membranes. Bright fluorescence indicates the percentage of cells in the sample which were permeabilized to the extent of permitting a high degree of dye uptake. Medium fluorescence represents cells which took up the dye but were not fully permeabilized, and faint fluorescence is baseline or control permeation.

Statistics: Asterisks indicate significant difference from the control for bright and faint fluorescence levels. Medium fluorescence in columnar cells was not significantly different from control staining. Goblet cells displayed more medium and less faint fluorescence than columnar cells for both detergents. There was no significant difference between saponin and digitonin, nor between 100µg ml^{-1} and 50µg ml^{-1} .

Figure 6.9 Ethidium bromide fluorescence after exposure to controls

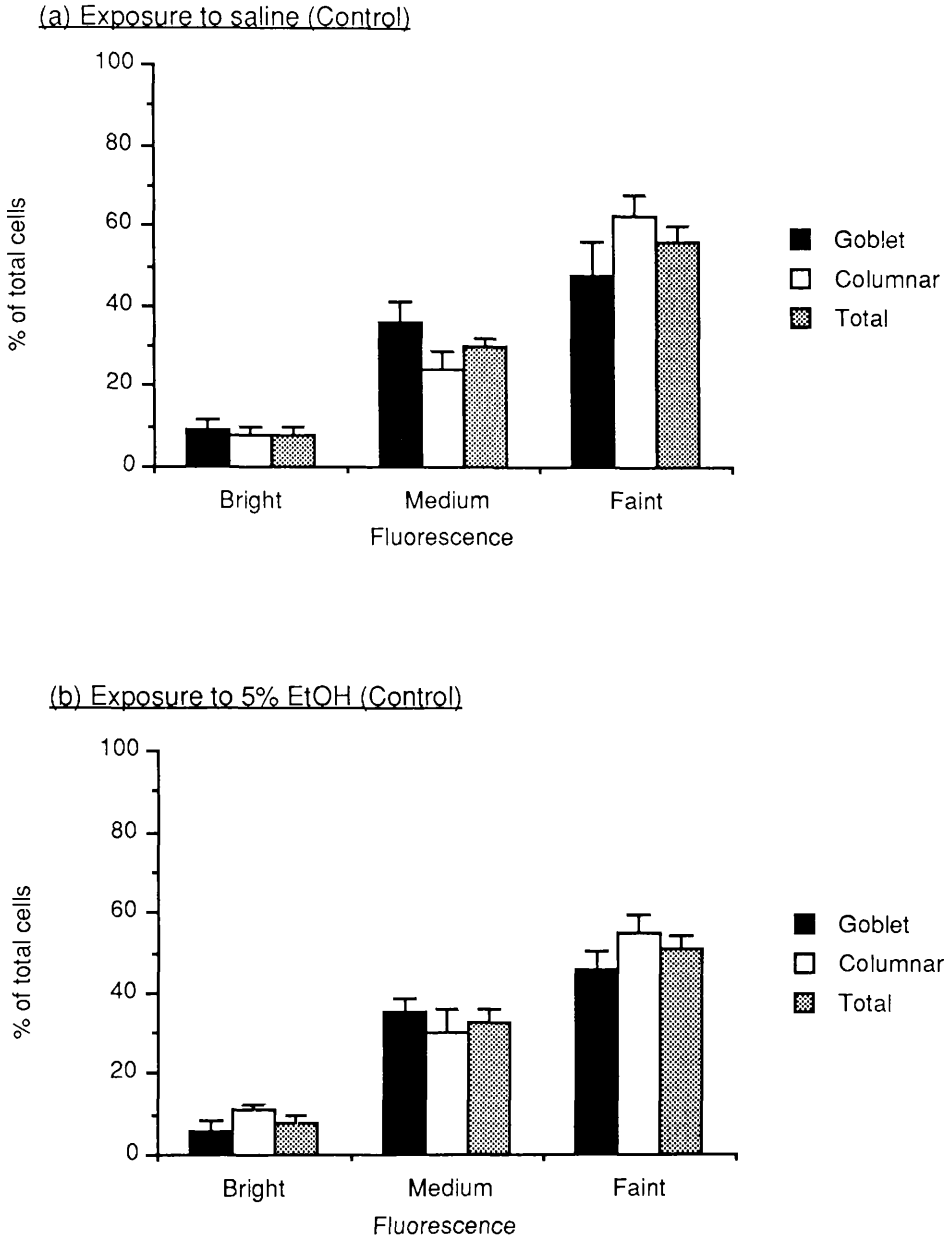

Ethidium Bromide uptake into isolated midgut cells. Parallel controls for detergent permeabilization. (a) Cells exposed to divalent-free saline (n=7). (b) Cells exposed to 5% EtOH in divalent-free saline (n=9). ±S.E.M. Ability to permeate goblet cell membranes was compared with ability to permeate columnar cell membranes. Bright fluorescence indicates the percentage of cells in the sample which were permeabilized to the extent of permitting a high degree of dye uptake. Medium fluorescence represents cells which took up the dye but were not fully permeabilized, and faint fluorescence is baseline or control permeation. There was no significant differences between the two controls.

Figure 6.10 Ethidium Bromide uptake into permeabilized midgut cells.

a. Under control conditions, cells were exposed to divalent-free *Manduca* saline before incubation in 50μM ethidium bromide. This fluorescence micrograph shows a goblet cell and a columnar cell displaying faint fluorescence compared with permeabilized cells (figs. b and c). Nb. when capturing the image, the camera compensates for the lack of brightness which causes faint cells to appear brighter on film.

b. Cells were exposed to 100μg ml^{-1} saponin before assaying fluorescence emission after ethidium bromide uptake. This micrograph show a bright goblet cell, a bright columnar cell and a medium fluorescent columnar cell.

c. Cells were exposed to 100μg ml^{-1} digitonin before assaying for ethidium bromide uptake. Brightly fluorescing goblet and columnar cells are shown.

Scale bars = 50μm

Figure 6.10 Ethidium Bromide uptake into permeabilized midgut cells.

a

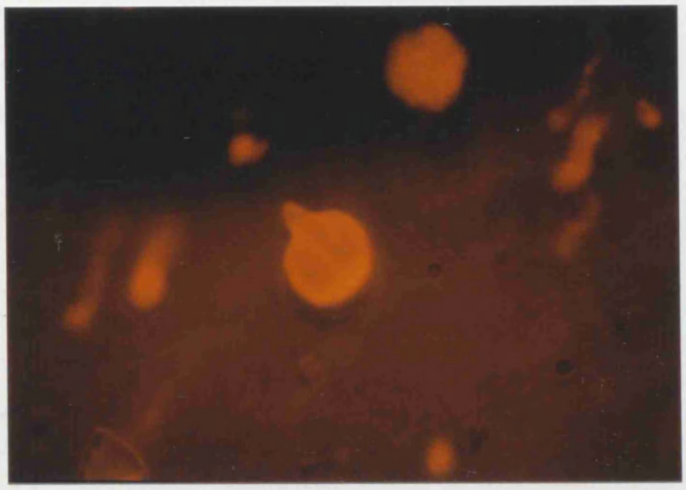

b

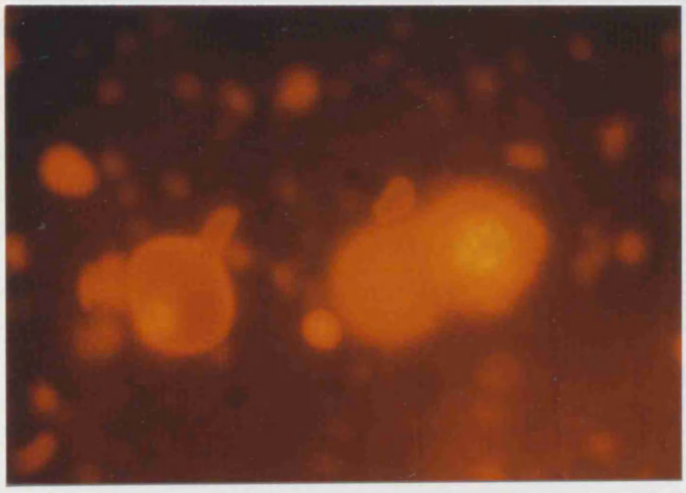

c

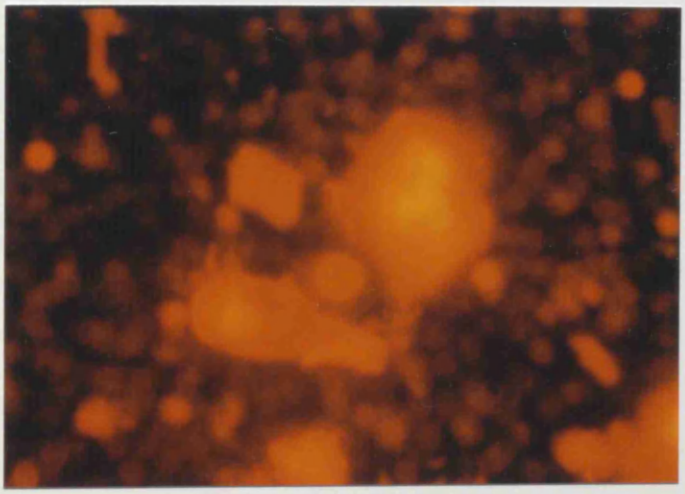

Figure 6.11 Effect of digitonin on SCC of middle midgut

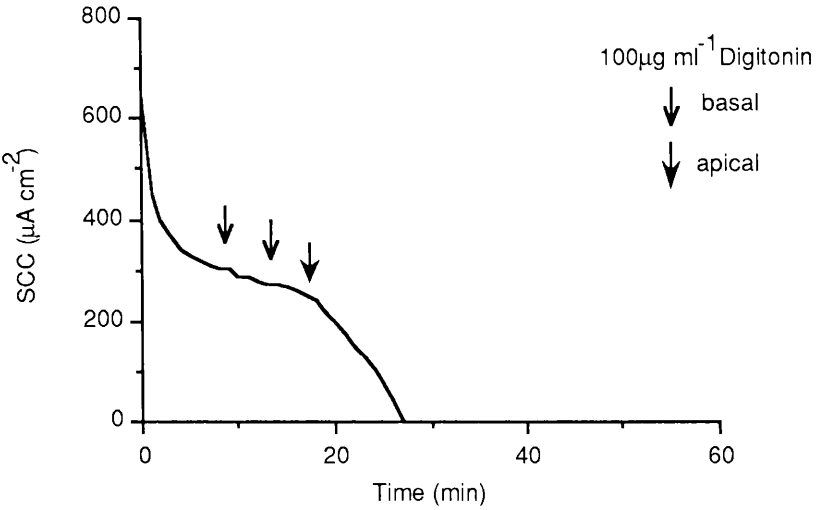

Permeabilization of the middle midgut under short circuit conditions using digitonin. 100μg ml^{-1} digitonin in divalent-free saline was added sequentially to the basal (twice) and apical (once) sides of the epithelium. A sharp drop in SCC (short circuit current) indicates successful permeabilization.

isolated cells) had little effect when added to the basal side; However, SCC was abolished relatively quickly when the same dose was applied to the apical side. A much greater dose of 400μg ml^{-1} was required to cause a decline of SCC when added to the basal side (Figure 6.12). Saponin had little permeabilizing effect, requiring 800μg ml^{-1} to cause just a slow decline (Figure 6.13).

One reason for the poor permeabilizing activity of basally applied agents could be that there is more connective tissue (basement membrane) and even a muscle cell layer to penetrate before the epithelial cell basal membrane can be targeted. Another possible explanation is that the basal side of the tissue does become permeabilized but the drop in SCC seen with higher doses is actually poration of the apical membrane (the site of the large electrochemical gradient) from the cytoplasmic side. Figure 6.14 shows that one application of 100μg ml^{-1} digitonin to the apical side only, caused an immediate drop in SCC. Once the current was almost at zero a 20mM addition of ATP to the apical (permeabilized) side produced a small rise in current indicating a transient enhancement of ion transport from basal to apical side, perhaps as the pump was fuelled. Making additions, such as they were, often had a disrupting effect on the SCC curves, so, open circuit voltage recording was employed for the remaining experiments.

6.2.2.3. Whole Tissue Permeabilization; Open Circuit Conditions

It was emphasised, using this recording parameter, that basal additions of permeabilizing agent (mainly digitonin) were followed by a 5 min lag time before a drop in TEP was seen (Figure 6.15). This supports the opinion that the basal membrane did not carry a significant electrical gradient which could be diminished on permeabilization. Alternatively, the underlying connective tissue might be a physical barrier to diffusion of the agent. Very high doses of digitonin were required to see any effect and the rate of decline seemed to be loosely dose-dependent suggesting that it was diffusional access to the membrane which was the rate limiting step for basal permeabilization (Figure 6.15b). Addition of 20mM ATP to basally permeabilized cells had little or no effect on increasing TEP transiently and in fact occasionally it acted as a permeabilizing agent speeding the rate of decline. This finding could mean that the cytoplasmic

Figure 6.12 Effect of basal digitonin on SCC of middle midgut

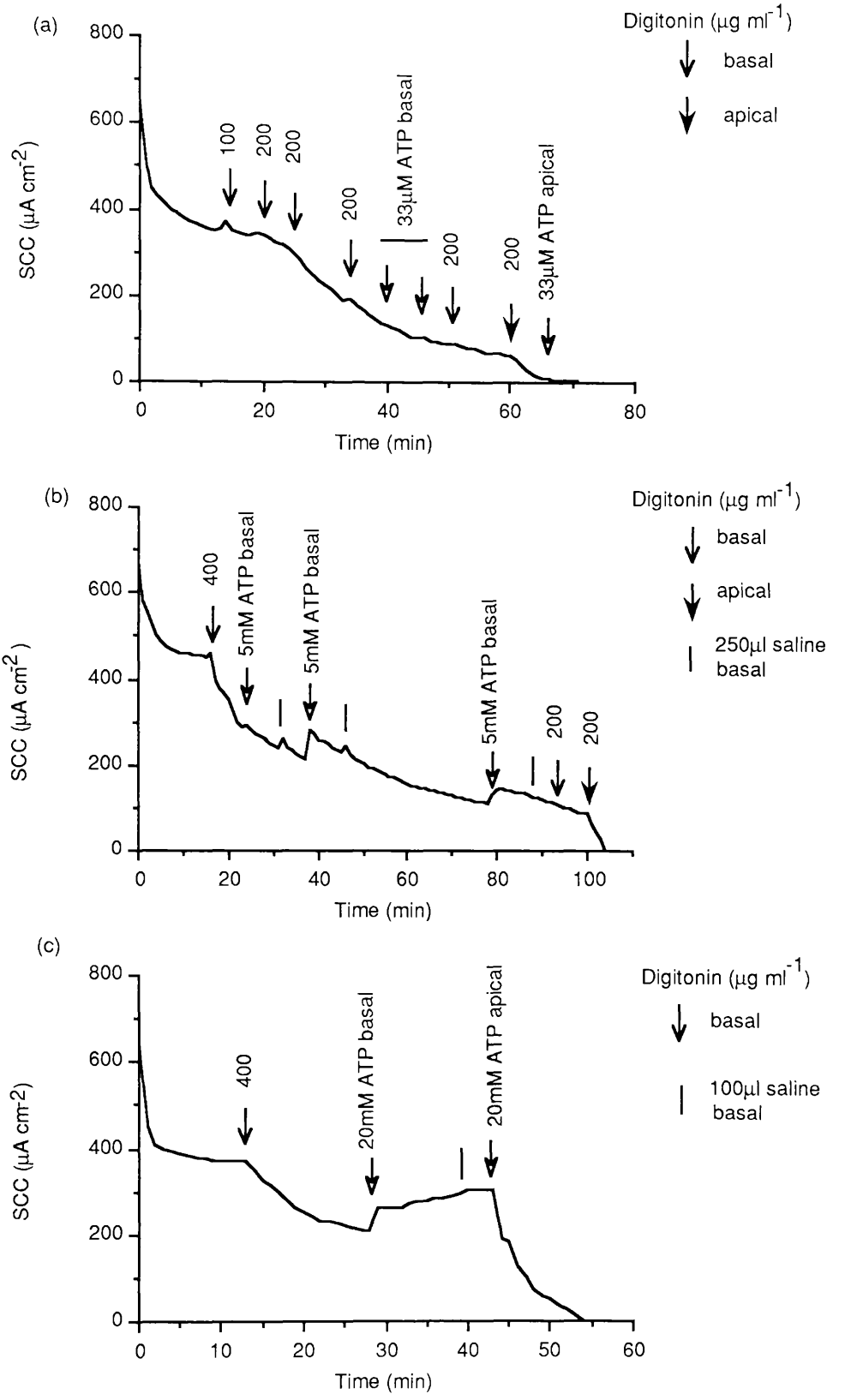

Permeabilization of the middle midgut under short circuit conditions using digitonin. Digitonin was added to the basal and apical sides of the epithelium at the concentrations shown in divalent-free saline (the numbered arrows). Permeabilization is indicated by a drop in SCC. ATP, at various concentrations, was applied to different sides of the epithelium after permeabilization. a, b and c are 3 separate experiments.

Figure 6.13 Effect of basal saponin on SCC of middle midgut

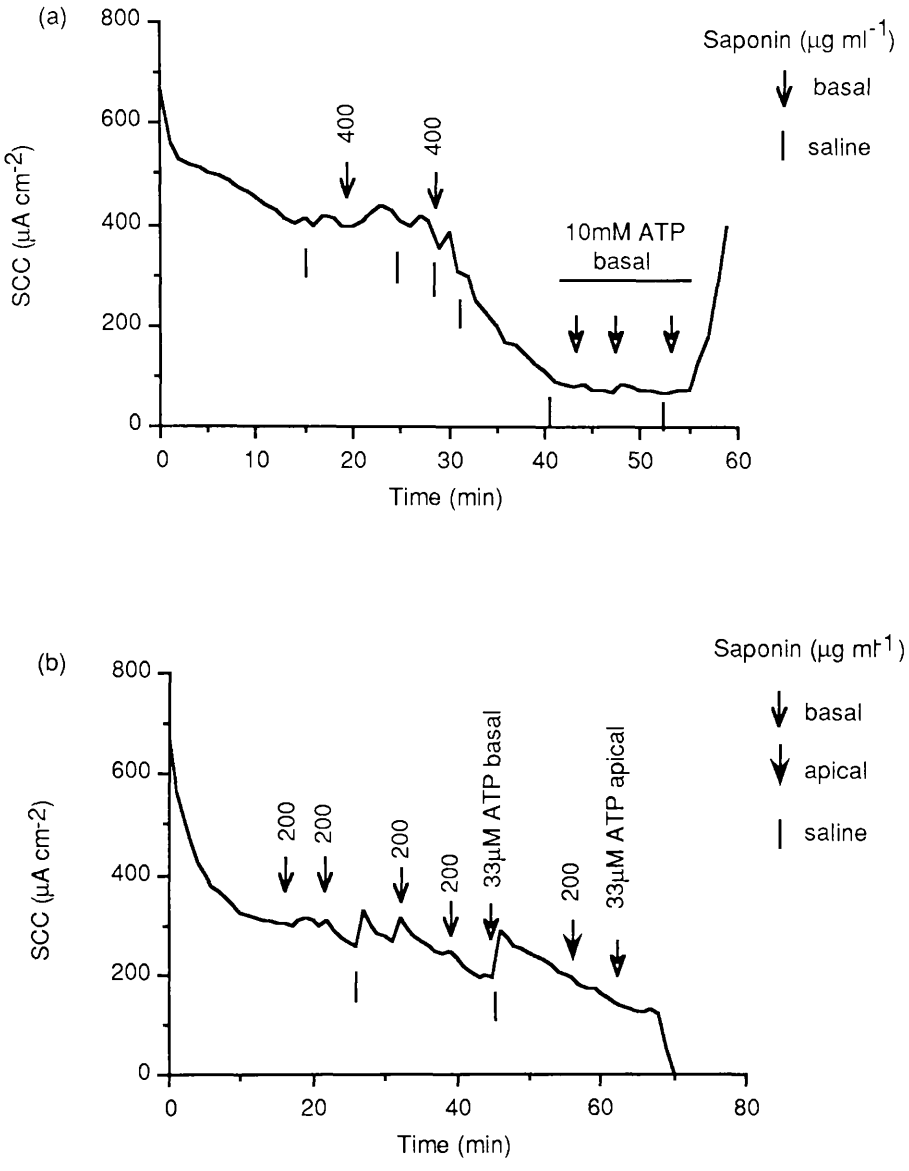

Permeabilization of the middle midgut under short circuit conditions using Saponin. Saponin was added mainly to the basal but also to the apical side of the epithelium at the concentrations indicated by the numbered arrows. Permeabilization is indicated by a sharp drop in SCC. ATP at various concentrations was applied to either side following permeabilization. a and b are 2 separate experiments.

Figure 6.14 Effect of apical digitonin on SCC of middle midgut

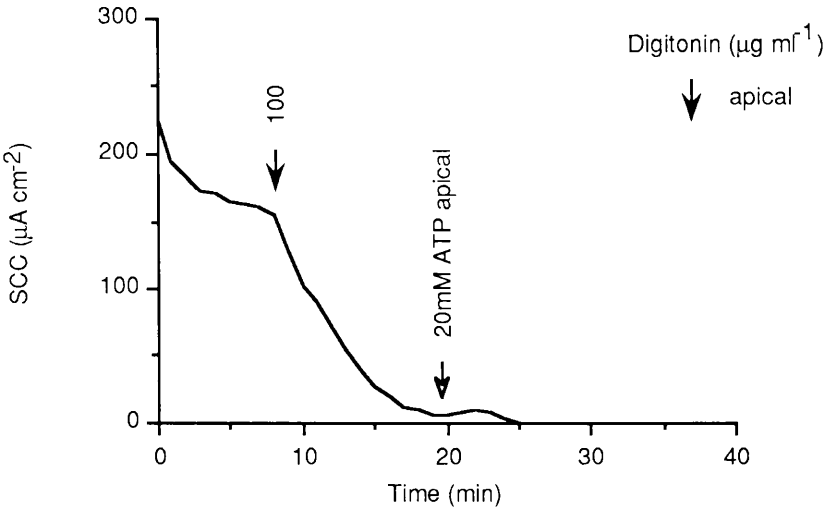

Permeabilization of the middle midgut under short circuit conditions using digitonin. Digitonin was added to the apical side at a concentration of 100μg ml^{1} in divalent-free saline. Permeabilization is indicated by a drop in SCC. Addition of 20mM ATP to the apical side following permeabilization had the effect shown.

Figure 6.15 Effect of basal digitonin on TEP of middle midgut

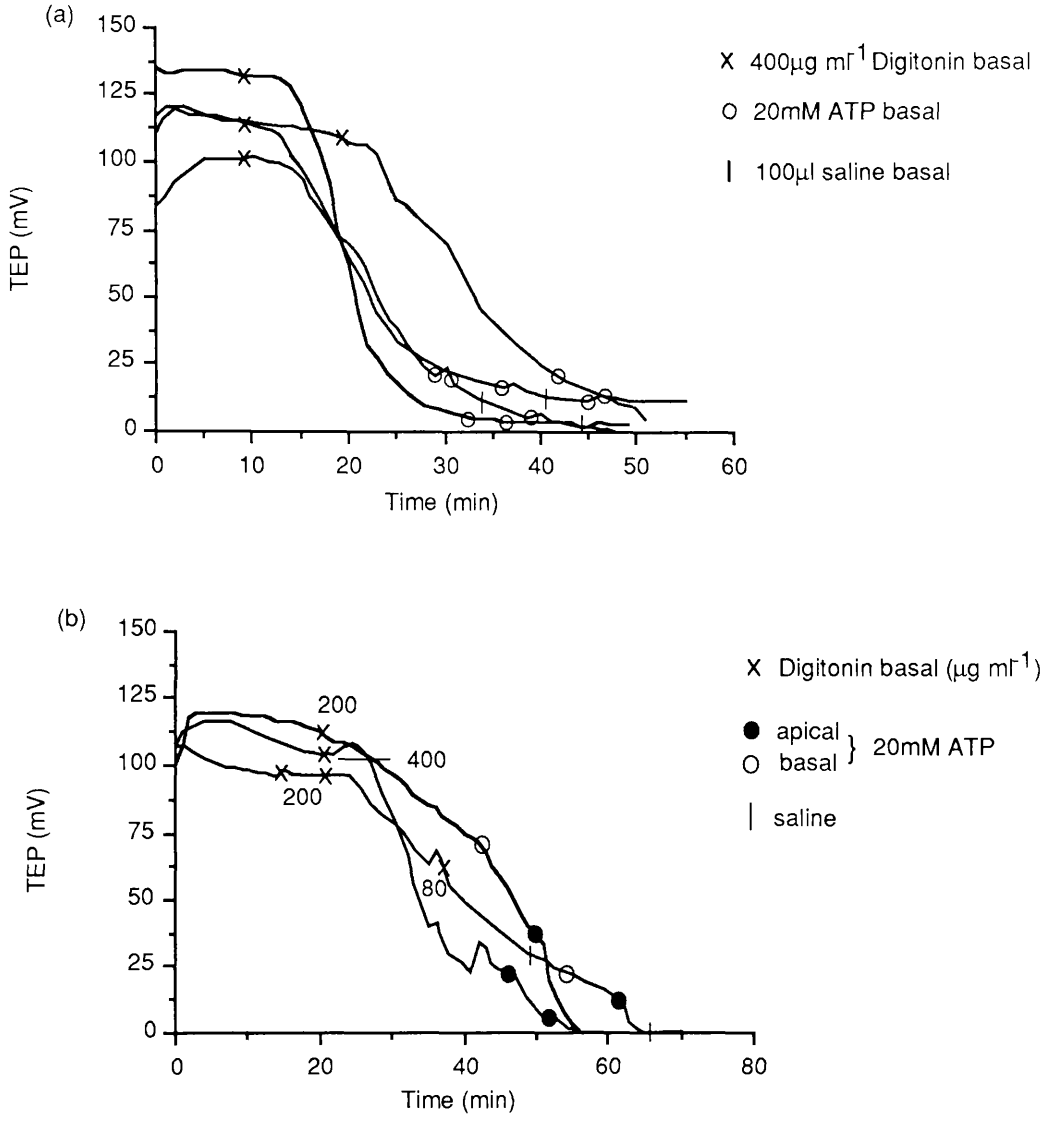

Permeabilization of middle midgut under open circuit conditions using digitonin. Digitonin was added at the concentrations indicated to the basal side. Following permeabilization, 20mM ATP was added to either the basal or apical side of the epithelium and the effects recorded. The results from 7 experiments are shown but are presented on 2 graphs (a and b) for simplicity.

side of the apical membrane, or the pump itself, had been affected by the high dose of digitonin and could no longer be electrically stimulated.

Digitonin added to the apical side caused a rapid decline of TEP even at doses as low as 50μg ml^{-1} (Figure 6.16). Subsequent ATP additions almost always induced a transient rise in TEP of about 4-5mV for a duration of 5 min. It could be a matter of access as the pump is located apically in the tissue therefore apical ATP additions could diffuse readily to their intended site. Another explanation could be that the lower doses of detergent used to reduce the TEP on the apical side, did less damage to the cytoplasmic face of the membrane than the higher dose required for the same effect on the basal side.

Saponin, at 400μg ml^{-1}, had less of an effect on the basal membrane than the same concentration of digitonin (figure 6.17), in contrast to the findings with isolated cells that both detergents were equally efficient agents for permeabilizing midgut cells (Figure 6.8a). The conclusions drawn from these results are based on the assumption that permeabilization of the apical membrane is a prerequisite for loss of TEP, which it might not be. Instead, disruption of the ionic and metabolic constituents of the cytoplasm following membrane poration by these agents could indirectly affect the ion transporting capabilities of the tissue cells.

Even ATP reduces TEP when added to the apical side in divalent-free conditions (Figure 6.18). The concentration of 20mM used here was much greater than that used for isolated cell permeabilization, hence the speed of the response. When ATP was added after TEP had fallen to near zero with apical digitonin permeabilization (Figure 6.16), the cells were probably fully permeabilized with the electrochemical gradient lost completely. So, ATP^{4-} simply entered the goblet cells, became neutralised by the divalents present and diffused to the catalytic site of ion pumps, which were transiently fuelled. The small values obtained for these rises should be expected as the epithelium was probably in a condition unsuitable for supporting any significant ionic or electrical gradients.

Figure 6.16 Effect of apical digitonin on TEP of middle midgut

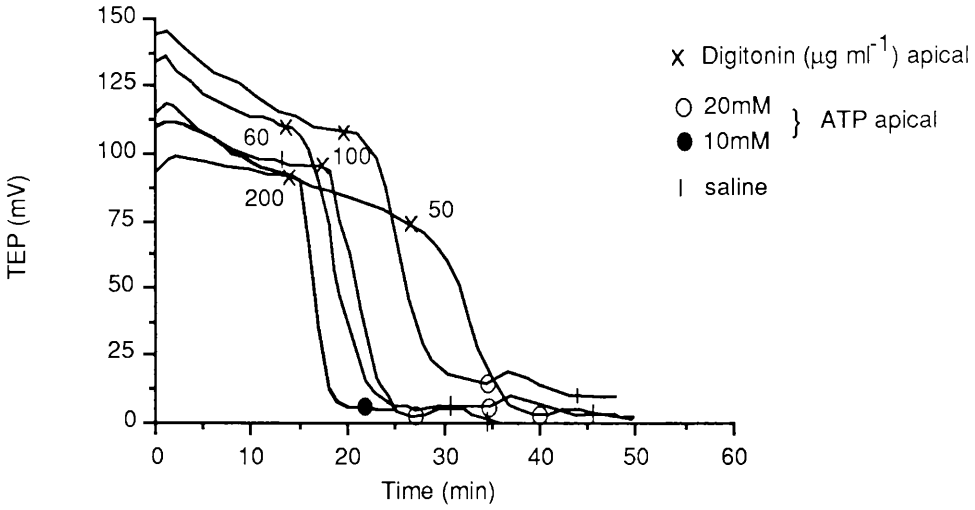

Permeabilization of middle midgut under open circuit conditions using digitonin. Digitonin was added at the concentrations indicated to the apical side. Following permeabilization, 20mM ATP (or 10mM in one instance) was added to the apical side of the epithelium and the effects recorded. The results from 5 separate experiments are shown.

Figure 6.17 Effect of basal saponin on TEP of middle midgut

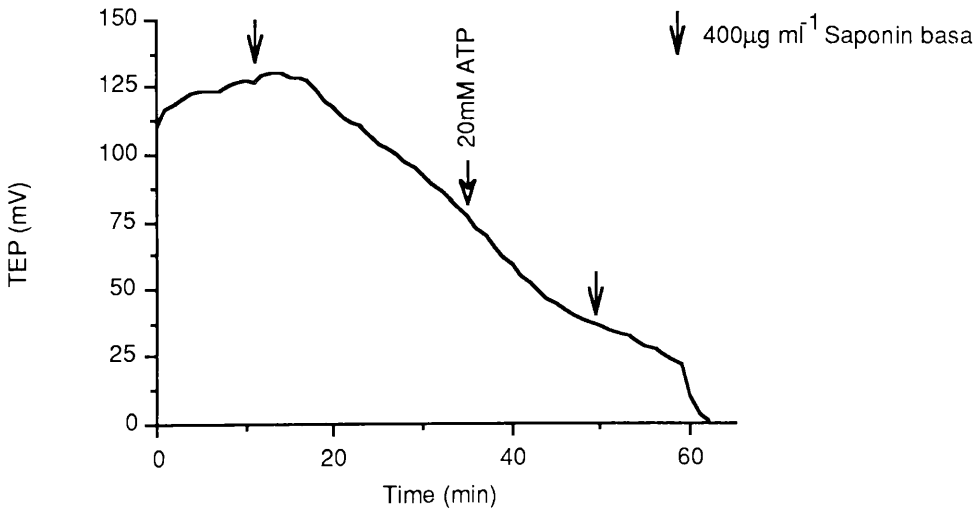

Permeabilization of the middle midgut under open circuit conditions using saponin. Saponin, in divalent-free saline, was added at a concentration of 400μg ml^{-1} to the basal side of the epithelium. 20mM ATP was also added to the basal side during the decline of transepithelial potential.

Figure 6.18 Effect of apical ATP on TEP of middle midgut

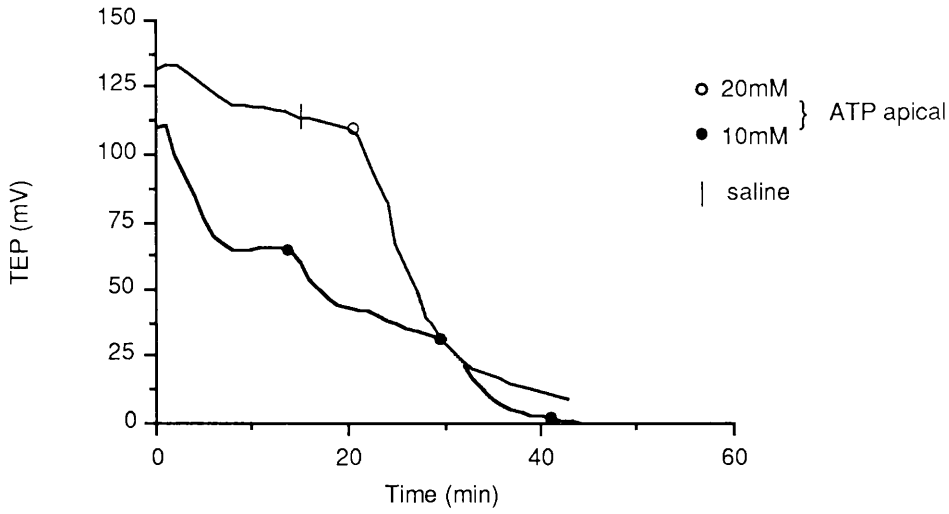

Permeabilization of middle midgut under open circuit conditions using ATP. ATP was added to the apical side of the midgut in divalent-free saline at the concentrations indicated. Permeabilization is seen as a drop in transepithelial potential (TEP). The results of 2 separate experiments are shown.

6.2.3. Discussion

Lepidopteran midgut epithelial cell membranes can be permeabilized using certain commonly employed agents, including ATP^{4-}, digitonin and saponin (Brooks and Treml 1983; Gomperts and Fernandez 1985; Smolen and Stoehr 1985; Wilson and Kirshner 1983). To date there is no record of the effectiveness of permeabilizing agents on any insect cells types. Both reversible and irreversible techniques were successful for both goblet and columnar cells, with no significant cell specificity observed. Steroid glycosides were more effective than even long exposure to ATP, as determined by the strength of fluorescence in cells caused by passive ethidium bromide uptake. It was difficult to assess permeabilization ability using this method as it required a qualitative assessment by eye. Ethidium bromide binds to DNA and RNA and so was brightest around cell nuclei. Quantitative analysis could be carried out using spectrofluorimetry; however, it was suffice to determine whether or not cells could be permeabilized, so that ATP or other moieties likely to enhance ATPase activity within the goblet cell cytoplasm could be introduced. This was achieved and by monitoring transepithelial potential (TEP), not only could permeabilization of the epithelium be followed, but the apical addition of ATP was seen to have a small stimulatory effect on the overall potential.

This technique of permeabilizing midgut cells with detergents or ATP, opens the way for a range of pharmacological studies, which at the very least could allow labelling of the cytoplasmic-facing proteins, like the ion transporting ATPase, whilst it is operating, or before any membrane isolation procedures have been carried out. The physiological effects of a range of pharmacological agents could be screened on this assay system. The results with ATP permeabilization at high concentration suggest a possible resealing process (by addition of divalents) which may be viable for various applications, such as introducing genes or gene products into the cytoplasm.

Chapter 7

7. Chapter 7 Discussion

There are several models for the transport of potassium ions from the haemolymph into the lumen of Lepidopteran larvae (Dow et al. 1984; Dow and O'Donnell 1990; Harvey et al. 1981; Harvey et al. 1983b; Harvey and Nedergaard 1964; Harvey and Zehran 1972; Wieczorek et al. 1989). Harvey originated the model that a K^+ ATPase was resident on the goblet cell apical membrane and that it was responsible for transporting K^+ ions electrogenically from the basal to the apical side of the midgut. Dow (1984) expanded on this model and suggested that the active transport of K^+ was indirectly responsible for generating the high luminal pH measured (Dow 1984). The presence of carbonic anhydrase at this region facilitated the generation of bicarbonate ions in the cavity, the membrane of which was by then highly polarized by active K^+ ion transport. This electrical potential difference also drove protons, which had been stripped from bicarbonate, back across the membrane into the cytoplasm, in accordance with the Nernst equation. K^+ and carbonate ions then leaked into the lumen resulting in a very high pH there. This theory applied only to the front two thirds of the midgut where the high luminal pH had been recorded, and not necessarily to the posterior region in which the pH could be seen to fall along its length. The posterior third did display electrogenicity with similar properties (Cioffi and Harvey 1981), although it was not coupled to alkali generation.

Some support for this regional specialization of transport properties can be obtained from the results of Ridgway and Moffett (1986) who reported a localization of carbonic anhydrase at the goblet cell apical membranes in the front two thirds of the midgut, and at the columnar cell apical membrane in the posterior third (Ridgway and Moffett 1986). This also suggested that the electrogenic transport found in the posterior region could be for regulation of pH in the blood and other tissues. The extent of alkalinization in the lumen would imply parallel acidification of the blood and / or epithelial cell cytoplasm. However, direct measurements of pH in these compartments gave values of pH 6.7 and 7 respectively (Dow 1984; Roos and Boron 1981). Homoeostasis is evident by the measured fall in pH in the posterior lumen, following the rise in anterior and middle regions, suggesting that there is recycling of acid / base equivalents. The

movement of protons away from the luminal side in the front two-thirds of the midgut therefore has a low impact on the blood pH overall.

As well as osmotic regulation by the Malpighian tubules (Bradley 1983; O'Donnell and Maddrell 1984), the posterior region may be involved in excreting protons back into the lumen, possibly via the columnar cell microvilli, which have associated matrix material not unlike that found in the goblet cavity (Dow et al. 1984; Harvey et al. 1983a). If there is a Cl^-/HCO_3^- exchange mechanism at the brush border, as indicated by the presence of carbonic anhydrase (Ridgway and Moffett 1986), then this could be driven indirectly by electrogenic K^+ transport in the posterior region and may help to regulate overall pH.

In another model, proposed by Wieczorek et al. (1989), which has been receiving considerable attention, the electrogenic pump is an H^+ ATPase. Active transport of protons into the cavity energizes an electroneutral H^+/K^+ exchange antiporter, resulting in K^+ transfer from the blood to the lumen, but not directly resulting in high pH. An anionic conductance is also present in the membrane, and depending on which anion is transported there could be variations in cavity pH, i.e. Cl^- would cause acidification, HCO_3^- would be less acidic, and shutting off the conductance would result in alkalinization. It is possible that Cl^- dominates in the posterior midgut and is therefore the anion conducted across the cavity membrane thereby causing acidification, whereas bicarbonate may be the subject of the anionic conductance in the anterior and middle regions. The fixed negatively charged mucopolysaccharides present in the cavity may influence anionic conductance in this way (Dow et al. 1984; Gupta et al. 1985).

Moffett has recently measured the pH of cavities in the posterior region and found it to be 7.23, which is close to neutral. This finding contradicts Wieczorek's theory as there would not be enough energy contained in the proton gradient to drive K^+ flux across the membrane. This could be resolved by having an exchange stoichiometry of at least $2H^+ / K^+$. Cavity pH has not yet been measured directly in anterior and middle midgut; however, if it too is near neutral then another mechanism present somewhere between the cavity and the lumen must bring about the high pH found in the lumen. The flexibility of this system with respect to pH in

the cavity allows the results obtained during this study to be interpreted in accordance with an H^+ ATPase; however, this interpretation often appears slightly contrived. The results are better explained in the context of Dow's model (1984). Another point in favour of the H^+ ATPase model is that from an evolutionary stand-point, these vacuolar-type pumps are ubiquitous and conserved, and they have been known to energize other transport processes in a similar way to the proposed model (Nelson 1987; Nelson and Taiz 1989).

Some recent sequencing work on the pump suggests that a 69kDa polypeptide isolated from the protein is identical to that of other known vacuolar ATPases (Harvey, pers. comm.). There are still some gaps in the model; How is pH generated? What is the anion transported? What is the role of the cavity? This controversy is currently being reviewed and the end result may be something of a compromise, or a completely new model, such as a K^+ / H^+ exchange ATPase working in the opposite direction from that in mammalian gastric mucosa (Al-Awqati 1986; Nelson 1987; Nelson and Taiz 1989; Pedersen and Carafoli 1987a; Pedersen and Carafoli 1987b).

Microelectrode impalements of cavities in isolated tissue showed that there was a high potential difference across the goblet cell apical membrane, and that the resistance in the cavity was such that the cavity was electrically isolated from the midgut lumen, supporting the predictions of the model proposed by Dow (1984) and emphasising the importance of the cavity. This p.d. could be generated by either an electrogenic K^+ ATPase, or an electrogenic H^+ ATPase, although no proton ATPases nor any other type of ion-motive ATPases have been discovered to date with an electron motive force (emf) quite as high as the 270mV estimated from these measurements (Harvey et al. 1983a). A K^+/ H^+ exchanger could also be present on this membrane and along with some kind of conductance of H^+ across the energized membrane could result in extreme alkalinization of the cavity. These results alone did not discriminate between the two models, as the electrical element of transport could be independent of the type of ion transported, providing it was a monovalent cation; However, the experiments carried out with acridine orange on transporting midgut were thought-provoking.

Actively transporting midgut tissue *in vitro* (~60-140mV) when stained with acridine orange, appeared under fluorescence as a green epithelial sheet filled with unstained black holes which correspond to alkaline (or at least non-acidic) goblet cavities. Non-transporting epithelia also displayed green cytoplasmic staining but had red, acridine orange filled cavities suggestive of acidity. Why, if the electrogenic element was an H^+ ATPase, should blocking this pump result in acidification of the cavity lumen? Perhaps the energy used in pumping one proton drove more than one proton back across the membrane, for instance by having extremely electroresponsive K^+ / H^+ exchanger. Therefore losing the driving force for the antiporter would result in proton accumulation within the cavity. It is perhaps easier to believe that an electrogenic K^+ ATPase is responsible for facilitating H^+ movement out of the cavity and that its inhibition would result in cavity acidification.

When K^+ was omitted from the bathing solution, not only were red cavities found, which could be explained in the context of the H^+ ATPase model by the failure of the electroneutral K^+ / H^+ antiporter, but there was also a rapid fall off in transepithelial potential difference to 0 mV followed by a reversal of potential. In short, the electrogenic transport was lost in the absence of potassium ions, which, according to Wieczorek's model, are transferred from blood to lumen by electroneutral means. One way to explain these results with an H^+ ATPase could be to say that the K^+ / H^+ exchange is coupled to the anionic conductance step which is affected by inhibition of the antiporter in K^+ -free conditions. Conductance of Cl^- into the cavity for instance would result in acidification as well as balancing out the charge transferred by active H^+ transport.

Many of the problems associated with these models could be resolved with further physiological and biochemical experiments, as have been used previously and in this study; however, it is imperative that the structure and evolution of the pump is defined and molecular biology will no doubt provide most of the answers. Some progress has already been made in this area with respect to the ion transport ATPase of *Manduca sexta* midgut, as a 69kDa polypeptide which has been isolated and partially purified from goblet cell apical membranes appears to have an amino acid sequence identical to that of other known vacuolar ATPases (Harvey pers comm.; Schweikl et al. 1989; Schweikl et al. 1987).

The ability to isolate, separate and maintain insect midgut cells in culture could be useful for several reasons. For instance, membrane proteins would be guaranteed to have originated from specific cells, such as goblet cells. Also, expression systems could be set up once cell lines have been established and viruses, which are specific for the midgut, could be used to express the pump and mutations of the pump subunits *in vitro* (Hammock et al. 1990). Further manipulation could yield interesting conclusions about the nature and origin of the transport mechanism.

Although many isolation and separation methods were attempted during the course of this study, with some reasonably enriched populations being obtained, purity of the samples was low. For instance, when immobilized lectin was used to sequester columnar cells from a heterogeneous population of midgut cells, the results were ambiguous depending on the method used. In general, one thing that emerged was that goblet cells were more robust than columnar cells as they survived isolation and various treatments after isolation much better than columnar cells with their delicate microvilli. As goblet cells are the site of active transport, this means that inducing a certain amount of strain on a mixed cell suspension could potentially yield a reasonably pure population of goblet cells which one could then manipulate biochemically. Cells of both types did survive primary culture for periods exceeding two weeks and there is potential for such manipulations as well as for employing molecular biological expression systems, such as the baculovirus expression system currently in use in cell lines of *Drosophila* for expression of juvenile hormone esterase (Hammock et al. 1990).

One of the ultimate applications of these systems could be in the insecticide industry where it may be possible to specifically target an individual insect pest species and eliminate them by causing them to express proteins and hormones that normally result in their metamorphosis, or not, as the case may be. Over- or under-expression of the K^+ ATPase could potentially have dire consequences for a feeding larva. Under-expression of active transport would result in lower, or no, driven amino acid and nutrient uptake, whereas over-expression could make their gut contents indigestible and upset homoeostasis, perhaps by

over acidification of the blood and tissues in response to higher alkalinization of the gut lumen.

There is still a long and interesting study to be completed regarding not only ion transport in Lepidopteran midgut, which promises to begin a debate on the nature of the pump, (Is it a K^+ ATPase or an H^+ ATPase?), but also with the advent of new biochemical, molecular biological and physiological techniques (such as confocal fluorescence microscopy and voltage- and ion- specific dyes) many transport processes will become elucidated. The ancestral origin of the pumps could then be defined so that a broader, fundamental idea of the function of ion transport in cells and tissues becomes clear.

Ion transport processes are the physiological basis for many higher functions, for instance, it now seems that pH is the cue for division in some if not all cell types. It will therefore be interesting to see the ever reducing gap between physiology and molecular biology finally bridged.

If the "unique" K^+ ATPase of insect tissues is proved to be so, then this will be an interesting phenomenon in itself. How did this pump evolve? Perhaps it will be homologous to certain other ion pumps, which are sometimes conspicuous by their absence in certain congenital and hereditary diseases, such as the chloride transporter in cystic fibrosis. On the other hand if the pump turns out to be a proton ATPase then this opens doors to speculation on how and why this particular pump is as active as it is. Again, how did it evolve? Could its energetic coupling characteristics be mimicked in systems which are deficient in this activity? There are endless possibilities for the application of knowledge gained from such a phenomenal system, not least the self satisfaction of deciphering a mechanism of nature out of pure scientific interest.

References

REFERENCES

Adang, M. J. and K. D. Spence. (1982). Biochemical comparisons of the peritrophic membranes of the Lepidoptera *Orgyia pseudotsugata* and *Manduca sexta*. *Comp. Biochem. Physiol.* **73B**: 645-649.

Al-Awqati, Q. (1986). Proton translocating ATPases. *Ann. Rev. Cell Biol.* **2**: 179-199.

Alberts, B., D. Bray, J. Lewis, M. Raff, K. Roberts and J. D. Watson. (1989). Molecular biology of the cell. New York, Garland.

Amsterdam, A. and J. D. Jamieson. (1972). Structural and functional characterization of isolated pancreatic cells. *Proc. natn. Acad. Sci. U.S.A.* **69**: 3028-3032.

Anderson, D. T. (1973). Embryology and phylogeny in annelids and arthropods. Pergamon, Oxford.

Anderson, E. and W. R. Harvey. (1966). Active transport by the Cecropia midgut II. Fine structure of the midgut epithelium. *J. Cell Biol.* **31**: 107-134.

Aplin, J. D. (1981). Protein-derivatized glass coverslips for the study of cell-to-substratum adhesion. *Anal. Biochem.* **113**: 144-148.

Ashhurst, D. E. (1968). The connective tissue of insects. *A. Rev. Ent.* **13**: 45-74.

Ashhurst, D. E. and A. J. Bailey. (1980). Locust collagen: morphological and biochemical characterization. *Eur. J. Biochem.* **103**: 75-83.

Baines, D. M. (1978). Observations on the peritrophic membrane of Locusta *Migratoria migratorioides* (R. & F.) nymphs. *Acrida*. **7**: 11-22.

Berenbaum, M. (1980). Adaptive significance of midgut pH in larval Lepidoptera. *Amer.naturalist* . **115**: 138-146.

Bernays, E. A. (1981). Plant tannins and insect herbivores: an appraisal. *Ecol.Entomol.* . **6**: 353-360.

Blankmeyer, J. T. and W. R. Harvey. (1978). Identification of active cell in potassium transporting epithelium. *J. exp. Biol.* **77**: 1-13.

Blinks, J. R., W. G. Weir, P. Hess and F. G. Prendergast. (1982). Measurement of Ca^{2+} concentrations in living cells. *Prog. Biophys. Molec. Biol.* **40**: 1-114.

Bowman, B. J. and E. J. Bowman. (1986). H^+-ATPases from mitochondria, plasma membranes and vacuoles of fungal cells. *J. Membr. Biol.* **94**: 83-97.

Bowman, E. J., A. Siebers and K. A. Altendorf. (1988). Bafilomycins: A class of inhibitors of membrane ATPases from microorganisms, animal cells and plant cells. *Proc. natn. Acad. Sci. USA.* **85**: 7972-7976.

Bradley, T. J. (1983). Functional design of microvilli in the Malpighian tubules of the insect *Rhodnius prolixus*. *J. Cell Sci.* **60**: 117-135.

Bradley, T. J. (1984). Mitochondrial placement and function in insect ion-transporting cells. *Amer. Zool.* **24**: 157-167.

Brandt, C. R., M. J. Adang and K. D. Spence. (1978). The peritrophic membrane: ultrastructural analysis and function as a mechanical barrier to microbial infection in *Orgyia pseudotsugata*. *J. Inv. Path.* **32**: 12-24.

Brooks, J. C. and S. Treml. (1983). Catecholamine secretion by chemically skinned cultured chromaffin cells. *J. Neurochem.* **40**: 468-473.

Burton, R. F. (1975). Ringer Solutions and Physiological Salines. Bristol, Wright. Scientechnica.

Chamberlin, M. E. (1990). Ion transport across the midgut of the tobacco hornworm *(Manduca sexta)*. *J. exp. Biol.* **150**: 425-442.

Chamberlin, M. E. (1989). Metabolic stimulation of transepithelial potential difference across the midgut of the tobacco hornworm *(Manduca sexta)*. *J. exp. Biol.* **141**: 295-311.

Chess, L., R. P. MacDermott and S. F. Schlossman. (1974). Immunologic functions of isolated human lymphocyte subpopulations. I. Quantitative

isolation of human T and B cells and response to mitogens. *J. Immunol.* **113**: 1113-1121.

Cioffi, M. (1979). The morphology and fine structure of the larval midgut of a moth *(Manduca sexta)* in relation to active ion transport. *Tissue Cell.* **11**: 467-479.

Cioffi, M. (1980). Apocrine secretion in the midgut of the tobacco hornworm larva, *Manduca sexta*. *Amer. Zool.* **20**: 1207.

Cioffi, M. (1984). Comparative ultrastructure of arthropod transporting epithelia. *Amer. Zool.* **24**: 139-156.

Cioffi, M. and W. R. Harvey. (1981). Comparison of K^+ transport in three structurally distinct regions of the insect midgut. *J. exp. Biol.* **91**: 103-116.

Cioffi, M. and M. G. Wolfersberger. (1983). Isolation of separate apical, lateral and basal plasma membrane from cells of an insect epithelium. A procedure based on tissue organization and ultrastructure. *Tissue Cell.* **15**: 781-803.

Crawford, D. N. and W. R. Harvey. (1988). Barium and calcium block *Bacillus thuringiensis* ssp *kurstaki* δ-endotoxin inhibition of potassium current across isolated midgut of larval *Manduca sexta*. *J. exp. Biol.* **137**: 277-286.

Currie, D. A., M. J. Milner and C. W. Evans. (1988). The growth and differentiation *in vitro* of leg and wing imaginal disc cells from *Drosophila melanogaster*. *Development.* **102**: 805-814.

de Duve, C., T. de Barsy, B. Poole, A. Trouet, P. Tulkens and F. Van Hoof. (1974). Commentary, lysomotropic drugs. *Biochem. Pharmacol.* **23**: 2495-2531.

De Jong, S., J. G. Zijlstra, H. Timmer-Bosscha, N. H. Mulder and E. G. E.

De Vries. (1986). Detection of DNA cross-links in tumour cells with the ethidium bromide fluorescence assay. *Int. J. Cancer.* **37**: 557-561.

Decker, R. S., M. L. Decker, V. Thomas and J. W. Fuselar. (1985). Responses of cultured cardiac monocytes to lysomotropic compounds and methylated amino acids. *J. Cell. Sci.* **74**: 119-135.

Dow, J. A. T. (1984). Extremely high pH in biological systems: A model for carbonate transport. *Am. J. Physiol.* **246** (RICP 15): R633-R635.

Dow, J. A. T. (1986). Insect midgut function. Advances in Insect Physiology. New York, Academic Press.

Dow, J. A. T., B. L. Gupta, T. A. Hall and W. R. Harvey. (1984). X-ray microanalysis of elements in frozen hydrated sections of an electrogenic K^+ transport system: The posterior midgut of tobacco hornworm *(Manduca sexta) in vivo* and *in vitro*. *J. Membr. Biol.* **77**: 223-241.

Dow, J. A. T. and W. R. Harvey. (1988). The role of midgut electrogenic K^+ pump potential difference in regulating lumen K^+ and pH in larval Lepidoptera. *J. exp. Biol.* **140**: 455-463.

Dow, J. A. T., W. R. Harvey, M. G. Wolfersberger and B. Boyes. (1985). Short communication: An improved chamber for short circuiting of epithelia. *J. exp. Biol.* **114**: 685-689.

Dow, J. A. T. and M. J. O'Donnell. (1990). Reversible alkalinization by *Manduca sexta* midgut. *J. exp. Biol.* **150**: 247-256.

Dow, J. A. T. and J. M. Peacock. (1989). Microelectrode evidence for the electrical isolation of goblet cell cavities in *Manduca sexta* middle midgut. *J. exp. Biol.* **143**: 101-114.

Dunn, L. A. and R. W. Holz. (1983). Catecholamine secretion from digitonin-treated adrenal medullary chromaffin cells. *J. Biol. Chem.* **258**: 4989-4993.

Endo, Y. and J. Nishiitsutsuji-Uwo. (1980). Mode of action of *Bacillus thuringiensis* δ-endotoxin: histopathological changes in the silkworm midgut. *J. Invert. Pathol.* **36**: 90-103.

Endo, Y. and J. Nishiitsutsuji-Uwo. (1981). Gut endocrine cells in insects: the ultrastructure of the gut endocrine cells of the Lepidopterous species. *Biomed. Res.* **2**: 270-280.

Epstein, W. (1985). The Kdp system: A bacterial K^+ transport ATPase. *Curr. Top. Membr. Transp.* **23**: 153-175.

Fast, P. G. (1981). Bacteria: the crystal toxin of *Bacillus thuringiensis*. Microbial control of pests and plant diseases. New York, Academic Press.

Fausto-Sterling, A. (1983). Paper in 24th Annual National Drosophila Conference.

Fehon, R. (1983). Paper in 24th Annual National Drosophila Conference.

Findlay, I. (1988). ATP^{4-} and ATP.Mg inhibit the ATP-sensitive K^+ channel of rat ventricular myocytes. *Pflugers Arch. Eur. J. Physiol.* **412**: 37-41.

Fistrom, J. W., R. Logan and C. Murphy. (1973). The synthetic and minimal culture requirements for evagination of imaginal discs of *Drosophila melanogaster in vitro*. *Devl. Biol.* **33**: 441-456.

Florkin, M. and C. Jeuniaux. (1974). Haemolymph: Composition. Physiology of Insecta. New York London, Academic Press.

Flower, N. E. and B. K. Filshie. (1976). Goblet cell membrane differentiation in the midgut of a Lepidopteran larva. *J. Cell Sci.* **20**: 357-375.

Fraser, M. J. (1989). Expression of eukaryotic genes in insect cell cultures. *In Vitro Cell. Devl. Biol.* **25**: 225-235.

Freshney, I. R. (1986). Animal cell culture: a practical approach. Oxford, IRL.

Futai, M. and H. Kanazawa. (1983). Structure and function of proton-translocating adenosine triphosphatase (F_0F_1): Biochemical and molecular biological approaches. *Microbiol. Rev.* **47**: 285-312.

Garcia, S. T., A. McQuillan and L. Panasci. (1988). Correlation between the cytotoxicity of melphalan and DNA crosslinks as detected by the ethidium bromide fluorescence assay in the F1 variant of B16 melanoma cells. *Biochem. Pharmacol.* **37**(16): 3189-3192.

Giordana, B., P. Parenti, G. M. Hanozet and V. F. Sacchi. (1985). Electrogenic K^+-basic amino acid cotransport in the midgut of Lepidopteran larvae. *J. Membr. Biol.* **88**: 45-53.

Giordana, B. and F. Sacchi. (1977). Some ionic and electrical parameters of the intestinal epithelium in three mature larvae of Lepidoptera. *Comp. Biochem. Physiol.* **56A**: 95-99.

Giordana, B., V. F. Sacchi and G. M. Hanozet. (1982). Intestinal amino acid absorption in Lepidopteran larvae. *Biochim. Biophys. Acta.* **692**: 81-88.

Goldschmidt, R. (1915). Some experiments on spermatogenesis *in vitro*. *Proc. natn. Acad. Sci. (Balt.).* **1**: 220-222.

Gomperts, B. D. and J. M. Fernandez. (1985). Techniques for membrane permeabilization. *TIBS.* **10**: 414-417.

Gordon, J. L. (1986). Extracellular ATP: Effects, sources and fate. *Biochem. J.* **233**: 309-319.

Grace, T. D. C. (1958). The prolonged growth and survival of ovarian tissue of the promethea moth *(Callosarnia promethea) in vitro*. *J. Gen. Physiol.* **41**: 1027-1033.

Grace, T. D. C. (1962). Establishment of four strains of cells from insect tissues grown *in vitro*. *Nature.* **195**: 788-789.

Griego, V. M., L. J. Fancher and K. D. Spence. (1980). Scanning electron microscopy of the disruption of tobacco hornworm, *Manduca sexta*, midgut by *Bacillus thuringiensis* endotoxin. *J. Inv. Path.* **35**: 186-189.

Guilbault, G. G. and D. N. Kramer. (1964). Fluorimetric determination of lipase, acylase, alpha- and gamma- chymotrypsin and inhibitors of these enzymes. *Anal. Chem.* **36**: 409-412.

Gupta, B. L., J. A. T. Dow, T. A. Hall and W. R. Harvey. (1985). Electron probe X-ray microanalysis of the effects of *Bt.* var *kurstaki* crystal protein insecticide on ions in an electrogenic K^+ transporting epithelium of the larval midgut in the Lepidopteran, *Manduca sexta, in vitro*. *J. Cell Sci.* **74**: 137-152.

Haider, M. Z. and D. J. Ellar. (1987). Characterization of the toxicity and cytopathic specificity of a cloned *Bacillus thuringiensis* crystal protein using insect cell culture. *Molec. Microbiol.* **1**: 59-66.

Hakim, R. S., K. M. Baldwin and P. Bayer. (1986). Embryonic development of the insect midgut. *Amer. Zool.* **66**: A12

Hall, J. L. and D. A. Baker. (1977). Oxidative Phosphorylation. Cell membranes and ion transport. New York London, Longman.

Halliwell, J. V. and M. J. Whitaker. (1987). Using microelectrodes. Microelectrode Techniques. The Plymouth Workshop Handbook. Cambridge, Company of Biologists.

Hammock, B. D., B. C. Bonning, R. D. Possee, T. N. Hanzlick and S. Maeda. (1990). Expression and effects of the juvenile hormone esterase in a baculovirus. *Nature.* **344**: 458-461.

Hanozet, G. M., B. Giordana, V. F. Sacchi and P. Parenti. (1989). Amino acid transport systems in brush border membrane vesicles from Lepidopteran enterocytes. *J. exp. Biol.* **143**: 87-100.

Harikumar, P. and J. P. Reeves. (1986). Lysosomal Proton Pump. New Insights into Cell and Membrane Transport Processes. New York London, Plenum.

Harper, E., S. Seifter and B. Scharrer. (1967). Electron microscopic and biochemical characterization of collagen in blatterian insects. *J. Cell Biol.* **33**: 385-393.

Harrison, R. (1907). Observations on the living developing nerve fibre. *Anat. Rec. Balt.* **1**: 116-118.

Harvey, G. T. and S. S. Sohi. (1985). Isoenzyme characterization of 28 cell lines from five insect species. *Can. J. Zool.* **63**: 2270-2276.

Harvey, W. R. (1980). Water and ions in the gut. VBW 80: Insect biology in the future. London, Academic Press.

Harvey, W. R., M. Cioffi, J. A. T. Dow and M. G. Wolfersberger. (1983a). Potassium ion transport ATPase in insect epithelia. *J. exp. Biol.* **106**: 91-117.

Harvey, W. R., M. Cioffi and M. G. Wolfersberger. (1981). Portasomes as coupling factors in active ion transport and oxidative phosphorylation. *Am. Zool.* **21**: 775-791.

Harvey, W. R., M. Cioffi and M. G. Wolfersberger. (1983b). Chemiosmotic potassium ion pump of insect epithelia. *Am. J. Physiol.* **244**: R163-R175.

Harvey, W. R., M. Cioffi and M. G. Wolfersberger. (1986). Transport physiology of Lepidopteran midgut in relation to the action of *Bt* δ-endotoxin. Fundamental and applied aspects of invertebrate pathology. Wangeningenen, Foundation IVth Intl. Colloq. Invert. Path.

Harvey, W. R., J. A. Haskell and S. Nedergaard. (1968). Active transport by the cecropia midgut III: midgut potential generated directly by active K^+ transport. *J. exp. Biol.* **48**: 1-12.

Harvey, W. R., J. A. Haskell and K. Zerahn. (1967). Active transport of potassium and oxygen consumption in the isolated midgut of *H.cecropia. J. exp. Biol.* **46**: 235-248.

Harvey, W. R. and S. Nedergaard. (1964). Sodium-independent active transport of potassium in the isolated midgut of the Cecropia silkworm. *Proc. natl. Acad. Sci. (USA).* **51**: 757-765.

Harvey, W. R. and M. G. Wolfersberger. (1979). Mechanism of inhibition of active potassium transport in isolated midgut of *Manduca sexta* by *Bacillus thuringiensis* endotoxin. *J. exp. Biol.* **83**: 293-304.

Harvey, W. R., J. L. Wood, R. P. Quatrale and A. M. Jungreis. (1975). Cation distributions across the larval and pupal midgut of the Lepidopteran, *Hyalophora cecropia, in vivo. J. exp. Biol.* **63**: 321-330.

Harvey, W. R. and K. Zehran. (1972). Active transport of potassium and other alkali metals by the isolated midgut of the silkworm. *Curr. Top. Membr. Transp.* **3**: 367-410.

Haskell, J. A., R. D. Clemons and W. R. Harvey. (1965). Active transport by the Cecropia midgut. I. Inhibitors, stimulants and potassium-transport. *J. Cell Comp. Physiol.* **65**: 45-56.

Hatefi, Y. (1985). The mitochondrial electron transport and oxidative phosphorylation system. *Ann. Rev. Biochem.* **54**: 1015-1069.

Hellstrom, U., M.-L. Dillner, S. Hammarstrom and P. Perlmann. (1976). Fractionation of human T-lymphocytes on wheatgerm agglutinin-sepharose. *J. exp. Medicine.* **144**: 1381-1385.

Himeno, M., N. Koyama, T. Funato and T. Komano. (1985). Mechanism of action of *Bacillus thuringiensis* insecticidal delta- endotoxin on insect cells *in vitro*. *Agric. Biol. Chem.* **49**: 1461-1468.

Hink, W. F. and R. L. Hall. (1989). Recently established invertebrate cell lines. Invertebrate Cell System Applications. Boca Raton, FL, CRC Press.

Hofer, M. (1981). Active Transport. Transport across biological membranes. Boston London, Pitman Advanced Publishing Program.

Howell, T. W., S. Cockcroft and B. D. Gomperts. (1987). Essential synergy between Ca^{2+} and guanine nucleotides in exocytotic secretion from permeabilized rat mast cells. *J. Cell Biol.* **105**: 191-197.

Humbert, W. (1978). Cytochemistry and X-ray microprobe analysis of the midgut of *Tomocerus minor Lubbock* (Insecta, Collembola) with special reference to the physiological significance of the mineral concretions. *Cell. Tiss. Res.* **187**: 397-416.

Ivie, G. W., D. L. Bull, R. C. Beier, N. W. Pryor and E. M. Oertli. (1983). Metabolic detoxification-mechanisms of insect resistance to plant sporalens. Science. **221**: 374-376.

Jones, B. M. (1962). The cultivation of insect cells and tissues. *Biol. Rev.* **37**: 512-536.

Jorgensen, P. L. (1982). Mechanism of the Na^+ K^+ pump. Protein structure and conformations of the pure (Na^+ + K^+) ATPase. *Biochim. Biophys. Acta.* **694**: 27-68.

Jungreis, A. M., P. Jatlow and G. R. Wyatt. (1973). Inorganic ion composition of haemolymph of the Cecropia silkmoth: changes with diet and ontogeny. *J. Insect Physiol.* **19**: 225-233.

Keynes, R. D. (1969). From frog skin to sheep rumen: A survey of transport of salts and water across multicellular structures. *Quart. Rev. Biophys.* **2**: 177-281.

Kimmich, G. A. (1970). Preparation and properties of mucosal epithelial cells isolated from small intestine of the chicken. *Biochemistry.* **9**: 3659-3668.

Klein, U., S. Weerth, M. Schindlbeck, H. Schweikl and H. Wieczorek. (1988). Proton transport and proton ATPase in K^+-transporting plasma membranes of *Manduca sexta* midgut epithelium. *Verh. Dtsch. Zool. Ges.* **81**: 309-310.

Knowles, B. H., P. H. Francis and D. J. Ellar. (1986). Structurally related *Bacillus thuringiensis* δ-endotoxins display major differences in insecticidal activity *in vivo* and *in vitro*. *J. Cell Sci.* **84**: 221-236.

Knowles, B. H., W. E. Thomas and D. J. Ellar. (1984). Lectin-like binding of *Bacillus thuringiensis* var *kurstaki* Lepidopteran- specific toxin as an initial step in insecticidal action. *FEBS lett.* **168**: 197-202.

Kobayashi, Y. and H. Ando. (1983). Embryonic development of the alimentary canal and ectodermal derivatives in the primitive moth, *Neomicropteryx nipponensis* (Lepidoptera, Micropterygidae). *J. Morphol.* **176**: 289-314.

Koefoed, B. M. (1985). A simple mechanical method to isolate the basal lamina of insect midgut epithelial cells. *Tissue Cell.* **17** (5): 763-768.

Kurtti, T. J. (1976). Phenotypic variations of cell lines from cockroach embryos. Invertebrate Tissue Culture: Research Applications. New York, Academic Press.

Lane, N. J. and H. I. Skaer. (1980). Intercellular junctions in insect tissues. *Adv. Insect Physiol.* **15**: 35-213.

Lane, N. J. and L. S. Swales. (1982). Stages in the assembly of pleated and smooth septate junctions in developing insect embryos. *J. Cell Sci.* **56**: 245-262.

Levinson, G. and T. J. Bradley. (1984). Removal of insect basal laminae using elastase. *Tissue Cell.* **16** (3): 367-376.

Ling, G. and R. W. Gerard. (1949). The normal membrane potential of frog sartorius fibers. *J. Cell Comp. Physiol.* **30**: 383-396.

Lis, H. and N. Sharon. (1986). Lectins as molecules and tools. *Ann. Rev. Biochem.* **55**: 35-67.

Maddrell, S. H. P., N. J. Lane, J. B. Harrison, B. O. C. Gardiner. (1985). DNA replication in binucleate cells of the Malpighian tubules of Hemipteran insects. *Chromosoma* . **91**: 201-209.

Maddrell, S. H. P. and B. O. C. Gardiner. (1980). The permeability of the cuticular lining of the insect alimentary canal. *J. exp. Biol.* **85**: 227-237.

Maddrell, S. H. P., J. A. Overton, D. J. Ellar and B. H. Knowles. (1989). Action of activated 27000 Mr toxin from *Bacillus thuringiensis* var. *israelensis* on Malpighian tubules of the insect *Rhodnius prolixus. J. Cell. Sci.* **94**: 601-608.

Makarow, M. and L. T. Nevalainen. (1987). Transport of a fluorescent macromolecule via endosomes to the vacuole in *S. cerevisae. J. Cell Biol.* **104**: 67-75.

Mandel, L. J., D. F. Moffett, T. G. Riddle and M. M. Grafton. (1980). Coupling between oxidative metabolism and active transport in the midgut of tobacco hornworm. *Am. J. Physiol.* **238**: C1-C9.

Mandel, M., Y. Moriyama, J. D. Hulmes, Y. E. Pan, H. Nelson and N. Nelson. (1988). cDNA sequence encoding the 16kD proteolipid of chromaffin granules implies gene duplication in the evolution of H^+ ATPases. *Proc. natn. Acad. Sci. (USA).* **85**: 5521-5524.

Manderino, G. L., G. T. Gooch and A. B. Stavitsky. (1978). Preparation, characterization and functions of rabbit lymph node cell populations. I.

Preparation of KLH primed T and B memory cells with anti-Fab affinity columns. *Cell. Immunol.* **41**: 264-275.

Marks, E. P. (1976). The uses of cell and organ cultures in insect endocrinology. Invertebrate Tissue Culture: Research Applications. New York London, Academic Press.

Martin, J. S. and M. M. Martin. (1983). Tannin assays in ecological studies: Precipitation of ribulose-1, 5-bisphosphate carboxylase-oxygenase by tannic acid, quebracho and oak *(Quercus)* foliage extracts. *J. Chem. Ecol.* **9**: 285-294.

McIntosh, A. H. (1976). Agar suspension culture for the cloning of invertebrate cells. Invertebrate Tissue Culture: Research Applications. New York, Academic Press.

Metz, J., W. G. Forssmann and S. Ito. (1977). Exocrine pancreas under experimental conditions. III. Membrane and cell junctions in isolated acinar cells. *Cell Tiss. Res.* **177**: 459-474.

Milner, M. J. and J. Muir. (1987). The cell biology of Drosophila wing metamorphosis *in vitro*. *Wilhelm Roux's Arch. Devl. Biol.* **196**: 191-201.

Mitchell, P. (1966). Chemiosmotic coupling in oxidative and photosynthetic phosphorylation. *Biol. Rev.* **41**: 445-502.

Mitsuhashi, J. (1976). Establishment and characterization of cell lines from the pupal ovaries of *Papilio xuthus*. Invertebrate Tissue Culture: Research Applications. New York, Academic Press.

Mitsuhashi, J. (1982). Media for insect cell culture. Advances in Cell Culture. New York, Academic Press.

Miya, K. (1976). Ultrastructural changes of embryonic cells during organogenesis in the silkworm, *Bombyx mori*. *J. Fac. Agric. Iwate Uni.* **13**: 95-122.

Moffett, D. F. (1980). Voltage-current relation and K^+ transport in tobacco hornworm *(Manduca sexta)* midgut. *J. Membr. Biol.* **54**: 213-219.

Moffett, D. F., R. L. Hudson, S. B. Moffett and R. L. Ridgway. (1982). Intracellular K^+ activities and cell membrane potentials in a K^+ transporting epithelium, the midgut of tobacco hornworm *(Manduca sexta). J. Membr. Biol.* **70**: 59-68.

Moffett, D. F. and A. R. Koch. (1988a). Electrophysiology of K^+ transport by midgut epithelium of Lepidopteran insect larvae II: The transapical electrochemical gradients. *J. exp. Biol.* **135**: 39-49.

Moffett, D. F. and A. R. Koch. (1988b). Electrophysiology of K^+ transport by midgut epithelium of Lepidopteran insect larvae I: The transbasal electrochemical gradient. *J. exp. Biol.* **135**: 25-38.

Moffett, D. F., C. J. Smith and J. M. Green. (1983). Effects of caffeine, cAMP and A23187 on ion transport by the midgut of tobacco hornworm. *Comp. Biochem. Physiol.* **75C**: 305-310.

Mori, H. (1983). Origin, development, functions and phylogeny of the embryonic midgut epithelium in insects. *Ent. gen.* **8**: 135.

Moriyama, Y., T. Takano and S. Ohkuma. (1982). Acridine orange as a fluorescent probe for lysosomal proton pump. *J. Biochem.* **92**: 1333-1336.

Nedergaard, S. (1977). Amino acid transport. Transport of ions and water in animals. London, Academic Press.

Nelson, N. (1987). The vacuolar proton ATPase of eukaryote cells. *Bioessays.* **7**(6): 251-254.

Nelson, N. and L. Taiz. (1989). The evolution of H^+-ATPases. *TIBS.* **14**: 113-116.

Nicola, N. A., A. W. Burgess, D. Metcalf and F. L. Battye. (1978). Separation of mouse bone marrow cells using wheat germ agglutinin affinity chromatography. *Aus. J. exp. Biol. A.K.* **56**: 663-679.

O'Donnell, M. J. and S. H. P. Maddrell. (1984). *In Vitro* techniques for studies of Malpighian tubules. Measurement of ion transport and metabolic rate in insects. New York, Springer Verlag.

Ohkuma, S. and B. Poole. (1981). Cytoplasmic vacuolation of mouse peritoneal macrophages and the uptake into lysosomes of weakly basic substances. *J. Cell Biol.* **90**: 656-664.

Paul, J. (1975). Cell and Tissue Culture. Edinburgh, Churchill Livingstone.

Pedersen, P. L. and E. Carafoli. (1987a). Ion motive ATPases: I. Ubiquity, properties and significance to cell function. *TIBS.* **12**: 146-150.

Pedersen, P. L. and E. Carafoli. (1987b). Ion motive ATPases: II. Energy coupling and work output. *TIBS.* **12**: 186-189.

Poole, B. and S. Ohkuma. (1981). Effect of weak base on the intralysosomal pH in mouse peritoneal macrophages. *J. Cell Biol.* **90**: 665-669.

Pope, A. J. and R. A. Leigh. (1988). Dissipation of pH gradients in tonoplast vesicles and liposomes by mixtures of acridine orange and anions. Implications for the use of acridine orange as a pH probe. *Plant Physiol.* **86**: 1315-1322.

Rabon, E., J. Cuppoletti, D. Malinowska, A. Smolka, H. F. Helander, J. Mendlein and G. Sachs. (1983). Proton secretion by the gastric parietal cell. *J. exp. Biol.* **106**: 119-133.

Reynolds, S. E., S. F. Nottingham and A. E. Stephens. (1985). Food and water economy and its relation to growth in fifth instar larvae of the tobacco hornworm, *Manduca sexta. J. Insect Physiol.* **31**: 119-127.

Riddiford, L. M. (1976). Hormonal control of insect epidermal cell commitment *in vitro. Nature.* **259**: 115-117.

Ridgway, R. L. and D. F. Moffett. (1986). Regional differences in the histochemical localization of carbonic anhydrase in the midgut of tobacco hornworm *(Manduca sexta). J. exp. Zool.* **237**: 407-412.

Rink, T. J., R. Y. Tsien and T. Pozzan. (1982). Cytoplasmic pH and free Mg^{2+} in lymphocytes. *J. Cell Biol.* **95**: 189-196.

Romrell, L. J., M. R. Coppe, D. R. Munro and S. Ito. (1975). Isolation and separation of highly enriched fractions of viable mouse gastric parietal cells by velocity sedimentation. *J. Cell Biol.* **65**: 428-438.

Roos, A. and W. F. Boron. (1981). Intracellular pH. *Physiol. Rev.* **61**: 296-434.

Rossier, B. C., K. Geering and J. P. Kraehenbuhl. (1987). Regulation of the sodium pump: How and why? *TIBS.* **12**: 483-487.

Rothman, J. H., C. T. Yamashiro, C. K. Raymond, P. M. Kane and T. H.

Stevens. (1989). Acidification of the lysosome-like vacuole and the vacuolar H^+ ATPase are deficient in two yeast mutants that fail to sort vacuolar proteins. *J. Cell Biol.* **109** (1): 93-100.

Ryerse, J. S. (1978). Ecdysterone switches off fluid secretion at pupation in insect Malpighian tubules. *Nature.* **271**: 745-746.

Ryerse, J. S. (1979). Developmental changes in Malpighian tubule cell structure. *Tissue Cell.* **11**: 533-552.

Ryerse, J. S. (1980). The control of Malpighian tubule developmental physiology of 20-hydroxyecdysone and juvenile hormone. *J. Insect Physiol.* **26**: 449-457.

Sacchi, V. F., G. Cattaneo, M. Carpentieri and G. Giordana. (1981). l-Phenylalanine active transport in the midgut of *Bombyx mori* larva. *J. Insect Physiol.* **27**: 211-214.

Sacchi, V. F., G. M. Hanozet and B. Giordana. (1984). Gamma-aminoisobutyric acid transport in the midgut of two Lepidopteran larvae. *J. exp. Biol.* **108**: 329-339.

Sacchi, V. P., P. Parenti, G. M. Hanozet, B. Giordana, P. Luthy and M. G. Wolfersberger. (1986). *Bt.* toxin inhibits K^+ gradient dependent amino acid transport across the brush border membrane of *Pieris brassicae* midgut cells. *FEBS 3904.* **204** (2): 213-218.

Sachs, G., B. Wallmark, G. Saccomani, E. Rabon, H. B. Stewart, D. R. di Bona and T. Berglindh. (1982). The ATP-dependent component of gastric acid secretion. *Curr. Top. Membr. Transp.* **16**: 135-159.

Sang, J. H. (1981). Drosophila cells and cell lines. Advances in Cell Culture. New York, Academic Press.

Santos, C. D., A. F. Ribeiro, C. Ferreira and W. R. Terra. (1984). The larval midgut of the cassava hornworm *(Erinnyis ello)* Ultrastructure, fluid fluxes and the secretory activity in relation to the organization of digestion. *Cell Tiss. Res.* **237**: 565-574.

Satmary, W. M. and T. J. Bradley. (1984). Dissociation of insect Malpighian tubules into single viable cells. *J. Cell Sci.* **72**: 101-109.

Schweikl, H., U. Klein, M. Schindlbeck and H. Wieczorek. (1989). A vacuolar-type ATPase, partially purified from potassium transporting plasma membranes of tobacco hornworm midgut. *J. Biol. Chem.* **264**: 11136-11142.

Schweikl, H., M. Schindlbeck, U. Klein and H. Wieczorek. (1987). Solubilization and partial purification of a K^+ -stimulated ATPase activity from K^+ transporting membranes of insect midgut epithelium. *Verh. Dtsch. Zool. Ges.* **80**: 225.

Serrano, R. (1984). Plasma membrane ATPase of fungi and plants as a novel type of proton pump. *Curr. Top. Cell Reg.* **23**: 87-126.

Skaer, R. J. (1981). Cellular sieving by a natural, high-flux membrane. *J. microsc.* **124**: 331-333.

Smith, D. S., K. Compher, M. Janners, C. Lipton and L. W. Wittle. (1969). Cellular organization and ferritin uptake in the midgut epithelium of a moth, *Ephestia kuhniella*. *J. Morph.* **127**: 41-72.

Smolen, J. E. and S. J. Stoehr. (1985). Micromolar concentrations of free calcium provoke secretion of lysozyme from human neutrophils permeabilized with saponin. *J. Immunol.* **134**: 1859-1865.

Sohi, S. S. (1980). The effect of pH and osmotic pressure on the growth and survival of 3 Lepidopteran cell lines. Invertebrate Systems *in Vitro*. Amsterdam, Elsevier / North Holland Bio-medical Press.

Spies, A. G. and K. D. Spence. (1985). Effect of sublethal *Bacillus thuringiensis* crystal endotoxin treatment on the larval midgut of a moth, *Manduca sexta* : SEM study. *Tissue Cell.* **17** (3): 379-394.

Sutcliffe, D. W. (1963). The chemical composition of haemolymph in insects and some other invertebrates in relation to their phylogeny. *Comp. Biochem. Physiol.* **9**: 121-135.

Suzuki, N. and H. Ando. (1981). Alimentary canal formation in the scorpion fly, *Panorpa pryeri Maclachlan* (Mecoptera: Panorpidae). *Int. J. Insect Morph. Embryol.* **10**: 345-354.

Terra, W. R. and C. Ferreira. (1983). Further evidence that enzymes involved in the final stages of digestion by Rhynchosciara do not enter the endoperitrophic space. *Insect Biochem.* **13**: 143-150.

Thomas, M. V. and T. E. May. (1984a). Active potassium ion transport across the caterpillar midgut. I. Tissue electrical properties and potassium ion transport inhibition. *J. exp. Biol.* **108**: 273-291.

Thomas, M. V. and T. E. May. (1984b). Active potassium ion transport across the caterpillar midgut. II. Intracellular microelectrode studies. *J. exp. Biol.* **108**: 293-304.

Trager, W. (1935). Cultivation of the virus of grasserie in silkworm tissue cultures. *J. exp. Med.* **61**: 501-514.

Turbeck, B. O. (1974). A study of the concentrically laminated concretions 'spherites' in the regenerative cells of the midgut of Lepidopterous larvae. *Tissue Cell.* **6**: 627-640.

Turbeck, B. O. and B. Foder. (1970). Studies on a carbonic anhydrase from the midgut epithelium of larvae of Lepidoptera. *Biochim. Biophys. Acta.* **212**: 134-138.

Ussing, H. H. and K. Zerahn. (1951). Active transport of sodium as the source of electric current in the short-circuited isolated frog skin. *Acta. Physiol. Scand.* **23**: 110-127.

Vaughn, J. L., R. D. Stone and G. K. Zhu. (1989). The effect of dissolution procedures on the infectivity of the nuclear polyhedrosis polyhedra-derived virions for cell cultures. Invertebrate Cell System Applications. Boca Raton, FL, CRC Press.

Vitellaro-Zuccarello, L., V. F. Sacchi, G. Monticelli and B. Giordana. (1985). The colon of *Leucophaea maderae*: fine structure and physiological features. *Tissue Cell* . **17**: 395-404.

Waku, Y. and K.-I. Sumimoto. (1971). Metamorphosis of midgut epithelial cells in the silkworm *(Bombyx mori L.)* with special regard to the calcium salt deposits in the cytoplasm I. Light microscopy. *Tissue Cell.* **3**: 127-136.

Warner, A. E. and C. M. Bate. (1987). Techniques for dye injection and cell labelling. Microelectrode Techniques. The Plymouth Workshop Handbook. Cambridge, Company of Biologists.

Waterhouse, D. F. (1949). The hydrogen ion concentration in the alimentary canal of larval and adult Lepidoptera. *Aust. J. Sci. Res., Ser. B.* **132**: 428-437.

Whetton, A. D., S. J. Huang and P. N. Monk. (1988). Adenosine triphosphate can maintain multipotent haemopoeitic stem cells in the absence of interleukin 3 via a membrane permeabilization mechanism. *Biochem. Biophys. Res. Comm.* **152** (3): 1173-1178.

Wieczorek, H. (1982). A biochemical approach to the electrogenic potassium pump of insect sensilla: potassium sensitive ATPase in the labellum of the fly. *J. comp. Physiol.* **148A**: 303-311.

Wieczorek, H. and W. Gnatzy. (1985). The electrogenic K^+ pump of insect cuticular sensilla. *Insect Biochem.* **15** (2): 225-232.

Wieczorek, H., S. Weerth, M. Schindlbeck and U. Klein. (1989). A vacuolar type proton pump in a vesicle fraction enriched with K^+-transporting plasma

membranes from tobacco hornworm midgut. *J. Biol. Chem.* **264**: 11143-11148.

Wieczorek, H., M. G. Wolfersberger, M. Cioffi and W. R. Harvey. (1986). Cation-stimulated ATPase activity in purified plasma membranes from tobacco hornworm midgut. *Biochimica. Biophys. Acta.* **857**: 271-281.

Wilson, S. P. and N. Kirshner. (1983). Calcium-evoked secretion from digitonin -permeabilized adrenal medullary chromaffin cells. *J. Biol. Chem.* **258**: 4994-5000.

Wolfersberger, M. G. and K. M. Giangiacomo. (1983). Active K^+ transport by the isolated Lepidopteran larval midgut: Stimulation of net K^+ flux and elimination of the slower phase decline of the short circuit current. *J. exp. Biol.* **102**: 199-210.

Wolfersberger, M. G., W. R. Harvey and M. Cioffi. (1982). Transepithelial potassium transport in insect midgut by an electrogenic alkali metal ion pump. *Curr. Top. Membr. Transp.* **16**: 109-133

Wolfersberger, M. G., C. Hofmann and P. Luthy. (1985). Interaction of *Bacillus thuringiensis* δ-endotoxin with membrane vesicles isolated from Lepidopteran larval midgut. *Pers. Comm.*

Wolfersberger, M. G., D. D. Spaeth and J. A. T. Dow. (1986). Permeability of the peritrophic membrane of tobacco hornworm larval midgut. *Amer. Zool.* **66**: A74.

Wood, J. L., P. S. Farrand and W. R. Harvey. (1969). Active transport of potassium by the cecropia midgut VI. Microelectrode potential profile. *J. exp. Biol.* **50**: 169-178.

Wood, J. L. and W. R. Harvey. (1976). Active transport of calcium across the isolated midgut of *Hyalophora cecropia*. *J. exp. Biol.* **65**: 347-360.

Wood, J. L. and W. R. Harvey. (1979). Influx theory and size of potassium and rubidium pools in the midgut of *Hyalophora cecropia*. *J. exp. Biol.* **82**: 1-9.

Wood, J. L. and R. B. Moreton. (1978). Refinements in the short- circuit technique and its application to active potassium transport across the cecropia midgut. *J. exp. Biol.* **77**: 123-140.

Wyatt, S. S. (1956). Culture *in vitro* of tissue from the silkworm *Bombyx mori*. *J. Gen. Physiol.* **39**: 841-852.

Xie, X.-S. and D. K. Stone. (1986). Isolation and reconstitution of the clathrin-coated vesicle proton-translocating complex. *J. Biol. Chem.* **261**: 2492-2495.

Yamamoto, R. T. (1969). Mass rearing of the tobacco hornworm II. larval rearing and pupation. *J. Econ. Entomol.* **62**: 1427-1431.

Zerahn, K. (1977). Potassium transport in insect midgut. Transport of ions and water in animals. New York, Academic.